ISSN (1230-0322)
2023, Vol. 73, No. 1

Food

Polish Journal of Food and Nutrition Sciences

formerly Acta Alimentaria Polonica

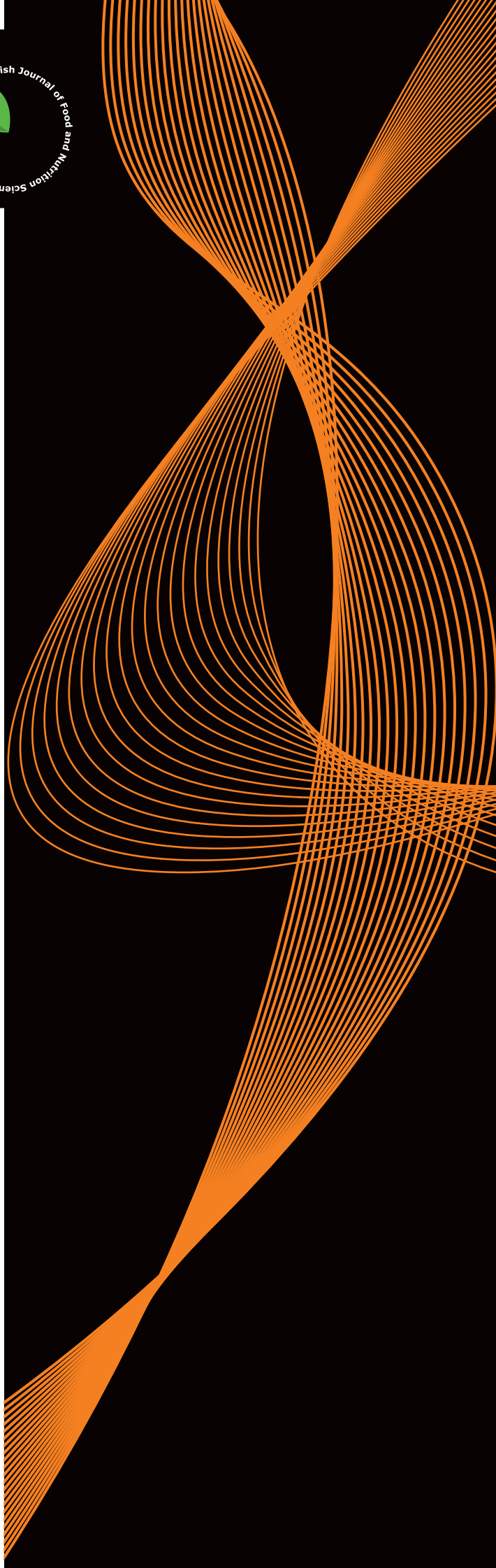

Published

by Institute of Animal Reproduction and Food Research of the Polish Academy of Sciences, Olsztyn

Published since 1957 as
Roczniki Chemii i Technologii Żywności and Acta Alimentaria Polonica (1975–1991)

SCOPE: The Journal covers fundamental and applied research in food area and nutrition sciences with a stress on interdisciplinary studies in the areas of food, nutrition and related subjects.

POLICY: Editors select submitted manuscripts in relation to their relevance to the scope. Reviewers are selected from the Advisory Board and from Polish and international scientific centres. Identity of reviewers is kept confidential.

AUTHORSHIP FORMS referring to Authorship Responsibility, Conflict of Interest and Financial Disclosure, Copyright Transfer and Acknowledgement, and Ethical Approval of Studies are required for all authors.

FREQUENCY: Quarterly – one volume in four issues (March, June, September, December).

COVERED by Web of Science, Current Contents/Agriculture, Biology & Environmental Sciences, Journal Citation Reports and Science Citation Index Expanded, BIOSIS (Biological Abstracts), SCOPUS, FSTA (formerly: Food Science and Technology Abstracts), CAS (Chemical Abstracts), AGRICOLA, AGRO-LIBREX data base, EBSCO, FOODLINE, Leatherhead FOOD RA data base FROSTI, AGRIS and Index Copernicus data bases, Biblioteka Nauki ICM, Biblioteka Narodowa - POLONA, and any www browser; ProQuest: The Summon, Bacteriology Abstracts, Immunology Abstracts.

EDITORIAL AND BUSINESS CORRESPONDENCE: Submit contributions (see Instructions to Authors) and address all communications regarding subscriptions, changes of address, etc. to:

CORRESPONDENCE TO: Ms. Joanna Molga
Polish Journal of Food and Nutrition Sciences
Institute of Animal Reproduction and Food Research
of Polish Academy of Sciences
ul. Tuwima 10, 10-747 Olsztyn, Poland
e-mail: pjfns@pan.olsztyn.pl; http://journal.pan.olsztyn.pl

Polish Journal of Food and Nutrition Sciences

ADVISORY BOARD OF PJFNS 2023–2026

Contents

covered by CURRENT CONTENTS/AGRICULTURE, BIOLOGY & ENVIRONMENTAL SCIENCES, JOURNAL CITATION REPORTS AND SCIENCE CITATION INDEX EXPANDED, BIOSIS, SCOPUS, IFIS Publishing and CAS abstracts, and AGRO-Librex, FROSTI, PSJC, AGRIS and Index Copernicus data bases

Ministerstwo
Edukacji i Nauki

W latach 2022–2024 kwartalnik naukowy ***Polish Journal of Food and Nutrition Sciences*** realizuje projekt nr RCN/SP/0520/2021/1 finansowany ze środków budżetu państwa – Ministerstwo Edukacji i Nauki w ramach programu „Rozwój czasopism naukowych". Dofinansowanie wynosi 120 000 zł. W ramach projektu podejmowane są działania zmierzające do podniesienia poziomu praktyk wydawniczych i edytorskich, zwiększenia wpływu czasopism na rozwój nauki oraz utrzymania się czasopism w międzynarodowym obiegu naukowym.

Ministry of Education and Science
Republic of Poland

In the years 2022–2024, the scientific quarterly ***Polish Journal of Food and Nutrition Sciences*** accomplishes a project no. RCN/SP/0520/2021/1 financed from the state budged – Ministry of Education and Science Republic of Poland in the framework of a program "Development of scientific journals". The financing amounts to 120,000 PLN. The program aims at improving the level of publishing and editing practices, increasing the impact of scientific journals on science development, and extending the international range of scientific journals.

Subscription
2023 – One volume, four issues per volume. Annual subscription rates are: Poland 150 PLN, all other countries 80 EUR. Prices are subject to exchange rate fluctuation. Subscription payments should be made by direct bank transfer to Bank Gospodarki Żywnościowej, Olsztyn, Poland, account No 17203000451110000000452110 SWIFT code: GOPZPLWOLA with corresponding banks preferably. Subscription and advertising offices at the Institute of Animal Reproduction and Food Research of Polish Academy of Sciences, ul. J. Tuwima 10, 10-747 Olsztyn, Poland, tel./fax (48 89) 5234670, fax (48 89) 5240124, e-mail: pjfns@pan.olsztyn.pl; http://journal.pan.olsztyn.pl

Zamówienia prenumeraty: Joanna Molga (e-mail: pjfns@pan.olsztyn.pl)

Wersja pierwotna (referencyjna) kwartalnika PJFNS: wersja papierowa (ISSN 1230–0322)
Nakład: 70 egz.; Ark. wyd. 16,9; Ark. druk. 14
Skład i druk: ITEM

REVIEW ARTICLE
http://journal.pan.olsztyn.pl

Polish Journal of Food and Nutrition Sciences
2023, Vol. 73, No. 1, 5–23
DOI: 10.31883/pjfns/159361
ISSN 1230-0322, e-ISSN 2083-6007

Phenolic Compounds in Agro-Industrial Waste of Mango Fruit: Impact on Health and Prebiotic Effect – a Review

Mayra Nicolás-García[1], Anahí Jobeth Borrás-Enríquez[2], Jorge Luis González-Escobar[1]*, Oscar de Jesús Calva-Cruz[3], Viridiana Pérez-Pérez[1], Mayra Sánchez-Becerril[1]

[1]Tecnológico Nacional de México/Tecnológico de Estudios Superiores de San Felipe del Progreso. División de Ingeniería en Industrias Alimentarias. Av. Instituto Tecnológico, S/N, ejido de San Felipe del Progreso, 50640, San Felipe del Progreso, Estado de México, México
[2]Tecnológico Nacional de México/Tecnológico de Estudios Superiores de San Felipe del Progreso. División de Ingeniería en Energías Renovables. Av. Instituto Tecnológico, S/N, ejido de San Felipe del Progreso, 50640, San Felipe del Progreso, Estado de México, México
[3]IPICYT, Instituto Potosino de Investigación Científica y Tecnológica A.C., Camino a La Presa San José 2055, Col. Lomas 4a Sección, San Luis Potosí, SLP, 78216, México

The fruit processing industry generates huge amounts of waste annually, causing severe environmental problems. Mango processing produces around 20 million tons of wastes from the non-consumed fraction, mainly peels and seeds, which constitute 30–60% of the fruit weight. However, various phytochemicals found in these residues have been implicated in preventing cancer and also cardio-metabolic and gastrointestinal diseases. Particularly, phenolic compounds hold a promising potential to be utilized as modulatory agents of the human gut microbiota (prebiotics-like actions). This review article mainly discusses the effect of phenolics from mango wastes on gut microbiota modulation and its beneficial repercussions for human health. Moreover, it also discusses the importance of phenolic compounds of mango peel and seed kernel residues, their extraction, identification, and quantification.

Key words: mango processing, mango wastes, phytochemicals, biological properties, gut health

ABBREVIATIONS

ABTS, 2,2'-azinobis (3-ethylbenzothiazoline 6-sulfonate); Ace, Acetone; AMPK, AMP-activated protein kinase; BHA, Butylhydroxy-anisole; BHT, Butylhydroxytoluene; CAA, Cellular antioxidant activity; COX-2, Cyclooxygenase-2; DW, Dry weight; DCM, Dichloromethane; DPPH$^{\bullet}$, 2,2-Diphenyl-1-picrylhydrazyl radical; DSS, Dextran sulfate sodium; EC_{50}, Half maximal effective concentration; EtOH, Ethanol; FRAP, Ferric reducing antioxidant power; FW, Fresh weight; GC–QTOF-MS, Gas chromatography with quadrupole-time-of-flight mass spectrometry; GLUT4, Glucose transporter 4; GM-CSF, Granulocyte-macrophage colony-stimulating factor; GRO, Growth-regulated oncogene; HbA1c, Glycosylated hemoglobin levels; HepG2, Hepatocellular carcinoma; HPLC, High-performance liquid chromatography; HPLC-DAD--ESI-QTOF-MS, HPLC-DAD coupled to electrospray ionization quadrupole-time-of-flight mass spectrometry; HPLC-DAD-MS, HPLC-DAD with mass spectrometry; HPTLC, High-performance thin layer chromatography; HSP, Hansen's solubility parameters; IC_{50}, Half-maximal inhibitory concentration; iNOS, inudcible nitric oxide synthase; IL-6, Interleukin-6; IL-8, Interleukin-8; ISAPP, International Scientific Association of Probiotics and Prebiotics; LC-QTOF-MS/MS, Liquid chromatography coupled to quadrupole-time-of-flight tandem mass spectrometry; MCP-1, Monocyte chemoattractant protein-1; MCS, Mangiferin calcium salt; MeOH, Methanol; NAFLD, Non-alcoholic fatty liver disease; NF-κB, Nuclear factor κB; ORAC, Oxygen radical absorbance capacity;

***Corresponding Author:**
e-mail: jorge.ge@sfelipeprogreso.tecnm.mx (J.L. González-Escobar)

Submitted: 26 November 2022
Accepted: 16 January 2023
Published on-line: 21 February 2023

PAI-1, Plasminogen Activator Inhibitor-1; PLE, Pressurized liquid extraction; RP-HPLC-ESI-MS, Reversed-phase HPLC coupled to electrospray ionization mass spectrometry; SCCAI, Simple clinical colitis activity index; SCFAs, Short-chain fatty acids; TNF-α, Tumor necrosis factor-α; UHPLC, Ultra high performance liquid chromatography; UPLC-DAD-ESI-MS, UHPLC with diode array detector coupled to electrospray ionisation mass spectrometry; UPLC-ESI-QTOF-MS, UPLC coupled to electrospray ionization quadrupole-time-of-flight mass spectrometry.

INTRODUCTION

The mango (*Mangifera indica* L.), belonging to the Anacardiaceae family, comprises 70 genera and around 1000 varieties that differ in the fruit size, shape, color, and composition. This is one of the most important tropical fruit crops in the world [Alañón *et al.*, 2021a; Ediriweera *et al.*, 2017; Nguyen *et al.*, 2022]. According to the Food and Agriculture Organization (FAO) of the United Nations, the leading tropical fruits in 2019 include pineapple (41%), avocado (29%), and mango (26%), with a trade of 7.8 million tons worldwide. Still, the tropical product with the most significant expansion is mango and its export production for 2019 was 2,042,125 tons worldwide [FAO, 2020]. Mango consumption trend is related to its sensory, nutritional, and functional qualities [Ballesteros-Vivas *et al.*, 2019a; Borrás-Enríquez *et al.*, 2021; Lim *et al.*, 2019]. Many varieties or cultivars from Thailand, Mexico, Egypt, the tropical coasts of Spain, North India, Ecuador, China, and Colombia provide good-quality fruits of industrial importance, among which there are Mango Hindi [Abdel-Aty *et al.*, 2018], Keitt [Abbasi *et al.*, 2017; Alañón *et al.*, 2021a, b; Kim *et al.*, 2018], Kent [Alañón *et al.*, 2021a, b; Marcillo-Parra *et al.*, 2021], Osteen [Alañón *et al.*, 2021a, b; López-Cobo *et al.*, 2017], Halden [Castañeda-Valbuena *et al.*, 2021; Marcillo-Parra *et al.*, 2021], Hilacha [Hoyos-Arbeláez *et al.*, 2018], Bombay Green, Dashe Hari, Langra and Chausa [Jyotshna *et al.*, 2015], Sensation [Hu *et al.*, 2018; López-Cobo *et al.*, 2017], Xiangya [Hu *et al.*, 2018], Tommy Atkins [Castro-Vargas *et al.*, 2019; Marcillo-Parra *et al.*, 2021], Luzon, Narcissus, Royal Mango, Big Tainong, Australian Mango, Thai Mango, Samall Tainong and Egg Mango [Abbasi *et al.*, 2017], Manila [Gómez-Maldonado *et al.*, 2020; Soria-Lara *et al.*, 2020], Manililla [Borrás-Enríquez *et al.*, 2021], and Ataulfo [Anaya-Loyola *et al.*, 2020; De Ancos *et al.*, 2018; Hernández-Maldonado *et al.*, 2019].

The industrial processing of mangoes entails mainly extracting juices and producing nectars, concentrates, sauces, or jams with a high nutritional value [Anaya-Loyola *et al.*, 2020; Castañeda-Valbuena *et al.*, 2021; Sáyago-Ayerdi *et al.*, 2019]. However, 30–60% of residues are generated during processing, including peel (12–20%) and seed (10–25%). Overall, the seed accounts for 20 to 60% of the whole fruit, as shown in Figure 1 [Lim *et al.*, 2019; Mwaurah *et al.*, 2020; Sánchez-Camargo *et al.*, 2021; Torres-León *et al.*, 2017]. Unfortunately, around 20 million tons of these residues are discarded per year, promoting water and air pollution, vegetation damage, and greenhouse gas emissions [Castañeda-Valbuena *et al.*, 2021; Mutua *et al.*, 2017; Sáyago-Ayerdi *et al.*, 2019]. Nonetheless, agro-industrial by-products, such as mango peels and seeds, are a source of nutrients and bioactive compounds. For instance, the mango seed contains carbohydrates (58–80 g/100 g), proteins (6–13 g/100 g) with high levels of essential amino acids, and lipids (6–16 g/100 g) with oleic and stearic acids [Borrás-Enríquez *et al.*, 2021; Lebaka *et al.*, 2021; Torres-León *et al.*, 2016]. On the other hand, mango phenolic compounds are one of the most important biologically active components [Ballesteros-Vivas *et al.*, 2019a; Torres-León

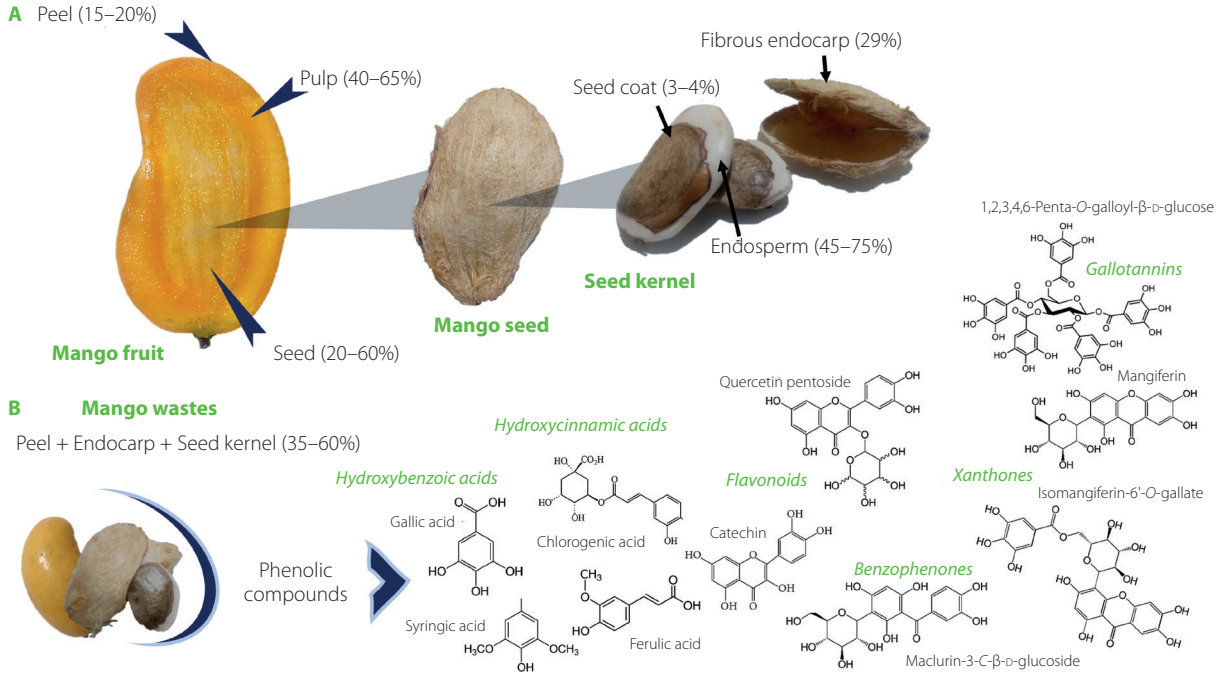

Figure 1. (A) Structural components of the mango fruit (*M. indica* L.); (B) main phenolic compounds in mango agro-industrial residues [De Ancos *et al.*, 2018; Ediriweera *et al.*, 2017].

et al., 2021]. Phenolic compounds have recently gained more interest due to their beneficial health properties as antioxidants and antimicrobials agents. Several studies have reported that some compounds in mango (found in peel and seed kernel) can prevent diseases related to oxidative stress, such as cancer, arthritis, atherosclerosis, type 2 diabetes, cardiovascular diseases as well as Alzheimer's and Parkinson's diseases [Kim *et al.*, 2018; Lin *et al.*, 2020; Lopez-Martinez *et al.*, 2022; Torres-León *et al.*, 2021]. The high flavonoid content is widely linked to antioxidant and antiproliferative activity [Abbasi *et al.*, 2017; Soria-Lara *et al.*, 2020]. Additionally, the high phenolic compound content has been reported to beneficially modify the gut microbiota profile [Bento-Silva *et al.*, 2020; Kim *et al.*, 2018]. In this context, the mango wastes contain diverse and valuable compounds that offer uncountable benefits to human health. Therefore, the main goal of this review article was to understand the bioactive potential of phenolic compounds from mango by-products, mainly in the context of prebiotics-like actions. It also discusses extraction methods used for phenolic identification and quantification.

PHENOLIC COMPOUNDS IN MANGO BY-PRODUCTS

Composition, distribution, extraction, and identification

Phenolic compounds from mango residues can be classified into phenolic acids, flavonoids, gallates and gallotannins, ellagitannins, and others (benzophenones, xanthones, and lignans) [Ballesteros-Vivas *et al.*, 2019a; De Ancos *et al.*, 2018; Torres-León *et al.*, 2021] as listed in Table 1. These compounds can be found in both free and bound forms [Alañón *et al.*, 2021a; Gómez-Caravaca *et al.*, 2016; Pacheco-Ordaz *et al.*, 2018a]. Generally, the bound compounds are low molecular weight phenolics that may be interacting with macromolecules or cell wall components such as dietary fiber; these can be phenolic acids such as gallic, *p*-hydroxybenzoic, vanillic, protocatechuic, *p*-coumaric, ferulic, ellagic, as well as *trans* and *cis*-*p*-coumaric acids [Abbasi *et al.*, 2017; Anaya-Loyola *et al.*, 2020; Hernández-Maldonado *et al.*, 2019]. Gómez-Caravaca *et al.* [2016] reported ellagic acid as the main bound phenolic in the pulp and peel fruit, as well as the husk and the seed kernel. The authors have remarked that this compound is responsible for 88.7% of the bound phenolics in the peel of mango fruit. Nonetheless, the variation of phenolic composition and biological activities in mango depends on the plant variety or cultivar, its geographic origin, growing conditions, age, fruit harvest time, degree of maturity, processing, and storage conditions [Abdel-Aty *et al.*, 2018; Alañón *et al.*, 2021a; Marcillo-Parra *et al.*, 2021; Sáyago-Ayerdi *et al.*, 2019]. For example, fisetin and mangiferin have been found in higher contents in the mango peel of the cultivar Xiao Tainong compared to other varieties [Abbasi *et al.*, 2017]. It has also been reported that the Keitt mango peel had a significantly higher total phenolic content than the Kent and Osteen varieties; mainly due to the presence of galloyl glucose, 5-galloylquinic acid, digalloylquinic acid, hexagalloyl glucose, and galloyl glucoside [Alañón *et al.*, 2021a]. Moreover, it was reported that green mango peels had about 45% higher content of phenolics than ripe mango. This trend has been associated with the mango ripening process because physiological, biochemical, and molecular changes develop, inducing the degradation, synthesis, or accumulation of phenolic compounds [Alañón *et al.*, 2021b; Hu *et al.*, 2018].

Nowadays, phenolics from natural sources are attracting increased attention for their bioactivities. For that reason, many studies have focused on improving extraction techniques and characterization of phenolic profiles. Due to the vast diversity of phenolic compounds, no common global strategy has been developed to carry out their extraction and identification. They differ in physical and chemical properties, and above all in solubility, which is why the efficiency of their extraction process depends mainly on the solvents and techniques used. Moreover, the source from which they are obtained determines the extraction process since phenolic compounds can interact with other components of the matrix and, as mentioned above, can be present in the tissues in free or bound form [Abbasi *et al.*, 2017; Alañón *et al.*, 2021a; Pacheco-Ordaz *et al.*, 2018a]. Hence, the need arises to develop the optimum and appropriate methods for their proper extraction and purification. Essential factors for optimal extraction, such as pH, time, and temperature, have been considered [Ballesteros-Vivas *et al.*, 2019a; Castañeda-Valbuena *et al.*, 2021; Martínez-Ramos *et al.*, 2020]. However, the most important aspect is the solvent type used (Table 1). The solvents used so far in the case of mango by-products included ethanol (50, 80, 96, and 100%, *v/v*) [Azhar *et al.*, 2019; Buelvas-Puello *et al.*, 2021; Gómez-Maldonado *et al.*, 2020], methanol (50 and 100%, *v/v*) [Castro-Vargas *et al.*, 2019; Hoyos-Arbeláez *et al.*, 2018], ethyl acetate [Ballesteros-Vivas *et al.*, 2019a; Torres-León *et al.*, 2021], and hexane [Martínez-Ramos *et al.*, 2020; Torres-León *et al.*, 2021].

Numerous phenolic compounds have been identified and characterized through different approaches. For instance, Ballesteros-Vivas *et al.* [2019a] identified xanthones, phenolic acids, flavonoids, and gallotannins in mango seed kernels. Different contents of mangiferin were determined, depending on the solvent type and extraction method used, *i.e.*: 13.27 mg/g when absolute ethanol and pressurized liquid were applied; 13.60 and 12.34 mg/g when kernels were macerated in 50% (*v/v*) and absolute ethanol, respectively. In turn, Martínez-Ramos *et al.* [2020] reported that the ethanol-to-acetone ratio of the extraction mixture affected the extraction efficiency of phenolic compounds from mango peel residues during conventional and ultrasound-assisted processes. Furthermore, they showed that the composition of solvent mixtures and ultrasonic power influenced the solvent-solute interaction. On the other hand, Castañeda-Valbuena *et al.* [2021] established that variations in the solvent-solid ratio and solvent concentration used to obtain mango peel and seed extracts influenced their antioxidant capacity evaluated by different methods (DPPH, ABTS, and FRAP assays). The conventional and new alternative techniques deployed so far for the extraction of phenolic compounds from residues mango include: maceration [Ballesteros-Vivas *et al.*, 2019a; Borrás-Enríquez *et al.*, 2021; Safdar *et al.*, 2017], agitation [El-Kady *et al.*, 2017; Martínez-Ramos *et al.*, 2020], Soxhlet and solvent extraction

Table 1. Phenolic compounds identified in mango by-products.

Class/ Subclass	Compound	Content			Extraction solvent	Analytical method	References
		Peel	Seed kernel	Unit (based on DW)			
Phenolic acids/Hydroxybenzoic acids and derivatives	Gallic acid	2.30-25.62	2.52-26.08	mg/100 g	80% MeOH	HPLC-DAD--ESI-QTOF--MS	Alañón *et al.* [2021a, b]; Gómez-Caravaca *et al.* [2016]
		28.60-43.10	nd		70% Ace	HPLC-UV/Vis	Marcillo-Parra *et al.* [2021]
	p-Hydroxybenzoic acid	nd	0.54	mg/g	80% EtOH	HPLC	Gómez-Maldonado *et al.* [2020]
	p-Hydroxybenzoic acid glucoside	0.64-17.24	6.06-11.01	mg/100 g	80% MeOH	HPLC-DAD--ESI-QTOF--MS	Alañón *et al.* [2021a, b]; Gómez-Caravaca *et al.* [2016]; López-Cobo *et al.* [2017]
	p-Hydroxybenzoic acid glucoside isomer I	6.34-16.66	nd	µg/100 g			López-Cobo *et al.* [2017]
	p-Hydroxybenzoic acid isomer I	968.36-2186.12	835.62-2186.12				
	p-Hydroxybenzoic acid isomer II	173.97-982.15	729.36-982.15				
	p-Hydroxybenzoic acid isomer III	nd	259.42-846.12				
	Dihydroxybenzoic acid glucoside	0.30-3	1.13-4.53	mg/100 g			Alañón *et al.* [2021a, b]
	Protocatechuic acid	158.44-434.24	295.82-479.05	µg/100 g			López-Cobo *et al.* [2017]
	Syringic acid	7.47-24.09	25.44-54.47	mg/100 g			Gómez-Caravaca *et al.* [2016]; López-Cobo *et al.* [2017]
	Vanillic acid	nd	21.6	mg/100 g	80% EtOH	HPLC	El-Kady *et al.* [2017]
		30.47-48.21	nd	µg/100 g	80% MeOH	HPLC-DAD--ESI-QTOF--MS	López-Cobo *et al.* [2017]
	Vanillic acid glucoside	11.6-62.69	6.75-16.86	mg/100 g			Alañón *et al.* [2021a, b]; López-Cobo *et al.* [2017]
	Ethyl 2,4-dihydroxy-3-(3,4,5--trihydroxybenzoyl)oxybenzoate	7.17	6.29				Gómez-Caravaca *et al.* [2016]
	Ellagic acid	nd	2613	mg/100 g	80% EtOH	HPLC	El-Kady *et al.* [2017]
		0.40-1.30	6.66-614.89		80% MeOH	HPLC-DAD--ESI-QTOF--MS	Alañón *et al.* [2021a, b]; Gómez-Caravaca *et al.* [2016]
Phenolic acids/Hydroxycinnamic acids and derivatives	Caffeic acid	nd	2.04	mg/g	80% EtOH	HPLC	Gómez-Maldonado *et al.* [2020]
	Chlorogenic acid	42.07	nd	µg/g	50% MeOH		Safdar *et al.* [2017]
	Chlorogenic acid	nd	8.50	mg/100 g	80% MeOH		Abdel-Aty *et al.* [2018]
	p-Coumaric acid	nd	12.50				
	trans-p-Coumaric acid	107.88-1081.61	107.88-155.55	µg/100 g	80% MeOH	HPLC-DAD--ESI-QTOF--MS	Alañón *et al.* [2021a, b]; López-Cobo *et al.* [2017]
	cis-p-Coumaric acid	752.87-861.14	nd				
	p-Coumaric acid glucoside	0.30-11.58	1.51	mg/100 g			
	Ferulic acid	80.58-382.81	341.11-382.81	µg/100 g			López-Cobo *et al.* [2017]
	Ferulic acid hexoside	1.20-2.10	nd	mg/100 g			Alañón *et al.* [2021a, b]
	Sinapic acid	nd	17.63		80% EtOH	HPLC	El-Kady *et al.* [2017]
	Sinapic acid hexoside	0.80-1.10	nd	mg/100 g	80% MeOH	HPLC-DAD--ESI-QTOF--MS	Alañón *et al.* [2021a, b]; Gómez-Caravaca *et al.* [2016]; López-Cobo *et al.* [2017]
	Sinapic acid hexoside-pentoside	10.40-50.99	nd				
	Dihydro sinapic acid hexoside--pentoside	4.80-62.59	nd				

Table 1. Continued.

Class/ Subclass	Compound	Content			Extraction solvent	Analytical method	References
		Peel	Seed kernel	Unit (based on DW)			
Flavonoids/ Flavanones	Eriodictyol	nd	2.98-5.35	mg/100 g	80% MeOH	HPLC-DAD--ESI-QTOF--MS	López-Cobo *et al.* [2017]
	Hesperidin	nd	3000			HPLC	Abdel-Aty *et al.* [2018]
Flavonoids/ Flavanols	Catechin	0.03-0.25	nd	mg/100 g	80% Ace	HPLC	Abbasi *et al.* [2017]
		88.50	nd	µg/g	50% EtOH		Safdar *et al.* [2017]
		6.37-27.87	3.57-25.37	mg/100 g	80% MeOH	HPLC-DAD--ESI-QTOF--MS	Alañón *et al.* [2021a, b]; Gómez-Caravaca *et al.* [2016]
	Epicatechin	9.01-9.24	nd	mg/100 g	70% Ace	HPLC-UV/ Vis	Marcillo-Parra *et al.* [2021]
Flavonoids/ Flavonols	Fisetin	1.86-17.49	nd	mg/100 g	80% Ace	HPLC	Abbasi *et al.* [2017]
	Kaempferol	nd	4		80% EtOH		El-Kady *et al.* [2017]
	Kaempferol	31.73	nd	µg/g	50% EtOH		Safdar *et al.* [2017]
	Myricetin	7.05	nd				
	Myricetin	nd	4.92	mg/g	80% EtOH		Gómez-Maldonado *et al.* [2020]
	Quercetin	35.20	nd	µg/g	50% MeOH		Safdar *et al.* [2017]
		nd	3.87	mg/g	80% EtOH		Gómez-Maldonado *et al.* [2020]
		2.05-3.32	nd	mg/100 g	70% Ace	HPLC-UV/ Vis	Marcillo-Parra *et al.* [2021]
	Quercetin arabinofuranoside	4.19-19.41	nd	mg/100 g	80% MeOH	HPLC-DAD--ESI-QTOF--MS	Alañón *et al.* [2021a, b]; Gómez-Caravaca *et al.* [2016]; López-Cobo *et al.* [2017]
	Quercetin hexoside	1.43	nd	g/kg	50% EtOH	HPLC-DAD	De Ancos *et al.* [2018]
	Quercetin pentoside	1.72	nd				
	Quercetin glucoside	19.50-188.69	1.02-2.26	mg/100 g	80% MeOH	HPLC-DAD--ESI-QTOF--MS	Alañón *et al.* [2021a, b]; López-Cobo *et al.* [2017]
	Quercetin galactoside	10.90-120.17	0.18				
	Quercetin pentoside	1.72	nd				
	Quercetin xyloside	2.70-39.18	nd				
	Rhamnetin hexoside	5.22-28.03	nd				López-Cobo *et al.* [2017]
	Rutin	98.43	nd	µg/g	50% MeOH	HPLC	Safdar *et al.* [2017]
		nd	2.95	mg/g	80% EtOH		Gómez-Maldonado *et al.* [2020]
		26.60-46.50	nd	mg/100 g	70% Ace	HPLC-UV/ Vis	Marcillo-Parra *et al.* [2021]
	Apigenin	nd	0.53	mg/g	80% EtOH	HPLC	Gómez-Maldonado *et al.* [2020]
Flavonoids/ Anthocyanins	Cyanidin 3-*O*-β-D--galactopyranoside	0.138-1.108	nd	mg/100 g	80% MeOH	HPLC-DAD--ESI-QTOF--MS	López-Cobo *et al.* [2017]
	7-*O*-Methylcyanidin 3-*O*-β-D--galactopyranoside	0.58-3.63	nd				
	Petunidin rutinoside-(*p*--coumaric acid) gallate	0.38-0.59	0.37-0.46				

Table 1. Continued.

Class/ Subclass	Compound	Content			Extraction solvent	Analytical method	References
		Peel	Seed kernel	Unit (based on DW)			
Gallotannins and gallic acid derivatives	Tannic acid	nd	987	mg/100 g	80% MeOH	HPLC	Abdel-Aty et al. [2018]
	Coumaroyl galloyl glucoside	2.34-19.50	nd			HPLC-DAD--ESI-QTOF--MS	Alañón *et al.* [2021a, b]; Gómez-Caravaca *et al.* [2016]; López-Cobo *et al.* [2017]
	Coumaroyl galloyl glucoside isomer I	4.35- 4.43	nd				López-Cobo *et al.* [2017]
	Coumaroyl galloyl glucoside pentoside	0.80-2.24	nd				Alañón *et al.* [2021a]; López-Cobo *et al.* [2017]
	Coumaroyl galloyl glucoside pentoside isomer I	1.85-1.99	nd				López-Cobo *et al.* [2017]
	Galloyl glucoside	0.44-109.60	154-271				Alañón *et al.* [2021a, b]; López-Cobo *et al.* [2017]
	Galloyl glucoside isomer I	59.88-372.97	63.10-101.36	mg/100 g	80% MeOH	HPLC-DAD--ESI-QTOF--MS	López-Cobo *et al.* [2017]
	Galloyl glucoside isomer II	7.56-14.13	nd				
	Galloyl glucoside isomer III	3.09-5.03	nd				
	Galloyl glucoside isomer IV	2.53-4.09	nd				
	Galloylglucose isomer V	1.80-3.78	nd				
	Galloyl glucose isomer VI	18.91-29.64	nd				
	Galloyl diglucoside	3.80-51.81	2.54-11.28				Alañón *et al.* [2021a, b]
	Galloyl diglucoside isomer II	1.90-3.90	nd				López-Cobo *et al.* [2017]
	Galloyl diglucoside isomer III	8-16	1.43-5.19				
	Galloyl diglucoside isomer IV	28.67-63.26	6.33-13.44	mg/100 g	80% MeOH	HPLC-DAD--ESI-QTOF--MS	Gómez-Caravaca *et al.* [2016]; López-Cobo *et al.* [2017]
	3-Galloylquinic acid	1-3	1.95-2.78				Alañón *et al.* [2021a, b]
	5-Galloylquinic acid	0.20-200.20	3.57-84.46				Alañón *et al.* [2021a, b]; López-Cobo *et al.* [2017]
	7-*O*-Galloyltricetiflavan	0.10-2.80	4.90-13.99				Alañón *et al.* [2021a, b]; Gómez-Caravaca *et al.* [2016]
	Digallic acid	0.70-10.83	1.04-3.64				Alañón *et al.* [2021a, b]; Gómez-Caravaca *et al.* [2016]
	m-Digallic acid methyl ester	2.68	nd	g/kg	50% EtOH	HPLC-DAD	De Ancos *et al.* [2018]
	Digalloyl glucose	20.10-47.28	0.70-4.23	mg/100 g	80% MeOH	HPLC-DAD--ESI-QTOF--MS	Alañón *et al.* [2021a, b]; Gómez-Caravaca *et al.* [2016]
	Digalloyl glucose isomer I	0.63-3.21	nd				López-Cobo *et al.* [2017]
	Digalloylquinic acid	0.50-74.20	1.11				Alañón *et al.* [2021a, b]
	3,5-Digalloylquinic acid	2.69	nd				López-Cobo *et al.* [2017]
	5-(Digalloyl)quinic acid	0.34-10.12	nd				
	Ethyl 2,4-dihydroxy-3-(3,4,5--trihydroxybenzoyl) oxy)--benzoate	7.17	5.85-11.30				
	Trigalloyl glucose	6.1-17.70	0.44-3.15				Alañón *et al.* [2021a, b]; Gómez-Caravaca *et al.* [2016]

Table 1. Continued.

Class/ Subclass	Compound	Content			Extraction solvent	Analytical method	References
		Peel	Seed kernel	Unit (based on DW)			
Gallotannins and gallic acid derivatives	Trigalloyl glucose isomer I	1.22-1.53	nd	mg/100 g	80% MeOH	HPLC-DAD--ESI-QTOF--MS	López-Cobo *et al.* [2017]
	Tetragalloyl glucose	3.4-11.6	23.21-68.98				Alañón *et al.* [2021a, b]
	Tetragalloyl glucose isomer I	1.87-4.71	1.04-3.52				López-Cobo *et al.* [2017]
	Tetragalloyl glucose isomer II	4.54-6.37	2.14-6.78				
	Tetragalloyl glucose isomer III	1.12-2.37	0.46-0.67				
	Pentagalloyl glucose	24.02-36.63	92.60-207.41				
	Hexagalloylglucose	21.03-73.10	61.67-172.99				Alañón *et al.* [2021a, b]; Gómez-Caravaca *et al.* [2016]
	Hexagalloylglucose isomer I	17.44-73.81	10.00-46.56				López-Cobo *et al.* [2017]
	Hexagalloylglucose isomer II	11.74-36.26	7.98-29.91				
	Hexagalloylglucose isomer III	3.33-27.70	0.98-15.54				
	Hexagalloylglucose isomer IV	0.46-4.60	0.54-10.25				
	Heptagalloyl glucose	35.10-57.8	6.15				Alañón *et al.* [2021a, b]
	Heptagalloylglucose isomer III	3.71-35.04	nd				López-Cobo *et al.* [2017]
	Heptagalloylglucose isomer IV	7.35-48.18	0.59-2.32				
	Heptagalloylglucose isomer V	7.80-44.86	2.03-5.24				
	Heptagalloylglucose isomer VI	5.27-28.43	0.05-1.03				
	Heptagalloylglucose isomer VII	4.56-23.33	0.02-0.51				
	Heptagalloylglucose isomer VIII	1.38-7.38	nd				
	Hydroxybenzoyl galloyl glucoside	0.58-2.22	nd				
	Ethyl gallate	1.38	nd	g/kg	50% EtOH	HPLC-DAD	De Ancos *et al.* [2018]
	Methyl gallate	51.10-167.60	94.43-558.86	mg/100 g	80% MeOH	HPLC-DAD--ESI-QTOF--MS	Alañón *et al.* [2021a, b]; López-Cobo *et al.* [2017];
	Methyl digallate ester	46.73-66.55	19.61-47.65				López-Cobo *et al.* [2017]
Benzophenones	Iriflophenone glucoside	nd	0.61-10.89	mg/100 g	80% MeOH	HPLC-DAD--ESI-QTOF--MS	Alañón *et al.* [2021b]; López-Cobo *et al.* [2017]
	Maclurin *C*-glucoside	nd	4.38-11.40				Alañón *et al.* [2021b]; Gómez-Caravaca *et al.* [2016]
	Maclurin *C*-glucoside isomer I	1.05-3.64	4.17-11.77				Gómez-Caravaca *et al.* [2016]; López-Cobo *et al.* [2017]
	Maclurin-3-*C*-β-D-glucoside	0.42	nd	g/kg	50% EtOH	HPLC-DAD	De Ancos *et al.* [2018]
	Maclurin-3-*C*-(2-*O*-galloyl)- β-D--glucoside	1.59	nd				
	Maclurin-3-*C*-(2,3-di-*O*-galloyl)--β-D-glucoside	1.33	nd				
	Maclurin-3-*C*-(6'-*p*--hydroxybenzoyl glucoside	1.21	nd				
	Maclurin galloyl glucoside	2.36-4.73	0.07-9.63	mg/100 g	80% MeOH	HPLC-DAD--ESI-QTOF--MS	Alañón *et al.* [2021a, b]; Gómez-Caravaca *et al.* [2016]; López-Cobo *et al.* [2017]
	Maclurin digalloyl glucoside	0.30-1.89	0.47-6.21				

Table 1. Continued.

Class/ Subclass	Compound	Content			Extraction solvent	Analytical method	References
		Peel	Seed kernel	Unit (based on DW)			
Xanthones	Lupeol	0.05-0.30	nd	mg/100 g	EtOH-Ace (7:3, *v/v*)	HPTLC	Jyotshna *et al.* [2015]
	Mangiferin	4.14-29.78	22.48-148.12	mg/100 g	80% MeOH	HPLC-DAD--ESI-QTOF--MS	Alañón *et al.* [2021a, b]; Gómez-Caravaca *et al.* [2016]; López-Cobo *et al.* [2017]
	Mangiferin-6´-*O*-gallate	1.57	nd	g/kg	50% EtOH	HPLC-DAD	De Ancos *et al.* [2018]
	Mangiferin-3-*C*-(2,3-di-*O*-galloyl)--β-D-glucoside	1.44	nd				
	Isomangiferin-6´-*O*-gallate	1.34	nd				
	Methoxylmangiferin	nd	2.24 - 4.43	mg/100 g	80% MeOH	HPLC-DAD--ESI-QTOF--MS	López-Cobo *et al.* [2017]
Lignans	Pentadecenylresorcinol	3.87-16.50	0.53-0.96	µg/g	DCM	GC-QTOF--MS	López-Cobo *et al.* [2017]
	Pentadecylresorcinol	56.58-110.76	0.84-2.96				
	Heptadecadienylresorcinol	224.77-602.26	0.84-2.96				
	Heptadecenylresorcinol	271.40-873.99	3.29-14.32				
	Heptadecylresorcinol	116.9	nd				
	Nonadecenylresorcinol	4.92-44.61	1.14-7.74				
Others	Pyrogallol	nd	1337.66	mg/100 g	80% EtOH	HPLC	El-Kady *et al.* [2017]
	Catechol	nd	202				

DW, dry weight; EtOH, ethanol; MeOH, methanol; Ace, acetone; DCM, dichloromethane; nd, not detected; HPLC, high-performance liquid chromatography; HPLC-DAD, HPLC with a diode-array detector; HPLC-UV/Vis, HPLC with UV-vis detection; HPLC-DAD-ESI-QTOF-MS, HPLC-DAD coupled to electrospray ionisation-quadrupole-time-of-flight mass spectrometry (ESI-QTOF--MS); HPTLC, high-performance thin layer chromatography; GC-QTOF-MS, gas chromatography with quadrupole-time-of-flight mass spectrometry.

[Buelvas-Puello *et al.*, 2021; Castro-Vargas *et al.*, 2019; Torres--León *et al.*, 2021], solid-liquid extraction, ultrasound-assisted extraction [Borrás-Enríquez *et al.*, 2021; Castañeda-Valbuena *et al.*, 2021; Lopez-Martinez *et al.*, 2022], microwave-assisted extraction [Martínez-Ramos *et al.*, 2020; Sánchez-Camargo *et al.*, 2021; Torres-León *et al.*, 2017], extraction assisted by fermentation [Torres-León *et al.*, 2021], high hydrostatic pressure [Cádiz-Gurrea *et al.*, 2020; Sánchez-Camargo *et al.*, 2021], extraction with supercritical fluids [Ballesteros-Vivas *et al.*, 2019b; Buelvas-Puello *et al.*, 2021; Sánchez-Camargo *et al.*, 2019], and extraction with pressurized fluids [Santana *et al.*, 2019].

Recent trends in the valorization of agro-industrial wastes are focused on minimizing the environmental impact through the circular economy model. In this context, green techniques are essential to reduce the adverse effects on human health and the environment. Thereby, using green solvents in phenolic extraction provides more environmentally friendly and sustainable processes [Cádiz-Gurrea *et al.*, 2020; Oliver-Simancas *et al.*, 2021]. Ballesteros-Vivas *et al.* [2019a] proposed the integrated approach of green extraction, based upon sequential pressurized liquid extraction (PLE) to obtain fractions rich in bioactive compounds. The extraction of bioactive components with high antioxidant and antiproliferative capacity from residues of the mango seeds was optimized; the most efficient proved to be the mixture of ethanol/ethyl acetate (50:50, *v/v*) at 25°C and 1.01 bar, based on Hansen's solubility parameters (HSP). PLE is an alternative technology to reduce environmental pollution generated by standard extraction methods. This technique allows for higher extraction yields of bioactive compounds with lower solvent consumption and shorter extraction time [Cádiz--Gurrea *et al.*, 2020].

Regarding the identification and quantification (Table 1) of the phenolic compounds of mango residues, various methods based on liquid chromatography (HPLC, UPLC) with detection by UV-Vis detector or DAD were used [Buelvas-Puello *et al.*, 2021; Lopez-Martinez *et al.*, 2022; Sánchez-Camargo *et al.*, 2019]. The techniques combining liquid chromatography with mass spectrometry were also often applied: RP-HPLC-ESI-MS [Torres-León *et al.*, 2017, 2021], HPLC-DAD-MS [Hernández-Maldonado *et al.*, 2019], HPLC-DAD-ESI-QTOF-MS [Alañón *et al.*, 2021a, b; Gómez-Caravaca *et al.*, 2016; López--Cobo *et al.*, 2017], [UPLC-DAD-ESI-MS [Navarro *et al.*, 2019], UPLC-ESI-QTOF-MS [Anaya-Loyola *et al.*, 2020; Hu *et al.*, 2018], and LC-QTOF-MS/MS [Ballesteros-Vivas *et al.*, 2019a; Sánchez--Camargo *et al.*, 2021]. Other chromatographic techniques successfully used to identify mango bioactive compounds were HPTLC [Jyotshna *et al.*, 2015] and GC-QTOF-MS [López--Cobo *et al.*, 2017].

Mango agro-industrial wastes contain xanthonoids in the *C*-glucoside form, such as mangiferin. This polyphenol and some of its derivatives, such as methoxymangiferin and isomangiferin, have been detected in the peel and kernel residues [Alañón *et al.*, 2021a, b; Anaya-Loyola *et al.*, 2020; Marcillo-Parra *et al.*, 2021]. Mangiferin has been reported to possess numerous beneficial properties, such as antioxidant, anti-inflammatory, antiviral, antiparasitic, and antimicrobial activities [Anaya-Loyola *et al.*, 2020; Hernández-Maldonado *et al.*, 2019; Vazquez-Olivo *et al.*, 2019]. Mango residues also contain gallic acid, its numerous derivatives and gallotannins. Gallotannins are hydrolysable tannins with a structure of polymeric chains of gallic acid esterified with glucose. Gallotannins and their derivatives represent 20–28% of the total phenolic content in the mango peel. Overall, they are recognized as mango nutraceutical components for their pharmacological effects and functional properties [Alañón *et al.*, 2021a]. Interestingly, the gallotannins identified in the mango seed kernels were considered as an indicator of the degree of maturation among multiple mango varieties [Alañón *et al.*, 2021b; Torres-León *et al.*, 2021]. Yet, another study with residues of the Ataulfo variety identified 47 phenolic compounds by UPLC-ESI-QTOF MS [Anaya-Loyola *et al.*, 2020]. Of these, 35 were detected in the extractable fraction and 12 in the fraction after acid hydrolysis. The extractable fraction contained gallotannins, such as heptagalloyl hexose, hexagalloyl hexose, pentagalloyl hexose, tetragalloyl hexose, and some gallic acid derivatives (gallic acid hexoside, gallic acid dihexoside, and galloylquinic acid). In contrast, the fraction obtained after hydrolysis contained 59% of ellagic acid and 22.4% of gallic acid, and other phenolics, like rhamnetin, syringic acid, and vanillic acid.

Mango peel

Among the mango peel phenolic compounds identified, worthy of special attention are mangiferin, gallic acid, quercetin, hydrolysable tannins, syringic acid, ferulic acid, and protocatechuic acid [Anaya-Loyola *et al.*, 2020; Borrás-Enríquez *et al.*, 2021; Pacheco-Ordaz *et al.*, 2018a; Soria-Lara *et al.*, 2020]. A study conducted by Tan *et al.* [2020] identified 651 secondary metabolites in the peel of two mango varieties by the metabolome approach, of which 257 corresponded to phenolic compounds, including numerous anthocyanin proanthocyanidins, and hydrolysable tannins, as well as gallocatechin, gallocatechin gallate, epicatechin, epicatechin gallate epicatechin 3-*O*-gallate, protocatechuic aldehyde, 3,4-dihydroxybenzoic acid, and ellagic acid. Navarro *et al.* [2019] also detected various gallotannins with different degrees of polymerization, including monogalloyl hexose up to undecagalloyl hexose. A comparative study of the total phenolic content of the mango different tissues demonstrated the peels from fruits with commercial maturity had a higher content (59.75 mg gallic acid equivalent (GAE)/g) than the pulp (10.73 mg GAE/g). More than 100 phenolic compounds (free and bound) were found in the peel, including phenolic acids, benzophenones, flavonoids, and gallotannins (mono/digalloyl) [Alañón *et al.*, 2021a]. Monogalloyl derivatives represented around 34–37% of phenolics, with galloyl glucose prevailing. Regarding gallates, the digalloyl derivatives accounted for 16–29%, with high contents of digalloyl glucose, digalloylquinic acid, digallic acid, and the digallic acid methyl ester. The flavonoid fraction (10–19%) included flavonols (quercetin and its glycosides with glucosyl, galactosyl, xylosyl, arabinopyrosyl, and arabinofurosyl moieties) and flavanols (catechin and 7-*O*-galloyltricetyl flavane). Phenolic acids, like vanillic, *p*-hydroxybenzoic, ellagic, *p*-coumaric, sinapic, and ferulic acid, were also found, accounting for 5–10% of the peel phenolics [Alañón *et al.*, 2021a]. Benzophenones, including maclurin, and their derivatives have been also identified in the peel with maclurin galloyl glucoside being the most abundant. Among xanthones, mangiferin has been found to be one of the major compounds in mango peel and recognized currently as one of the strongest antioxidants [Hernández-Maldonado *et al.*, 2019; Marcillo-Parra *et al.*, 2021; Navarro *et al.*, 2019; Vazquez-Olivo *et al.*, 2019].

Mango seed kernel

Mango seed is constituted by kernel or embryo (45–75%), the shell of fibrous endocarp (29%), and seed coat (3%) (Figure 1). Although the mango seed generates a large mass of waste products, little progress has been made on the valorization of these by-products since the only recycling strategy has focused on converting waste into animal feeds. Notwithstanding, these residues are a good source of bioactive compounds. Therefore, using this waste appropriately could generate bio-products with added value [Ballesteros-Vivas *et al.*, 2019a; Borrás-Enríquez *et al.*, 2021; Mutua *et al.*, 2017].

The total phenolic content of mango kernel is 28 times higher (78–80.5 mg GAE/g) than that of the pulp (2.1–4.2 mg GAE/g). Moreover, contents of some individual phenolics, as gallic acid and its derivatives, in mango kernels are higher than in other fruits' seeds, such as longan (*Dimocarpus longan* Lour.) seed [Alañón *et al.*, 2021b]. Phenolic acids (gallic, ellagic, protocatechuic, ferulic, caffeic, coumaric, cinnamic, vanillic, and 4-caffeylquinic acid), flavonoids (rhamnetin-3-(6'-2-butenoil-hexoside), quercetin, kaempferol, rutin, and anthocyanins), tannins and derivatives (ethyl galate and penta-*O*-galloyl glucoside), xanthones (mangiferin, isomangiferin, homomangiferin), and benzophenones were identified in the phenolic profile in several studies [Lebaka *et al.*, 2021; Mwaurah *et al.*, 2020; Torres-León *et al.*, 2017]. Therein, penta-*O*-galloyl glucoside is an important compound linked with antimicrobial, anti-inflammatory, antiproliferative, anticancer, antidiabetic, and antioxidant properties. Likewise, phenolics have been reported with bioactivity in breast, liver, leukemia, cervix, prostate, lung, and colon cancer cell lines [Ballesteros-Vivas *et al.*, 2019a; Castro-Vargas *et al.*, 2019; Kim *et al.*, 2018; Torres-León *et al.*, 2021]. Hesperidin and compounds with monogalloyl moiety (galloyl glucose, galloyl diglucose, 5-galloylquinic acid, 3-galloylquinic acid, methyl galate, and ethyl gallate) have also been detected in high contents [Abdel-Aty *et al.*, 2018; Alañón *et al.*, 2021b; Ballesteros-Vivas *et al.*, 2019a]. Derivatives of digallic acid (from gallic acid esterification), including digallic acid, digalloyl glucose, digallic acid methyl ester and digallic quinic acid have

been detected as well [Alañón *et al.*, 2021a, b; Gómez-Caravaca *et al.*, 2016].

In the mango seed kernel, various flavan-3-ols have been found, like catechin, epicatechin, and epicatechin gallate. Quercetin and quercetin glucoside have been identified in lesser amounts [Ballesteros-Vivas *et al.*, 2019a; Gómez-Maldonado *et al.*, 2020]. On the other hand, Alañón *et al.* [2021b] found high contents of maclurin *C*-glucoside, digalloylmaclurin glucoside, mangiferin, 5-galloylquinic acid, and trigalloyl glucose in the Keitt cultivar seed, and mainly hexa- and hepta-gallotannins in the Osteen variety. In the same research, iriflophenone glucoside was identified, being a characteristic benzophenone from the kernel, since it has not been found either in peel or pulp [Alañón *et al.*, 2021b; Gómez-Caravaca *et al.*, 2016; López-Cobo *et al.*, 2017]. Detection of xanthones in the seed kernel is strongly linked to the presence of mangiferin being the major compound [Ballesteros-Vivas *et al.*, 2019a; Lim *et al.*, 2019; Torres-León *et al.*, 2021]. Nonetheless, xanthones with other structures beside mangiferin which is *C*-glycoside, have been identified including mangiferin gallate and 3-*O*-methyl mangiferin (homomangiferin) [Ballesteros-Vivas *et al.*, 2019a].

Roles of phenolic compounds from mango wastes in human health promotion and disease prevention

Phenolic compounds exhibit a wide range of bioactivities exerting beneficial effects on health, such as anti-allergenic, hypolipidemic, antidiabetic, antiatherogenic, anti-inflammatory, anti-microbial, antiviral, immunomodulatory, antiproliferative, anticarcinogenic, antioxidant, anti-thrombotic, cardioprotective, and vasodilatory effects, as shown in Table 2. In this context, some mechanisms of their action in preventing or reducing the risk of various chronic diseases have been discovered [Abbasi *et al.*, 2017; Alañón *et al.*, 2021a, b; Kim *et al.*, 2018; Lin *et al.*, 2020].

Antidiabetic effects

Diabetes mellitus is one of the major metabolic diseases characterized by hyperglycemia resulting from insufficient insulin production or diminished tissue responses to insulin. In addition, cardiovascular diseases, renal failure, blindness, neurological problems, colon cancer, and others have been linked with diabetes. Hence, research about the suppression of diabetic complications is very significant. In this sense, several efforts have been made in scientific research to elucidate possible mechanisms of action of phytochemicals, such as phenolic compounds [Azhar *et al.*, 2019; Fernández-Ochoa *et al.*, 2020; Rodríguez-González *et al.*, 2017]. For instance, Rodríguez-González *et al.* [2017] evaluated antidiabetic properties of the mango by-product, which is peel and remnant pulp. A reduction in serum glucose in diabetic rats fed mango by-product was observed, which was not associated with either intestinal absorption of glucose or protection of the islets of Langerhans. In addition, polyphenol- and carotenoid-rich extracts caused an insulin-mimetic effect on 3T3-L1 adipocyte cells and reduced the concentration of triglycerides in the serum. Likewise, diabetic nephropathy was improved by the antioxidant activity at the renal level. This antidiabetic effect was associated with the high soluble fiber content and the presence of phenolic compounds, such as ellagic acid, gallic acid, quercetin, and epicatechin gallate. In another study, consumption of mango pulp for six weeks had a beneficial effect on lean and obese individuals [Fang *et al.*, 2018]. The effects were linked to lowering blood pressure in lean individuals and reducing levels of proinflammatory cytokines (IL-8 and MCP-1) and cardiometabolic risk biomarkers (PAI-1 and HbA1c) in obese individuals. Thereby, mango consumption reduces the risk of developing chronic obesity-related diseases, mainly by metabolite bioactivities, such as gallotannin derivatives that modulate inflammation and metabolic functions. Other phytochemicals from mango fruits and their by-products have also been linked with antidiabetic effects. In particular, mangiferin has been reported to promote glucose uptake at the cellular level through glucose transporter 4 (GLUT4) expression. It has also been linked to glycolipid metabolism enhancement, gluconeogenesis inhibition in the liver, and reduction of glucose production, blood glucose levels, and liver injury [Azhar *et al.*, 2019; Fernández-Ochoa *et al.*, 2020; Lin *et al.*, 2020; Rodríguez-González *et al.*, 2017; Soria-Lara *et al.*, 2020]. Nonetheless, mangiferin derivatives or isomers could exhibit different mechanisms of action to promote health effects. For example, Lin *et al.* [2020] evaluated the effects of oral administration of mangiferin and its derivative called mangiferin calcium salt (MCS). Here, MCS exhibited better efficiency compared to mangiferin not only in the absorption process but also in the therapeutic effect in rats with type 2 diabetes and NAFLD by regulating glucose and lipid metabolism.

Mango seed kernels have also been reported to exert antidiabetic effects (in addition to their anti-tyrosinase, anti-inflammatory, anti-obesity, and hepatoprotective activities) [Abdel-Aty *et al.*, 2018]. For example, a study by Azhar *et al.* [2019] disclosed a hypoglycemic effect in diabetic rats administrated 200 mg/kg of the ethanolic extract of the mango seed. There was an increase in insulin production in the pancreas and a decrease in the level of glycosylated hemoglobin (HbA1c). These effects were attributed to flavonoids and phenolic acids contained in the mango seed.

Antimicrobial effects

The phenolic compounds of mango seed have shown antifungal and antibacterial effects against Gram-positive bacteria [Asif *et al.*, 2016; Gómez-Maldonado *et al.*, 2020; Mutua *et al.*, 2017]. In addition, some studies have demonstrated antimicrobial activity of gallotannins and their metabolites. For instance, gallic acid inhibited the growth of such pathogens as *Clostridium perfringens* that induces diseases, like *e.g.* colitis [Hernández-Maldonado *et al.*, 2019; Kim *et al.*, 2018]. In this setting, Manila mango kernel extract with phenolics has shown antimicrobial activity against *Colletotrichum brevisporum* [Gómez-Maldonado *et al.*, 2020]. This *in vitro* study revealed that the extract (3 g/L) caused 100% inhibition of mycelial growth after 9 days and 0% spore germination after 20 h. Thereby, this evidence exposes the potential application of the mango kernel extract with phenolics as an antimicrobial agent [Gómez-Maldonado *et al.*, 2020].

Table 2. Biactivities of mango by-product extracts.

Bioactivity	Extract	Mango structure	Model	Assay	Results	Reference
Antidiabetic activity	Methanol extract	Peel	*In vivo*	Male Wistar rats	Mango-supplemented diet exerted a significant antioxidant effect in the liver of diabetic rats, likely due to its phenolic compounds, like mangiferin.	Fernández--Ochoa *et al.* [2020]
	Aqueous extract	Seed kernel	*In vivo*	Pancreatic lipase inhibition activity (Wistar strain male albino rats)	Significant reduction in body weights, fat pad weights and organ weights of treated animals was found. Elevated levels of glucose, insulin, leptin and lipid profiles were normalized upon treatment with the extract. Antioxidant status was also brought back to normal upon treatment. Pronounced anti-obesity activity was demonstrated and this effect may be due the pancreatic lipase inhibitory activity.	Kumaraswamy *et al.* [2020]
Antioxidant activity	Ethyl acetate extracts	Peel and seed kernel	*In vitro*	DPPH radical scavenging activity, ferric ion reducing power (FRAP), ABTS radical cation scavenging activity, and nitric oxide radical (NO) scavenging activity.	Mango peel extracts and seed kernel extracts exhibited better radical scavenging activity compared to pulp extracts.	Kuganesan *et al.* [2017]
	Water and ethanol extracts	Peel	*In vitro*	ABTS radical cation scavenging activity and DPPH radical scavenging activity.	Extracts had high total phenolic content and possessed the high DPPH radical and ABTS radical cation scavenging activities which may be attributed to the high contents of *p*-hydroxybenzoic acid, gallic acid, and pyrogallol.	Huang *et al.* [2018]
Antibacterial activity	Water and ethanol extracts	Peel	*In vitro*	Standard method of diffusion disc plates on agar.	The extracts exhibited antibacterial activities against the five bacteria tested. The Gram-negative bacteria (*Escherichia coli* ATCC 11775, *Salmonella typhimurium* ATCC 13311, and *Vibrio parahaemolyticus* ATCC 17802) were more sensitive than the Gram-positive ones (*Staphylococcus aureus* ATCC 12600 and *Bacillus cereus* ATCC 14579).	Huang *et al.* [2018]
	Aqueous extracts	Seed	*In vitro*	Minimum inhibitory concentration (MIC) method and ROS assay.	Gold nanoparticles with aqueous extract efficiently inhibited the growth of *Escherichia coli* and *Staphylococcus aureus*.	Vimalraj *et al.* [2018]
Anti-inflammatory activity	Ethyl acetate extracts	Peel and seed kernels	*In vitro*	Human Red Blood Cell (HRBC) membrane stabilization assay.	The peel and seed kernel extracts showed significantly different inhibition of hemolysis, ranging from (IC_{50}) 151 g/mL to 197 µg/mL and from 128 to 248 µg/mL, respectively.	Kuganesan *et al.* [2017]
	Water and ethanol extracts	Peel	*In vitro*	Nitrite oxide in culture media (Murine macrophage cell lines RAW 264.7).	The results indicate that compressional--puffed ethanol extracthad apparent anti-infammatory activity, and thus it may have potential as a natural and safe agent in the protection of human health by modulating the immune system.	Huang *et al.* [2018]
Antiproliferative and anticancer activity	Ethanolic extracts	Peel	*In vitro*	Colorimetric assay based on the metabolic use of 3-(4,5-dimethylthiazol-2--yl)-2,5-diphenyltetrazo-lium bromide (MTT) by viable cells (HT29, Caco-2, and HCT116 colon cancer cells).	Already after 24 h extract treatment, viability of all the analyzed colon cancer cells was reduced in a dose-dependent manner. The effect started at 180 µg/mL of extract, and at 600 µg/mL concentration the evaluated residual viability amounted to 46%, 35%, and 44% in HT29, Caco-2, and in HCT116 cells, respectively. This effect further increased by prolonging the incubation time of cells in the presence of MPE, reaching the maximum at 48 h of treatment with 360 µg/mL dose.	Lauricella *et al.* [2019]

Table 2. Continued.

Bioactivity	Extract	Mango structure	Model	Assay	Results	Reference
Antiproliferative and anticancer activity	Aqueous extracts	Seed	*In vivo*	Chorioallantoic membrane model (CAM) angiogenesis assay.	The result suggests that the gold nanoparticles with aqueous extract inhibited the angiogenic process by down regulating Ang-1/Tie2 pathway.	Vimalraj *et al.* [2018]
	Aqueous extracts	Seed	*In vitro*	Human gastric cancer cell.	Biocompatibility assessment indicated the non-toxic nature of gold nanoparticles with extract towards mesenchymal stem cells at 25 µg/mL and suppressed the growth of human gastric cancer cells.	Vimalraj *et al.* [2018]

Antioxidant effects

Mangoes are endowed with considerable antioxidant properties because of their phenolic compounds, such as gallic acid, galloyl derivatives, flavonol glycosides, and benzophenones [Fang *et al.*, 2018; Kim *et al.*, 2017]. Notably, antioxidant activity of mango phytochemicals has been implicated in treating chronic diseases, such as diabetes, hypertension, and dyslipidemia [Mutua *et al.*, 2017; Torres-León *et al.*, 2021]. However, both phenolic content and antioxidant capacity in mango seem to differ across plant cultivars, fruit maturity stages, and fruit parts [Hoyos-Arbeláez *et al.*, 2018]. Interestingly, higher antioxidant capacity has been reported in the mango peel than in the peels of other fruits [Sáyago-Ayerdi *et al.*, 2019]. Nonetheless, the mango kernel has the highest antioxidant activity owing to gallic acid, a compound with high radical scavenging activity [Hoyos-Arbeláez *et al.*, 2018] that was found in higher content in kernel residues from the seed compared to the peel [Alañón *et al.*, 2021a, b; Ballesteros-Vivas *et al.*, 2019a; Torres-León *et al.*, 2021].

Several studies have evaluated the antioxidant activity of different fruit constituents, finding exciting results. For example, Abassi *et al.* [2017] evaluated cellular antioxidant activity (CAA) of various mango cultivars. They found a higher activity of peel residues than mango pulp, which contained a large content of flavonoids. Another cultivar, Xiao Tainong, with high CAA (2,986 µmol quercetin equivalent (QE)/100 g FW), has been found with compounds such as fisteine and mangiferin. Velderrain-Rodríguez *et al.* [2018] evaluated the antioxidant activity of three fractions of a phenolic extract from mango peel (free, acid, and alkaline fraction). The alkaline and acid fractions presented higher antioxidant capacity (DPPH/FRAP/ORAC assays) mainly attributed to the presence of free gallic acid. Recent studies have revealed that seed extracts of a "Haden" mango obtained by ultrasound-assisted extraction had a remarkable antioxidant capacity measured by DPPH, ABTS, and FRAP assays, and it was higer than that of peels. It has also been observed that changes in such variables as solvent concentration and solvent:solid ratio impact the phenolic content and affected the antioxidant capacity evaluated by different methods [Castañeda-Valbuena *et al.*, 2021]. El-Kady *et al.* [2017] analyzed antioxidant activity of ethanolic extracts of seed kernel in which 20 phenolic compounds were identified and found a higher DPPH radical scavenging activity (96.86%) compared to synthetic antioxidants like – butylated hydroxytoluene (BHT) (94.9%) and ascorbic acid (91.5%). Moreover, Castro-Vargas *et al.* [2019] reported a 57% reduction in lipid oxidation and a 75% growth of human cancer cell lines by the antioxidant effects exerted by the phenolic extracts of mango residues, such as seed kernel. The antioxidant effect of mangiferin and other phenolic compounds from mango seed kernels has also been reported [Ballesteros-Vivas *et al.*, 2019a].

Immunomodulation: anti-inflammatory effects

The phenolic compounds of fruits and vegetables are considered natural anti-inflammatory substances that inhibit the activation of nuclear factor κB (NF-κB). For example, anti-inflammatory activity of mango phenolics has been reported which consisted in inhibiting inducible nitric oxide synthase (iNOS), cyclooxygenase-2 (COX-2), and the tumor necrosis factor-α (TNF-α) *in vitro* and *in vivo* [Kim *et al.*, 2017]. In this study, a significantly reduced simple clinical colitis activity index (SCCAI) was observed upon a daily intake (200-400 g) of mango pulp for eight weeks. In addition, reduced plasma levels of pro-inflammatory cytokines were detected, such as interleukin-8 (IL-8) (16.2%), growth-regulated oncogene (GRO) (25%), and granulocyte-macrophage colony-stimulating factor (GM-CSF) (28.6%) [Kim *et al.*, 2020].

High methyl gallate content has been found in the kernel of the mango seed [Alañón *et al.*, 2021b; Torres-León *et al.*, 2021]. Previous studies have evidenced the anti-inflammatory activity of methyl gallate on inflammatory bowel disease [Anzoise *et al.*, 2018]. For example, Anzoise *et al.* [2018] reported that methyl gallate reduced intestinal motility, decreasing peristalsis by 74.5% (dose 100 mg/kg) and 58.82% (dose 300 mg/kg), with a greater effect observed for the 100 mg/kg dose applied in a colitis model to observe the effect on inflammatory bowel disease. Likewise, a decrease in inflammatory mediators (COX-2), cytokines such as interleukin-6 (IL-6), TNF-α, and the severity of microscopic tissue damage induced by acetic acid was detected. In this same sense, pyrogallol, a metabolite produced by the microbial decarboxylation of the gallic acid present in mango, has been reported to exert anti-inflammatory activities in breast cancer and obese patients [Fang *et al.*, 2018; Kim *et al.*, 2018]. Likewise, the anti-inflammatory effect of mango phenolic compounds has been reported in ulcerative colitis *in vitro* model [Kim *et al.*, 2017].

It is well known that phenolic compounds contribute to the modulation of the immune response by reducing

inflammatory bowel disorders [Anzoise *et al.*, 2018]. Some phytochemicals from mango residues have been linked to immunomodulatory activities. For instance, it has been noted that the consumption of mango juice by-products in children decreased the incidence of gastrointestinal and respiratory diseases, remarking the immunomodulatory properties by the modulation of immune-related proteins [Anaya-Loyola *et al.*, 2020]. In this context, mangiferin from mango agro-industrial wastes has also been demonstrated to possess immunomodulatory properties [Alañón *et al.*, 2021b; Lin *et al.*, 2020; Vazquez-Olivo *et al.*, 2019].

- Antiproliferative and anticancer effects

Phenolic compounds have demonstrated antiproliferative and chemopreventive effects through modulating the cell cycle, metastasis, angiogenesis, and apoptosis. In addition, they have also been shown that significantly inhibit colon carcinogenesis by reducing oxidative stress and activating Akt and NF-κB signaling intermediates [Ballesteros-Vivas *et al.*, 2019a; Castro-Vargas *et al.*, 2019; Kim *et al.*, 2017, 2018]. Several phenolic compounds of the mango peel and kernel belonging to phenolic acids, flavonoids, xanthones, benzophenones, gallotannins, and gallate derivatives have been linked to cancer prevention by antiproliferative effects on cell lines, such as leukemia, breast, lung, liver, cervix, prostate, and colon [Ballesteros-Vivas *et al.*, 2019a; Velderrain-Rodríguez *et al.*, 2018]. However, the biological activity of phenolics depends on their molecular structure. For example, the anticarcinogenic activity of gallotannins has been associated with the number of galloyl groups in the structure [Navarro *et al.*, 2019]. This activity could be associated with cytotoxicity mechanisms involving apoptosis induction through an increase in Bax/Bcl-2 protein levels, the arrest of the cell cycle in the S phase, and the inhibition of NF-κB activation, with the consequent downregulation of inflammatory cytokines [Navarro *et al.*, 2019].

The inhibition of metastasis and proliferation of hepatocellular carcinoma (HepG2) have been evaluated using mango peel residues, observing high EC_{50} values of 2.35 mg/mL [Abbasi *et al.*, 2017]. Velderrain-Rodríguez *et al.* [2018] also assessed the antiproliferative and the pro-apoptotic effect of mango peel extracts (free, acid, and alkaline fractions) against human colon adenocarcinoma cells (LS180) and mouse connective cells (L929). The three fractions were moderately effective against LS180 cells (IC_{50}=~137 µg/mL), primarily to the cytotoxic effect of quercetin. Both free and alkaline fractions inhibited the growth of normal L929 cells (IC_{50}=~197 and ~94 µg/mL, respectively). Gallic acid was the main antioxidant and responsible for the antiproliferative effect, followed by mangiferin, quercetin, and syringic acid. On the other hand, Sánchez-Camargo *et al.* [2021] evaluated the antiproliferative effect of the extract from mango peel containing gallic acid and some derivatives, such as galloyl esters, as well as mangiferin, gallate derivatives, quercetin, and quercetin glycosides. The results showed a high antioxidant capacity and a relevant antiproliferative activity against the human colon adenocarcinoma cell line (HT-29) after 24 h of treatment (IC_{50}=22.98 µg/mL). In turn, Kim *et al.* [2018] have noted that gallic acid and pyrogallol from mango reduced cell proliferation by 37 and 78% in an *in vitro* model with HT-29 colon cancer cells. Also ellagic acid and ethyl gallate have been identified, which have been shown to exhibit anticancer capacity on cancer cell lines, as HTC116 and Caco-2, by the induction of apoptosis [Ballesteros-Vivas *et al.*, 2019a].

The development of different techniques for the extraction, fractionation, and purification of phenolic compounds from the mango seed kernel has made it possible to evaluate their antiproliferative activity against the human tumor cell lines. For instance, Ballesteros-Vivas *et al.* [2019b] noted a significant potentiating effect on the inhibition of cell proliferation (70.51%) in the colon cell line HT-29 using an enriched phenolic extract obtained by the supercritical antisolvent fractionation (SAF) approach. Another study carried out by Castro-Vargas *et al.* [2019] evaluated the antiproliferative effect of a methanolic extract obtained by the traditional method from mango kernel in human cancer cell lines, such as MDA-MB-231 (breast), PC-3 (prostate), A-549 (lung), and HT-29 (colon). Surprisingly, a 75% decrease in the viability of HT-29, MDA-MB-231, and PC-3 cells was also observed.

POTENTIAL PREBIOTIC EFFECT AND ITS RELATIONSHIP WITH GUT HEALTH

Few investigations have highlighted mango residues as a potential novel source of prebiotics. Herein, we discuss the beneficial effects of phenolic compounds from mango residues on modulating the gut microbiota [Anaya-Loyola *et al.*, 2020; Anzoise *et al.*, 2018; Hernández-Maldonado *et al.*, 2019; Kim *et al.*, 2018]. Several studies have shown that the consumption of mango and by-products helps prevent gastrointestinal diseases and other related. In this context, mechanisms of action of the phenolic compounds associated with modulation of inflammation and prevention of colon cancer correlate with the gut microbiota's functional composition [Anzoise *et al.*, 2018; Hernández-Maldonado *et al.*, 2019; Kim *et al.*, 2018]. Therefore, dietary fiber and phenolics of mango residues can be considered prebiotics since both modulate the gut microbiome. In addition, the International Scientific Association of Probiotics and Prebiotics (ISAPP) recently published that phenolic compounds from plants can meet prebiotic criteria. In this sense, the ISAPP defines a prebiotic as a substrate selectively used by the host microorganism, conferring a health benefit [Anaya-Loyola *et al.*, 2020; Hu *et al.*, 2018; Sáyago-Ayerdi *et al.*, 2019]. Currently, there is a plentitude of supporting evidence showing that mango and by-products consumption helps prevent gastrointestinal diseases. In this sense, it has been suggested that phytochemicals could play an essential role in the gut microbiota's modulation by both antimicrobial and prebiotic properties.

- **Bioaccessibility and bioavailability of phenolic compounds**

In the case of phenolic compounds, bioaccessibility refers to the phenolic fraction released from the food matrix during gastrointestinal phase digestion and made available for intestinal absorption. In contrast, bioavailability relates to the phenolic

fraction or its derivatives that reach the bloodstream by intestinal absorption and become available for body functions at the site of action [Blancas-Benitez *et al.*, 2015; Hernández-Maldonado *et al.*, 2019; Jamar *et al.*, 2017; Peanparkdee & Iwamoto, 2022]. Therefore, the biological contribution of phenolic compounds in the human body depends on numerous factors, such as the host condition, its gut microbiota, and the chemical and structural nature of the molecules. Firstly, the bioaccessibility and bioavailability of different phenolics vary depending on the individual's physical condition, including digestive/absorptive/metabolic/response capability and effective dose. After ingestion, the release of phenolic compounds begins with the cellular compartmentalization and enzymatic hydrolysis of salivary α-amylases. Then, in the gastric phase, they interact with endogenous enzymes influencing the digestibility of the components of the food matrix, such as starch (α-amylase), lipids (pancreatic lipase), and proteins (pepsin and trypsin) [Peanparkdee & Iwamoto, 2022; Wu *et al.*, 2017]. Then, multiple enzymes endowed with diverse metabolic capacities in the human gut microbiome contribute to the absorption of phenolics by their transformation or degradation [Bento-Silva *et al.*, 2020; Blancas-Benitez *et al.*, 2015; Hernández--Maldonado *et al.*, 2019; Jamar *et al.*, 2017; Pacheco-Ordaz *et al.*, 2018a; Vazquez-Olivo *et al.*, 2019; Velderrain-Rodríguez *et al.*, 2018]. However, it has been reported that up to 65% of anthocyanins present in the diet are not absorbed in the gastrointestinal tract [Tian *et al.*, 2019]. The phenolic compounds' absorption also depends on their molecular structure, composition (free form or interacting with another component), and the degree of polymerization, which influences their solubility, permeability, and molecular stability.

Many authors have focused on knowing the bioaccessibility and bioavailability of mango phenolic. For instance, Blancas--Benitez *et al.* [2015] determined the phenolic bioaccessibility in the mango peel using an *in vitro* digestion system. As a result, a relative bioaccessibility of 43.53% was found. The vanillic acid and hydroxycinnamic acids were accessible for absorption in the small intestine and available to exert beneficial health effects. Hernández-Maldonado *et al.* [2019] found that 54% of the phenolic compounds in a mango-based bar were absorbed during the gastrointestinal phase, while 46% were hydrolyzed in the colon. Both research results regarding low bioaccessibility could be associated with the instability of the compounds that tend to degrade during intestinal digestion, such as phenolic acids, catechin, quercetin, resveratrol, and rutin [Peanparkdee & Iwamoto, 2022; Tian *et al.*, 2019]. In this same sense, resistant compounds that reach the small intestine have also been observed. For example, Velderrain-Rodríguez *et al.* [2018] determined the absorption probability of phenolics from the Ataulfo mango peel in enterocytesin. They found a wide range of compounds with different relative absorption rates, such as *p*-coumaric and 2-hydroxycinnamic acid (89%), ferulic acid (86%), syringic acid (83%), protocatechuic acid (82%), gallic acid (75%), catechin (71%), quercetin (64%), ellagic acid (60%), mangiferin (40%), and rutin (16%). Herein, gallic acid and derivatives showed an absorption percentage higher than 57%, indicating better cell permeability. This result could potentially be associated with the antiproliferative effect reported for gallic acid. In addition, Pacheco-Ordaz *et al.* [2018a] evaluated the acid and alkaline hydrolysis of Ataulfo mango peel extracts using Caco-2 cell monolayers as a model for intestinal epithelial permeability. They reported gallic acid from an alkaline fraction presented an apparent permeability coefficient of 2.61×10^{-6} cm/s compared to the standard of 2.48×10^{-6} cm/s. Overall, the results suggest that most phenolic compounds (except for rutin) could be considered bioaccessible at the intestinal level; and some compounds could be even absorbed.

The conjugation of hydroxybenzoic acids limits bioaccessibility and bioavailability of some oligomers, such as gallotannins and ellagotannins formed from gallic acid and ellagic acid, respectively [Bento-Silva *et al.*, 2020; Velderrain-Rodríguez *et al.*, 2018]. Under gastrointestinal phase conditions, these compounds are hydrolyzed to simple molecules, like gallic acid [Anaya-Loyola *et al.*, 2020]. However, branched-chain tannins that are not absorbable in their native form can be hydrolyzed and decarboxylated by microbial enzymes. The resulting metabolites, such as gallic acid and pyrogallol, can be absorbed in the colon [Kim *et al.*, 2018]. In this same sense, mangiferin also is a compound with low absorption and little bioavailability compared to other phenolic components. Thereby, it should form complexes with other molecules to improve its solubility, food release, bioavailability, and other properties [Lin *et al.*, 2020; Velderrain-Rodríguez *et al.*, 2018]. However, compounds such as mangiferin gallate can undergo hydrolysis during gastric digestion, which leads to the mangiferin release [Hernández-Maldonado *et al.*, 2019]. On the contrary, hydroxycinnamic acids and kaempferol require intestinal enzymes for absorption. In this regard, chlorogenic acid is a compound with low intestinal absorption. However, its bioavailability depends also on the metabolism of the gut microbiota. It has even been reported that it promotes the modulation of the colonic microbiota through stimulating the growth of *Bifidobacterium spp.*, *Clostridium coccoides*, and *Eubacterium rectale* [Coman & Vodnar, 2020]. Therefore, these scientific works suggest that the mango wastes' phenolic compounds can be modified not only to enhance their intestinal absorption but also to achieve their profiles enhancing the gut microbiota.

Understanding the bioaccessibility and bioavailability of phenolic compounds is crucial to establishing a functional characterization. For that reason, many researchers have focused on deciphering these mechanisms through different approaches. For instance, a significant effect on the release of phenolic compounds during an *in vitro* gastrointestinal simulation was observed in a study using a mango product with high total soluble phenolic contents. Herein, gastric digestion showed a release rate of 9% higher than the intestinal phase [Hernández-Maldonado *et al.*, 2019]. These results could be associated with covalent interactions of the phenolic compounds with the polysaccharides of the cell wall [Hernández-Maldonado *et al.*, 2019; Wu *et al.*, 2017]. In addition, glycosidic bonds from polyphenols can be broken down by acid hydrolysis, causing the release of aglycones [Pacheco-Ordaz *et al.*, 2018a].

In the intestinal section, the release of phenolic compounds is affected by pH changes and enzymes activity (mainly pancreatin and α-amylase). Both factors weaken molecular interactions in the food matrix, promoting bond hydrolysis. Particularly, intestinal esterases hydrolyze ester bonds between carbohydrates linked to phenolic compounds and other cell wall components in plants, increasing the bioavailability of phenolic compounds. They may be then absorbed by the gastrointestinal barrier and get into blood circulation. Generally, phenolic compounds are not fully absorbed by their structural complexity, and around 90% of these compounds reach the colon where they are fermented by intestinal microorganisms. Here, about 2,671 microbial species exist, constituting the human gut microbiota [Lagier *et al.*, 2018; Ye *et al.*, 2022]. These microorganisms are genetically endowed with enzymes such as esterases, lipases, carbohydrates, and proteases. Among them, α-L-rhamnosidases, β-D-glucosidase, and β-D--glucuronidases allow the release, absorption, and production of metabolites, such as bioactive phenolic acids, including gallic acid, protocatechuic acid, syringic acid, and vanillic acid [Bento-Silva *et al.*, 2020; Coman & Vodnar, 2020; Hernández-Maldonado *et al.*, 2019; Jamar *et al.*, 2017; Pacheco-Ordaz *et al.*, 2018a; Tian *et al.*, 2019].

Interestingly, a recent study evaluated the phenolic compounds' bioaccessibility in a mango pulp and peel-based bar during gastrointestinal phase and after fermentation [Hernández-Maldonado *et al.*, 2019]. The results of this research identified not only phenolic acids (gallic, ferulic, coumaric, and caffeic acid) but also flavonoids and xanthones (quercetin, gallocatechin, mangiferin, and mangiferin gallate), reporting their 53.78% bioaccessibility. Likewise, products after fermentation were hydroxyphenolic acids and acetic acids as the primary short-chain fatty acids. In addition, norathyriol classified as xanthone (aglycone) was identified after 12 h of fermentation. Mango peel's total soluble phenolic bioaccessibility has been reported at 44%. Soluble and released by hydrolysis phenolics represent only 11.46% of the insoluble fiber content. Hence then, non-bioaccessible and released soluble phenolics can reach the colon and potentially be used as substrates by the colonic microbiota [Hernández-Maldonado *et al.*, 2019; Sáyago-Ayerdi *et al.*, 2019]. Thereby, the insoluble fiber composition can influence microbiota composition changes during the fermentation process.

The gut microbiota plays a critical function in the biotransformation of phytochemicals, modulating the phenolic compounds' bioavailability and promoting gut health [Bento-Silva *et al.*, 2020; Hernández-Maldonado *et al.*, 2019; Kim *et al.*, 2018]. Therefore, the consumption of probiotics, prebiotics (dietary fiber), and phenolic compounds is recommended for better gut health, considering that phenolic molecules have the same biological effect as prebiotics [Hernández-Maldonado *et al.*, 2019; Ye *et al.*, 2022].

Gut health and modulation of the gut microbiota

The intake of fruits and vegetables is closely related with gut health because their bioactive compounds exert beneficial effects, such as phenolic compounds that remain bioaccessible after the gastrointestinal phase in the non-digestible fraction [Hernández-Maldonado *et al.*, 2019; Kim *et al.*, 2020; Pacheco-Ordaz *et al.*, 2018a]. Hydroxycinnamic acids, gallotannins, and other compounds interacting with the fiber have been found therein [Hernández-Maldonado *et al.*, 2019; Sáyago-Ayerdi *et al.*, 2019; Velderrain-Rodríguez *et al.*, 2018]. Also flavonoids and xanthones associated with the insoluble fiber fraction have been identified in mango, including quercetin, kaempferol, and mangiferin. Notably, as shown by assays with the fecal microbiota, this flavonoid-xanthone fraction produces compounds that benefit gut health, such as hydroxyphenolic acids and other derivatives [Hernández-Maldonado *et al.*, 2019; Kim *et al.*, 2018].

Regarding gastrointestinal infectious diseases, dietary fiber intake has been shown to help mitigate disorders, including constipation and diarrhea associated with gut microbiota changes. In addition, dietary fiber is related to bioactive components such as phenolic compounds, which are bioaccessible once released in the digestive tract [Anaya-Loyola *et al.*, 2020; Hernández--Maldonado *et al.*, 2019]. Thereby, diarrhea reduction can be associated with the content of gallotannins, such as penta-, hexa- and heptagalloyl glucose, in mango residues, which inhibit the growth of pathogenic microorganisms, like *Campylobacter jejuni* involved in acute diarrhea [Anaya-Loyola *et al.*, 2020; Kim *et al.*, 2018; Vazquez-Olivo *et al.*, 2019].

In another study, a reduction in flatulence and abdominal inflammation was reported in children who consumed a beverage from mango juice residues (peel and pulp), which was constituted by dietary fiber with a high content of extractable polyphenols (mono- to heptagalloyl hexosides and mangiferin) and polyphenols released by hydrolysis [Anaya-Loyola *et al.*, 2020]. Methyl gallate has also been demonstrated to exert antidiarrheal, spasmolytic, anti-inflammatory, and antioxidant effects in preclinical models of intestinal inflammation [Anzoise *et al.*, 2018]. The cited authors also showed it reduced intestinal motility, decreasing peristalsis by 74.5% (100 mg/kg) and 58.82% (300 mg/kg), and observed a greater effect of the 100 mg/kg dose applied in a preclinical model with intestinal disorders.

Multiple factors are involved in the gut health, such as a balanced microbial composition, intestinal permeability, healthy epithelial barrier, and a vigorous colonic mucosa. Any disorder of these factors can cause oxidative stress and induce development of intestinal diseases, including obesity, inflammatory bowel disease, mucosal ulceration, ulcerative colitis, and Crohn's disease [Hernández-Maldonado *et al.*, 2019; Kim *et al.*, 2020; Ye *et al.*, 2022]. Particularly, inflammatory bowel disease is characterized by chronic inflammation and dysbiosis, which are the main factors for the development of gastrointestinal neoplasms or colon cancer. Worthy of mention is that 60% of stomach cancer and 43% of colon cancer are attributed to low consumption of vegetables [Anzoise *et al.*, 2018; Kim *et al.*, 2018; Navarro *et al.*, 2019; Vazquez-Olivo *et al.*, 2019].

The gut microbiota plays an important role in food digestion, immunity and other metabolic functions. The human intestinal microbial communities are defined by host genetics, intestinal dysbiosis, endogenous factors (antibiotics and xenobiotics

consumption), and other environmental factors. However, dietary components play a crucial role in regulating microbial profiles, mainly fiber and phenolic compounds [Bento-Silva *et al.*, 2020; Kim *et al.*, 2018]. From this perspective, phenolic compounds have become relevant for health since they can modify the gut microbiota, increasing the release of metabolites with more significant bioactivity [Hernández-Maldonado *et al.*, 2019; Kim *et al.*, 2018]. Moreover, phenolic molecules with a higher degree of polymerization, as gallotannins, have been linked with substantial anti-inflammatory and anticancer properties [Navarro *et al.*, 2019]. For example, Kim *et al.* [2020] demonstrated that gallotannins and gallic acid mitigated intestinal inflammation and carcinogenesis by intestinal microbiome modulation. Mangiferin has also been reported to improve intestinal inflammation in a murine model with induced colitis [Kim *et al.*, 2018; Vazquez-Olivo *et al.*, 2019]. On the other hand, Navarro *et al.* [2019] identified 71 compounds, including 32 gallates and gallotannins with different degrees of polymerization, 7 hydroxybenzophenone derivatives (maclurin and iriflophenone), 6 xanthonoids (isomangiferin derivatives and mangiferin), 11 phenolic acids, and 8 flavonoids (derived from rhamnetin and quercetin), when evaluating the cytotoxic effect of mango peel extracts on different human carcinoma cells related to the digestive tract, and concluded that gallotannins and xantonoids play an essential role in toxicity against cancer cells.

The mango's phenolic compounds and their derivatives have also been noted to participate in processes linked to immune system regulation by gut microbiota modulation. For instance, using a rat model with DSS-induced colitis, Kim *et al.* [2020] surveyed a mango polyphenol concentrate. They found significant changes in the profiles of bacteria belonging to the Firmicutes Phylum (*Lactobacillus plantarum*, *Lactococcus lactis*, and *Clostridium butyrium*). Consequently, the production of short-chain fatty acids (SCFAs) was induced as butyrate and valerate. It was also observed a suppression of HDAC1 activity and an increase of AMPK activity together with levels of autophagy biomarkers; thereby, the mango phenolic compounds intake could mitigate intestinal inflammation. In addition, other studies have demonstrated that quercetin can modify the gut microbiota, improving the *Bifidobacteria* growth and the ratio of Firmicutes decreasing to Bacteroidetes. Interestingly, by conducting an *in vitro* gut simulation to evaluate a mango by-product rich in polyphenols and dietary fiber, Sayago-Ayerdi *et al.* [2019] detected an increase in *Bifidobacterium* relative abundance at 24 h and increased microbial genera diversity at 72 h, including mainly *Lactobacillus*, *Dorea*, and *Lactococcus*. In this sense, through a human clinical study, Kim *et al.* [2018] showed that mango intake encouraged the growth of *Lactobacillus* genera (*L. plantarum*, *L. reuteri*, and *L. lactis*), promoting butyrate production. Furthermore, mango consumption mitigated intestinal inflammation by decreasing the production of pro-inflammatory cytokines.

APPLICATIONS OF AGRO-INDUSTRIAL WASTES

New research challenges have opened an approach to food applications of valuable waste products. In this context, functional foods or dietary supplements have been designed with mango by-products implemented as active ingredients [Alañón *et al.*, 2021a; Anaya-Loyola *et al.*, 2020; Ballesteros-Vivas *et al.*, 2019a; Oliver-Simancas *et al.*, 2021]. Currently, the trend of developing new products in various sectors of the food industry, such as chicken patties and meat sausages in the meat industry, as well as dairy-based drinks and cheeses in the dairy industry, that are based among others on industrial by-products has been increasing [Gupta *et al.*, 2022; Iuit-González *et al.*, 2019; Oliver-Simancas *et al.*, 2021]. Several products have been reported to be developed from mango wastes, such as macaroni, noodles, films, yogurt, beverages, and bakery food products, like snacks, bread, biscuits, cakes, and mango-based bars [Abbasi *et al.*, 2017; Hernández-Maldonado *et al.*, 2019; Marcillo-Parra *et al.*, 2021; Melo *et al.*, 2019]. Mango seed kernel has been deployed to develop biodegradable films, edible coatings for tomato [Nawab *et al.*, 2017] and peach [Torres-León *et al.*, 2018], as packaging in chili [Nawab *et al.*, 2018], and to prepare extruded and deep-fried pellets [Patiño-Rodríguez *et al.*, 2021]. It has been reported that phenolic compounds present in mango by-products preoved well as probiotic enhancers that can be applied in yogurts, cheeses, olives, sauerkraut and other functional foods [Pacheco-Ordaz *et al.*, 2018b; Tirado-Kulieva *et al.*, 2021]. Pérez-Chabela *et al.* [2022] evaluated the effect of mango peel as a functional ingredient in yogurt. They observed that physicochemical characteristics, such as titratable acidity and pH, were accepted by consumers. The addition of this mango by-product had an effect because it inhibited undesirable microorganisms and promoted the proliferation of lactic acid bacteria, indicating that it presents prebiotic capacity. On the other hand, Das *et al.* [2019] incorporated up to 40% of mango kernel flour in the formulation of cakes and compared them with those made with 100% wheat flour. They observed that mango kernel flour affected the nutritional composition of the cakes. In addition, Iuit-González *et al.* [2019] developed a jam based on mango peel, evaluating the incorporation of 20 and 30%, the latter being the most preferred by the panelists. They indicated that the mango jam complied with the specifications of the Mexican Official Standard No. NOM-130-SSA1-1995 [Norma Oficial Mexicana, 1997]. Mango by-products have also been used as vegetable oil stabilizers to prevent oxidation [El-Kady *et al.*, 2017, Sánchez-Camargo *et al.*, 2019]. Thereby the synthetic antioxidants linked to harmful health events, such as butylhydroxyl anisole and butylated hydroxytoluene, could be substituted with antioxidants from natural sources. Another significant finding on mango residues is their antimicrobial properties, which allow their application as antimicrobial agents to prevent food poisoning and infections caused by pathogenic microorganisms in the food industry [Mutua *et al.*, 2017].

Understanding the underlying mechanisms of bioactive components from mango wastes opens new pharmacotherapy treatment options to avoid side effects associated with chronic-degenerative diseases [Marcillo-Parra *et al.*, 2021]. On the other hand, phenolic extracts from mango residues have also been used in combined therapy with conventional drugs to treat gastrointestinal diseases due to their potential to reduce levels

of inflammatory biomarkers and modulate the gut microbiota [Hernández-Maldonado *et al.*, 2019; Kim *et al.*, 2020].

Overall, mango residues are a low-cost source of phenolic compounds applicable in the food, cosmetic, and pharmaceutical industries, allowing the increase in the valorization of these residues and the reduction of their environmental effects [Alañón *et al.*, 2021a; Borrás-Enríquez *et al.*, 2021; Castro-Vargas *et al.*, 2019; El-Kady *et al.*, 2017; Lin *et al.*, 2020; Marcillo-Parra *et al.*, 2021; Mutua *et al.*, 2017; Torres-León *et al.*, 2021].

CONCLUSION

Mango processing industries bring about a massive volume of residues causing environmental problems. Nonetheless, several phytochemicals in the peel and seed kernel of the mango have been linked to preventing several diseases, such as cancer, cardio-metabolic diseases, and gastrointestinal diseases. The molecules present in mango waste have been reported to be involved in the gut microbiota modulation showing a prebiotic effect and improving gut health. These therapeutic effects make the mango by-products viable bioactive ingredients for use in the design of functional and nutraceutical foods for health improvement.

ACKNOWLEDGEMENTS

This study was supported by the Cátedras COMECyT-EDOMEX program of the Consejo Mexiquense de Ciencia y Tecnología del Estado de México, Mexico provided to Mayra Nicolás García (CAT2021-0048).

RESERCH FUNDING

This study received no external funding.

CONFLICT OF INTERESTS

The authors of the manuscript declare that they have no conflict of interest.

ORCID IDs

A.J. Borrás-Enríquez https://orcid.org/0000-0003-2695-5289
O. de Jesús Calva-Cruz https://orcid.org/0000-0002-9360-8781
J.L. González-Escobar https://orcid.org/0000-0002-6548-5913
M. Nicolás-García https://orcid.org/0000-0003-0077-0219
V. Pérez-Pérez https://orcid.org/0000-0003-3442-6969
M. Sánchez-Becerril https://orcid.org/0000-0002-8076-2640

REFERENCES

1. Abbasi, A.M., Liu, F., Guo, X., Fu, X., Li, T., Liu, R.H. (2017). Phytochemical composition, cellular antioxidant capacity and antiproliferative activity in mango (*Mangifera indica* L.) pulp and peel. *International Journal of Food Science and Technology*, *52*(3), 817–826. https://doi.org/10.1111/ijfs.13341
2. Abdel-Aty, A.M., Salama, W.H., Hamed, M.B., Fahmy, A.S., Mohamed, S.A. (2018). Phenolic-antioxidant capacity of mango seed kernels: therapeutic effect against viper venoms. *Revista Brasileira de Farmacognosia*, *28*(5), 594–601. https://doi.org/10.1016/j.bjp.2018.06.008
3. Alañón, M.E., Pimentel-Moral, S., Arráez-Román, D., Segura-Carretero, A. (2021a). Profiling phenolic compounds in underutilized mango peel by-products from cultivars grown in Spanish subtropical climate over maturation course. *Food Research International*, *140*, art. no. 109852. https://doi.org/10.1016/j.foodres.2020.109852
4. Alañón, M.E., Pimentel-Moral, S., Arráez-Román, D., Segura-Carretero, A. (2021b). HPLC-DAD-Q-ToF-MS profiling of phenolic compounds from mango (*Mangifera indica* L.) seed kernel of different cultivars and maturation stages as a preliminary approach to determine functional and nutraceutical value. *Food Chemistry*, *337*, art. no. 127764. https://doi.org/10.1016/j.foodchem.2020.127764
5. Anaya-Loyola, M.A., García-Marín, G., García-Gutiérrez, D.G., Castaño-Tostado, E., Reynoso-Camacho, R., López-Ramos, J.E., Enciso-Moreno, J.A., Pérez-Ramírez, I.F. (2020). A mango (*Mangifera indica* L.) juice by-product reduces gastrointestinal and upper respiratory tract infection symptoms in children. *Food Research International*, *136*, art. no. 109492. https://doi.org/10.1016/j.foodres.2020.109492
6. Anzoise, M.L., Basso, A.R., Del Mauro, J.S., Carranza, A., Ordieres, G.L., Gorzalczany, S. (2018). Potential usefulness of methyl gallate in the treatment of experimental colitis. *Inflammopharmacology*, *26*(3), 839–849. https://doi.org/10.1007/s10787-017-0412-6
7. Asif, A., Farooq, U., Akram, K., Hayat, Z., Shafi, A., Sarfraz, F., Sidhu, M.A.I., Rehman, H.U., Aftab, S. (2016). Therapeutic potentials of bioactive compounds from mango fruit wastes. *Trends in Food Science and Technology*, *53*, 102–112. https://doi.org/10.1016/j.tifs.2016.05.004
8. Azhar, A., Aamir, K., Asad, F., Kazi, H.A., Farooqui, M.U. (2019). Therapeutic effect of mango seed extract in diabetes mellitus. *The Professional Medical Journal*, *26*(09), 1551–1556. https://doi.org/10.29309/TPMJ/2019.26.09.4023
9. Ballesteros-Vivas, D., Álvarez-Rivera, G., Morantes, S.J., Sánchez-Camargo, A.P., Ibáñez, E., Parada-Alfonso, F., Cifuentes, A. (2019a). An integrated approach for the valorization of mango seed kernel: Efficient extraction solvent selection, phytochemical profiling and antiproliferative activity assessment. *Food Research International*, *126*, art. no. 108616. https://doi.org/10.1016/j.foodres.2019.108616
10. Ballesteros-Vivas, D., Alvarez-Rivera, G., Ocampo, A.F.G., Morantes, S.J., Sánchez-Camargo, A.P., Cifuentes, A., Parada-Alfonso, F., Ibáñez, E. (2019b). Supercritical antisolvent fractionation as a tool for enhancing antiproliferative activity of mango seed kernel extracts against colon cancer cells. *The Journal of Supercritical Fluids*, *152*, art. no. 104563. https://doi.org/10.1016/j.supflu.2019.104563
11. Bento-Silva, A., Koistinen, V.M., Mena, P., Bronze, M.R., Hanhineva, K., Sahlstrøm, S., Kitrytė, V., Moco, S., Aura, A.-M. (2020). Factors affecting intake, metabolism and health benefits of phenolic acids: do we understand individual variability? *European Journal of Nutrition*, *59*(4), 1275–1293. https://doi.org/10.1007/s00394-019-01987-6
12. Blancas-Benitez, F.J., Mercado-Mercado, G., Quirós-Sauceda, A.E., Montalvo-González, E., González-Aguilar, G.A., Sáyago-Ayerdi, S.G. (2015). Bioaccessibility of polyphenols associated with dietary fiber and *in vitro* kinetics release of polyphenols in Mexican 'Ataulfo' mango (*Mangifera indica* L.) by-products. *Food and Function*, *6*(3), 859–868. https://doi.org/10.1039/C4FO00982G
13. Borrás-Enríquez, A.J., Reyes-Ventura, E., Villanueva-Rodríguez, S.J., Moreno-Vilet, L. (2021). Effect of ultrasound-assisted extraction parameters on total polyphenols and its antioxidant activity from mango residues (*Mangifera indica* L. var. *Manililla*). *Separations*, *8*(7), art. no. 94. https://doi.org/10.3390/separations8070094
14. Buelvas-Puello, L.M., Franco-Arnedo, G., Martínez-Correa, H.A., Ballesteros-Vivas, D., Sánchez-Camargo, A.P., Miranda-Lasprilla, D., Narváez-Cuenca, C.-E., Parada-Alfonso, F. (2021). Supercritical fluid extraction of phenolic compounds from mango (*Mangifera indica* L.) seed kernels and their application as an antioxidant in an edible oil. *Molecules*, *26*(24), art. no. 7516. https://doi.org/10.3390/molecules26247516
15. Cádiz-Gurrea, M.L., Villegas-Aguilar, M.C., Leyva-Jiménez, F.J., Pimentel-Moral, S., Fernández-Ochoa, Á., Alañón, M.E., Segura-Carretero, A. (2020). Revalorization of bioactive compounds from tropical fruit by-products and industrial applications by means of sustainable approaches. *Food Research International*, *138*, art. no. 109786. https://doi.org/10.1016/j.foodres.2020.109786
16. Castañeda-Valbuena, D., Ayora-Talavera, T., Luján-Hidalgo, C., Álvarez-Gutiérrez, P., Martínez-Galero, N., Meza-Gordillo, R. (2021). Ultrasound extraction conditions effect on antioxidant capacity of mango by-product extracts. *Food and Bioproducts Processing*, *127*, 212–224. https://doi.org/10.1016/j.fbp.2021.03.002
17. Castro-Vargas, H.I., Ballesteros Vivas, D., Ortega Barbosa, J., Morantes Medina, S.J., Aristizabal Gutiérrez, F., Parada-Alfonso, F. (2019). Bioactive phenolic compounds from the agroindustrial waste of Colombian mango cultivars 'sugar mango' and 'Tommy Atkins'—An alternative for their use and valorization. *Antioxidants*, *8*(2), art. no. 41. https://doi.org/10.3390/antiox8020041
18. Coman, V., Vodnar, D.C. (2020). Hydroxycinnamic acids and human health: Recent advances. *Journal of the Science of Food and Agriculture*, *100*(2), 483–499. https://doi.org/10.1002/jsfa.10010
19. Das, P.C., Khan, M.J., Rahman, M.S., Majumder, S., Islam, M.N. (2019). Comparison of the physico-chemical and functional properties of mango kernel flour with wheat flour and development of mango kernel flour based composite cakes. *NFS Journal*, *17*, 1–7. https://doi.org/10.1016/j.nfs.2019.10.001

20. De Ancos, B., Sánchez-Moreno, C., Zacarías, L., Rodrigo, M.J., Ayerdí, S.S., Benítez, F.J.B., Domínguez-Avila, J.A., González-Aguilar, G.A. (2018). Effects of two different drying methods (freeze-drying and hot air-drying) on the phenolic and carotenoid profile of 'Ataulfo' mango by-products. *Journal of Food Measurement and Characterization*, *12*(3), 2145–2157. https://doi.org/10.1007/s11694-018-9830-4
21. Ediriweera, M.K., Tennekoon, K.H., Samarakoon, S.R. (2017). A review on ethnopharmacological applications, pharmacological activities, and bioactive compounds of *Mangifera indica* (Mango). *Evidence-Based Complementary and Alternative Medicine*, *2017*, art. no. 6949835. https://doi.org/10.1155/2017/6949835
22. El-Kady, T.M.A., El-Rahman, M.K.A., Toliba, A.O., Abo El-maty, S.M. (2017). Evaluation of mango seed kernel extract as natural occurring phenolic rich antioxidant compound. *Bulletin of the National Nutrition Institute of the Arab Republic of Egypt*, *48*(1), 1–30. https://doi.org/10.21608/bnni.2017.4239
23. Fang, C., Kim, H., Barnes, R.C., Talcott, S.T., Mertens-Talcott, S.U. (2018). Obesity-associated diseases biomarkers are differently modulated in lean and obese individuals and inversely correlated to plasma polyphenolic metabolites after 6 weeks of mango (*Mangifera indica* L.) consumption. *Molecular Nutrition and Food Research*, *62*(14), art. no. 1800129. https://doi.org/10.1002/mnfr.201800129
24. FAO (2020). *Major tropical fruits – Preliminary market results 2019*. Food and Agriculture Organization of the United Nations, Rome, Italy.
25. Fernández-Ochoa, Á., Cázares-Camacho, R., Borrás-Linares, I., Domínguez-Avila, J.A., Segura-Carretero, A., González-Aguilar, G.A. (2020). Evaluation of metabolic changes in liver and serum of streptozotocin-induced diabetic rats after Mango diet supplementation. *Journal of Functional Foods*, *64*, art. no. 103695. https://doi.org/10.1016/j.jff.2019.103695
26. Gómez-Caravaca, A.M., López-Cobo, A., Verardo, V., Segura-Carretero, A., Fernández-Gutiérrez, A. (2016). HPLC-DAD-q-TOF-MS as a powerful platform for the determination of phenolic and other polar compounds in the edible part of mango and its by-products (peel, seed, and seed husk). *Electrophoresis*, *37*(7–8), 1072–1084. https://doi.org/10.1002/elps.201500439
27. Gómez-Maldonado, D., Lobato-Calleros, C., Aguirre-Mandujano, E., Leyva-Mir, S.G., Robles-Yerena, L., Vernon-Carter, E.J. (2020). Antifungal activity of mango kernel polyphenols on mango fruit infected by anthracnose. *LWT – Food Science and Technology*, *126*, art. no. 109337. https://doi.org/10.1016/j.lwt.2020.109337
28. Gupta, A.K., Gurjar, P.S., Beer, K., Pongener, A., Ravi, S.C., Singh, S., Verma, A., Singh, A., Thakur, M., Tripathy, S., Verma, D.K. (2022). A review on valorization of different byproducts of mango (*Mangifera indica* L.) for functional food and human health. *Food Bioscience*, *48*, art. no. 101783. https://doi.org/10.1016/j.fbio.2022.101783
29. Hernández-Maldonado, L.M., Blancas-Benítez, F.J., Zamora-Gasga, V.M., Cárdenas-Castro, A.P., Tovar, J., Sáyago-Ayerdi, S.G. (2019). *In vitro* gastrointestinal digestion and colonic fermentation of high dietary fiber and antioxidant-rich mango (*Mangifera indica* L.) "Ataulfo"-based fruit bars. *Nutrients*, *11*(7), art. no. 1564. https://doi.org/10.3390/nu11071564
30. Hoyos-Arbeláez, J., Blandón-Naranjo, L., Vázquez, M., Contreras-Calderón, J. (2018). Antioxidant capacity of mango fruit (*Mangifera indica*). An electrochemical study as an approach to the spectrophotometric methods. *Food Chemistry*, *266*, 435–440. https://doi.org/10.1016/j.foodchem.2018.06.044
31. Hu, K., Dars, A.G., Liu, Q., Xie, B., Sun, Z. (2018). Phytochemical profiling of the ripening of Chinese mango (*Mangifera indica* L.) cultivars by real-time monitoring using UPLC-ESI-QTOF-MS and its potential benefits as prebiotic ingredients. *Food Chemistry*, *256*, 171–180. https://doi.org/10.1016/j.foodchem.2018.02.014
32. Huang, C.-Y., Kuo, C.-H., Wu, C.-H., Kuan, A.-W., Guo, H.-R., Lin, Y.-H., Wang, P.-K. (2018). Free radical-scavenging, anti-inflammatory, and antibacterial activities of water and ethanol extracts prepared from compressional-puffing pretreated mango (*Mangifera indica* L.) peels. *Journal of Food Quality*, *2018*, art. no. 1025387. https://doi.org/10.1155/2018/1025387
33. Iuit-González, M., Betancur-Ancona, D., Santos-Flores, J., Cantón-Castillo, C.G. (2019). Marmalade enriched with dietary fiber from Mango (*Mangifera indica* L.) peel. *Revista Tecnología en Marcha*, *32*(1), 193–201 (in Spanish, English abstract). https://doi.org/10.18845/tm.v32i1.4128
34. Jamar, G., Estadella, D., Pisani, L.P. (2017). Contribution of anthocyanin-rich foods in obesity control through gut microbiota interactions. *BioFactors*, *43*(4), 507–516. https://doi.org/10.1002/biof.1365
35. Jyotshna, Srivastava, P., Killadi, B., Shanker, K. (2015). Uni-dimensional double development HPTLC-densitometry method for simultaneous analysis of mangiferin and lupeol content in mango (*Mangifera indica*) pulp and peel during storage. *Food Chemistry*, *176*, 91–98. https://doi.org/10.1016/j.foodchem.2014.12.034
36. Kim, H., Banerjee, N., Barnes, R.C., Pfent, C.M., Talcott, S.T., Dashwood, R.H., Mertens-Talcott, S.U. (2017). Mango polyphenolics reduce inflammation in intestinal colitis—involvement of the miR-126/PI3K/AKT/mTOR axis *in vitro* and *in vivo*. *Molecular Carcinogenesis*, *56*(1), 197–207. https://doi.org/10.1002/mc.22484
37. Kim, H., Krenek, K.A., Fang, C., Minamoto, Y., Markel, M.E., Suchodolski, J.S., Talcott, S.T., Mertens-Talcott, S.U. (2018). Polyphenolic derivatives from mango (*Mangifera Indica* L.) modulate fecal microbiome, short-chain fatty acids production and the HDAC1/AMPK/LC3 axis in rats with DSS-induced colitis. *Journal of Functional Foods*, *48*, 243–251. https://doi.org/10.1016/j.jff.2018.07.011
38. Kim, H., Venancio, V.P., Fang, C., Dupont, A.W., Talcott, S.T., Mertens-Talcott, S.U. (2020). Mango (*Mangifera indica* L.) polyphenols reduce IL-8, GRO, and GM-SCF plasma levels and increase *Lactobacillus* species in a pilot study in patients with inflammatory bowel disease. *Nutrition Research*, *75*, 85–94. https://doi.org/10.1016/j.nutres.2020.01.002
39. Kuganesan, A., Thiripuranathar, G., Navaratne, A.N., Paranagama, P.A. (2017). Antioxidant and anti-inflammatory activities of peels, pulps and seed kernels of three common mango (*Mangifera indical* L.) varieties in Sri Lanka. *International Journal of Pharmaceutical Sciences and Research*, *8*(1), 70–78. https://doi.org/10.13040/IJPSR.0975-8232.8(1).70-78
40. Kumaraswamy, A., Gurunagarajan, S., Pemiah, B. (2020). Scientific evaluation of anti-obesity potential of aqueous seed kernel extract of *Mangifera indica* Linn. in high fat diet induced obese rats. *Obesity Medicine*, *19*, art. no. 100264. https://doi.org/10.1016/j.obmed.2020.100264
41. Lagier, J.-C., Dubourg, G., Million, M., Cadoret, F., Bilen, M., Fenollar, F., Levasseur, A., Rolain, J.-M., Fournier, P.-E., Raoult, D. (2018). Culturing the human microbiota and culturomics. *Nature Reviews Microbiology*, *16*(9), 540–550. https://doi.org/10.1038/s41579-018-0041-0
42. Lauricella, M., Lo Galbo, V., Cernigliaro, C., Maggio, A., Palumbo Piccionello, A., Calvaruso, G., Carlisi, D., Emanuele, S., Giuliano, M., D'Anneo, A. (2019). The anti-cancer effect of *Mangifera indica* L. peel extract is associated to γH2AX-mediated apoptosis in colon cancer cells. *Antioxidants*, *8*(10), art. no. 422. https://doi.org/10.3390/antiox8100422
43. Lebaka, V.R., Wee, Y.-J., Ye, W., Korivi, M. (2021). Nutritional composition and bioactive compounds in three different parts of mango fruit. *International Journal of Environmental Research and Public Health*, *18*(2), art. no. 741. https://doi.org/10.3390/ijerph18020741
44. Lim, K.J.A., Cabajar, A.A., Lobarbio, C.F.Y., Taboada, E.B., Lacks, D.J. (2019). Extraction of bioactive compounds from mango (*Mangifera indica* L. var. Carabao) seed kernel with ethanol–water binary solvent systems. *Journal of Food Science and Technology*, *56*(5), 2536–2544. https://doi.org/10.1007/s13197-019-03732-7
45. Lin, H., Teng, H., Wu, W., Li, Y., Lv, G., Huang, X., Yan, W. Lin, Z. (2020). Pharmacokinetic and metabolomic analyses of mangiferin calcium salt in rat models of type 2 diabetes and non-alcoholic fatty liver disease. *BMC Pharmacology and Toxicology*, *21*(1), 1–12. https://doi.org/10.1186/s40360-020-00438-x
46. López-Cobo, A., Verardo, V., Diaz-de-Cerio, E., Segura-Carretero, A., Fernández-Gutiérrez, A., Gómez-Caravaca, A.M. (2017). Use of HPLC- and GC-QTOF to determine hydrophilic and lipophilic phenols in mango fruit (*Mangifera indica* L.) and its by-products. *Food Research International*, *100*(3), 423–434. https://doi.org/10.1016/j.foodres.2017.02.008
47. Lopez-Martinez, L.X., Campos-Gonzalez, N., Zamora-Gasga, V.M., Domínguez-Avila, J.A., Pareek, S., Villegas-Ochoa, M.A., Sáyago-Ayerdi, S.G., González-Aguilar, G.A. (2022). Optimization of ultrasound treatment of beverage from mango and carrot with added turmeric using response surface methodology. *Polish Journal of Food and Nutrition Sciences*, *72*(3), 287–296. https://doi.org/10.31883/pjfns/152432
48. Marcillo-Parra, V., Anaguano, M., Molina, M., Tupuna-Yerovi, D.S., Ruales, J. (2021). Characterization and quantification of bioactive compounds and antioxidant activity in three different varieties of mango (*Mangifera indica* L.) peel from the Ecuadorian region using HPLC-UV/VIS and UPLC-PDA. *NFS Journal*, *23*, 1–7. https://doi.org/10.1016/j.nfs.2021.02.001
49. Martínez-Ramos, T., Benedito-Fort, J., Watson, N.J., Ruiz-López, I.I., Che-Galicia, G., Corona-Jiménez, E. (2020). Effect of solvent composition and its interaction with ultrasonic energy on the ultrasound-assisted extraction of phenolic compounds from Mango peels (*Mangifera indica* L.). *Food and Bioproducts Processing*, *122*, 41–54. https://doi.org/10.1016/j.fbp.2020.03.011
50. Melo, P.E.F., Silva, A.P.M., Marques, F.P., Ribeiro, P.R.V., Souza Filho, M.S.M., Brito, E.S., Lima, J.R., Azeredo, H.M.C. (2019). Antioxidant films from mango kernel components. *Food Hydrocolloids*, *95*, 487–495. https://doi.org/10.1016/j.foodhyd.2019.04.061

51. Mutua, J.K., Imathiu, S., Owino, W. (2017). Evaluation of the proximate composition, antioxidant potential, and antimicrobial activity of mango seed kernel extracts. *Food Science and Nutrition*, *5*(2), 349–357. https://doi.org/10.1002/fsn3.399
52. Mwaurah, P.W., Kumar, S., Kumar, N., Panghal, A., Attkan, A.K., Singh, V.K., Garg, M.K. (2020). Physicochemical characteristics, bioactive compounds and industrial applications of mango kernel and its products: A review. *Comprehensive Reviews in Food Science and Food Safety*, *19*(5), 2421–2446. https://doi.org/10.1111/1541-4337.12598
53. Navarro, M., Arnaez, E., Moreira, I., Quesada, S., Azofeifa, G., Wilhelm, K., Vargas, F., Chen, P. (2019). Polyphenolic characterization, antioxidant, and cytotoxic activities of *Mangifera indica* cultivars from Costa Rica. *Foods*, *8*(9), art. no. 384. https://doi.org/10.3390/foods8090384
54. Nawab, A., Alam, F., Haq, M.A., Haider, M.S., Lutfi, Z., Kamaluddin, S., Hasnain, A. (2018). Innovative edible packaging from mango kernel starch for the shelf life extension of red chili powder. *International Journal of Biological Macromolecules*, *114*, 626–631. https://doi.org/10.1016/j.ijbiomac.2018.03.148
55. Nawab, A., Alam, F., Hasnain, A. (2017). Mango kernel starch as a novel edible coating for enhancing shelf-life of tomato (*Solanum lycopersicum*) fruit. *International Journal of Biological Macromolecules*, *103*, 581–586. https://doi.org/10.1016/j.ijbiomac.2017.05.057
56. Nguyen, T.V.L., Nguyen, Q.D., Nguyen, P.B.D. (2022). Drying kinetics and changes of total phenolic content, antioxidant activity and color parameters of mango and avocado pulp in refractance window drying. *Polish Journal of Food and Nutrition Sciences*, *72*(1), 27–38. https://doi.org/10.31883/pjfns/144835
57. Norma Oficial Mexicana (1997). Especificaciones sanitarias para alimentos envasados en recipientes de cierre hermético y sometidos a tratamiento térmico (NOM-130-SSA1-1995) (in Spanish). https://dof.gob.mx/nota_detalle.php?codigo=4901457&fecha=21/11/1997#gsc.tab=0
58. Oliver-Simancas, R., Labrador-Fernández, L., Díaz-Maroto, M.C., Pérez-Coello, M.S., Alañón, M.E. (2021). Comprehensive research on mango by-products applications in food industry. *Trends in Food Science and Technology*, *118*, 179–188. https://doi.org/10.1016/j.tifs.2021.09.024
59. Pacheco-Ordaz, R., Antunes-Ricardo, M., Gutiérrez-Uribe, J.A., González--Aguilar, G.A. (2018a). Intestinal permeability and cellular antioxidant activity of phenolic compounds from mango (*Mangifera indica* cv. Ataulfo) peels. *International Journal of Molecular Sciences*, *19*(2), art. no. 514. https://doi.org/10.3390/ijms19020514
60. Pacheco-Ordaz, R., Wall-Medrano, A., Goñi, M.G., Ramos-Clamont-Montfort, G., Ayala-Zavala, J.F., González-Aguilar, G.A. (2018b). Effect of phenolic compounds on the growth of selected probiotic and pathogenic bacteria. *Letters in Applied Microbiology*, *66*(1), 25–31. https://doi.org/10.1111/lam.12814
61. Patiño-Rodríguez, O., Bello-Pérez, L.A., Agama-Acevedo, E., Pacheco-Vargas, G. (2021). Effect of deep frying unripe mango kernel flour extrudate: Physicochemical, microstructural and starch digestibility characteristics. *LWT – Food Science and Technology*, *145*, art. no. 111267. https://doi.org/10.1016/j.lwt.2021.111267
62. Peanparkdee, M., Iwamoto, S. (2022). Encapsulation for improving *in vitro* gastrointestinal digestion of plant polyphenols and their applications in food products. *Food Reviews International*, *38*(4), 335–353. https://doi.org/10.1080/87559129.2020.1733595
63. Pérez-Chabela, M.L., Cebollón-Juárez, A., Bosquez-Molina, E., Totosaus, A. (2022). Mango peel flour and potato peel flour as bioactive ingredients in the formulation of functional yogurt. *Food Science and Technology*, *42*, art. no. e38220. https://doi.org/10.1590/fst.38220
64. Rodríguez-González, S., Gutiérrez-Ruíz, I.M., Pérez-Ramírez, I.F., Mora, O., Ramos-Gomez, M., Reynoso-Camacho, R. (2017). Mechanisms related to the anti-diabetic properties of mango (*Mangifera indica* L.) juice by-product. *Journal of Functional Foods*, *37*, 190–199. https://doi.org/10.1016/j.jff.2017.07.058
65. Safdar, M.N., Kausar, T., Nadeem, M. (2017). Comparison of ultrasound and maceration techniques for the extraction of polyphenols from the mango peel. *Journal of Food Processing and Preservation*, *41*(4), art. no. e13028. https://doi.org/10.1111/jfpp.13028
66. Sánchez-Camargo, A.P., Ballesteros-Vivas, D., Buelvas-Puello, L.M., Martinez--Correa, H.A., Parada-Alfonso, F., Cifuentes, A., Ferreira, S.R.S., Gutiérrez, L.F. (2021). Microwave-assisted extraction of phenolic compounds with antioxidant and anti-proliferative activities from supercritical CO_2 pre-extracted mango peel as valorization strategy. *LWT – Food Science and Technology*, *137*, art. no. 110414. https://doi.org/10.1016/j.lwt.2020.110414
67. Sánchez-Camargo, A.P., Gutiérrez, L.F., Vargas, S.M., Martinez-Correa, H.A., Parada-Alfonso, F., Narváez-Cuenca, C.E. (2019). Valorisation of mango peel: Proximate composition, supercritical fluid extraction of carotenoids, and application as an antioxidant additive for an edible oil. *The Journal of Supercritical Fluids*, *152*, art. no. 104574. https://doi.org/10.1016/j.supflu.2019.104574
68. Santana, Á.L., Queirós, L.D., Martinez, J., Macedo, G.A. (2019). Pressurized liquid- and supercritical fluid extraction of crude and waste seeds of guarana (*Paullinia* cupana): Obtaining of bioactive compounds and mathematical modeling. *Food and Bioproducts Processing*, *117*, 194–202. https://doi.org/10.1016/j.fbp.2019.07.007
69. Sáyago-Ayerdi, S.G., Zamora-Gasga, V.M., Venema, K. (2019). Prebiotic effect of predigested mango peel on gut microbiota assessed in a dynamic *in vitro* model of the human colon (TIM-2). *Food Research International*, *118*, 89–95. https://doi.org/10.1016/j.foodres.2017.12.024
70. Soria-Lara, D.M., Jiménez-García, S.N., Botello-Álvarez, J.E., Miranda-López, R. (2020). Main changes on the polyphenols profile and antioxidant capacity in Manila mango (*Mangifera indica* L.). *Archivos Latinoamericanos de Nutrición*, *70*(4), 269–281. https://doi.org/10.37527/2020.70.4.005
71. Tan, L., Jin, Z., Ge, Y., Nadeem, H., Cheng, Z., Azeem, F., Zhan, R. (2020). Comprehensive ESI-Q TRAP-MS/MS based characterization of metabolome of two mango (*Mangifera indica* L) cultivars from China. *Scientific Reports*, *10*(1), art. no. 20017. https://doi.org/10.1038/s41598-020-75636-y
72. Tian, L., Tan, Y., Chen, G., Wang, G., Sun, J., Ou, S., Chen, W., Bai, W. (2019). Metabolism of anthocyanins and consequent effects on the gut microbiota. *Critical Reviews in Food Science and Nutrition*, *59*(6), 982–991. https://doi.org/10.1080/10408398.2018.1533517
73. Tirado-Kulieva, V., Atoche-Dioses, S., Hernández-Martínez, E. (2021). Phenolic compounds of mango (*Mangifera indica*) by-products: Antioxidant and antimicrobial potential, use in disease prevention and food industry, methods of extraction and microencapsulation. *Scientia Agropecuaria*, *12*(2), 283–293. https://doi.org/10.17268/sci.agropecu.2021.031
74. Torres-León, C., de Azevedo Ramos, B., dos Santos Correia, M.T., Carneiro-da--Cunha, M.G., Ramirez-Guzman, N., Alves, L.C., Brayner, F.A., Ascacio-Valdes, J., Álvarez-Pérez, O.B., Aguilar, C.N. (2021). Antioxidant and anti-staphylococcal activity of polyphenolic-rich extracts from Ataulfo mango seed. *LWT – Food Science and Technology*, *148*, art. no. 111653. https://doi.org/10.1016/j.lwt.2021.111653
75. Torres-León, C., Rojas, R., Contreras-Esquivel, J.C., Serna-Cock, L., Belmares--Cerda, R.E., Aguilar, C.N. (2016). Mango seed: Functional and nutritional properties. *Trends in Food Science and Technology*, *55*, 109–117. https://doi.org/10.1016/j.tifs.2016.06.009
76. Torres-León, C., Rojas, R., Serna-Cock, L., Belmares-Cerda, R., Aguilar, C.N. (2017). Extraction of antioxidants from mango seed kernel: Optimization assisted by microwave. *Food and Bioproducts Processing*, *105*, 188–196. https://doi.org/10.1016/j.fbp.2017.07.005
77. Torres-León, C., Vicente, A.A., Flores-López, M.L., Rojas, R., Serna-Cock, L., Alvarez-Pérez, O.B., Aguilar, C.N. (2018). Edible films and coatings based on mango (var. Ataulfo) by-products to improve gas transfer rate of peach. *LWT – Food Science and Technology*, *97*, 624–631. https://doi.org/10.1016/j.lwt.2018.07.057
78. Vazquez-Olivo, G., Antunes-Ricardo, M., Gutiérrez-Uribe, J.A., Osuna-Enciso, T., León-Félix, J., Heredia, J.B. (2019). Cellular antioxidant activity and *in vitro* intestinal permeability of phenolic compounds from four varieties of mango bark (*Mangifera indica* L.). *Journal of the Science of Food and Agriculture*, *99*(7), 3481–3489. https://doi.org/10.1002/jsfa.9567
79. Velderrain-Rodríguez, G.R., Torres-Moreno, H., Villegas-Ochoa, M.A., Ayala--Zavala, J.F., Robles-Zepeda, R.E., Wall-Medrano, A., González-Aguilar, G.A. (2018). Gallic acid content and an antioxidant mechanism are responsible for the antiproliferative activity of 'Ataulfo' mango peel on LS180 cells. *Molecules*, *23*(3), art. no. 695. https://doi.org/10.3390/molecules23030695
80. Vimalraj, S., Ashokkumar, T., Saravanan, S. (2018). Biogenic gold nanoparticles synthesis mediated by *Mangifera indica* seed aqueous extracts exhibits antibacterial, anticancer and anti-angiogenic properties. *Biomedicine and Pharmacotherapy*, *105*, 440–448. https://doi.org/10.1016/j.biopha.2018.05.151
81. Wu, P., Bhattarai, R.R., Dhital, S., Deng, R., Chen, X.D., Gidley, M.J. (2017). *In vitro* digestion of pectin- and mango-enriched diets using a dynamic rat stomach--duodenum model. *Journal of Food Engineering*, *202*, 65–78. https://doi.org/10.1016/j.jfoodeng.2017.01.011
82. Ye, S., Shah, B.R., Li, J., Liang, H., Zhan, F., Geng, F., Li, B. (2022). A critical review on interplay between dietary fibers and gut microbiota. *Trends in Food Science and Technology*, *124*, 237–249. https://doi.org/10.1016/j.tifs.2022.04.010

ORIGINAL ARTICLE
http://journal.pan.olsztyn.pl

Polish Journal of Food and Nutrition Sciences
2023, Vol. 73, No. 1, 24–31
DOI: 10.31883/pjfns/157248
ISSN 1230-0322, e-ISSN 2083-6007

Oxidative Stability and Quality Parameters of Veal During Ageing

Mateja Lušnic Polak[1,*], Mojca Kuhar[1], Iva Zahija[1], Lea Demšar[1], Tomaž Polak[1]

[1]Biotechnical Faculty, University of Ljubljana, Jamnikarjeva 101, 1000 Ljubljana, Slovenia

The objective of the present study was to evaluate the effects of the ageing period (1, 7, 14, and 21 days) on the quality parameters, sensory attributes, and oxidative stability of loins (*longissimuss lumborum* muscle) obtained from twelve Simmental calves less than 8 months old and slaughtered in a commercial processing plant. After 21 days, the colour of veal samples became yellower (increase in *b** colour parameter value), and the instrumentally-measured texture improved (Warner-Bratzler shear force decreased from 84.61 N to 56.79 N). Ageing time enhanced sensory-evaluated tenderness, juiciness, aroma, and flavour. The amount of the lipid oxidation products determined as thiobarbituric acid reactive substance content remained unchanged; in contrast, the amount of protein carbonyls increased, without compromising veal quality.

Key words: ageing, veal, quality parameters, TBARs, protein carbonyls

INTRODUCTION

Meat ageing is a common name for many biochemical processes, such as enzymatic degradation of proteins and, to a lesser extent, enzymatic degradation of lipids. In the process of proteolysis, endogenous proteolytic enzymes cause fragmentation of the microstructure of muscle fibres, resulting in improved tenderness of the meat [Franco *et al.*, 2009; Kemp *et al.*, 2010]. During the degradation of myofibrillar proteins, peptides and amino acids are released that act as water-soluble flavour precursors [Koutsidis *et al.*, 2008]. The result is an improvement in the aroma and flavour of the meat, which acquires the desired gastronomic properties, mainly related to the aroma and flavour specific of aged meat [Lee *et al.*, 2021]. The speed and extent of ageing depend on several factors, such as the species, age, diet, and breed of the animal, as well as the type of muscle. The meat of young animals is, in contrast to the meat of older animals, generally considered softer and requires less time to reach the same degree of tenderness. Veal is the meat of cattle up to 8 months old and should be characterised by a tender texture, pale pink colour, high water content, and low-fat content [Government of the Republic of Slovenia Regulation, 2019]. The most important factor determining the acceptability of veal and influencing the consumer's purchase decision is tenderness [Reicks *et al.*, 2011]. Although veal is considered tender meat than beef and is usually not aged, some studies have confirmed the positive influence of ageing on its tenderness, juiciness, and overall acceptability [Baldi *et al.*, 2015; Revilla & Vivar-Quintana, 2006].

Oxidation is one of the main causes of meat deterioration, along with microbial spoilage. Muscle lipids and proteins are susceptible to oxidation as a result of internal and external factors. Meat contains several endogenous initiators of oxidation, such as ferrous heme pigments, transition metal ions, and oxidative enzymes. The ageing of meat can enhance oxidative degradation. Meat is subjected to oxidation of lipids and proteins, resulting in the formation of various oxidation products, including carbonyl groups and lipid oxidation products, such

***Corresponding Author:**
Tel.: +386-1-320-37-42, e-mail: **mateja.lusnic@bf.uni-lj.si** (M. Lušnic Polak)

Submitted: 27 September 2022
Accepted: 7 December 2022
Published on-line: 11 January 2023

as thiobarbituric acid reactive substances (TBARs). Lipid oxidation is often responsible for quality loss *via* rancid flavour development [Domínguez *et al.*, 2019; Popova *et al.*, 2009]. To reduce the unbeneficial effects of oxidation processes on meat quality, the meat industry uses vacuum packaging, which exerts a strong oxidation-inhibiting effect. Bonny *et al.* [2017] showed that TBAR levels were the lowest in vacuum-packed beef samples compared to the modified atmosphere-packed (MAP) samples. Similar results were observed for carbonyl group content, where vacuum packaging presented significantly lower carbonyl content after 10 days than MAP treatments. The effects of lipid oxidation on meat aroma and overall quality have been thoroughly studied, while the effects of protein oxidation are still poorly understood [Lund *et al.*, 2011]. The formation of carbonyl and sulfhydryl groups causes meat to lose functional groups, leading to the formation of intra- and/or inter-protein disulfide cross-links. These factors have a strong influence on the functionality of muscle proteins and, consequently, reduce the water-holding capacity. The chemical changes that occur during protein oxidation are responsible for changes in protein solubility, protein fragmentation, and protein aggregation. Protein oxidation can affect eating quality of meat, including especially its tenderness, juiciness, flavour, and discoloration [Bao & Ertbjerg, 2019].

We are aware that there are many studies on meat ageing, but there are few on the topic of veal ageing and practically none addressing longer ageing periods. Although veal is considered to be more tender than beef, based on promising results of limited similar studies, we believe that ageing will result in additional improvement in its tenderness, aroma, and flavour. Therefore, the objective of the present study was to determine the effects of 21-day ageing of veal on its quality parameters and sensory attributes. Since the oxidation process in meat is related to its quality and consumer acceptance, the extent of lipid and protein oxidation of veal was determined as well.

MATERIALS AND METHODS

Experimental design

In the experimental part of the study, twelve calves (Simmental breed) were randomly selected and purchased at a local butcher (Ljubljana, Slovenia). The calves were from Slovenian breeding and rearing and slaughtered on the same day in a commercial slaughterhouse at less than 8 months of age. The average cold carcass weight was 104±8 kg. The procedures of the preslaughter period, slaughter and primary processing of carcasses were conducted according to standard technology [Council Regulation, 2009; Government of the Republic of Slovenia Regulation, 2018]. Carcasses were chilled at 4±1°C for 24 h, and the *longissimus lumborum* (LL) section of the *longissimus thoracis et lumborum* muscle was removed from both the left and the right side of the carcass. The muscles were separated from the bone and divided, perpendicular to the muscle fibres, into four approximately equal parts. Samples were weighed, vacuum-packed in polyvinylidene chloride (PVDC) laminate bags (Cryovac, Elmwood Park, NJ, USA), and randomly selected for different ageing periods (7, 14, and 21 days *postmortem*, *pm*). Samples in group 1 (24 h *pm*) were immediately analysed for meat quality parameters.

The ageing period was selected based on the results of sensory analysis of the preliminary study, which included four calves (Simmental breed) from Slovenian breeding and rearing. The experimental design was similar to that of the main experiment, with the only difference being the duration of ageing. After 28 days of ageing, the panelists evaluating sensory attributes of meat perceived its off-aroma and off-flavour (aroma/flavour associated with meat at the end of shelf life), thus the ageing period in the main experiment was 21 days instead of 28 days.

Ageing took place in a cooling chamber at a constant temperature of 2±1°C. After each ageing period, one part of the sample was immediately analysed for meat quality parameters, and another part of the sample was vacuum-packed and frozen at −21±1°C until contents of protein carbonyl and TBARs were determined. Before analysis, the meat samples were thawed at 4±1°C for 24 h.

Analysis of meat quality parameters

After each ageing period, weep loss (expressed as a percentage of excreted meat juice during ageing) was determined. Then, a 3–4 cm thick slice with core temperature of 2±1°C was cut from the corresponding sample, in which the pH value was measured directly using a combined glass-gel spear electrode (Type 03, Testo Pty Ltd, Croydon South, Australia) with a thermometer (Type T, Testo Pty Ltd) connected to a pH metre (Testo 230, Testo Pty Ltd). The reading accuracy was 0.01 pH units.

Colour parameters of the meat samples were measured using a CR-400 colorimeter (Konica Minolta Optics, Inc., Osaka, Japan) with standard illuminant C and 0° viewing angle. The CIE L^* (lightness), a^* (redness), and b^* (yellowness) values were determined at four different points on the freshly-cut surface after 30 min of bloom time at 4±1°C. The surface of meat sample was drained of excreted meat juice before measurement. The remaining piece of the raw sample was weighed, and colour and marbling were visually evaluated by a sensory panel.

The samples were then vacuum-packed and heat-treated in a combi oven (Rational FRIMA SCC61, Landsberg am Lech, Germany) at 75°C for 1 h using the *sous-vide* (vacuum cooking) method. After the heat treatment, cooking loss was determined and expressed as a percentage of excreted meat juice during heat treatment. The remaining sensory properties (juiciness, tenderness, aroma and flavour) were evaluated on the warm part of the sample.

To evaluate the sensory qualities, a panel of six panellists qualified and experienced in the field of meat products was appointed. The panel was trained in sensory profiling of veal from the Slovenian market in five training sessions. In the first session, the panellists were trained on samples of unaged veal (24 h *pm*). In the four following sessions, samples of aged veal (with different ageing times: 7, 14, 21, and 28 days) were served. The panellists evaluated the sensory characteristics of the veal and agreed on descriptors and their definitions. The sensory evaluation of veal was conducted under defined, precisely prescribed, controlled

and reproducible operating conditions. These included: arrangement of laboratory, samples, accessories and organization of assessment [ISO, 2007; ISO, 2012]. Assessment of the coded samples took place in a standard sensory laboratory. Regarding sensory evaluation, the thermally-treated samples with discarded edges were cut into 1 cm^3 cubes, and two cubes per panellist were wrapped in aluminium foil and randomly presented to the panellists for evaluation. To neutralise the taste, the panel used the middle dough of white bread and water.

The analytical-descriptive test [Gašperlin *et al.*, 2014] was carried out by scoring the sensory attributes according to a non-structured scale from 1 to 7 points, whereby a higher score indicated a stronger expression of a particular attribute. The definitions of the descriptors are listed in Table 1.

After each ageing period, marbling and colour were visually assessed on raw samples. After thermal treatment, the aroma and flavour of the samples were assessed immediately after un-wrapping the aluminium foil. The juiciness and tenderness were assessed by tasting the samples. The samples were served and scored in four sessions (after each ageing period), and their attributes were recorded individually.

The Warner-Bratzler shear force (WBSF) was measured according to the procedure of Campo *et al.* [2000], with some modifications. The analysis was performed using the TAXT plus texture analyser (Stable Micro Systems Ltd., Godalming, United Kingdom) with a 50 kg load cell. The shear force (N) was measured perpendicular to the muscle slices (10×10×40 mm) cooled to room temperature (20±1°C) in four parallels as the resistance of the sample to cutting by blade set consists of guillotine edge and a Warner-Bratzler blade (HDP/BS) with the operating conditions: blade speed 50 mm/min, penetration into the muscle 10.5 mm.

TBAR and protein carbonyl content determination

The extent of lipid oxidation of veal samples was monitored by measuring TBAR content as described by Penko *et al.* [2015]. Briefly, to 0.100±0.001 g of a homogenised sample, 1 mL of 35% trichloroacetic acid, and 2 mL of 0.36% thiobarbituric acid (in 0.1 M Na_2SO_3) were added and mixed intensively for 5 min on an orbital shaker (KS260, IKA, Staufen, Germany), followed by the addition of 1 mL of 0.9% butylated hydroxytoluene in *n*-hexane. The samples were heated at 90°C for 30 min in a thermoblock (VLM EC1, Bielefeld, Germany). After cooling to room temperature, 1 mL of trichloroacetic acid and 2 of mL chloroform were added and then centrifuged at 1,500×*g*, 6 min (5810 centrifuge, Eppendorf, Darmstadt, Germany). After centrifugation, the absorbance in the supernatant was measured at 532 nm with a Cary 8454 UV-Vis spectrophotometer (Agilent Technologies, Waldbronn, Germany). 1,1,3,3-Tetraethoxypropane was used as a standard for the determination of TBARs. Results were expressed in mg of malondialdehyde equivalents per kg of meat.

A modified spectrophotometric method of Soglia *et al.* [2016] was used to determine protein carbonyl content of meat. In brief, 1,000 g of muscle sample was homogenised in 10 mL of ice-cold 0.15 M KCl solution. To 100 µL of the homogenate, 1 mL of 10% trichloroacetic acid was added. A blank was prepared by adding 1 mL of 10% trichloroacetic acid to 100 µL of distilled water. After centrifugation at 4,000×*g* for 6 min (Eppendorf 5810 centrifuge), the supernatant was removed, and 400 µL sodium dodecyl sulfate was added to the residue. After heating (10 min, 90°C) and sonication (30 min, 40°C) (3510 ultrasonic cleaner, Branson, Danbury, CT, USA), the samples were treated with 0.8 mL of a 0.3% (*w/v*) solution of 2,4-dinitrophenylhydrazine (DNPH) in 3 M HCl. To the blank, 0.8 mL of 3 M HCl was added. After incubation (30 min), 400 µL of 40% trichloroacetic acid was added and centrifuged (4,000×*g*, 6 min). The supernatant was removed, and 1 mL ethanol-ethyl acetate mixture (1:1, *v:v*) was added to the residue. After centrifugation (4,000×*g*, 10 min), the supernatant was again removed. This procedure was repeated three times. To the dried precipitate, 1.5 mL of 6 M guanidine hydrochloride in 20 mM sodium phosphate buffer (pH 6.5) was added. After overnight incubation (4°C), the samples were filtered by 0.45 µm Phenex regenerated cellulose (RC) syringe filters (Phenomenex, Torrance, CA, USA), and carbonyl groups were detected, by reactivity of carbonyl groups with DNPH to form protein-bound 2,4-dinitrophenylhydrazones, at wavelengths of 370 nm and 280 nm with a Cary 8454 UV-Vis spectrophotometer (Agilent Technologies). The protein carbonyl

Table 1. Definitions of descriptors for the sensory evaluation of veal.

Descriptor	Definition	Scale
Colour	Colour typical for veal (visual evaluation)	1 – too light 4 – pale pink (optimal) 7 – too dark
Marbling	The proportion of intramuscular fat (visual evaluation)	1 – absence of marbling 7 – extreme marbling
Juiciness	The degree of juiciness perceived after the first three chews between the molar teeth	1 – extremely dry 7 – extremely juicy
Tenderness	Perception of tenderness after the first three chews between the molar teeth	1 – extremely tough 7 – extremely tender
Aroma	Aroma associated with cooked veal loin	1 – absence of veal aroma 7 – fully expressed veal aroma
Flavour	Flavour associated with cooked veal loin	1 – absence of veal flavour 7 – fully expressed veal flavour

content, expressed as nmol/mg of protein, was calculated according to the following equation:

$$\text{Content of protein carbonyls} = \frac{A_{370}}{22{,}000 \times [A_{280} - (A_{370} \times 0.43)]} \times 10^6 \quad (1)$$

where: 22,000 – absorption coefficient of protein-bound 2,4-dinitrophenylhydrazones at 370 nm; A_{370} – absorbance at 370 nm; A_{280} – absorbance at 280 nm; and 0.43 – correction factor.

Statistical analysis

To determine the effects of variability and the characteristics of its influence on some physical, chemical, and instrumental parameters of veal, the univariate UNIANOVA test (IBM SPSS Statistics version 22.0, Chicago, IL, USA) was used, where the model included fixed effects of ageing time (A_i; 1, 7, 14, 21 days) and repetition (animal) (R_j; 1–12). The model was represented as equation (2).

$$y_{ijk} = \mu + Ai + Rj + e_{ijk} \quad (2)$$

where: y was the observed parameter, μ – the general mean, and e – a residual random term with variance σ_e^2. The effect of calf sex was not observed. The Shapiro-Wilk test for the sensory parameters did not show a normal distribution of the data ($p<0.05$), so the Kruskal-Wallis test was used to evaluate the influence of ageing time on the above traits. Since this non-parametric test does not allow us to evaluate the differences between ageing days, the UNIANOVA test was also performed and was upgraded with a post-hoc multiple comparison least significant difference (LSD) test. Sensory trait values were compared at each day with a significance level of 0.05.

RESULTS AND DISCUSSION

The results referring to weep loss during ageing, cooking loss during heat treatment, pH values, instrumentally-measured colour parameters and texture are summarised in Table 2. The pH values of the veal samples varied from 5.66 (24 h *pm*) to 5.72 (after 21 days). The pH value measured after 24 h *pm* indicated normal muscle quality. The pH values in the present study are similar to those reported by other authors [Revilla & Vivar-Quintana, 2006].

During the 21 days, the veal samples released a noticeable amount of meat juice (Table 2). Weep loss during ageing is caused by denaturation of muscle proteins and decreased ability to bind water [Wiklund *et al.*, 2010]. The highest percentage weep loss was observed after 21 days (6.97%), but without statistical differences ($p>0.05$) compared to day 7 (1.17%) and day 14 (3.43%). One of the possible explanations is that vacuum packaging protects against high water losses. Shi *et al.* [2020], who investigated different packaging methods, reported that the lowest weep losses occurred in wet-aged beef samples due to vacuum packing. Vacuum packaging inhibited evaporation of water, so weep losses decreased. In contrast, dry-aged beef samples had the highest weep losses compared to beef samples aged under various moisture-permeable packages [Laster *et al.*, 2008].

The ageing process affected the cooking loss ($p<0.001$) of veal during heat treatment (Table 2). The highest cooking loss was determined for meat aged for 14 days (22.63%) and similarly maintained at 21 days *pm* (21.78%). Mungure *et al.* [2016] found a significant increase in cooking loss in beef samples after 21 days of ageing (37.51%) compared to 3-day aged beef. The mentioned value was higher than the cooking loss observed in our experiment at day 21. Weight loss during heat treatment depends on the method, temperature and duration of heat treatment, so comparison with other studies is difficult. Longer heat treatment and higher temperature affect the increase in cooking loss, which could be due to increased myosin denaturation and possible weakening of myofibril structure [Zielbauer *et al.*, 2016].

Colour plays an important role in the appearance, presentation, and acceptability of veal [Klont *et al.*, 2000]. Colour parameters of meat 24 h *pm* in our study are shown in Table 2. The values of L^*, a^* and b^* were similar to those reported by Hulsegge *et al.* [2001], who performed measurements on *rectus abdominis* muscle. Instrumental colour measurements on the *rectus abdominis* and *pectoralis superficialis* muscle are

Table 2. pH value, weep and cooking losses, as well as instrumentally-measured colour parameters and texture of veal after different ageing periods.

Parameter		Ageing period (day)				p_A	p_R	SE	Mean across days *pm*
		1	7	14	21				
pH		5.66^b	5.71^a	5.65^b	5.72^a	0.065	0.653	0.05	5.79
Weep loss (%)		0.0	1.17	3.43	6.97	0.153	-	1.3	2.9
Cooking loss (%)		16.02^b	17.40^b	22.63^a	21.78^a	<0.001	-	2.8	19.5
Colour parameter	L^*	48.36	49.93	50.30	49.12	0.318	0.001	3.33	49.43
	a*	11.79^b	13.32^a	12.41^{ab}	13.40^a	0.054	<0.001	2.67	12.79
	b*	2.80^c	5.60^a	3.29^{bc}	3.77^b	<0.001	0.025	1.12	3.86
Texture parameter, WBSF (N)		84.61^a	53.48^b	63.47^b	56.79^b	<0.001	0.501	24.14	64.59

pm, *postmortem*; WBSF, Warner-Bratzler shear force; p_A, statistical probability of ageing effect; p_R, statistical probability of repetition (animal) effect; SE, standard error of mean. Data with different superscript letters within a row (differences between days of ageing) differ significantly ($p\leq0.05$).

recommended for objective evaluation of veal colour [Horcada *et al.*, 2013]. For the results obtained after different ageing period (Table 2), there were no significant differences ($p>0.05$) in the L^* values, while significant differences were in parameter b^* with a maximum value observed after 7 days of ageing (5.60, $p<0.001$). Differences observed in parameter a^* were mainly due to the repetition (animal) effect. A possible explanation for increase in parameter b^* is in oxidation of myoglobin to metmyoglobin as a result of dissolved oxygen in the meat [Henriott *et al.*, 2020]. An increase in brightness may have a positive effect on the appearance of veal, while an increase in redness may be a negative factor [Baldi *et al.*, 2015]. Similarly to our results, Vieira *et al.* [2006] found no significant effect of a 14-day ageing period on the a^* values of beef *longissimus thoracis* muscle. In contrast, Florek *et al.* [2015] found significantly higher values of L^*, a^*, and b^* parameters in LL muscle after 12 days of ageing, regardless of the calf slaughter age. Similar findings were observed by Vitale *et al.* [2014], who reported higher baseline values of L^*, a^* and b^* in aged beef (3, 6, 8, 14, and 21 days) than in unaged beef. These results are consistent with Bruce *et al.* [2004], who demonstrated an increase in L^*, a^*, and b^* values of *longissimus toracis* for 14 days of vacuum-packaged meat compared to unaged meat (24 h *pm*). The differences in L^*, a^*, and b^* values between aged and unaged meat could be explained by a higher blooming ability of vacuum-aged meat [Oliete *et al.*, 2006].

Ageing had a significant ($p<0.001$) effect on instrumentally-measured texture of heat-treated meat (Table 2). After 21 days of ageing, the WBSF decreased by approximately 33% (from 84.61 N to 56.79 N), and the lowest value was observed after 7 days *pm* (53.48 N), without significant differences ($p>0.05$) compared to day 14 and day 21. A slight increase was observed after 14 days, which could be related to a higher cooking loss. At this point, it should be noted that the values of measured WBSF obtained in our study are very difficult to compare with other studies, because different blade sets (*e.g.*, standard blade, "V" slot blade, rectangular slot blade) and different dimensions and shapes (rectangular or oval) of the sample were used for force measurement. For this reason, comparison with other studies is only possible in relative terms. In this case, our results are in agreement with the results of the study by Baldi *et al.* [2015], who reported a decrease in WBSF for *longissimus dorsi* muscle of veal within 8 days, without further improvement in tenderness. Also similarly to our findings, Franco *et al.* [2009] found that beef aged for 21 days did not differ in WBSF from beef aged for 8 or 14 days. Another difference between our study and some other studies was in the storage of the aged veal samples. In our case, we performed the WBSF measurements immediately after each ageing period. Some other authors reported that the veal samples were frozen before measurements [Baldi *et al.*, 2015; Campo *et al.*, 2000; Revilla *et al.*, 2006]. The data in the literature indicate a positive effect of freezing on the tenderness of the meat, attributed to mechanical damage of the myofibrillar structure of the meat by the ice crystals [Cho *et al.*, 2017; Dang *et al.*, 2021; Lagerstedt *et al.*, 2008; Vieira *et al.*, 2006].

The ageing period affected several sensory attributes of veal (Table 3). After 21 days, the juiciness (by 0.46 points), tenderness (by 1.33 points), aroma (by 0.32 points), and flavour (by 0.41 points) of veal improved significantly ($p\leq0.05$). Similar results were obtained in a preliminary study, in which tenderness, aroma, and flavour improved (increase in scores) up to 21 days; later, at day 28, no further improvement in tenderness, but off-aroma and off-flavour were noted (data not shown). Kaniou *et al.* [2001] reported an increase in the content of biogenic amines during the ageing of vacuum-packed beef. The highest levels of putrescine and cadaverine were found after 26 days. High levels of putrescine and cadaverine are known to enhance histamine or tyramine toxicity. This is another reason why we decided to use a 21-day ageing period.

The most important quality characteristic of meat is tenderness, a highly variable attribute that depends on many intrinsic and extrinsic factors and their interactions. According to the Government of Republic of Slovenia Regulation [2019], calves are slaughtered at less than 8 months of age; consequently, consumers expect tender meat. In our study, tenderness was rated at 6.51 points (Table 3), which is almost the maximum value for this attribute. Both, sensorial and instrumental methods confirmed improvement in tenderness of veal, although some differences between methods were observed. The lowest WBSF

Table 3. Sensory attributes of veal after different ageing periods.

Sensory attribute	Ageing period (day)				X^2	p_A (Kruskal Wallis test)	SE	Mean across days *pm*
	1	7	14	21				
Colour (1–4–7)	4.08^a	4.08^a	3.69^b	3.82^b	15.90	0.001	0.47	3.9
Marbling (1–7)	1.65^c	1.65^c	1.85^b	2.06^a	8.31	0.040	0.82	1.8
Juiciness (1–7)	5.43^b	5.58^b	5.53^b	5.89^a	22.68	<0.001	0.40	5.6
Tenderness (1–7)	5.18^d	5.71^c	6.18^b	6.51^a	89.50	<0.001	0.42	5.9
Aroma (1–7)	6.00^c	6.00^c	6.13^b	6.32^a	53.20	<0.001	0.17	6.1
Flavour (1–7)	6.08^c	6.15^c	6.28^b	6.49^a	47.95	<0.001	0.22	6.3

pm, *postmortem*, (1–7); scale from 1 to 7 points (a higher score indicates a stronger expression of a particular attribute); p_A, statistical probability of ageing effect; SE, standard error of mean. Data with different superscript letters within a row (differences between days of ageing) differ significantly ($p\leq0.05$, least significant difference test).

was measured on day 7, while from a sensory point of view, the highest score for tenderness was achieved after 21 days of ageing. The reason for this deviation may be in the sensory perception of tenderness, which is indirectly related to juiciness [Choe *et al.*, 2016]. This coincides with the increase in juiciness (the highest value for juiciness was observed after 21 days of ageing). The increase in juiciness is the result of the activation of calpains during *postmortem* aging period, which influences the increase in the amount of free water in meat [Jaspal *et al.*, 2021]. Sensory-rated colour scores for the fresh cut veal sample decreased significantly during ageing, from 4.08 on the first day to 3.69 after 14 days (Table 3). The colour was described as brighter, which is desirable for veal and in accordance with an increase in parameter *b** (yellowness) ($p<0.001$). Marbling varied from 1.65 points to 2.06 points ($p=0.040$), the differences were minimal and probably due to the influence of the individual animal in the experiment. It is difficult to compare our results directly with other studies because no study has been conducted with the same ageing conditions. Revilla & Vivar-Quintana [2006] reported that the quality of veal improved during ageing; tenderness, colour, and odour were the main attributes affected by ageing, and a 7-day ageing period seemed to be sufficient to obtain veal of high quality. Baldi *et al.* [2015] found that during a 4-day ageing period, the tenderness and juiciness of *longissimus dorsi* muscle significantly improved ($p<0.001$), while ageing had no effect on aroma and flavour.

The results regarding the development of oxidation in vacuum-packed veal samples are presented in Table 4. The ageing process had no effect on TBAR formation ($p=0.589$), indicating that the selected ageing conditions were appropriate. Campo *et al.* [2006] related TBAR values to the sensory attributes of beef. Higher TBAR values indicate a higher degree of oxidation, but not always a change in sensory attributes [Penko *et al.*, 2015]. The cut-off point for consumer detection of rancidity is between 1.0 and 3.0 mg malondialdehyde/kg, according to Campo *et al.* [2006]. In the current study, TBAR values ranged from 0.24 to 0.27 mg malondialdehyde/kg, well below the critical level at which rancidity is detected; hence, the sensory attributes of veal were not affected. One of the possible explanations for the minimal formation of TBARs in our experiment could be in the vacuum packaging of the samples. Both lipid and protein oxidation increased during storage due to the high oxygen content in the packaging atmosphere [Lund *et al.*, 2007]. Clausen *et al.* [2009] reported very low TBAR values for vacuum-stored samples (23 days *pm*), while a sharp increase in lipid oxidation was observed for samples stored 6 days after vacuum packaging in MAP. In contrast, Popova *et al.* [2009] reported that 14 days of vacuum storage affected lipid oxidation in beef samples and it was higher than that in nonvacuum-packed meat, with a significant difference observed in the content of TBARs on the first and sixth day of storage. According to Insausti *et al.* [2021], lipid oxidation is directly related to the formation of metmyoglobin during meat display; meat with a higher pigment content is more oxidized and therefore less stable in colour. Veal is considered a younger animal meat and has less available myoglobin for the oxidation process.

The total amount of protein carbonyls in the veal samples increased significantly during ageing (3.98 nmol/mg protein at day 1 *vs.* 6.13 nmol/mg protein at day 21) (Table 4). The highest increase was observed after 14 days of ageing (6.22 nmol/mg protein). Popova *et al.* [2009] reported that a significantly higher amount of carbonyls was formed (20 nmol/mg proteins) after 6 days of ageing of beef in a vacuum package at a temperature of 4°C compared to our results. According to the authors, during a 10-day storage of bovine LL muscle and *diaphragma pedialis*, the total protein carbonyl content increased from 3.1 to 5.1 nmol/mg protein and from 4.8 to 6.9 nmol/mg protein. Large content variability could be explained by differing ageing conditions, especially temperature, muscle type, packaging method, and duration [Estévez, 2011]. Oxidation of myofibrillar proteins during storage can have a significant effect on muscle condition. Under highly oxidative conditions, intermolecular cross-links can be formed, affecting proteins that are less susceptible to enzymatic proteolysis and reducing the development of tenderness due to proteolysis in meat [Davies, 2005]. In our study, a relationship between meat tenderness and the protein oxidation process was not found; in contrast, meat tenderness improved during ageing. The selected ageing conditions in our experiment were suitable to obtain the protein carbonyl content at a low level. The process of protein oxidation during storage of meat in the refrigerator is probably slower than the process of oxidation under conditions where radicals are formed more rapidly, such as heat treatment, freezing and thawing, irradiation and packaging of meat in an oxygen-rich atmosphere. This is one of the current research areas that can help us better understand the formation of protein carbonyls related to oxidative changes in meat [Estévez *et al.*, 2019].

CONCLUSIONS

According to the current situation of veal on the Slovenian market and promising results of limited studies considered ageing

Table 4. Oxidation parameters of veal after different ageing periods.

Parameter	Ageing period (day)				p_A	p_R	SE	Mean across days *pm*
	1	7	14	21				
TBARs (mg malondialdehyde/kg)	0.24	0.23	0.23	0.27	0.589	0.630	0.05	0.24
Protein carbonyls (nmol/mg proteins)	3.98^b	4.03^b	6.22^a	6.13^a	<0.001	0.436	0.99	5.09

pm, *postmortem*; TBARs, thiobarbituric acid reactive substances; p_A, statistical probability of ageing effect; p_R, statistical probability of repetition (animal) effect; SE, standard error of mean. Data with different superscript letters within a row (differences between days of ageing) differ significantly ($p\leq0.05$).

as a routine processing of veal to improve meat quality and to find the best compromise between the improvement in sensory properties and minimising loss of colour, lipid, and protein stability, the results obtained in the present study fully confirm that 21-day *pm* ageing under vacuum conditions at a temperature of 2±1°C reflects improvements of some sensory characteristics, especially tenderness, juiciness, aroma, and flavour. The intensity of lipid oxidation was low, as the content of TBARs during ageing remained below the threshold for the detection of rancid odour. In contrast, the duration of ageing affected the formation of protein carbonyls as their content increased with time without compromising meat quality. These results are promising for the use of veal ageing in the meat industry and gastronomy.

RESEARCH FUNDING

The work was financially supported by the research programs funded by the Slovenian Research Agency (P4-0234).

CONFLICT OF INTERESTS

The authors declare no conflict of interest.

ORCID IDs

L. Demšar https://orcid.org/0000-0003-2408-4256
M. Kuhar https://orcid.org/0000-0003-4261-752X
M. Lušnic Polak https://orcid.org/0000-0001-9768-3028
T. Polak https://orcid.org/0000-0001-9024-3855
I. Zahija https://orcid.org/0000-0002-7864-8136

REFERENCES

1. Baldi, G., Ratti, S., Bernardi, C.E.M., Dell'Orto, V., Corino, C., Compiani, R., Sgoifo Rossi, C.A. (2015). Effect of ageing time in vacuum package on veal *longissimus dorsi* and *biceps femoris* physical and sensory traits. *Italian Journal of Food Science*, *27*(3), 290–297. https://doi.org/10.14674/1120-1770/ijfs.v271
2. Bao, Y., Ertbjerg, P. (2019). Effects of protein oxidation on the texture and water-holding of meat: a review. *Critical Reviews in Food Science and Nutrition*, *59*(22), 3564–3578. https://doi.org/10.1080/10408398.2018.1498444
3. Bonny, D.S.S., Li, X., Li, Z., Li, M., Du, M., Gao, L., Zhang, D. (2017). Colour stability and lipid oxidation of beef *longissimus lumborum* under different packaging conditions. *Polish Journal of Food and Nutrition Sciences*, *67*(4), 257–281. https://doi.org/10.1515/pjfns-2017-0016
4. Bruce, H.L., Stark, J.L., Beilken, S.L. (2004). The effects of finishing diet and *post-mortem* ageing on the eating quality of the *M. longissimus thoracis* of electrically stimulated Brahman steer carcasses. *Meat Science*, *67*(2), 261–268. https://doi.org/10.1016/j.meatsci.2003.10.014
5. Campo, M.M., Nute, G.R., Hughes, S.I., Enser, M., Wood, J.D., Richardson, R.I. (2006). Flavour perception of oxidation in beef. *Meat Science*, *72*(2), 303–311. https://doi.org/10.1016/j.meatsci.2005.07.015
6. Campo, M.M., Santolaria, P., Sañudo, C., Lepetit, J., Olleta, J.L., Panea, B., Albertí, P. (2000). Assessment of breed type and ageing time effects on beef meat quality using two different texture devices. *Meat Science*, *55*(4), 371–378. https://doi.org/10.1016/S0309-1740(99)00162-X
7. Cho, S., Kang, S.M., Seong, P., Kang, G., Kim, Y., Kim, J., Chang, S., Park, B. (2017). Effect of aging and freezing conditions on meat quality and storage stability of 1++ grade Hanwoo steer beef: Implications for shelf life. *Korean Journal for Food Science of Animal Resources*, *37*(3), 440–448. https://doi.org/10.5851/kosfa.2017.37.3.440
8. Choe, J.-H., Choi, M.-H., Rhee, M.-S., Kim, B.-C. (2016). Estimation of sensory pork loin tenderness using Warner-Bratzler shear force and texture profile analysis measurements. *Asian-Australasian Journal of Animal Sciences*, *29*(7), 1029–1036. https://doi.org/10.5713/ajas.15.0482
9. Clausen, I., Jakobsen, M., Ertbjerg, P., Madsen, N.T. (2009). Modified atmosphere packaging affects lipid oxidation, myofibrillar fragmentation index and eating quality of beef. *Packaging Technology and Science*, *22*(2), 85–96. https://doi.org/10.1002/pts.828
10. Council Regulation (EC) No. 1099/2009 on the protection of animals at the time of killing (2009). *Official Journal of the European Union*, *L 303*, 1–30.
11. Dang, D.S., Bastarrachea, L.J., Martini, S., Matarneh, S.K. (2021). Crystallization behavior and quality of frozen meat. *Foods*, *10*(11), art. no. 2707. https://doi.org/10.3390/foods10112707
12. Davies, M.J. (2005). The oxidative environment and protein damage. *Biochimica et Biophysica Acta - Proteins and Proteomics*, *1703*(2), 93–109. https://doi.org/10.1016/j.bbapap.2004.08.007
13. Domínguez, R., Pateiro, M., Gagaoua, M., Barba, F.J., Zhang, W., Lorenzo, J.M. (2019). A comprehensive review on lipid oxidation in meat and meat products. *Antioxidants*, *8*(10), art. no. 429. https://doi.org/10.3390/antiox8100429
14. Estévez, M. (2011). Protein carbonyls in meat systems: A review. *Meat Science*, *89*(3), 259–279. https://doi.org/10.1016/j.meatsci.2011.04.025
15. Estévez, M., Padilla, P., Carvalho, L., Martín, L., Carrapiso, A., Delgado, J. (2019). Malondialdehyde interferes with the formation and detection of primary carbonyls in oxidized proteins. *Redox Biology*, *26*, art. no. 101277. https://doi.org/10.1016/j.redox.2019.101277
16. Florek, M., Domaradzki, P., Stanek, P., Litwińczuk, Z., Skałecki, P. (2015). *Longissimus lumborum* quality of Limousin suckler beef in relation to age and *postmortem* vacuum ageing. *Annals of Animal Science*, *15*(3), 785–798. https://doi.org/10.1515/aoas-2015-0019
17. Franco, D., Bispo, E., González, L., Vázquez, J.A., Moreno, T. (2009). Effect of finishing and ageing time on quality attributes of loin from the meat of Holstein–Fresian cull cows. *Meat Science*, *83*(3), 484–491. https://doi.org/10.1016/j.meatsci.2009.06.030
18. Gašperlin, L., Skvarča, M., Žlender, B., Lušnic, M., Polak, T. (2014). Quality assessment of Slovenian *krvavica*, a traditional blood sausage: sensory evaluation. *Journal of Food Processing and Preservation*, *38*(1), 97–105. https://doi.org/10.1111/j.1745-4549.2012.00750.x
19. Government of the Republic of Slovenia Regulation (2018). Rules on the classification and labelling of bovine and pig carcasses. *Official Gazette of the Republic of Slovenia*, *83*, 13306 (in Slovenian).
20. Government of the Republic of Slovenia Regulation (2019). Rules on the quality of meat of slaughter animals and game. *Official Gazette of the Republic of Slovenia, 67*, 8003 (in Slovenian).
21. Henriott, M.L., Herrera, N.J., Ribeiro, F.A., Hart, K.B., Bland, N.A., Calkins, C.R. (2020). Impact of myoglobin oxygenation level on color stability of frozen beef steaks. *Journal of Animal Science*, *98*(7), art. no. skaa193. https://doi.org/10.1093/jas/skaa193
22. Horcada, A., Juárez, M., Molina, A., Valera, M., Beriain, M.J. (2013). Instrumental colour measurement as a tool for light veal carcasses online evaluation. *Archives Animal Breeding*, *56*(1), 851–860. https://doi.org/10.7482/0003-9438-56-085
23. Hulsegge, B., Engel, B., Buist, W., Merkus, G.S.M., Klont, R.E. (2001). Instrumental colour classification of veal carcasses. *Meat Science, 57*(2), 191–195. https://doi.org/10.1016/S0309-1740(00)00093-0
24. Insausti, K., Murillo-Arbizu, M.T., Urrutia, O., Mendizabal, J.A., Beriain, M.J., Colle, M.J., Bass, P.D., Arana, A. (2021). Volatile compounds, odour and flavour attributes of lamb meat from the Navarra breed as affected by ageing. *Foods*, *10*(3), art. no. 493. https://doi.org/10.3390/foods10030493
25. International Organization for Standardization (2007). *Sensory analysis — General guidance for the design of test rooms* (ISO Standard No. 8589:2007).
26. International Organization for Standardization (2012). *Sensory analysis — General guidelines for the selection, training and monitoring of selected assessors and expert sensory assessors* (ISO Standard No. 8586:2012).
27. Jaspal, M.H., Badar, I.H., Amjad, O.B., Yar, M.K., Ijaz, M., Manzoor, A., Nasir, J., Asghar, B., Ali, S., Nauman, K., Rahman, A., Wara, U.U. (2021). Effect of wet aging on color stability, tenderness, and sensory attributes of *Longissimus lumborum* and *Gluteus medius* muscles from water buffalo bulls. *Animals*, *11*(8), art. no. 2248. https://doi.org/10.3390/ani11082248
28. Kaniou, I., Samouris, G., Mouratidou, T., Eleftheriadou, A., Zantopoulos, N. (2001). Determination of biogenic amines in fresh unpacked and vacuum-packed beef during storage at 4°C. *Food Chemistry*, *74*(4), 515–519. https://doi.org/10.1016/S0308-8146(01)00172-8
29. Kemp, C.M., Sensky, P.L., Bardsley, R.G., Buttery, P.J., Parr, T. (2010). Tenderness – An enzymatic view. *Meat Science, 84*(2), 248–256. https://doi.org/10.1016/j.meatsci.2009.06.008
30. Klont, R.E., Barnier, V.M.H., van Dijk, A., Smulders, F.J.M., Hoving-Bolink, A.H., Hulsegge, B., Eikelenboom, G. (2000). Effects of rate of pH fall, time of deboning, aging period, and their interaction on veal quality characteristics. *Journal of Animal Science, 78*(7), 1845–1851. https://doi.org/10.2527/2000.7871845x
31. Koutsidis, G., Elmore, J.S., Oruna-Concha, M.J., Campo, M.M., Wood, J.D., Mottram, D.S. (2008). Water-soluble precursors of beef flavour. Part II: Effect of *post-mortem* conditioning. *Meat Science*, *79*(2), 270–277. https://doi.org/10.1016/j.meatsci.2007.09.010

32. Lagerstedt, Å., Enfält, L., Johansson, L., Lundström, K. (2008). Effect of freezing on sensory quality, shear force and water loss in beef *M. longissimus dorsi*. *Meat Science*, *80*(2), 457–461. https://doi.org/10.1016/j.meatsci.2008.01.009
33. Laster, M.A., Smith, R.D., Nicholson, K.L., Nicholson, J.D.W., Miller, R.K., Griffin, D.B., Harris, K.B., Savell, J.W. (2008). Dry *versus* wet aging of beef: Retail cutting yields and consumer sensory attribute evaluations of steaks from ribeyes, strip loins, and top sirloins from two quality grade groups. *Meat Science*, *80*(3), 795–804. https://doi.org/10.1016/j.meatsci.2008.03.024
34. Lee, D., Lee, H.J., Yoon, J.W., Kim, M., Jo, C. (2021). Effect of different aging methods on the formation of aroma volatiles in beef strip loins. *Foods*, *10*(1), art. no. 146. https://doi.org/10.3390/foods10010146
35. Lund, M.N., Heinonen, M., Baron, C.P., Estévez, M. (2011). Protein oxidation in muscle foods: A review. *Molecular Nutrition and Food Research*, *55*(1), 83–95. https://doi.org/10.1002/mnfr.201000453
36. Lund, M.N., Hviid, M.S., Skibsted, L.H. (2007). The combined effect of antioxidants and modified atmosphere packaging on protein and lipid oxidation in beef patties during chill storage. *Meat Science*, *76*(2), 226–233. https://doi.org/10.1016/j.meatsci.2006.11.003
37. Mungure, T.E., Bekhit, A.E.-D.A., Birch, E.J., Stewart, I. (2016). Effect of rigor temperature, ageing and display time on the meat quality and lipid oxidative stability of hot boned beef *Semimembranosus* muscle. *Meat Science*, *114*, 146–153. https://doi.org/10.1016/j.meatsci.2015.12.015
38. Oliete, B., Carballo, J.A., Varela, A., Moreno, T., Monserrat, L., Sánchez, L. (2006). Effect of weaning status and storage time under vacuum upon physical characteristics of meat of the Rubia Gallega breed. *Meat Science*, *73*(1), 102–108. https://doi.org/10.1016/j.meatsci.2005.11.004
39. Penko, A., Polak, T., Lušnic Polak, M., Požrl, T., Kakovič, D., Žlender, B., Demšar, L. (2015). Oxidative stability of *n*-3-enriched chicken patties under different package-atmosphere conditions. *Food Chemistry*, *168*, 372–382. https://doi.org/10.1016/j.foodchem.2014.07.075
40. Popova, T., Marinova, P., Vasileva, V., Gorinov, Y., Lidji, K. (2009). Oxidative changes in lipids and proteins in beef during storage. *Archiva Zootechnica*, *12*(3), 30–38.
41. Reicks, A.L., Brooks, J.C., Garmyn, A.J., Thompson, L.D., Lyford, C.L., Miller, M.F. (2011). Demographics and beef preferences affect consumer motivation for purchasing fresh beef steaks and roasts. *Meat Science*, *87*(4), 403–411. https://doi.org/10.1016/j.meatsci.2010.11.018
42. Revilla, I., Vivar-Quintana, A.M. (2006). Effect of breed and ageing time on meat quality and sensory attributes of veal calves of the "Ternera de Aliste" Quality Label. *Meat Science*, *73*(2), 189–195. https://doi.org/10.1016/j.meatsci.2005.11.009
43. Shi, Y., Zhang, W., Zhou, G. (2020). Effects of different moisture-permeable packaging on the quality of aging beef compared with wet aging and dry aging. *Foods*, *9*(5), art. no. 649. https://doi.org/10.3390/foods9050649
44. Soglia, F., Petracci, M., Ertbjerg, P. (2016). Novel DNPH-based method for determination of protein carbonylation in muscle and meat. *Food Chemistry*, *197*, 670–675. https://doi.org/10.1016/j.foodchem.2015.11.038
45. Vieira, C., García-Cachán, M.D., Recio, M.D., Domínguez, M., Sañudo Astiz, C. (2006). Effect of ageing time on beef quality of rustic type and rustic x Charolais crossbreed cattle slaughtered at the same finishing grade. *Spanish Journal of Agricultural Research*, *4*(3), 225–234. https://doi.org/10.5424/sjar/2006043-197
46. Vitale, M., Pérez-Juan, M., Lloret, E., Arnau, J., Realini, C.E. (2014). Effect of aging time in vacuum on tenderness, and color and lipid stability of beef from mature cows during display in high oxygen atmosphere package. *Meat Science*, *96*(1), 270–277. https://doi.org/10.1016/j.meatsci.2013.07.027
47. Wiklund, E., Dobbie, P., Stuart, A., Littlejohn, R.P. (2010). Seasonal variation in red deer (*Cervus Elaphus*) venison (*M. Longissimus dorsi*) drip loss, calpain activity, colour and tenderness. *Meat Science*, *86*(3), 720–727. https://doi.org/10.1016/j.meatsci.2010.06.012
48. Zielbauer, B.I., Franz, J., Viezens, B., Vilgis, T.A. (2016). Physical aspects of meat cooking: time dependent thermal protein denaturation and water loss. *Food Biophysics*, *11*(1), 34–42. https://doi.org/10.1007/s11483-015-9410-7

ORIGINAL ARTICLE
http://journal.pan.olsztyn.pl

Polish Journal of Food and Nutrition Sciences
2023, Vol. 73, No. 1, 32–38
DOI: 10.31883/pjfns/159037
ISSN 1230-0322, e-ISSN 2083-600

Effect of Packaging on Microbial Quality of Edible Flowers During Refrigerated Storage

Aleksandra Wilczyńska*, Anita Kukułowicz, Anna Lewandowska

Department of Quality Management, Gdynia Maritime University, Morska 81-87, 81-225 Gdynia, Poland

Edible flowers are food products that are usually eaten fresh without prior heat treatment. Due to their chemical composition and low degree of processing, they can be an excellent breeding ground for microorganisms, and thus a source of infection. Methods of their preservation include proper packaging and storage at low temperatures. Therefore the aim of this study was to evaluate the effect of type of packaging (vacuum-sealed polyamide/polyethylene bag and polyethylene terephthalate box) on the microbial contamination of edible flowers including nasturtium, calendula, and daisy during refrigerated storage. The counts of selected pathogenic bacteria, total yeasts and moulds on the day of harvesting and after 1–3 days of refrigerated storage were determined. The results showed that the edible flowers did not contain *Salmonella* sp. or *Escherichia coli* (except nasturtiums), while all flowers contained both yeast and moulds at counts about 4–5 log cfu/g, and *Staphylococcus aureus* at numbers ranging from 1.89 to 2.72 log cfu/g. The differences in the counts of moulds and *S. aureus* were statistically significant depending on the type of flower. Neither the type of packaging nor storage time under refrigerated conditions influenced the degree of microbial contamination of the flowers.

Key words: nasturtium, calendula, daisy, microbiological contamination, shelf life

INTRODUCTION

Plants have been a component of human diet since the earliest times. Strong passion for consuming plant products is noticeable in Asian countries, especially in Japan, Korea, China, and Vietnam, where the phenomenon of herbophilia has been observed for years [Pinakin *et al.*, 2020]. Also, a common phenomenon is the consumption of edible flowers, called florifagia. Edible flowers (EF) are defined as flowers that can be safely consumed by humans [Lu *et al.*, 2016; Purohit *et al.*, 2021]. However, despite the fairly widespread use of flowers as food, there is still no general classification of them into edible and inedible. Edible flowers are niche products in Poland, due to their low availability (seasonality) and no traditions of their consumption. They are still treated as a decorative element of dishes and not as a source of nutrients. Nevertheless, in Poland, as in the other European countries, consumer interest in EF and dishes based on them has increased in recent years. The market for the sale of EF is expanding and, accordingly, adequate packaging for transport and trade needs to be ensured. The EF are usually packed individually and in flower boxes [Fernandes *et al.*, 2020b].

The interest in EF is growing mainly due to their aesthetic properties: unique flavours, aromas, and colours, as well as their nutritional values [Takahashi *et al.*, 2020]. EF are a rich source of carbohydrates and proteins, and do not contain excessive lipids. They also contain dietary minerals (calcium, iron, potassium, magnesium, phosphorous, and zinc) and vitamins [dos Santos *et al.*, 2018; Purohit *et al.*, 2021]. Moreover, EF represent a source of many biologically active substances, including phenolic

***Corresponding Author:**
Tel.: +386-1-320-37-42, e-mail: a.wilczynska@wznj.umg.edu.pl (A. Wilczyńska)

Submitted: 30 August 2022
Accepted: 4 January 2023
Published on-line: 20 January 2023

compounds [Fernandes *et al.*, 2017; Lu *et al.*, 2016; Mlcek & Rop, 2011]. Therefore, there are numerous health benefits from EF consumption, due to their antianxiety, anticancer, antidiabetic, anti-inflammatory, antioxidant, diuretic, anthelmintic, immunomodulatory, and antimicrobial effects [Demasi *et al.*, 2021a; Devecchi *et al.*, 2021; Lu *et al.*, 2016; Navarro-González *et al.*, 2015; Pinakin *et al.*, 2020; Skrajda-Brdak *et al.*, 2020; Zhao *et al.*, 2021].

It should be remembered, however, that in addition to compounds with a health-promoting effect, EF can be a source of anti-nutritional and even toxic substances [Klintschar *et al.*, 1999; Kristanc & Kreft, 2016 ; Lara-Cortés *et al.*, 2013; Sotelo *et al.*, 2007]. They may contain environmental pollution residues (such as heavy metals), as well as substances used in agriculture (pesticides, fertilizers) and various types of pathogenic microorganisms [Matyjaszczyk & Śmiechowska, 2019]. Due to the high content of water and nutrients, EF provide an excellent medium for many species of microorganisms, including yeasts and moulds. The EF processing may increase the risk of contamination with, among others, contaminants, total aerobic mesophilic bacteria, *Salmonella* sp., *Escherichia coli*, coliforms, yeasts, and moulds [Fernandes *et al.*, 2020a]. Subsequently, the use of contaminated EF, as an ingredient in ready-to-eat food, contributes to food spoilage and may cause foodborne outbreaks [Matyjaszczyk & Śmiechowska, 2019; Wilczyńska *et al.*, 2021]. At this point, it should be emphasized that there are no requirements for the production process and conditions for harvesting and storing edible flowers. Legal regulations relating to quality and safety assurance for EF consumption have not been developed; only Regulation (EC) No. 258/97 of the European Parliament and of the Council of 27 January 1997 concerning novel foods and novel food ingredients, provides some information about the safety of EF [Regulation (EC), 1997].

EF are usually consumed either fresh or minimally processed [Fernandes *et al.*, 2020b; Takahashi *et al.*, 2020]. Low-temperature storage is widely used as an effective preservation method to maintain the quality and extend the shelf life of EF [Fernandes *et al.*, 2019; Shantamma *et al.*, 2021]. The packaging of EF, as in the case of other fresh or minimally processed products, plays also an important role in maintaining their quality – it is a barrier between the product and the external environment and protects them against pollution, mechanical damage, and desiccation [Hussein *et al.*, 2015]. The type of packaging materials is an important factor in controlling flower deterioration. Therefore, the aim of this study was to evaluate the effect of the vacuum-sealed polyamide/polyethylene (PA/PE) bag and polyethylene terephthalate (PET) box packaging on the microbial contamination of selected edible flowers during refrigerated storage.

MATERIALS AND METHODS

Collection and storage of flowers

The research materials consisted of selected edible flowers: nasturtium (*Tropaeolum* L.), calendula (*Calendula officialis* L.), and daisy (*Bellis perennis* L.), which were freshly harvested during the 2021 harvest season directly from a commercial farm – Ogrodnictwo Lawenda, Gdańsk, Poland. The flowers were picked by hand while maintaining hygiene rules. Immediately after collection, all samples were packed in disposable food packaging (PET boxes) and then transported in a portable refrigerator to the laboratory, where the flowers were divided into three groups. One group was used for microbiological tests (day 0); from each type of flowers, 10 g were taken twice in order to obtain parallel replicates (n=6). The second group was packed in PET boxes (3 boxes of each type of flowers, 50 g each), and the third was packed in vacuum-sealed PA/PE bags (3 bags of each type of flowers, 50 g each) using a CVP-350/MS vacuum packer (CAS, Warsaw, Poland). The packed flowers, both in PET boxes and vacuum-sealed PA/PE bags, were kept in a refrigerator at 4±0.5°C for 3 days. On each day of storage, two parallel samples of 10 g of each type of flowers were taken from both PA/PE bags and PET boxes for microbiological tests (n=36). The whole experiment was repeated three times, at weekly intervals, producing a total of 126 samples that were analysed. The appearance of the stored flowers (colour, freshness, and wilting) was assessed through a daily visual inspection made by the same person.

Microbiological analyses

Microbiological analyses were performed on day 0 (control) and 1, 2, and 3 days of flower storage according to the methodology detailed in our previous article [Wilczyńska *et al.*, 2021]. Ten grams of each flower type were collected in a laminar air flow chamber and then homogenised together with 90 mL of a Ringer's solution using a Stomacher lab-blender 400 (Seward, Worthing, United Kingdom). Homogenates were subjected to further dilution. The counts of *Staphylococcus aureus, Escherichia coli*, yeasts, and moulds on the flowers was determined using the pour-plate technique. The conditions for carrying out analyses are presented in Table 1. The presence of *Salmonella* sp. was determined using

Table 1. The conditions of microbiological analyses conducted with the pour-plate technique.

Microorganism	Medium	Culture conditions
Escherichia coli	Coli ID (bioMerieux, Warsaw, Poland)	37°C, 48 h
Staphylococcus aureus	Baird-Parker agar + rabbit plasma fibrinogen (Merck, Darmstadt, Germany)	37°C, 48 h
Moulds and yeasts	Yeast extract glucose chloramphenicol agar (Merck, Darmstadt, Germany)	25°C, 120 h
Salmonella sp.	Buffered peptone water (Biomaxima, Lublin, Poland)	35°C, 24 h
	Brilliance™ *Salmonella* agar (Oxoid, Hampshire, United Kingdom)	35°C, 48 h

chromogenic Brilliance™ *Salmonella* agar for isolation and initial differentiation. *Salmonella* sp. were pre-multiplied in buffered peptone water for approx. 24 h at 35°C, and then 0.1 mL was placed on the prepared chromogenic medium and incubated at 35°C for 48 h. The results of these analyses were given as the logarithm of colony-forming units per gram of flower (log cfu/g).

Statistical analysis

The mean and standard deviations were calculated using Statistica v. 13.1 software (StatSoft, Tulsa, OK, USA). One-way and two-way analysis of variance (ANOVA) was conducted to investigate the overall effect of packaging type and storage time (days) on the extent of EF contamination with individual microorganisms. The Tukey test was used to determine significant differences between means ($p<0.05$).

RESULTS AND DISCUSSION

The visual assessment of the flowers showed that slight changes took place during the three-day refrigerated storage of nasturtium and calendula. Flowers packed both in PET boxes and vacuum-sealed PA/PE bags gently turned brown and withered. Only the daisies were unchanged in colour and showed faint signs of wilting (Figure 1). However, further sensory analysis should be carried out by qualified panellists to check how the appearance and condition of flowers will be affected by prolonged storage under refrigerated conditions. According to Demasi *et al.* [2021b], the visual appearance of most of the EF (thirteen species out of the 17 analysed in their study, including nasturtium and calendula) should be acceptable for seven days if stored at 4°C.

The degree of microbiological contamination of the EF on the harvesting day is shown in Table 2. None of the flowers was contaminated with *Salmonella* sp., which proves that proper agricultural and hygienic practices were followed in EF production and harvesting. According to Matyjaszczyk & Śmiechowska [2019], all cases of microbial contamination of EF recorded in the Rapid Alert System for Food and Feed (RASFF) were associated with the presence of different *Salmonella* sp. serotypes. *Salmonella* sp. is a bacterium that is quite common in the environment, but the sources of infection are mainly food products of animal origin [Ehuwa *et al.*, 2021]. It is an indicator of the hygienic condition of food products. In the case of products of plant origin, contamination with this bacterium may occur during cultivation and various post-harvest operations. The sources of contamination with *Salmonella* during processing and post-harvest operations may include workers, equipment as well as inadequate process management and packaging [Ehuwa *et al.*,

Figure 1. Flower appearance after 3 days of refrigerated storage; A – nasturtiums in vacuum-sealed polyamide/polyethylene (PA/PE) bags, B – calendula in vacuum-sealed PA/PE bags, C – daisy in vacuum-sealed PA/PE bags, D – nasturtiums in polyethylene terephthalate (PET) box, E – calendula in PET box, F – daisy in PET box.

Table 2. Counts of *Escherichia coli, Salmonella* sp., *Staphylococcus aureus*, yeasts, and moulds on flowers (log cfu/g) on harvest day.

Flower	*Escherichia coli*	*Salmonella*	*Staphylococcus aureus*	Moulds	Yeasts
Nasturtium	1.19±1.48	nd	2.05±0.56^{b}	5.06±0.48^{a}	4.48±0.76^{a}
Calendula	nd	nd	1.89±0.16^{b}	4.40±1.07^{a}	4.18±1.12^{a}
Daisy	nd	nd	2.72± 0.32^{a}	3.90±0.26^{b}	4.56±0.59^{a}

nd, not detected in samples. Results are expressed as mean ± standard deviation. Different letters in column show significant differences between means at $p<0.05$.

2021; Popa & Popa, 2021]. A major contributor to foodborne illness outbreaks is post-processing contamination [Jung *et al.*, 2014; Matyjaszczyk & Śmiechowska, 2019].

The results indicate that the nasturtium was the only flower type contaminated with *E. coli* (Table 2). Fernandes *et al.* [2020a] reported that counts for total coliforms and *E. coli* were less than 1 log cfu/g in the fresh flowers they analysed. *E. coli* is one of the most common indicators of food contamination, the absence of *E. coli* proves that the sanitary conditions or hygiene practices during or after food production have been maintained. The presence of coliforms on nasturtiums in our study, may be due to the fact that they were grown in a site richly fertilized with natural manure, which could be a source of contamination.

The count of *S. aureus* ranged from 1.89 log cfu/g in calendula flowers to 2.72 log cfu/g in daisies (Table 2) and was significantly higher in daisies (F=328.53, p=0.00004). These contamination rates of EF with *S. aureus* were smaller than contamination rates of ready-to-eat salads estimated at an average of 3 log cfu/g by Habibi Najafi & Bahreini [2012] and Saifullah *et al.* [2018]. The presence of *S. aureus* is an indicator of poor hygienic conditions, as this bacterium is mainly transferred by personnel in contact with food [Habibi Najafi & Bahreini, 2012]. According to Microbiological Guidelines for Food [2014], the acceptable contamination level with *S. aureus* in ready-to-eat foods should not exceed 20 cfu/g, while the level observed in EF (approx. 2 log cfu/g) in the present study is defined as borderline. All samples were contaminated with *S. aureus*, which could lead to foodborne infection.

All flowers were contaminated with moulds at counts ranging from 3.90 to 5.06 log cfu/g, and with yeasts at counts ranging from 4.18 to 4.56 log cfu/g (Table 2). Mould number was significantly lower in daisies (F=3.76, p=0.03), while the number of yeasts did not differ significantly between the flower types ($p\geq0.05$). Habibi Najafi & Bahreini [2012] who tested ready-to-eat salads and fresh herbs in Mashhad (Iran), isolated a similar amount of yeasts and moulds at levels ranging between 3.85 and 6.7 log cfu/g. Adeyemi *et al.* [2019] reported that the fungal count ranged from 4.22 to 4.46 log cfu/g in fresh salads. In turn, Kowalska & Szczech [2022] detected moulds in 106 (87%) samples of leafy green vegetables and found the highest average count of moulds (5.40 log cfu/g) in rocket. In the last mentioned publication, it was also reported that almost all the vegetables examined were contaminated with yeasts (with the exception of two iceberg lettuce samples and one chive sample), and the average yeast count was the highest in lamb's lettuce, parsley, and rocket – 5.94, 5.63, and 5.62 log cfu/g, respectively. Lara-Cortés *et al.* [2016] determined the fungal count of about 5.7 log cfu/g on dahlia packaged in PET. In the present study, a similar number of fungi was detected in nasturtium while counts of yeasts and moulds in daisies and calendula were lower by around 1.5 logarithmic unit. Fernandes *et al.* [2020a] reported average counts of yeasts and moulds in fresh edible flowers at the level of 2 log cfu/g, which was much lower than in the present study. Additionally, it was found that the low-temperature conditions (–18°C) had a protective effect against the growth of some spoilage microorganisms and foodborne pathogens, as their counts decreased or remained the same after three-month storage under these conditions for most of the flowers.

Comparing the present study results with the general guidelines for the number of non-pathogenic microorganisms in various types of unprocessed vegetables and fruits causing spoilage of these products (established for moulds and yeasts at $\leq10^3$ cfu/g) [Ragaert *et al.*, 2010], it can be concluded that EF are heavily contaminated with these microorganisms. EF can be contaminated with moulds and yeasts at any stage of their life cycle: during cultivation, harvest, transport, and marketing [Tournas, 2005]. High levels of fungi found on flowers may affect their nutritional and sensory characteristics. This is because these microorganisms change and accelerate the aging process of stored flowers and can produce volatile compounds responsible for off-flavours and texture changes [Rawat, 2015]. The presence of moulds and yeasts is also undesirable due to their potential adverse effects on human health – some of them (*Aspergillus, Penicillium, Alternaria* or *Fusarium*) may produce mycotoxins and others may cause allergies (*Cladosporium, Alternaria*) [Habibi Najafi & Bahreini, 2012; Kowalska & Szczech, 2022; Tournas, 2005].

The types of flowers differed in terms of the count of moulds and *S. aureus*. It is difficult to identify the causes of these differences. In the world literature, there are only few articles on the microbial contamination of edible flowers. Some species of flowers may be resistant to microbiological inoculation due to the content of phenolic compounds. It has been proven that flavonoids, such as flavanones, flavones and flavonols, inhibit the growth of *Candida albicans* and *Aspergillus flavus* [Cushnie & Lamb, 2005; Prasad *et al.*, 2014; Selma *et al.*, 2009]. Quercetin inhibits the development of pathogenic microorganisms, *e.g. S. aureus, Enterococcus faecalis, Bacillus subtilis, E. coli*. Anthocyanins, in turn, exert bacteriostatic and bactericidal effects against many microorganisms (including *Staphylococcus, Klebsiella, Helicobacter, Bacillus*). Phenolic compounds also elicit an inhibitory effect on viruses [Cushnie & Lamb, 2005]. The contents of the above-mentioned compounds in the tested flowers vary from low to high; therefore, they may have different inhibitory effects against microorganisms [Pires *et al.*, 2021].

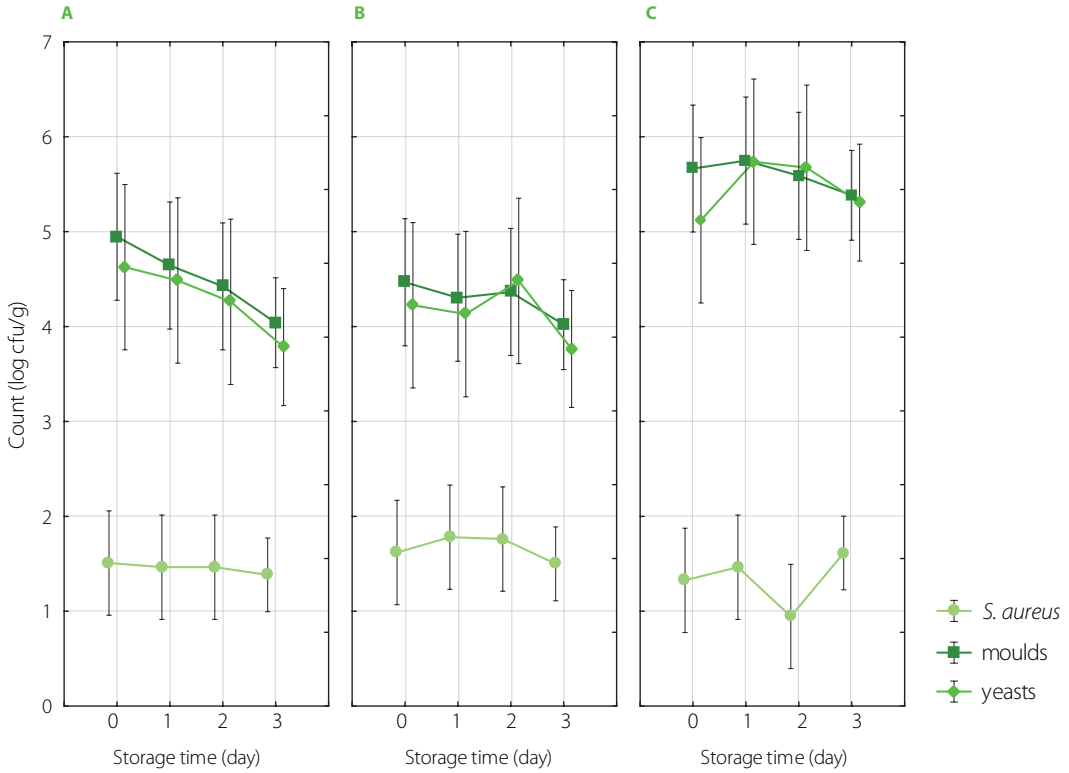

Figure 2. Counts of *Staphylococcus aureus*, yeasts, and moulds on edible flowers on harvesting day and after 1–3-day refrigerated storage (4°C); A – nasturtium, B – calendula, C – daisy.

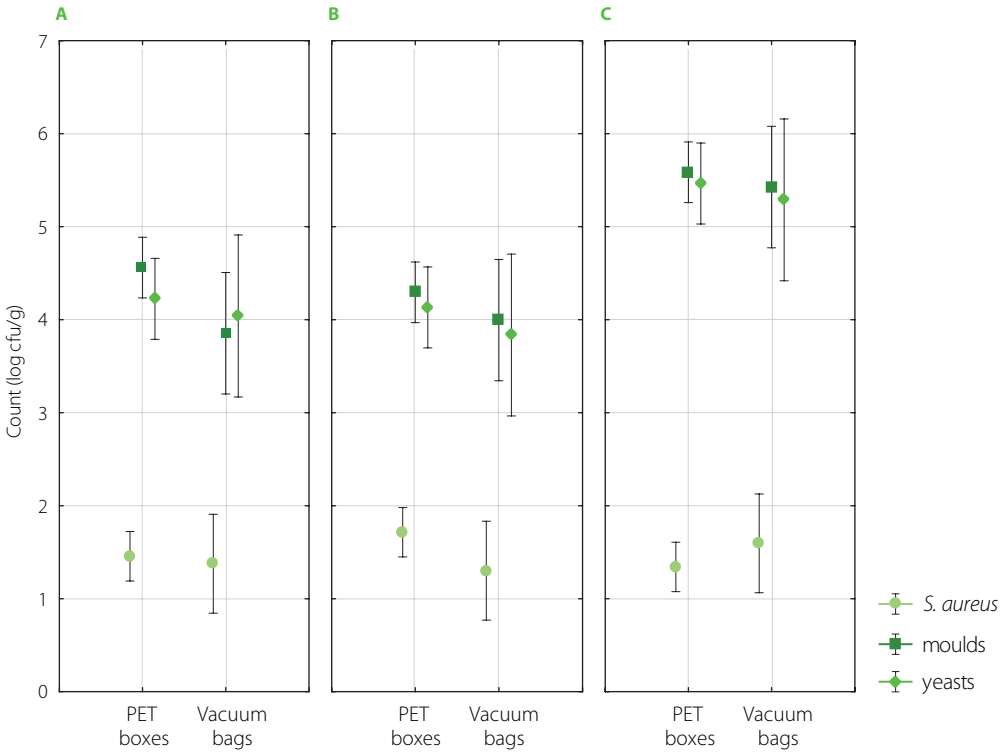

Figure 3. Counts of *Staphylococcus aureus*, yeasts, and moulds on edible flowers packed in polyethylene terephthalate (PET) boxes and vacuum-sealed polyamide/polyethylene (PA/PE) bags after 3-day refrigerated storage (4°C); A – nasturtium, B – calendula, C – daisy.

The counts of *S. aureus*, yeasts, and moulds on edible flowers on harvesting day and during successive storage at low temperature (4°C) are shown in Figure 2. Flowers stored for 3 days had similar counts of *S. aureus*, yeasts, and moulds. A slight decrease in the number of moulds and yeasts was noticed only in the case of nasturtium flowers (by 1 log cfu/g), but it was not a significant ($p \geq 0.05$) decrease. Figure 3 shows the differences in counts of *S. aureus*, yeasts, and moulds

on edible flowers packed in different packagings (PET box and vacuum-sealed PA/PE bags) after 3-day storage. The type of packaging did not significantly ($p \geq 0.05$) affect the number of microorganisms either. The counts of *S. aureus*, moulds, and yeasts were slightly lower after three days of refrigerated storage in vacuum-sealed PA/PE bags, but these differences were not statistically significant ($p \geq 0.05$). The two-way analysis of variance also showed that the combination of these factors (storage time and packaging type) had no significant effect on the development of microflora ($p \geq 0.05$).

Packaging is the main tool to protect flowers from desiccation and to preserve their frail structure. It provides a barrier between flowers and the outside environment, thereby minimising their exposure to pathogens and other contaminants [Hussein *et al.*, 2015]. Microbes have different growth requirements; hence, the use of different packaging methods can delay or prevent their growth [Fernandes *et al.*, 2019]. However, bacteria and fungi are unpredictable and some of them can still grow despite the measures taken, and cause spoilage of edible flowers [Rawat, 2015]. Also low-temperature storage is one of the easiest and simplest methods of EF preservation. It was observed that EF could be satisfactorily stored for 7 to 14 days at 4°C depending on species [Demasi *et al.*, 2021b]. The present study confirmed that combining two methods of preservation – storage in proper conditions (time, temperature) and packaging allowed maintaining an unchanged level of microbial contamination: there were no significant changes in the number of bacteria and moulds and yeasts after 3 days of refrigerated storage. However, there still remains the problem of preserving the appearance of the flowers during storage – how to store EF so that they retain their freshness and proper sensory characteristics as long as possible.

CONCLUSIONS

The present research indicated that the most important factors influencing the microbiological population on edible flowers, and thus the safety of their consumption, are pre-harvest factors. However, proper packaging and refrigerated storage for 3 days kept the microbiological contamination level unchanged. Neither the type of packaging nor storage in refrigerated conditions influenced the extent of microbial contamination of flowers. However, further research should be carried out into the long-term storage of packaged edible flowers under refrigeration conditions. It is also necessary to look for other ways to preserve EF. Taking into account results shown, it is necessary to inform the flowers suppliers that the level of microbiological contamination of flowers depends primarily on the growing conditions, but proper post-harvest treatment (appropriate harvesting, packaging, and storage) prevents cross-contamination and inhibits the further development of microorganisms.

RESEARCH FUNDING

Authors would like to thank Gdynia Maritime University for providing funds for this study (Project WZNJ/2022/PZ/01).

CONFLICT OF INTERESTS

Authors declare no conflict of interest.

ORCID IDs

A. Kukułowicz https://orcid.org/0000-0002-7520-7992
A. Wilczyńska https://orcid.org/0000-0003-4434-0819

REFERENCES

1. Adeyemi, O.A., Fejukui, B.M., Adeyemi, O.O. (2019). Microbial contamination of fresh vegetable salads from food vendors in Oyo Metropolis. *Nigerian Journal of Pure and Applied Sciences*, *32*(1), 3374–3379. https://doi.org/10.6084/m9.figshare.12284285
2. Cushnie, T.P.T., Lamb, A.J. (2005). Antimicrobial activity of flavonoids. *International Journal of Antimicrobial Agents*, *26*(5), 343–356. https://doi.org/10.1016/j.ijantimicag.2005.09.002
3. Demasi, S., Caser, M., Donno, D., Ravetto Enri, S., Lonati, M., Scariot, V. (2021a). Exploring wild edible flowers as a source of bioactive compounds: New perspectives in horticulture. *Folia Horticulturae*, *33*(1), 27–48. https://doi.org/10.2478/fhort-2021-0004
4. Demasi, S., Mellano, M.G., Falla, N.M., Caser, M., Scariot, V. (2021b). Sensory profile, shelf life, and dynamics of bioactive compounds during cold storage of 17 edible flowers. *Horticulturae*, *7*(7), art. no. 166. https://doi.org/10.3390/horticulturae7070166
5. Devecchi, A., Demasi, S., Saba F., Rosato, R., Gambino, R., Ponzo, V., De Francesco, A., Massarenti, P., Bo, S., Scariot, V. (2021). Compositional characteristics and antioxidant activity of edible rose flowers and their effect on phenolic urinary excretion. *Polish Journal of Food and Nutrition Sciences*, *71*(4), 383–392. https://doi.org/10.31883/pjfns/142639
6. dos Santos, A.M.P., Silva, E.F.R., dos Santos, W.N.L., da Silva, E.G.P., dos Santos, L.O., da S. Santos, B.R, da S. Sauthier M.C., dos Santos, W.P.C. (2018). Evaluation of minerals, toxic elements and bioactive compounds in rose petals (*Rosa* spp.) using chemometric tools and artificial neural networks. *Microchemical Journal*, *138*, 98–108. https://doi.org/10.1016/j.microc.2017.12.018
7. Ehuwa O., Jaiswal A.K., Jaiswal S. (2021). *Salmonella*, food safety and food handling practices. *Foods*, *10*(5), art. no. 907. https://doi.org/10.3390/foods10050907
8. Fernandes, L., Casal, S., Pereira, J.A., Lopes Pereira, E., Saraiva, J.A., Ramalhosa, E. (2020a). Freezing of edible flowers: Effect on microbial and antioxidant quality during storage. *Journal of Food Science*, *85*(4), 1151–1159. https://doi.org/10.1111/1750-3841.15097
9. Fernandes, L., Casal, S., Pereira, J.A., Saraiva, J.A., Ramalhosa, E. (2017). Edible flowers: A review of the nutritional, antioxidant, antimicrobial properties and effects on human health. *Journal of Food Composition and Analysis*, *60*, 38–50. https://doi.org/10.1016/j.jfca.2017.03.017
10. Fernandes, L., Casal, S., Pereira, J.A., Saraiva, J.A., Ramalhosa, E. (2020b). An overview on the market of edible flowers. *Food Reviews International*, *36*(3), 258–275. https://doi.org/10.1080/87559129.2019.1639727
11. Fernandes, L., Saraiva, J.A., Pereira, J.A., Casal, S., Ramalhosa, E. (2019). Post-harvest technologies applied to edible flowers: A review. Edible flowers preservation. *Food Reviews International*, *35*(2), 132–154. https://doi.org/10.1080/87559129.2018.1473422
12. Habibi Najafi, M.B., Bahreini, M. (2012). Microbiological quality of mixed fresh-cut vegetable salads and mixed ready-to-eat fresh herbs in Mashhad, Iran. *International Conference on Nutrition and Food Sciences IPCBEE*, *39*, 62–66.
13. Hussein, Z., Caleb, O.J., Opara, U.L. (2015). Perforation-mediated modified atmosphere packaging of fresh and minimally processed produce—A review. *Food Packaging and Shelf Life*, *6*, 7–20. https://doi.org/10.1016/j.fpsl.2015.08.003
14. Jung, Y., Jang, H., Matthews, K.R. (2014). Effect of the food production chain from farm practices to vegetable processing on outbreak incidence. *Microbial Biotechnology*, *7*(6), 517–527. https://doi.org/10.1111/1751-7915.12178
15. Klintschar, M., Beham-Schmidt, C., Radner, H., Henning, G., Roll, P. (1999). Colchicine poisoning by accidental ingestion of meadow saffron (*Colchicum autumnale*): Pathological and medicolegal aspects. *Forensic Science International*, *106*(3), 191–200. https://doi.org/10.1016/S0379-0738(99)00191-7
16. Kowalska, B., Szczech, M. (2022). Differences in microbiological quality of leafy green vegetables. *Annals of Agricultural and Environmental Medicine*, *29*(2), 238–245. https://doi.org/10.26444/aaem/149963
17. Kristanc, L., Kreft, S. (2016). European medicinal and edible plants associated with subacute and chronic toxicity part I: Plants with carcinogenic,

teratogenic and endocrine-disrupting effects. *Food and Chemical Toxicology*, *92*, 150–164.
https://doi.org/10.1016/j.fct.2016.04.007

18. Lara-Cortés, E., Osorio-Díaz, P., Jiménez-Aparicio, A., Bautista-Baños, S. (2013). Nutritional content, functional properties and conservation of edible flowers. Review. *Archivos Latinoamericanos de Nutricion*, *63*(3), 197–208 (in Spanish; English abstract).
19. Lara-Cortés, E., Troncoso-Rojas, R., Hernández-López, M., Bautista-Baños, S. (2016). Evaluation of the antimicrobial activity of cinnamaldehyde in the preservation of edible dahlia flowers, under different storage conditions. *Revista Chapingo Serie Horticultura*, *22*(3).
https://doi.org/10.5154/r.rchsh.2016.02.002
20. Lu, B., Li, M., Yin, R. (2016). Phytochemical content, health benefits, and toxicology of common edible flowers: A review (2000–2015). *Critical Reviews in Food Science and Nutrition*, *56*(sup1), S130–S148.
https://doi.org/10.1080/10408398.2015.1078276
21. Matyjaszczyk, E., Śmiechowska, M. (2019). Edible flowers. Benefits and risks pertaining to their consumption. *Trends in Food Science and Technology*, *91*, 670–674.
https://doi.org/10.1016/j.tifs.2019.07.017
22. *Microbiological Guidelines for Food (For ready-to-eat food in general and specific food items)* (2014). Centre for Food Safety, Food and Environmental Hygiene Department, Hong Kong, China, pp. 11–12.
23. Mlcek, J., Rop, O. (2011). Fresh edible flowers of ornamental plants – A new source of nutraceutical foods. *Trends in Food Science and Technology*, *22*(10), 561–569.
https://doi.org/10.1016/j.tifs.2011.04.006
24. Navarro-González, I., González-Barrio, R., García-Valverde, V., Bautista-Ortín, A.B., Periago, M.J. (2015). Nutritional composition and antioxidant capacity in edible flowers: Characterisation of phenolic compounds by HPLC-DAD-ESI/MS^n. *International Journal of Molecular Sciences*, *16*(1), 805–822.
https://doi.org/10.3390/ijms16010805
25. Pinakin, D.J., Kumar, V., Suri, S., Sharma, R., Kaushal, M. (2020). Nutraceutical potential of tree flowers: A comprehensive review on biochemical profile, health benefits, and utilization. *Food Research International*, *127*, art. no. 108724.
https://doi.org/10.1016/j.foodres.2019.108724
26. Pires, E.d.O., Jr., Di Gioia, F., Rouphael, Y., Ferreira, I.C.F.R., Caleja, C., Barros, L., Petropoulos, S.A. (2021). The compositional aspects of edible flowers as an emerging horticultural product. *Molecules*, *26*(22), art. no. 6940.
https://doi.org/10.3390/molecules26226940
27. Popa, G.L., Popa, M.I. (2021). *Salmonella* spp. infection – a continuous threat worldwide. *Germs*, *11*(1), 88–96.
https://doi.org/10.18683/germs.2021.1244
28. Prasad, V.G.N.V., Vamsi krishna, B., Swamy, P.L., Rao, T.S., Rao, G.S. (2014). Antibacterial synergy between quercetin and polyphenolic acids against bacterial pathogens of fish. *Asian Pacific Journal of Tropical Disease*, *4*(sup1), S326–S329.
https://doi.org/10.1016/S2222-1808(14)60464-3
29. Purohit, S.R., Rana, S.S., Idrishi, R., Sharma, V., Ghosh, P. (2021). A review on nutritional, bioactive, toxicological properties and preservation of edible flowers. *Future Foods*, *4*, art. no. 100078.
https://doi.org/10.1016/j.fufo.2021.100078
30. Ragaert, P., Jacxsens, L., Vandekinderen, I., Baert, L., Devlieghere, F. (2010). Microbiological and safety aspects of fresh-cut fruits and vegetables. In O. Martin-Belloso, R. Soliva Fortuny (Eds.), *Advances in Fresh-Cut Fruits and Vegetables Processing*, CRC Press, Boca Raton, Florida, USA, pp. 53–86.
https://doi.org/10.1201/b10263
31. Rawat, S. (2015). Food spoilage: Microorganisms and their prevention. *Asian Journal of Plant Science and Research*, *5*(4), 47–56.
32. Regulation (EC) No. 258/97 of the European Parliament and of the Council of 27 January 1997 concerning novel foods and novel food ingredients (2019). *Official Journal of the European Communities, L 43*, 14.2.1997, 1–6.
33. Selma, M.V., Espín, J.C., Tomás-Barberán, F.A. (2009). Interaction between phenolics and gut microbiota: Role in human health. *Journal of Agricultural and Food Chemistry*, *57*(15), 6485–6501.
https://doi.org/10.1021/jf902107d
34. Shantamma, S., Vasikaran, E.M., Waghmare, R., Nimbkar, S., Moses, J.A., Anandharamakrishnan, C. (2021). Emerging techniques for the processing and preservation of edible flowers. *Future Foods*, *4*, art. no. 100094.
https://doi.org/10.1016/j.fufo.2021.100094
35. Skrajda-Brdak, M., Dąbrowski, G., Konopka, I. (2020). Edible flowers, a source of valuable phytonutrients and their pro-healthy effects – A review. *Trends in Food Science and Technology*, *103*, 179–199.
https://doi.org/10.1016/j.tifs.2020.06.016
36. Sotelo, A., López-García, S., Basurto-Peña, F. (2007). Content of nutrient and antinutrient in edible flowers of wild plants in Mexico. *Plant Foods for Human Nutrition*, *62*(3), 133–138.
https://doi.org/10.1007/s11130-007-0053-9
37. Takahashi, J.A., Rezende, F.A.G.G., Moura, M.A.F., Dominguete, L.C.B., Sande, D. (2020). Edible flowers: Bioactive profile and its potential to be used in food development. *Food Research International*, *129*, art. no. 108868.
https://doi.org/10.1016/j.foodres.2019.108868
38. Tournas, V.H. (2005). Moulds and yeasts in fresh and minimally processed vegetables, and sprouts. *International Journal of Food Microbiology*, *99*(1), 71–77.
https://doi.org/10.1016/j.ijfoodmicro.2004.08.009
39. Wilczyńska, A., Kukułowicz, A., Lewandowska, A. (2021). Preliminary assessment of microbial quality of edible flowers. *LWT – Food Science and Technology*, *150*, art. no. 111926.
https://doi.org/10.1016/j.lwt.2021.111926
40. Zhao, M., Fan, J., Liu, Q., Luo, H., Tang, Q., Li, C., Zhao, J., Zhang, X. (2021). Phytochemical profiles of edible flowers of medicinal plants of *Dendrobium officinale* and *Dendrobium devonianum*. *Food Science and Nutrition*, *9*(12), 6575–6586.
https://doi.org/10.1002/fsn3.2602

ORIGINAL ARTICLE
http://journal.pan.olsztyn.pl

Polish Journal of Food and Nutrition Sciences
2023, Vol. 73, No. 1, 39–49
DOI: 10.31883/pjfns/159290
ISSN 1230-0322, e-ISSN 2083-6007

Effect of UV-C Postharvest Disinfection on the Quality of Fresh-Cut 'Tommy Atkins' Mango

Alba Mery Garzón-García[1, 2], Saúl Ruiz-Cruz[2]*, Saúl Dussán-Sarria[1], José Igor Hleap-Zapata[1], Enrique Márquez-Ríos[2], Carmen Lizette Del-Toro-Sánchez[2], José Agustín Tapia-Hernández[2], Dalila Fernanda Canizales-Rodríguez[3], Víctor Manuel Ocaño-Higuera[3]

[1]Facultad de Ingeniería y Administración, Universidad Nacional de Colombia - Sede Palmira / Faculty of Engineering and Administration, National University of Colombia-Palmira Campus, Carrera 32 No. 12-00, 763533, Palmira, Colombia
[2]Departamento de Investigación y Posgrado en Alimentos, Universidad de Sonora / Department of Research and Postgraduate in Food, University of Sonora, Blvd. Luis Encinas y Rosales s/n, Hermosillo 83000, Sonora, México
[3]Departamento de Ciencias Químico Biológicas, Universidad de Sonora / Department of Chemical-Biological Sciences, University of Sonora, Blvd. Luis Encinas y Rosales s/n, Hermosillo 83000, Sonora, México

Mango cv. 'Tommy Atkins' is a highly appreciated fruit for its organoleptic characteristics and its resistance to minimal processing. However, some operations as peeling and cutting can generate microbial contamination and loss of bioactive compounds. Ultraviolet short wave (UV-C) is an alternative technology for fresh-cut products that leads to microbial inactivation and the increase of beneficial compounds. The effect of a UV-C dose of 6 kJ/m^2 was evaluated on quality attributes of fresh-cut 'Tommy Atkins' mango during days 0, 3, 6, 9, and 12 of storage (5°C, relative humidity: 85-90%), and compared with a positive control (conventional method by immersion in 10 mg/L sodium hypochlorite solution) and a negative control (without treatment). Physicochemical analysis (titratable acidity, pH, total soluble solid content, and firmness), superficial color evaluation, determinations of microbial counts, contents of total carotenoids, phenolics and flavonoids, and antioxidant capacity assays were performed. The results showed that UV-C treatment allowed to preserve microbial safety and superficial color of stored fresh-cut mango, and to increase the content of total carotenoids, which was 19.34 and 26.50 mg β-carotene/100 g fresh weight (FW) for control and UV-C treated sample at day 12 of storage, respectively. The DPPH$^•$ scavenging activity of the UV-C treated mango was also higher (0.60 mM TE/g FW) compared to control (0.27 mM TE/g FW) at the end of storage. However, UV-C treatment caused loss of firmness. Some native microorganisms of mango adapted to the stress caused by the treatments and the storage.

Key words: minimal processing, surface color, native microorganisms, predictive microbiology, ultraviolet short wave irradiation

INTRODUCTION

Mango (*Mangifera indica* L.) is a tropical fruit with high production and consumption in the world due to its attractive sensorial attributes and nutritional value [Maldonado-Celis *et al.*, 2019]. It is a source of dietary fiber, vitamins, carbohydrates, fatty acids, and amino acids as well as presents a considerable biological activity by the high content of phenolic compounds, terpenoids, sterols, and carotenoids [Kumar *et al.*, 2021]. The main producing regions of mango in the world are Asia (60% of world production), Latin America (25%), and Africa (14%) [Santo *et al.*,

***Corresponding Author:**
Tel.: +52 6441250653, Fax: +52 6622592208, e-mail: saul.ruizcruz@unison.mx (S. Ruiz-Cruz)

Submitted: 23 September 2022
Accepted: 13 January 2023
Published on-line: 16 February 2023

2018]. There are more than 1,000 mango cultivars in the world, but the main cultivars harvested in Latin America for commercialization are 'Kent', 'Keitt', 'Ataulfo', 'Tommy Atkins', and 'Haden' [Kansci *et al.*, 2008]. 'Tommy Atkins' cultivar is one of the most appreciated as it is characterized by its large size and color, its resistance to handling, and its potential for minimal processing [Djioua *et al.*, 2010].

Fresh-cut fruits have similar properties to fresh fruits, and their consumption is implied to confer multiple benefits for human health, including the prevention of different chronic, degenerative, and cardiovascular diseases [Artés-Hernández *et al.*, 2017]. However, these products are highly susceptible to microbial growth because their protective tissue is removed and cell contents are released during cutting operation, thereby they serve as a substrate for microorganisms that cause decay and development of human pathogens [Artés-Hernández *et al.*, 2021]. Accordingly, it is important to comply with strict hygiene and manufacturing practices and to recognize critical control points during processing [De Corato, 2020]. For storage, it is necessary to ensure low temperatures and a packaging to control the fresh-cut fruit metabolic activity and accelerated microbial growth. Modified or controlled atmosphere are usually applied using polymeric films and containers, which allows to prevent the flow of respiratory gases, reduce O_2 concentration, and rise CO_2 concentration in the package headspace [Giannakourou & Tsironi, 2021].

With the increase in the consumption of fresh-cut fruits, a concern has arisen regarding the effectiveness of disinfection methods in reducing microorganisms that cause foodborne diseases [Hinojosa *et al.*, 2013]. Different chemical and physical methods have been studied for the disinfection of fresh-cut fruits. The ultraviolet short wave (UV-C) irradiation is an emerging physical technology that inactivates microorganisms and simultaneously induces defense mechanisms in plant. This leads to the production of phytoalexins after treatment and allows to improve the conservation and attributes of minimally-processed fruits [Zambrano-Zaragoza *et al.*, 2021]. These effects depend on the dose of UV-C, although the beneficial effects are attributed to short doses (low dose of radiation or short exposure times).

Different studies have indicated that UV-C treatment preserves quality attributes of fresh-cut mango during storage. González-Aguilar *et al.* [2007] found that irradiation of fresh-cut 'Tommy Atkins' mango for 1 to 10 min induced the accumulation of phenolics and increased antioxidant capacity during storage for 15 days at 5°C. UV-C treatment of 'Kent' mango slices for 30 s had a positive effect on the physicochemical characteristics and produced lower counts of mesophiles, psychrophiles and molds and yeasts, compared to control samples [Márquez-Villacorta *et al.*, 2011]. Irradiation of fresh-cut 'Kent' mango with 14 kJ/m^2 resulted in lower counts of mesophiles and molds and yeasts, and an increment of contents of total phenolics and flavonoids during 15 days of storage at 5°C [Márquez-Villacorta & Pretell-Vásquez, 2013]. However, the treatment doses should be determined empirically for the specific research material. In our preliminary studies, an optimal UV-C dose of 6 kJ/m^2 was estimated for the inactivation of less than 2 log cfu/g of *Escherichia coli* O157:H7, *Salmonella* Typhimurium and *Listeria monocytogenes* on fresh-cut 'Tommy Atkins' mango. The aim of this research was to evaluate the effects of this UV-C dose on the safety and quality attributes of fresh-cut 'Tommy Atkins' mango during refrigerated storage.

MATERIALS AND METHODS

Plant material

Mango fruits (*Mangifera indica* L. cv. 'Tommy Atkins') in stage 3 of maturity were purchased from a Hermosillo (México) local market. Stage of maturity was determined according to the total soluble solid content for this cultivar [Lopes *et al.*, 2021]. Ten kg of fruit with uniform size and maturity were stored at 5°C for 24 h. Subsequently, mangoes were washed, cleaned for 5 min with a 200 mg/L sodium hypochlorite solution, and left to dry in the air.

Fresh-cut mango processing

Peel and seed were removed from fruits. Pulp was cut into 10×60×20 mm spears and divided to three lots. The first lot (C, control) consisted of fresh-cut mango without treatment. The second lot (H) was immersed in a 10 mg/L sodium hypochlorite (NaClO) solution for 1 min and drained for 2 min [Djioua *et al.*, 2010]. A UV-C dose of 6 kJ/m^2 established by Rodríguez-Mijangos *et al.* [2014] was applied to the third lot (UV-C treatment) in a portable disinfection chamber. Groups of three spears were arranged in the center of the equipment at 75 mm from the radiation source for 26 min and 48 s. Approximately 90 g of fresh-cut fruit from each lot were distributed in polyethylene terephthalate (PET) containers (12 cm long, 10 cm wide, and 6 cm high). Fifteen containers per each lot were used for quality analyses. Fresh-cut mango was stored under refrigeration at 5°C with a relative humidity (RH) of 85-90% for 12 days.

Analyses of pH, titratable acidity, total soluble solid content, and firmness

Titratable acidity (TA), pH, total soluble solid (TSS) content, and firmness analyses were performed. pH was measured with a potentiometer (STARTER 2100, OHAUS, Nänikon, Switzerland). TA was assessed by titration with 0.1 N NaOH (Thermo Fisher Scientific, Waltham, MA, USA) considering citric acid as a predominant organic acid in mango. TSS content was determined according to International AOAC 932.12 method using a manual refractometer [AOAC, 2012]. Firmness was measured with a texture analyzer (EZ-S, Shimadzu, Kyoto, Japan) through a Warner-Bratzler shear force test following the methodology proposed by Lázaro & De Lorenzo [2015] with some modifications. The mango samples were cut crosswise with a 2 mm thick Warner-Bratzler steel blade at a test speed of 100 mm/s. Firmness was considered as the maximum force applied to break a piece of mango.

Measurements of color parameters

Mango surface color parameters were evaluated with a MiniScan XE plus portable colorimeter (HunterLab, Reston, VA, USA) in

CIELab tristimulus coordinates: L^* (lightness: white(+)/black(–)), a^* (red(+)/green(–)), and b^* (yellow(+)/blue(–)). Equipment was calibrated with a reflector plate (X=80.1, Y=85, Z=90.6) considering a standard illuminant D65 and a 10° observer. Chroma (C^*), hue angle ($h°$), and total color difference (ΔE) were calculated with the following formulas [Pathare *et al.*, 2013]:

$$C^* = (a^{*2} + b^{*2})^{\frac{1}{2}} \quad (1)$$

$$h° = tan^{-1}(b^* / a^*) \quad (2)$$

$$\Delta E = (\Delta L^{*2} + \Delta a^{*2} + \Delta b^{*2})^{\frac{1}{2}} \quad (3)$$

Microbial count analysis

According to Hinojosa *et al.* [2013], three randomized samples of 15 g for each treatment were individually homogenized in 135 mL of 0.1% peptone water (Difco, Fisher Scientific, Hampton, NH, USA) in a sterile stomacher bag (Nasco, Whirl-Pak, Madison, WI, USA) for 2 min. Serial dilutions were prepared with 0.1% peptone water. For each dilution, aliquots of 1 and 5 mL were plated in triplicate on different mediums (a total of six Petri dishes per sample). Plates with plate count agar (Difco) and violet red bile agar (BD, Franklin Lakes, NJ, USA) were incubated for approximately 48 h (Analog Incubator 132000, Boekel Scientific, Feasterville, PA, USA) for aerobic mesophilic and total coliform counts, respectively. Plates with plate count agar and potato dextrose agar (Difco) were incubated for 7 days at 5°C and 22°C to count psychrotrophic bacteria and yeast and molds, respectively. The results were expressed as log colony forming units (cfu) per g of fresh-cut mango. The microbial quality of fresh-cut mango was evaluated following Colombian microbial legislation for minimally processed fruits [Ministry of Health and Social Protection of Colombia, 2013].

Inactivation kinetic modelling

A model of inactivation of microorganisms was developed using the linear logarithmic equation and Weibull model as a function of storage days [van Boekel, 2002] using formulas (4) and (5), respectively.

$$\log(N / N_0) = -kt / 2.303 \quad (4)$$

$$\log(N / N_0) = (-1 / 2.303)(t / \alpha)^{\beta} \quad (5)$$

where: N_0 and N are the numbers of initial and surviving microorganisms, respectively, and t corresponds to time of storage (day), k is the inactivation rate constant (1/day), α is the characteristic time (day), and β is the shape factor.

The inactivation parameters were estimated with the averages of the logarithmic reductions of the microbial populations during the storage time. Linear least squares method and non-linear least squares method with the resolution of the Gauss-Newton algorithm (maximum number of iterations of 200 and a convergence tolerance of 0.00001) were used to fit the inactivation data of microorganisms to the logarithmic linear equation and to the Weibull model, respectively. The fit of the models was evaluated by calculating the coefficient of determination (R^2), the adjusted coefficient of determination (adjusted R^2), and the root mean square error (RMSE).

Extract preparation

Two grams of mango samples were added to 3 mL of absolute ethanol. The solutions were mixed (MX-S vortex mixer, Science Med, Helsinki, Finland), sonicated for 30 min (Branson 1800 Digital Bath, Emerson, St. Louis, MO, USA), and placed in refrigeration and darkness for night. Subsequently, these solutions were centrifuged at 257×*g* for 20 min (Compact II centrifuge, BD). The supernatant was used for the quantification of bioactive compounds.

Total carotenoid content determination

Following the method proposed by González-Vega *et al.* [2021], 300 µL of each extract were added in triplicate to wells of the microplate, and absorbance was measured at 450 nm in a 96-well microplate reader (Multiskan GO, Thermo Fisher Scientific). A calibration curve was plotted with concentrations between 0.002 and 0.1 mg/mL of β-carotene standard (Sigma-Aldrich, St. Louis, MO, USA) (R^2=0.991). Results were reported as mg β-carotene equivalents per 100 g of fresh weight (FW) of mango.

Determination of total phenolic and flavonoid contents

The total contents of phenolics and flavonoids were determined following Pérez-Perez *et al.* [2021] methodology. For total phenolic content, 10 µL of each extract and 25 µL of 0.2 M Folin-Ciocâlteu reagent solution (Sigma-Aldrich) were initially added to each well of the microplate. The mixture was left under refrigeration for 5 min and subsequently, 25 µL of 20% Na_2CO_3 and 140 µL of distilled water were added. The microplate was put to rest for 30 min, and the absorbance was measured at 760 nm on the microplate reader. A calibration curve was plotted with concentrations between 0.1 and 1 mg/mL of gallic acid standard (Sigma-Aldrich) (R^2=0.992). The results were expressed as mg gallic acid equivalents (GAE) per 100 g of FW of mango.

For total flavonoid content determination, 80 µL of each extract and 80 µL of an ethanolic solution of aluminum trichloride (20 g/L) were added to wells of the microplate. The microplate was shaken for 30 s and left in the dark for 1 h at 25°C. Subsequently, it was shaken once more for 30 s, and the absorbance was measured at 415 nm in the microplate reader. The calibration curve was plotted with the quercetin standard (Sigma-Aldrich), considering concentrations from 0 to 0.08 mg/mL (R^2=0.999). The results were reported as mg quercetin equivalents (QE) per 100 g of FW of mango.

Antioxidant capacity assays

Assays were performed following the methodology reported by Pérez-Perez *et al.* [2021] with some modifications. To determine the antioxidant capacity by scavenging 2,2-diphenyl-1-picrylhydrazyl (DPPH) radical, 1 mg of the DPPH radical (Sigma-Aldrich)

was weighed and dissolved in 1 mL of absolute ethanol. From this initial solution, 0.75 mL was added to 29.25 mL of ethanol. The absorbance of the resulting solution was adjusted to 0.7 at a wavelength of 515 nm. Next, 200 µL of the resulting solution and 20 µL of the extract were added to wells of the microplate. The absorbance was measured at 515 nm in the plate reader after 30 min of leaving the microplate to rest. A calibration curve was made with Trolox standard (Sigma-Aldrich) considering concentrations between 0 and 0.2 mg/mL (R^2=0.992). The results were expressed as mM Trolox equivalents (TE) per g of FW of mango.

For determination of the antioxidant capacity by 2,2′-azino--bis(3-ethylbenzothiazoline-6-sulfonic acid) (ABTS) assay, 19.3 mg of ABTS were dissolved in 5 mL of distilled water. Separately, 0.0378 g of potassium persulfate and 1 mL of distilled water were mixed. From the second solution, 88 µL were added to the first solution, and it was left to rest in the dark for 16 h under refrigeration. One mL of this last prepared solution containing generated ABTS radical cations was added to 88 mL of ethanol, and the absorbance was adjusted to 0.7 at a wavelength of 734 nm. For the measurement of the samples, 270 µL of the ABTS radical cation solution and 20 µL of each extract were taken. The absorbance was measured at 734 nm after 30 min of rest. The calibration curve was plotted with Trolox standard considering concentrations from 0 to 0.01 mg/mL (R^2=0.994). The results were expressed as mM TE/g FW.

For ferric reducing antioxidant power (FRAP) determination, the stock solutions were prepared: a 300 mM sodium acetate buffer at pH 3.6, a 20 mM $FeCl_3 \times 6H_2O$ solution, and a solution of 10 mM 2,4,6-tris(2-pyridyl)-*s*-triazine (TPTZ; Sigma-Aldrich) in 40 mM HCl. The working solution was obtained by adding the stock solutions in a 10:1:1 (*v/v/v*) ratio (buffer, $FeCl_3 \times 6H_2O$, and TPTZ-HCl, respectively). Then, 280 µL of the working solution and 20 µL of each extract were added to each well of the microplate. Absorbance was measured at 638 nm after 30 min of rest. The calibration curve was plotted with Trolox standard considering concentrations between 0 and 0.4 mg/mL (R^2=0.999). Results were reported as mM TE/g FW.

Statistical analysis

A completely randomized design with two factors and a 3×5 factorial arrangement was used. The first factor (A) was the treatment of disinfection of fresh-cut mango with three levels (without disinfection treatment or control (C), immersion in 10 mg/L sodium hypochlorite solution (H), and application of a UV-C dose of 6 kJ/m^2 (UV)). The second factor (B) corresponded to the sampling time during storage of fresh-cut mango in refrigeration, comprising five levels (0, 3, 6, 9, and 12 days). Fresh-cut mango from the control treatment was considered as a negative control, and from the treatment with NaClO as a positive control. Results were presented as the mean of three replicates. A two-way ANOVA and a Tukey's test were performed to compare mean values between treatments and evaluate the effect of factors on pH, TA, TSS content, firmness, color parameters, microbial counts, contents of total carotenoids, total phenolics and flavonoids, and antioxidant capacity of fresh-cut mango (p<0.05).

RESULTS AND DISCUSSION

Titratable acidity, pH, total soluble solid content, and firmness

The results of determinations of titratable acidity, pH, total soluble solid content, and firmness of mango treated with UV-C, immersed in sodium hypochlorite solution and without treatment during storage are shown in Figure 1. According to the two-way ANOVA, the disinfection treatment, the storage time, and the interaction between these factors had a significant effect on the physicochemical properties of fresh-cut mango (p<0.05). Values of pH indicated that fresh-cut mango from C (3.88–4.18) and H (3.75–3.95) treatments was entering the senescence stage. For mango irradiated with UV-C, pH started to decrease significantly since day 9 of storage. According to Zambrano-Zaragoza *et al.* [2021], UV-C treatment allows delaying senescence stage. The content of TSS of fresh-cut mango from UV treatment tended to increase until day 9 of storage. The increase in TSS content is attributed to the hydrolysis of polysaccharides and the accumulation of released soluble sugars as a result of fruit ripening during storage [George *et al.*, 2015; Khubone & Mditshwa, 2018]. On the other hand, TSS content of C sample remained almost constant and its content of H sample decreased slightly only at day 6 (14.13 °Brix) of storage (Figure 1). Treatments could affect the rate of transpiration, generating slight changes in the content of water in the fruit [Zambrano-Zaragoza *et al.*, 2021]. The titratable acidity of fresh-cut mango from C treatment exhibited an increase up to day 9 of storage (0.48–0.85 g/100 g) and then decreased slightly (to 0.76 g/100 g) (Figure 1). The reduction in acidity levels can be initially linked to the ripening of the fruit when organic acids are degraded [Barreto *et al.*, 2021]. For the samples from H and UV treatments, TA increased until day 3 of storage and then remained almost constant (Figure 1). The disinfection treatments and the modified atmosphere could slow down the respiration rate, and the utilization rate of the respiratory substrate was minimal through the storage period [Razali *et al.*, 2021].

The firmness of fresh-cut mango tended to decrease during refrigerated storage (Figure 1). According to Barreto *et al.* [2021], the reduction of firmness of minimally processed fruits is generated by the cutting operation and the high degree of injury to cellular tissues. The demethylation and depolymerization of pectin, generation of free radicals, enzymatic degradation of hemicellulose, solubilization of polyuronides, the release of galactose from pectic polymers, cell wall swelling, decreased water content and osmotic potential may occur in tissues and thus lower the fruit firmness [Barreto *et al.*, 2021; Márquez-Villacorta & Pretell-Vásquez, 2013]. In our study, it was found that mango irradiated with UV-C exhibited the lowest firmness for most of the storage time (2.10–5.63 N) compared to control (3.53–4.46 N) and H-treated (2.03–5.94 N) samples (Figure 1). Fruit softening is modulated by cell wall hydrolases,

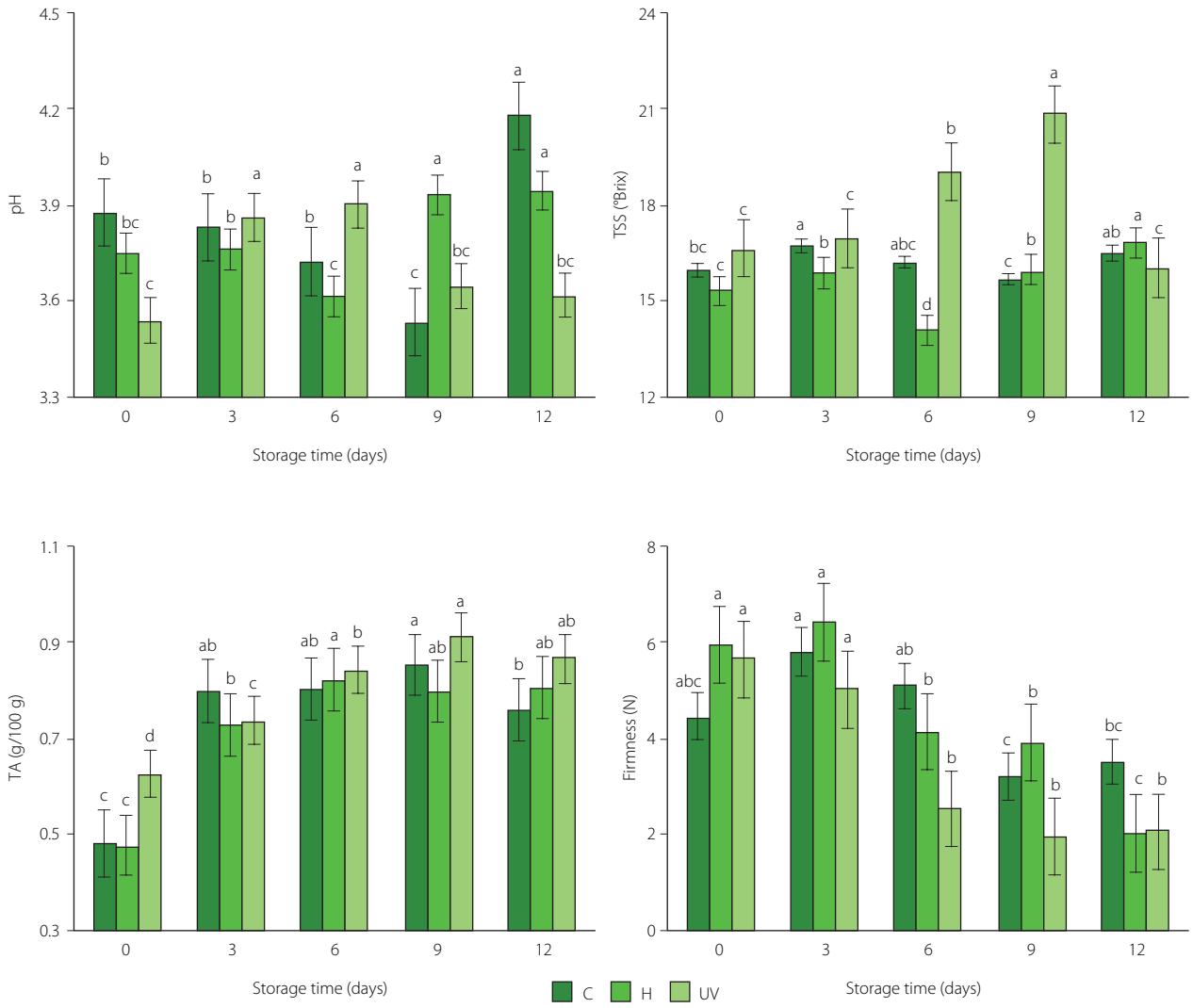

FIGURE 1. Values of pH, total soluble solid (TSS) content, titratable acidity (TA), and firmness of fresh-cut mango without treatment (control, C), immersed in sodium hypochlorite solution (H), and treated with ultraviolet short wave (UV-C, UV) during storage at 5°C for 12 days. Vertical lines above and below the points correspond to standard error. Different lowercase letters (a-d) above bars (separately for control and each treatment) indicate significant differences ($p<0.05$).

such as polygalacturonase, cellulase, β-galactose, and expansin, and UV-C treatment can alter the expression of genes involved in modifying cell wall structure [Kan *et al.*, 2021].

Color parameters

It was found that the disinfection treatment had no significant effect on *L** coordinate of fresh-cut mango ($p\geq0.05$). However, the storage time and the interaction of the factors had a significant effect on the values of this parameter ($p<0.05$). In Table 1, it is shown that *L** color coordinate of mango samples from C and UV treatments tended to increase slightly during storage, and to decrease for the samples from H treatment. Luminosity is considered an indicator of browning. The *L** value of the H-treated fresh-cut mango decreased during the storage possibly due to sample browning as a result of oxidation processes induced by NaClO. The disinfectants served as oxidizing agents [Hinojosa *et al.*, 2013]. In the case of UV-C treatment, inhibition of polyphenol oxidase (PPO) activity by radiation could occur [Barreto *et al.*, 2021] and result in the reduced browning of the fruits.

The disinfection treatment, the storage time, and the interaction between these factors had a significant effect on all other color parameters of fresh-cut mango ($p<0.05$). Low values of *a** coordinate represented tones between green and red. The values of *a** increased for the control sample, decreased for the samples from H treatment, and remained slightly constant for the samples from UV treatment during storage (Table 1). The increase in *a** coordinate value can be interpreted as the increase in orange or red pigments due to fruit ripening, and on the other hand, as enzymatic and non-enzymatic browning [Márquez-Villacorta & Pretell-Vásquez, 2013; Nguyen *et al.*, 2022]. Therefore, the radiation treatment allowed delaying some adverse processes linked to accelerated ripening and browning of the fruit, which possibly occurred in mango from C and H treatments, respectively. Positive values of *b** coordinate indicated yellow tones. This coordinate tended to remain constant for the samples from H and UV treatments during storage (Table 1). During mango ripening, green chloroplasts become chromoplasts with red and yellow tones. These tones in mango are mainly derived

TABLE 1. Color parameters of fresh-cut mango without treatment (control, C), immersed in sodium hypochlorite solution (H), and treated with ultraviolet short wave (UV-C, UV) during storage at 5°C for 12 days.

Color parameter	Treatment	Storage time (days)				
		0	3	6	9	12
*L**	C	54.17±0.07^{defg}	54.96±0.77^{cde}	56.62±0.18^{bc}	53.80±0.09^{defg}	57.69±0.40^{ab}
	H	57.54±0.36^{ab}	58.72±0.27^{a}	53.66±0.39^{efg}	52.64±0.06^{g}	54.20±0.10^{defg}
	UV	53.02±0.25^{fg}	54.32±0.16^{defg}	54.69±0.81^{def}	59.03±0.13^{a}	55.62±0.13^{cd}
*a**	C	8.23±0.16^{f}	13.51±0.15^{b}	11.09±0.15^{cd}	11.24±0.03^{cd}	15.05±0.18^{a}
	H	11.51±0.28^{cd}	11.93±0.26^{c}	8.06±0.09^{f}	7.013±0.03^{g}	6.78±0.09^{g}
	UV	9.88±0.21^{e}	11.99±0.12^{c}	13.58±0.20^{b}	10.92±0.07^{d}	11.58±0.01^{cd}
*b**	C	55.25±0.64^{d}	61.71±1.85^{c}	63.49±0.63^{bc}	68.14±0.20^{a}	67.65±0.83^{ab}
	H	62.27±1.11^{c}	61.80±0.85^{c}	55.40±1.35^{d}	60.02±0.17^{c}	60.91±0.65^{c}
	UV	67.06±0.47^{ab}	68.88±0.25^{a}	69.98±1.15^{a}	69.11±0.19^{a}	67.38±0.07^{ab}
*C**	C	55.86±0.66^{d}	63.17±1.90^{c}	64.45±0.65^{bc}	69.06±0.20^{a}	69.30±0.85^{a}
	H	63.33±1.14^{c}	62.94±0.86^{c}	55.98±1.33^{d}	60.43±0.17^{c}	61.29±0.66^{c}
	UV	67.78±0.49^{ab}	69.92±0.26^{a}	71.29±1.16^{a}	69.97±0.20^{a}	68.37±0.07^{ab}
h°	C	81.52±0.04^{bc}	77.65±0.10^{h}	80.09±0.04^{ef}	80.63±0.02^{de}	77.46±0.06^{h}
	H	79.53±0.07^{fg}	79.08±0.03^{g}	81.71±0.25^{b}	83.33±0.05^{a}	83.65±0.05^{a}
	UV	81.62±0.12^{b}	80.13±0.07^{e}	79.01±0.11^{g}	81.02±0.03^{cd}	80.24±0.01^{e}
Δ*E*	C	–	8.50±1.79^{bcd}	9.07±0.75^{b}	13.24±0.19^{a}	14.59±0.88^{a}
	H	–	1.83±0.21^{f}	8.73±0.97^{bc}	7.03±0.08^{bcd}	6.01±0.28^{bcde}
	UV	–	2.80±0.25^{ef}	5.04±1.31^{def}	5.36±0.20^{cdef}	2.25±0.09^{f}

Values are mean ± standard error. For each color parameter, means that do not share the same letter are significantly different ($p<0.05$). *L**, lightness; *a**, redness; *b**, yellowness; *C**, chroma; *h*°, hue angle; Δ*E*, total color difference.

from β-carotene, which is accumulated in the chromoplasts in the form of crystalloids [Miguel *et al.*, 2016]. For the control mango, *b** coordinate value increased throughout cold storage (Table 1). According to Rosalie *et al.* [2018], low temperatures can delay or block the accumulation of carotenoids in fruits, since it promotes oxidation in tissues.

The *C** value increased during storage for the control sample and tended to remain constant for the samples from H and UV treatments (Table 1). The increase in *C** value for the control sample indicated that the color became more saturated due to storage. This could stem from the appearance of some brown tones [Grasso *et al.*, 2022]. Values of *h*° increased significantly ($p<0.05$) after day 9 of storage for mango from H treatment. It can be attributed to the accelerated isomerization of carotenoids and oxidation by free radicals [Xiang *et al.*, 2020]. In turn, the *h*° values tended to decrease slightly for the control (from 81.52 to 77.46) and UV-C (from 81.62 to 80.24) treated samples throughout the storage (Table 1). A decrease in *h*° values indicates the yellowing of the fruit [Barreto *et al.*, 2021], while delay in color development is linked to a reduction in ripening and senescence [Khubone & Mditshwa, 2018]. According to the classification proposed in literature [Pathare *et al.*, 2013], the total color differences (Δ*E*) of the stored samples (relative to storage day 0) in our study were mostly classified as very different ($\Delta E>3$) and different ($1.5<\Delta E<3$). The Δ*E* increased significantly ($p<0.05$) throughout the storage of the control and H-treated samples. The UV-C-treated sample showed the least color change (the lowest Δ*E* value) after 12 days of storage. The irradiation of fresh-cut mango allowed to prevent the oxidation reactions associated with the activity of peroxidase (POD) and stabilize the pigments and color parameters [Zambrano-Zaragoza *et al.*, 2021].

Results of microbiological analysis

Figure 2 shows a significant increase in the native microbial population of fruit during storage. This increase may have been due to the handling of the samples during cutting and the high surface area/weight ratio of each sample [Artés-Hernández *et al.*, 2021]. By the two-way ANOVA, it was found that the disinfection treatment, the storage time, and their interaction had a significant effect on the native microorganisms of fresh-cut mango ($p<0.05$). The initial population of aerobic mesophiles was 1.69, 1.66, and 1.42 log cfu/g for the samples from C, H and UV treatments, respectively (Figure 2). This population increased notably for the samples from C and H treatments during the storage time. For UV-C irradiated samples, it remained stable after day 6

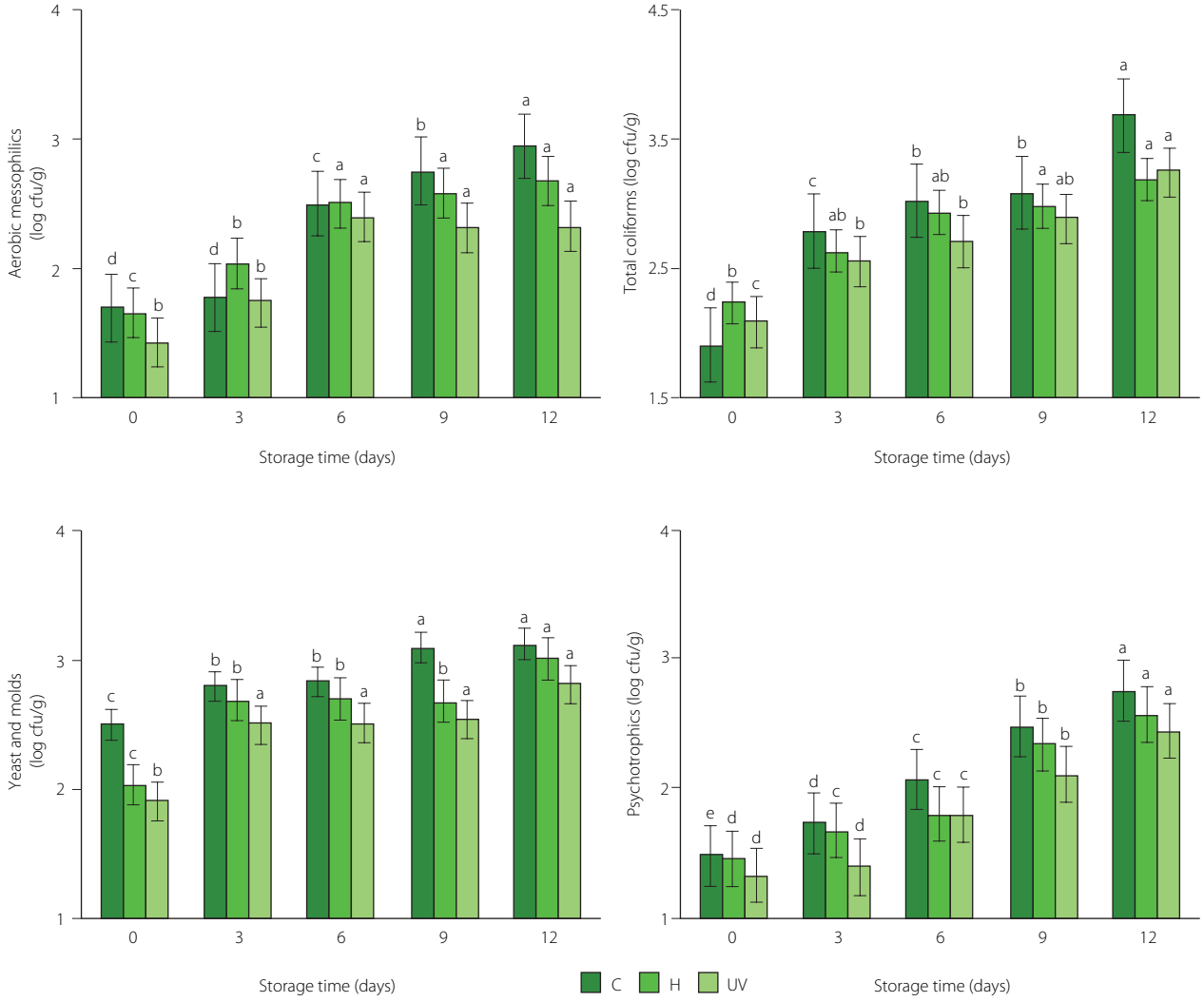

FIGURE 2. Aerobic mesophilic, total coliforms, yeast and molds, and psychrotrophic populations on fresh-cut mango without treatment (control, C), immersed in sodium hypochlorite solution (H), and treated with ultraviolet short wave (UV-C, UV) during storage at 5°C for 12 days. Vertical lines above and below the points correspond to standard error. Different lowercase letters (a-e) above bars (separately for control and each treatment) indicate significant differences (p<0.05).

of storage. The H and UV treatments reduced the population of aerobic mesophiles of mango by 0.26 and 0.62 log cfu/g, respectively, compared to C treatment at day 12 of refrigerated storage. For total coliforms, the initial population was 1.90, 2.23, and 2.08 log cfu/g for fresh-cut mango from C, H, and UV treatments, respectively. Total coliform count of the samples tended to increase during storage. At the end of storage, the treatments with disinfectant agents promoted a reduction of about 0.5 log cfu/g of enterobacteria population in contrast to C treatment. The initial population of psychrophiles was 1.47, 1.45, and 1.32 log cfu/g for fresh-cut mango from C, H, and UV treatments, respectively. Psychrotropic bacteria increased during storage in all samples. At the end of storage, the population reduction in the samples from H and UV treatments was 0.18 and 0.32 log cfu/g, respectively, in contrast to samples from C treatment.

According to Colombian microbiological requirements, the population of molds and yeasts limited the quality of fresh-cut mango (3 log cfu/g) [Ministry of Health and Social Protection of Colombia, 2013]. The samples from C and H treatments presented an acceptable level of quality until day 3 and 9 of storage, respectively (Figure 2). While the UV-treated samples had an acceptable level of quality throughout storage.

For kinetics inactivation (Table 2), Weibull model explained the inactivation of almost all native microorganisms of fresh-cut mango from different treatments. According to van Boekel [2002], the shape parameter (β) value lower than 1 indicated that some populations of native microorganisms had the ability to adapt to the stress applied with the treatments. While β>1 meant that in other populations, there remained cells that were damaged by the applied stress.

Bioactive compound contents

The disinfection treatment, the storage time, and their interaction had a significant effect on the total carotenoid and total flavonoid contents of fresh-cut mango (p<0.05). In turn, storage time had no effect on the total phenolic content of fresh-cut mango (p≥0.05). The content of total carotenoids was 5.77,

TABLE 2. Fitted and inactivation kinetic parameters of native microorganisms of fresh-cut mango without treatment (control, C), immersed in sodium hypochlorite solution (H), and treated with ultraviolet short wave (UV-C, UV) during storage at 5°C for 12 days.

Microbial population	Treatment	Kinetic parameters								
		Linear logarithmic equation				Weibull model				
		k (1/day)	R^2	Adjusted R^2	RMSE	α (day)	β	R^2	Adjusted R^2	RMSE
Aerobic mesophilic bacteria	C	0.267	0.931	0.908	0.290	4.209	1.072	0.861	0.815	0.297
	H	0.199	0.900	0.867	0.247	2.509	0.580	0.945	0.926	0.159
	UV	0.187	0.750	0.666	0.399	0.551	2.586	0.821	0.761	0.325
Total coliforms	C	0.297	0.893	0.858	0.423	0.967	0.525	0.965	0.954	0.251
	H	0.174	0.927	0.903	0.194	3.123	0.576	0.980	0.973	0.093
	UV	0.205	0.963	0.951	0.165	3.385	0.736	0.998	0.998	0.122
Yeast and molds	C	0.120	0.925	0.900	0.131	6.467	0.645	0.965	0.953	0.105
	H	0.151	0.747	0.662	0.361	0.986	0.274	0.927	0.903	0.170
	UV	0.141	0.781	0.708	0.308	1.609	0.306	0.945	0.927	0.139
Psychrotrophic bacteria	C	0.254	0.994	0.992	0.083	4.523	1.129	0.983	0.978	0.062
	H	0.224	0.953	0.938	0.203	5.811	1.354	0.973	0.964	0.159
	UV	0.225	0.969	0.958	0.163	6.136	1.430	0.945	0.927	0.105

k, inactivation rate constant; α, characteristic time; β, shape factor; R^2, coefficient of determination; RMSE, root mean square error.

11.42, and 20.95 mg β-carotene/100 g FW for C, H, and UV samples at the beginning of storage, respectively, and 19.34, 19.04, and 26.50 mg β-carotene/100 g FW at 12 day of storage, respectively, with maxima on day 3 of storage for the control and H-treated mango, and on day 6 of storage for the fruit from UV-C treatment (Figure 3). Accumulation of carotenoids during the storage could be influenced by the maturity of the fruit [Rosalie *et al.*, 2018]. Samples from control and H treatments which showed accelerated ripening and browning could reduce the accumulation of carotenoids due to metabolic processes. UV-C irradiation influenced carotenoid content due to physiological stress. UVR8 protein acts as a photoreceptor and interacts with another encoding protein COP1 to stimulate the production of carotenoids as a photoprotective effect [Castillejo *et al.*, 2022]. The increase in the content of total carotenoids is also related to the activation of carotene isomerase enzyme and the accumulation of phytoene synthase (PSY) and zeta-carotene desaturase (ZDS) gene transcripts [Khubone & Mditshwa, 2018].

The total phenolic content of fresh-cut mango of control and UV-C treated fruit was higher than that of the H samples at 6, 9, and 12 day of storage (Figure 3). This variation in the total phenolic content may be attributed to the various reasons. The release of phenolic compounds bound to cell wall polysaccharides and the depolymerization of phenolic polymers such as tannins [Xiang *et al.*, 2020] might have occurred. On the other hand, phenolics can be used as substrates for enzymes such as β-glucosidase, PPO, and POD [Velderrain-Rodríguez *et al.*, 2021]. These processes may occur to varying degrees in mango samples subjected to various treatments and thus result in different total phenolic content.

Fresh-cut mango showed a low content of flavonoids, which could be due to the low expression of the flavonol synthase in the ripening of the fruit, although the flavonol glycoside (quercetin 3-galactoside) is the major flavonoid of mango (22.1 mg/kg) [Maldonado-Celis *et al.*, 2019]. In our study, there were maxima in flavonoid content at days 3 (1.00 mg QE/100 g FW) and 6 (1.14 mg QE/100 g FW) of storage for the samples from C and UV treatments, respectively (Figure 3). The UV-C irradiation leads to the regulation of oxidative stress and the biosynthesis of key enzymes in the flavonoid biosynthetic pathway, such as phenylalanine ammonium lyase (PAL) and chalcone synthase (CHS) [Michailidis *et al.*, 2019]. The stress caused by UV-C can increase the production of reactive oxygen species (ROS), ROS scavenging compounds, and absorbers of UV radiation [Castillejo *et al.*, 2022]. UV-C stress can also activate the signaling pathway of the COP1 and UVR8 photoreception proteins to produce flavonoids [Li *et al.*, 2017].

■ Antioxidant capacity

It was established that the disinfection treatment, the storage time, and the interaction between the factors had significant effects on the antioxidant capacity of fresh-cut mango ($p<0.05$). Except that the storage time had no significant effect on the antioxidant capacity measured by DPPH assay of fresh-cut mango ($p\geq0.05$). At the end of storage, DPPH$^{\bullet}$ scavenging activity of the control (0.27 mM TE/g FW) was lower compared to both treated samples. For the fresh-cut mango treated with UV-C, DPPH$^{\bullet}$ scavenging activity was the highest (0.60 mM TE/g of FW). It could be due to the increase in the activity of PAL in response to external stress caused by fruit irradiation [Prajapati *et al.*, 2021].

The antioxidant capacity measured by ABTS assay tended to remain constant for the control sample (0.56–0.61 mM TE/g FW), and to increase for the samples from H treatment (0.39–0.56 mM TE/g FW) throughout storage (Figure 4). In

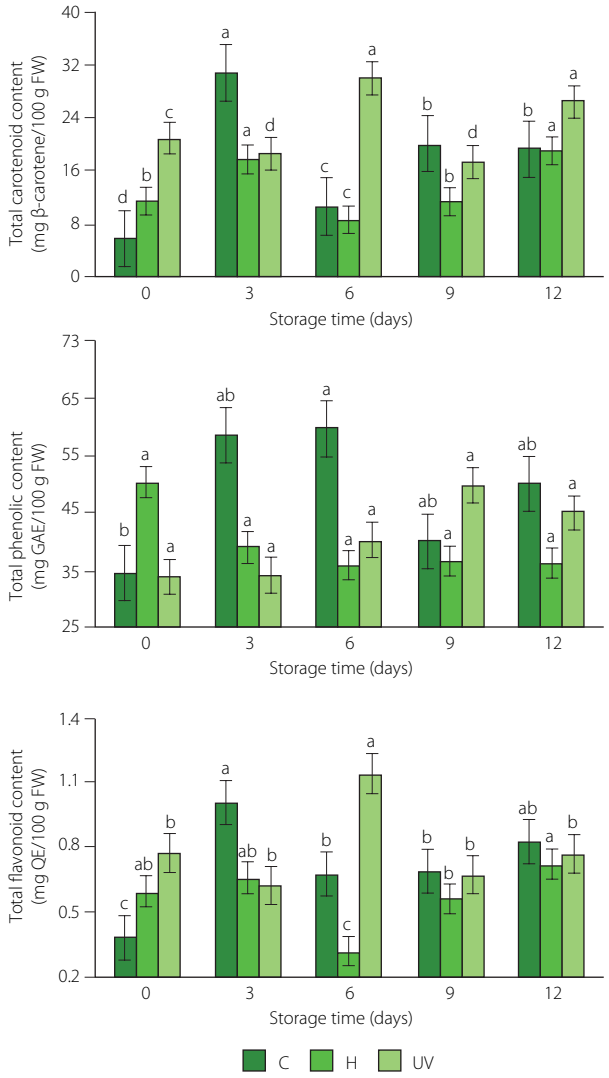

FIGURE 3. Contents of total carotenoids, total phenolics, and flavonoids of fresh-cut mango without treatment (control, C), immersed in sodium hypochlorite solution (H), and treated with ultraviolet short wave (UV-C, UV) during storage at 5°C for 12 days. Vertical lines above and below the points correspond to standard error. Different lowercase letters (a-d) above bars (separatly for control and each treatment) indicate significant differences (p<0.05). GAE, gallic acid equivalents; QE, quercetin equivalents; FW, fresh weight.

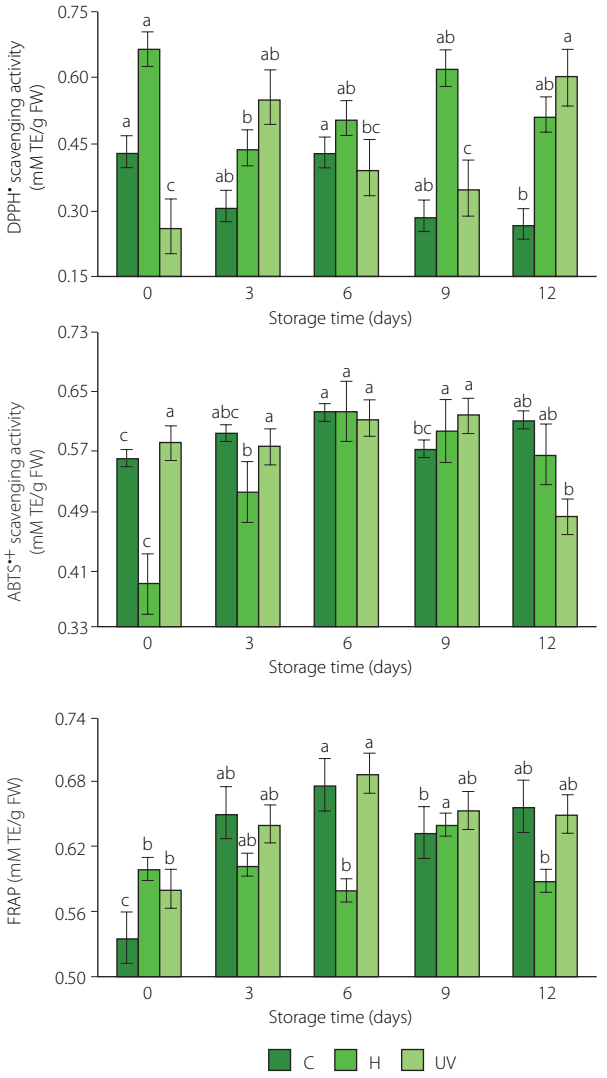

FIGURE 4. Antioxidant capacity determined as DPPH• and ABTS•+ scavenging activities and as ferric-reducing antioxidant power (FRAP) of fresh-cut mango without treatment (control, C), immersed in sodium hypochlorite solution (H), and treated with ultraviolet short wave (UV-C, UV) during storage at 5°C for 12 days. Vertical lines above and below the points correspond to standard error. Different lowercase letters (a-c) above bars (separatly for control and each treatment) indicate significant differences (p<0.05). TE, Trolox equivalents; FW, fresh weight.

turn, the activity of the samples treated with UV-C remained almost constant from day 0 to day 9 (0.58–0.62 mM TE/g FW). It is possible that UV-C affected the integrity of the cell structure and vacuoles, promoting the release of compounds with antioxidant activity [Rybak *et al.*, 2021]. At the end of the storage, ABTS•+ scavenging activity of the UV-C treated samples decreased (0.48 mM TE/g FW). Miguel *et al.* [2016] reported that the high activity of PPO and the low activity of PAL in mango during the beginning of senescence have an impact on its ABTS•+ scavenging activity.

The FRAP exhibited slight maxima on day 6 of storage for mango spears from C (0.68 mM TE/g FW) and UV (0.69 mM TE/g FW) treatments, and on day 9 of storage for the samples from H treatment (0.64 mM TE/g FW) (Figure 4). Low refrigeration temperature and UV-C irradiation stress activated the defense mechanism of enzymes related to the elimination of ROS and the biosynthesis of antioxidant compounds [Hinojosa *et al.*, 2013].

CONCLUSIONS

The UV-C treatment of fresh-cut 'Tommy Atkins' mango proved effective in preserving its quality attributes. The application of a UV-C dose of 6 kJ/m^2 promoted the conservation of microbial safety, the physicochemical properties (pH, TSS, and AT), the color parameters (L*, a*, and b*), the contents of total carotenoids, total phenolics, total flavonoids, and the antioxidant capacity measured by DPPH assay and as FRAP during fruit storage for 12 days at 5°C. However, this treatment promoted the loss of fruit firmness. In general, the disinfection treatment of fresh-cut mango with UV-C is a technological alternative to replace the conventional disinfection method with sodium hypochlorite immersion, since it provides the conservation of the quality

attributes of fruit, mitigates the adverse impact on the environment and on the health of consumers by the lack of dangerous chemicals applied during minimal processing.

ACKNOWLEDGEMENTS

The authors thank Universidad Nacional de Colombia for granting Honor Degree Scholarship.

RESEARCH FUNDING

This research received no external funding.

CONFLICT OF INTEREST

The authors declare no conflict of interest.

ORCID IDs

C.L. Del-Toro-Sánchez https://orcid.org/0000-0001-7029-7741
S. Dussán-Sarria https://orcid.org/0000-0001-9297-0781
A.M. Garzón-García https://orcid.org/0000-0002-5454-1000
J.I. Hleap-Zapata https://orcid.org/0000-0001-9692-5443
E. Márquez-Ríos https://orcid.org/0000-0001-7850-4960
V.M. Ocaño-Higuera https://orcid.org/0000-0001-7234-8370
S. Ruiz-Cruz https://orcid.org/0000-0002-7125-8952
J.A. Tapia-Hernández https://orcid.org/0000-0003-1124-7001

REFERENCES

1. AOAC International (2012). *Official Methods of Analysis of AOAC International*. 19th ed., Gaithersburg, MD, USA.
2. Artés-Hernández, F., Martínez-Hernández, G.B., Aguayo, E., Gómez, P.A., Artés F. (2017). Fresh-cut fruit and vegetables: Emerging eco-friendly techniques for sanitation and preserving safety. In I. Kahramanoglu (Ed.), *Postharvest Handling*, IntechOpen, London, UK, pp. 7-45. https://doi.org/10.5772/intechopen.69476
3. Artés-Hernández, F., Robles, P.A., Gómez, P.A., Tomás-Callejas, A., Artés, F., Martínez-Hernández, G.B. (2021). Quality changes of fresh-cut watermelon during storage as affected by cut intensity and UV-C pre-treatment. *Food and Bioprocess Technology*, *14*(3), 505–517. https://doi.org/10.1007/s11947-021-02587-1
4. Barreto, C.F., Navroski, R., Marques, L.O.D., Santos, R.F., Malgarim, M.B., Martins, C.R. (2021). Influência da radiação ultravioleta e aditivos na conservação de kiwis minimamente processados. *Brazilian Journal of Food Technology*, *24*, art. no. e2020024 (in Portuguese; English abstract). https://doi.org/10.1590/1981-6723.02420
5. Castillejo, N., Martínez-Zamora, L., Artés-Hernández, F. (2022). Postharvest UV radiation enhanced biosynthesis of flavonoids and carotenes in bell peppers. *Postharvest Biology and Technology*, *184*, art. no. 111774. https://doi.org/10.1016/j.postharvbio.2021.111774
6. De Corato, U. (2020). Improving the shelf-life and quality of fresh and minimally-processed fruits and vegetables for a modern food industry: A comprehensive critical review from the traditional technologies into the most promising advancements. *Critical Reviews in Food Science and Nutrition*, *60*(6), 940–975. https://doi.org/10.1080/10408398.2018.1553025
7. Djioua, T., Charles, F., Freire, M., Filgueiras, H., Ducamp-Collin, M.-N., Sallanon, H. (2010). Combined effects of postharvest heat treatment and chitosan coating on quality of fresh-cut mangoes (*Mangifera indica* L.). *International Journal of Food Science and Technology*, *45*(4), 849–855. https://doi.org/10.1111/j.1365-2621.2010.02209.x
8. Lopes, M.M.A., Lucena, H.H., Silveira, M.R.S., Garruti, D.S., Machado, T.F., Aragão, F.A.S., Silva, E.O. (2021). The use of electrolyzed water as a disinfectant for fresh cut mango. *Scientia Horticulturae*, *287*, art. no. 110227. https://doi.org/10.1016/j.scienta.2021.110227
9. González-Aguilar, G.A., Villegas-Ochoa, M.A., Martínez-Téllez, M.A., Gardea, A.A., Ayala-Zavala, J.F. (2007). Improving antioxidant capacity of fresh-cut mangoes treated with UV-C. *Journal of Food Science*, *72*(3), S197–S202. https://doi.org/10.1111/j.1750-3841.2007.00295.x
10. George, D.S., Razali, Z., Santhirasegaram, V., Somasundram, C. (2015). Effects of ultraviolet light (UV-C) and heat treatment on the quality of fresh-cut Chokanan mango and Josephine pineapple. *Journal of Food Science*, *80*(2), S426–S434. https://doi.org/10.1111/1750-3841.12762
11. Giannakourou, M.C., Tsironi, T.N. (2021). Application of processing and packaging hurdles for fresh-cut fruits and vegetables preservation. *Foods*, *10*(4), art. no. 830. https://doi.org/10.3390/foods10040830
12. González-Vega, R.I., Cárdenas-López, J.L., López-Elías, J.A., Ruiz-Cruz, S., Reyes-Díaz, A., Perez-Perez, L.M., Cinco-Moroyoqui, F.J., Robles-Zepeda, R.E., Borboa-Flores, J., Del-Toro-Sánchez, C.L. (2021). Optimization of growing conditions for pigments production from microalga *Navicula incerta* using response surface methodology and its antioxidant capacity. *Saudi Journal of Biological Sciences*, *28*(2), 1401–1416. https://doi.org/10.1016/j.sjbs.2020.11.076
13. Grasso, C., Forniti, R., Botondi, R. (2022). Post-harvest quality evaluation of "Soreli" kiwifruit at two ripening °Brix values from vineyards of different age under hail nets. *Foods*, *11*(3), art. no. 431. https://doi.org/10.3390/foods11030431
14. Hinojosa, A., Silveira, A.C., Ospina, M., Char, C., Sáenz, C., Escalona, V.H. (2013). Safety of ready-to-eat watercress using environmentally friendly sanitization methods. *Journal of Food Quality*, *36*(1), 66–76. https://doi.org/10.1111/jfq.12016
15. Kan, J., Hui, Y., Lin, X., Liu, Y., Jin, C. (2021). Postharvest ultraviolet-C treatment of peach fruit: Changes in transcriptome profile focusing on genes involved in softening and senescence. *Journal of Food Processing and Preservation*, *45*(10), art. no. e15813. https://doi.org/10.1111/jfpp.15813
16. Kansci, G., Koubala, B.B., Mbome, I.L. (2008). Biochemical and physicochemical properties of four mango varieties and some quality characteristics of their jams. *Journal of Food Processing and Preservation*, *32*(4), 644–655. https://doi.org/10.1111/j.1745-4549.2008.00204.x
17. Khubone, L.W., Mditshwa, A. (2018). The effects of UV-C irradiation on postharvest quality of tomatoes (*Solanum lycopersicum*). *Acta Horticulturae*, *1201*, 75–82. https://doi.org/10.17660/ActaHortic.2018.1201.11
18. Kumar, M., Saurabh, V., Tomar, M., Hasan, M., Changan, S., Sasi, M., Maheshwari, C., Prajapati, U., Singh, S., Prajapat, R.K., Dhumal, S., Punia, S., Amarowicz, R., Mekhemar, M. (2021). Mango (*Mangifera indica* L.) leaves: Nutritional composition, phytochemical profile, and health-promoting bioactivities. *Antioxidants*, *10*(2), art. no. 299. https://doi.org/10.3390/antiox10020299
19. Lázaro, A., De Lorenzo, C. (2015). Texture analysis in melon landraces through instrumental and sensory methods. *International Journal of Food Properties*, *18*(7), 1575–1583. https://doi.org/10.1080/10942912.2014.923441
20. Li, P., Yu, X., Xu, B. (2017). Effects of UV-C light exposure and refrigeration on phenolic and antioxidant profiles of subtropical fruits (litchi, longan, and rambutan) in different fruit forms. *Journal of Food Quality*, *2017*, art. no. 8785121. https://doi.org/10.1155/2017/8785121
21. Maldonado-Celis, M.E., Yahia, E.M., Bedoya, R., Landázuri, P., Loango, N., Aguillón, J., Restrepo, B., Guerrero Ospina, J.C. (2019). Chemical composition of mango (*Mangifera indica* L.) fruit: Nutritional and phytochemical compounds. *Frontiers in Plant Science*, *10*, art. no. 1073. https://doi.org/10.3389/fpls.2019.01073
22. Márquez-Villacorta, L., Pretell-Vásquez, C.P. (2013). UV-C Irradiation in tropical fruits minimally processed. *Scientia Agropecuaria*, *4*(3), 147–161 (in Spanish; English abstract). https://doi.org/10.17268/sci.agropecu.2013.03.01
23. Márquez-Villacorta, L., Pretell-Vásquez, C., Minchón-Medina, C. (2011). Effect of the disinfection treatment and storage time on physicochemical, microbiological, and sensory characteristics in slices of mango (*Mangifera indica*) Kent minimally processed. *Pueblo Continente*, *22*(2), 385–403 (in Spanish; English abstract).
24. Michailidis, M., Karagiannis, E., Polychroniadou, C., Tanou, G., Karamanoli, K., Molassiotis, A. (2019). Metabolic features underlying the response of sweet cherry fruit to postharvest UV-C irradiation. *Plant Physiology and Biochemistry*, *144*, 49–57. https://doi.org/10.1016/j.plaphy.2019.09.030
25. Miguel, A.C.A, Durigan, J.F., Marques, K.M., Morgado, C.M.A., Ferraudo, A.S. (2016). Prevention of chilling injury in "Tommy Atkins" mangoes previously stored at 5°C, using heat treatment and radiation UV (UV-C). *Revista Brasileira de Fruticultura*, *38*(1), 53–63. https://doi.org/10.1590/0100-2945-123/14
26. Ministry of Health and Social Protection of Colombia (2013). *La inocuidad de alimentos y su importancia en la cadena agroalimentaria* (in Spanish).
27. Nguyen, T.V.L., Nguyen, Q.D., Nguyen, P.B.D. (2022). Drying kinetics and changes of total phenolic content, antioxidant activity and color parameters of mango and avocado pulp in refractance window drying. *Polish Journal of Food and Nutrition Sciences*, *72*(1), 27–38. https://doi.org/10.31883/pjfns/144835
28. Pathare, P.B., Opara, U.L., Al-Said, F.A.-J. (2013). Colour measurement and analysis in fresh and processed foods: A review. *Food and Bioprocess Technology*, *6*(1), 36–60. https://doi.org/10.1007/s11947-012-0867-9
29. Pérez-Perez, L.M., Huerta-Ocampo, J.A., Ruiz-Cruz, S., Cinco-Moroyoqui, F.J., Wong-Corral, F.J., Rascón-Valenzuela, L.A., Robles-García, M.A., González-Vega, R.I., Rosas-Burgos, E.C., Corella-Madueño, M.A.G., Del-Toro-Sánchez, C.L. (2021).

Evaluation of quality, antioxidant capacity, and digestibility of chickpea (*Cicer arietinum* L. cv Blanoro) stored under N_2 and CO_2 atmospheres. *Molecules*, *26*(9), art. no. 2773.
https://doi.org/10.3390/molecules26092773

30. Prajapati, U., Asrey, R., Varghese, E., Singh, A.K., Singh, M.P. (2021). Effects of postharvest ultraviolet-C treatment on shelf-life and quality of bitter gourd fruit during storage. *Food Packaging and Shelf Life*, *28*, art. no. 100665. https://doi.org/10.1016/j.fpsl.2021.100665
31. Razali, Z., Somasundram, C., Nurulain, S.Z., Kunasekaran, W., Alias, M.R. (2021). Postharvest quality of cherry tomatoes coated with mucilage from dragon fruit and irradiated with UV-C. *Polymers*, *13*(17), art. no. 2919. https://doi.org/10.3390/polym13172919
32. Rodríguez-Mijangos, R., Gonzalez-Boué, G., Barffuson-Dominguez, F., Vargas-López, J.M., Yépiz-Gómez, M.S. (2014). Cámara de irradiación UV-C económica y sus potenciales aplicaciones en la desinfección de alimentos. *Epistemus*, *16*, 72–78 (in Spanish).
33. Rosalie, R., Léchaudel, M., Dhuique-Mayer, C., Dufossé, L., Joas, J. (2018). Antioxidant and enzymatic responses to oxidative stress induced by cold temperature storage and ripening in mango (*Mangifera indica* L. cv. 'Cogshall') in relation to carotenoid content. *Journal of Plant Physiology*, *224–225*, 75–85. https://doi.org/10.1016/j.jplph.2018.03.011
34. Rybak, K., Wiktor, A., Pobiega, K., Witrowa-Rajchert, D., Nowacka, M. (2021). Impact of pulsed light treatment on the quality properties and microbiological aspects of red bell pepper fresh-cuts. *LWT – Food Science and Technology*, *149*, art. no. 111906. https://doi.org/10.1016/j.lwt.2021.111906
35. Santo, D., Graça, A., Nunes, C., Quintas, C. (2018). *Escherichia coli* and *Cronobacter sakazakii* in 'Tommy Atkins' minimally processed mangos: Survival, growth and effect of UV-C and electrolyzed water. *Food Microbiology*, *70*, 49–54. https://doi.org/10.1016/j.fm.2017.09.008
36. van Boekel, M.A.J.S. (2002). On the use of the Weibull model to describe thermal inactivation of microbial vegetative cells. *International Journal of Food Microbiology*, *74*(1–2), 139–159. https://doi.org/10.1016/S0168-1605(01)00742-5
37. Velderrain-Rodríguez, G.R., Salmerón-Ruiz, M.L., González-Aguilar, G.A., Martín-Belloso, O., Soliva-Fortuny, R. (2021). Ultraviolet/visible intense pulsed light irradiation of fresh-cut avocado enhances its phytochemicals content and preserves quality attributes. *Journal of Food Processing and Preservation*, *45*(3), art. no. e15289. https://doi.org/10.1111/jfpp.15289
38. Xiang, Q., Fan, L., Zhang, R., Ma, Y., Liu, S., Bai, Y. (2020). Effect of UVC light-emitting diodes on apple juice: Inactivation of *Zygosaccharomyces rouxii* and determination of quality. *Food Control*, *111*, art. no. 107082. https://doi.org/10.1016/j.foodcont.2019.107082
39. Zambrano-Zaragoza, M.L., Quintanar-Guerrero, D., González-Reza, R.M., Cornejo-Villegas, M.A., Leyva-Gómez, G., Urbán-Morlán, Z. (2021). Effects of UV-C and edible nano-coating as a combined strategy to preserve fresh-cut cucumber. *Polymers*, *13*(21), art. no. 3705. https://doi.org/10.3390/polym13213705

ORIGINAL ARTICLE
http://journal.pan.olsztyn.pl

Polish Journal of Food and Nutrition Sciences
2023, Vol. 73, No. 1, 50–58
DOI: 10.31883/pjfns/159360
ISSN 1230-0322, e-ISSN 2083-6007

Use of Cashew Apple Pomace Powder in Pasta Making: Effects of Powder Ratio on the Product Quality

Thi Phuong Trang Nguyen[1,2], Thi Thu Tra Tran[1,2], Nu Minh Nguyet Ton[1,2], Van Viet Man Le[1,2*]

[1]Department of Food Technology, Ho Chi Minh City University of Technology (HCMUT), 268 Ly Thuong Kiet Street, District 10, Ho Chi Minh City, Vietnam
[2]Vietnam National University – Ho Chi Minh City (VNU-HCM), Linh Trung Ward, Thu Duc City, Ho Chi Minh City, Vietnam

The production of cashew apple juice generates fruit pomace which is rich in dietary fiber and phenolic compounds and shows high antioxidant capacity. In this research, the effects of different ratios of cashew apple pomace powder (CAPP) in the pasta formulation on the product quality were investigated. Increase in CAPP level in the pasta recipe from 0 to 20% enhanced the total dietary fiber and total phenolic content of the product by 4.1 times and 11.8 times, respectively, as well as improved the 2,2-diphenyl-1-picrylhydrazyl radical scavenging activity and ferric reducing antioxidant power by 18.2 times and 28.6 times, respectively. Nevertheless, the increased level of CAPP in the pasta recipe resulted in decreased cooking quality, textural properties and overall acceptability of the pasta. Pasta sample with 10% CAPP level in the recipe was considered high-fiber food with acceptable sensory quality. Therefore, CAPP may be considered a promising source of dietary fiber and antioxidants for the development of healthy food products.

Key words: antioxidant capacity, by-product, dietary fiber, pasta

INTRODUCTION

A balanced diet helps prevent malnutrition and certain diseases. Every day, people need food with sufficient energy content and fundamental nutrients including carbohydrates, protein, lipid, vitamins, and minerals [Stipanuk, 2019]. In addition, bioactive compounds are also important for daily diet since they have positive effects on human health. Nowadays, healthy food products have attracted great attention from consumers due to their different health-beneficial components [Bianchi *et al.*, 2021], such as dietary fiber and antioxidants.

The addition of dietary fiber and antioxidants to the formulation of conventional foods is a current trend in the development of healthy food products. According to Maphosa & Jideani [2016], increased consumption of dietary fiber improves the glucose and lipid metabolism as well as gut microbiota status, leading to the promotion of normal laxation and protective functions against colonic disorders and pathogens. Moreover, a high-fiber diet supports the treatment of eating disorders, diabetes, obesity, certain types of heart disease, and cancer. The recommended daily intake of dietary fiber should be about 35 g for an adult [Maphosa & Jideani, 2016]. Besides, antioxidants from foods can prevent or slow down oxidative damage of cell molecules by scavenging free radicals in human body. A diet rich in antioxidants may reduce the risk of various diseases including diabetes, cardiovascular diseases, inflammation, dementia, and various types of cancer, such as esophagus, stomach, and colon cancer [Tan *et al.*, 2018].

Pasta is widely selected for fiber and antioxidant fortification since it is an element of everyday diet in many countries and is poor in these components [Bianchi *et al.*, 2021]. Dietary fiber

***Corresponding Author:**
e-mail: lvvman@hcmut.edu.vn (Van Viet Man Le)

Submitted: 13 October 2022
Accepted: 16 January 2023
Published on-line: 21 February 2023

and antioxidants from many sources have been added to pasta recipes, such as whole cereal grain flours [Aravind *et al.*, 2012], powder from fruits [Bustos *et al.*, 2019], legumes [Wójtowicz & Mościcki, 2014], or vegetables [Kaur *et al.*, 2022]. Over the last decades, various by-product flours originating from food processing industry have been used in pasta formulation. Besides, these by-products contain not only dietary fiber and antioxidants but also different nutrients, such as protein and minerals, which are useful for human health. Nevertheless, the use of high ratio of food by-products in the recipe of pasta may decrease its textural profile, cooking quality and sensory properties [Bianchi *et al.*, 2021].

Cashew (*Anacardium occidentale* L.) trees are grown in tropical regions; among them Brazil, India, and Vietnam are countries with the largest export volume of cashew nuts in the world [Duarte *et al.*, 2017]. The cashew apple or cashew fruit is the pseudo--fruit above the cashew nut. After separation of cashew nut, the fruit is used to produce some value-added products, such as jam, sauce, and cashew apple juice. The obtained juice can also be used as the main material to manufacture cashew apple cordial, syrup, jelly, vinegar, and fermented beverages [Preethi *et al.*, 2021]. The production of cashew apple juice generates a by--product – cashew apple pomace, the predominant compounds of which are cellulose and hemicellulose. Polysaccharides of this by-product are treated with microbial carbohydrases to produce sugars which are subsequently used to obtain different products, such as bioethanol, enzymes, organic acids, and xylitol [Jeyavishnu *et al.*, 2021]. Recently, cashew apple pomace has been reported to contain not only phenolic compounds with high antioxidant activity but also different nutrients, including valuable proteins and minerals and therefore this by-product was added to the formulation of cereal extrudates to enhance their antioxidant activity and functional properties [Preethi *et al.*, 2021]. However, the use of cashew apple powder in pasta making has not been considered.

The purpose of this study was to evaluate the effects of cashew apple pomace ratios in pasta formulation on the proximate composition, antioxidant activity, physical properties, cooking properties, and consumer acceptability of the pasta.

MATERIALS AND METHODS

Materials

Ripe cashew apple (*Anacardium occidentale* L.) fruits without pestilence or damage were collected from a farm in Binh Phuoc province, Vietnam. After harvesting, the selected fruits were transported to Food Technology laboratory of Ho Chi Minh City University of Technology (Vietnam) and used for the preparation of cashew apple pomace powder within 24 h.

Durum wheat (*Triticum durum*) semolina was provided by Vietnam Flour Mills Co. (Ba Ria, Vung Tau province, Vietnam). Table salt was supplied by the Southern Salt Group Co. (Ho Chi Minh City, Vietnam).

Chemical reagents were purchased from Merck (Darmstadt, Germany) and they were of analytical grade. Enzyme preparations with α-amylase, glucoamylase, and protease activities were supplied by Novozymes (Bagsværd, Danmark) and used for analysis of dietary fiber.

Preparation of cashew apple pomace powder

Firstly, the nuts were manually removed; the fruits were washed with tap water, drained for 30 min, and squeezed for juice extraction. The obtained cashew apple pomace was cut into 3×2×1 cm pieces, which were subsequently blanched in 1% (*w/v*) sodium metabisulphite solution at 95°C for 10 min and drained for 10 min. The pomace was then dried at 55°C to less than 13 g/100 g moisture content, milled in a crusher, and sifted through a 70-mesh sieve. The cashew apple pomace powder (CAPP) was vacuum packed in polyethylene bags and stored at room temperature for experimentation.

Pasta making

A blend of durum wheat semolina and CAPP was used in the pasta recipe. There were five pasta samples in which the CAPP ratio was 0 (control), 5, 10, 15, and 20% of the blend weight.

The blend and table salt (0.5% on blend basis, *w/w*) were mixed in a stand mixer (Model HBD-805, Ukoeo, Zhuhai, China) with a paddle attachment for 2 min. To make a dough, distilled water at 42°C (47 g water/100 g flour) was added to the mixture and mixed at 120 rpm for 5 min. The dough was then kneaded using a dough hook at 120 rpm for 20 min before being fed to an extruder (Model HR2365/05, Philips Co., Shanghai, China). The die diameter was 1.6 mm and the extrusion pressure was 720 kgf/cm^2. The obtained pasta strands were oven-dried at 50°C for 8 h to less than 13 g/100 g moisture content. The dried pasta was kept at room temperature for 24 h before analysis.

Proximate composition analysis

Protein content was measured by AOAC International 992.23 method with a nitrogen-to-protein conversion factor of 6.25 [AOAC, 2000]. Lipid content was determined by AOAC International 920.85 method with diethyl ether solvent [AOAC, 2000]. Total starch content was quantified by spectrophotometric method, using dinitrosalicylic acid as reagent [Nielsen, 2017]. Total, soluble, and insoluble dietary fiber contents were estimated by AOAC International 985.29, 991.42, 993.19 methods, respectively [AOAC, 2000]. The moisture content was determined by drying at 105°C in a moisture analyzer (Model IR35, A&D Co., Tokyo, Japan) [Nielsen, 2017].

Determination of total phenolic content and antioxidant capacity

For the extraction of phenolics from durum semolina, CAPP, and uncooked pasta, each ground sample (1 g) was mixed with 10 mL of a 60% (*v/v*) acetone solution and left at room temperature for 30 min. The mixture was then filtered through an ashless filter paper. The filtrate was collected, filled to 100 mL with 60% (*v/v*) acetone solution, stored at –4°C away from light, and used within 2 days. The obtained extracts were used for determination of total phenolic content as well as 2,2-diphenyl-1-picrylhydrazyl (DPPH) radical scavenging activity and ferric reducing antioxidant power (FRAP).

Total phenolic content (TPC) was evaluated by spectrophotometric method, using Folin–Ciocalteu reagent; the analytical procedure was described by Biney & Beta [2014]. The results were shown as mg gallic acid equivalent per 100 g dry weight of sample (mg GAE/100 g dw).

The DPPH radical scavenging activity and FRAP were determined by spectrophotometric method following the procedures reported by Nguyen *et al.* [2020]. The results were expressed as µmol Trolox equivalent per 100 g dry weight of sample (µmol TE/100 g dw).

Water and oil holding capacity determination

The water holding capacity (WHC) was measured using the procedure described by Sangokunle *et al.* [2020] with some adjustments. About 1 g of the sample was soaked in 10 mL of distilled water and vortexed for 1 min. The mixture was left at room temperature for 2 h and then centrifuged at 1064×*g* (Certomat® BS-1, Sigma, Saint Louis, MO, USA) at room temperature for 10 min. The supernatant was removed while the sediment was weighed. The results were shown as g water/100 g dw.

The oil holding capacity (OHC) was quantified following the procedure described by Sangokunle *et al.* [2020] with some modifications. The sample (1 g) was soaked in 10 mL of soya oil and then vortexed for 1 min. The mixture was left at room temperature for 2 h and then centrifuged at 1064×*g* at room temperature for 10 min. The supernatant was decanted and the pellet was weighed. The results were expressed as g oil/100 g dw.

Cooking quality determination

The optimal cooking time (OCT), cooking loss, water absorption index (WAI), and swelling index (SI) were evaluated according to the procedure presented by Foschia *et al.* [2015] with minor modifications. The pasta sample (*ca.* 5 g) was cut into 5-cm strands and cooked in 50 mL of boiling distilled water. The OCT was recorded when white inner core of pasta just disappeared. At the end of cooking, the pasta strands were separated for draining for 4 min, and weighed (W_2). The cooked and drained pasta strands were dried at 105°C to constant weight (W_3). The cooking water was finally evaporated at 105°C to measure the total dry matter. The cooking loss was calculated as the percentage of the total dry matter of cooking water to the dry weight of raw pasta (W_1).

The SI (%) and WAI (%) were calculated according to Equations (1) and (2), respectively.

$$SI = (W_2 – W_3)/W_3 \quad (1)$$

$$WAI = (W_2 – W_1)/W_1 \quad (2)$$

Textural properties analysis

The textural properties of cooked pasta were determined with a texture analyzer (TA-XT Plus C, Stable Micro System, Godalming, United Kingdom) equipped with a Windows version of Exponent Connect Lite 7.0 software (Texture Technologies Co., Hamilton, MA, USA). A 70% axial compression of cooked pasta strand was done using a 40-mm diameter acrylic probe. The compression speed was 1 mm/s. After 1 s of the first compression, the second compression cycle was performed. The hardness, adhesiveness, springiness, cohesiveness, gumminess, and chewiness of cooked pasta samples were obtained from the force-time curve.

In the tensile strength test, cooked pasta strand was wound around parallel friction rollers two times (Pasta Tensile Rig, Stable Micro Systems). The extension speed was 1 mm/s. The tensile strength (TS, g/mm^2) and elongation rate (ER, %) were determined according Equations (3) and (4), respectively.

$$TS = F/S \quad (3)$$

where: F is the force at the break point (g), and S is the cross-sectional area of the cooked pasta strand (mm^2).

$$ER = [(D – D_0)/D_0] \times 100 \quad (4)$$

where: D is the distance at the break point (mm), and D_0 is the initial distance (mm).

Instrumental color measurement

Color of uncooked and ground pasta samples was determined using a Minolta chroma meter CM-3700A (Konica Minolta, Tokyo, Japan). The results were shown as L^* (lightness), a^* (redness), and b^* (yellowness) values. Color data were the mean of three replicate readings. The total color difference (ΔE) was determined as follows:

$$\Delta E = \sqrt{(L_0^* – L^*)^2 + (a_0^* – a^*)^2 + (b_0^* – b^*)^2} \quad (5)$$

where: L_0^*, a_0^* and $b_0^*$are the color values of the control pasta sample; and L^*, a^* and b^* are the color values of the CAPP added pasta sample.

Overall acceptability evaluation

Pasta samples were cooked for 1 min longer than the established optimal cooking time before being evaluated by 60 young adults aged from 18 to 25 to assess the overall acceptability, using a 9-point hedonic scale (from 1 – extremely dislike to 9 – extremely like). The evaluators were recruited from the students at Ho Chi Minh City University of Technology (Vietnam). The evaluators were provided with water to cleanse their palate before testing and between pasta samples. Five pasta samples were served in random order. The semi-consumer evaluation was conducted in a laboratory at ambient temperature.

Statistical analysis

All experiments were done in triplicate. The results were expressed as mean ± standard deviation. One-way analysis of variance (ANOVA), correlation coefficients between variables and Duncan's multiple range test with significance level of $p<0.05$ were done using Statgraphics Centurion 18.1.12 software (Statgraphics Technologies, Inc., The Plains, VA, USA).

RESULTS AND DISCUSSION

Proximate composition, antioxidant activity, and physical properties of cashew apple pomace powder and durum semolina used for pasta making

The proximate composition, antioxidant activity, and physical properties of CAPP and durum semolina used in the study were shown in Table 1. The CAPP contained more lipid and ash but had lower protein and starch content compared to the durum semolina. The total dietary fiber (TDF), insoluble dietary fiber (IDF), and soluble dietary fiber (SDF) content of CAPP was 20.1, 25.2, and 7.7 times, respectively, higher than that of durum semolina. The proximate composition of CAPP in this research was different to that reported by Duarte *et al.* [2017] or Preethi *et al.* [2021] due to the difference in cultivars of cashew apple, growing conditions of plant as well as cashew apple juice processing conditions.

The CAPP was rich in phenolics, the total content of which was about 50 times higher than that of durum semolina (Table 1). As a result, the DPPH radical scavenging activity, and ferric reducing antioxidant power of CAPP were 140 and 229 times, respectively, higher than those of durum semolina. Different phenolic compounds with high antioxidant activity were identified in cashew apple pomace, such as gallic acid, myricetin, and quercetin [Silveira *et al.*, 2021]. It can be suggested that the addition of CAPP to pasta recipe would improve dietary fiber content and antioxidant activity of the product.

Results in Table 1 also reveal that the CAPP was darker (lower L^* value) than the durum semolina. This can be explained by Maillard reactions between the residual reducing sugars and amino acids/proteins in cashew apple pomace (data not shown) during the drying process. In addition, the positive a^* and b^* values of CAPP color were recorded probably due to its red and yellow pigments, respectively. It is reported that the peel and pulp of ripen cashew apple contains carotenoids which exhibit red, yellow and other colors [Schweiggert *et al.*, 2016].

The WHC of CAPP was 2.8 times higher than that of semolina while their OHC was similar (values were not significantly different, $p<0.05$) (Table 1). The cashew apple fiber mainly consists of cellulose, hemicellulose, and lignin [Jeyavishnu *et al.*, 2021]. According to Chami Khazraji & Robert [2013], water molecules could rapidly interact with cellulose in both interfibrillar spaces and amorphous regions. Previous studies showed that red raspberry fruit pomace [Gouw *et al.*, 2017] and apple pomace [Wang *et al.*, 2019] with high cellulose content also had high WHC.

Table 1. Proximate composition, antioxidant activity, and physical properties of cashew apple pomace powder and durum wheat semolina used for pasta making.

	Cashew apple pomace powder	Durum wheat semolina
Protein (g/100 g dw)	12.5±0.6^b	14.9±0.5^a
Lipid (g/100 g dw)	10.8±0.2^a	2.8±0.1^b
Ash (g/100 g dw)	3.4±0.0^a	0.6±0.0^b
Starch (g/100 g dw)	19.3±1.0^b	80.9±0.8^a
TDF (g/100 g dw)	48.3±2.1^a	2.4±0.1^b
IDF (g/100 g dw)	42.9±2.3^a	1.7±0.1^b
SDF (g/100 g dw)	5.4±0.7^a	0.7±0.0^b
Total phenolics (mg GAE/100 g dw)	7101±119^a	143±3^b
Ferric reducing antioxidant power (µmol TE/100 g dw)	17168±100^a	75±2^b
DPPH radical scavenging activity (µmol TE/100 g dw)	20154±700^a	114±7^b
L^*	72.6±0.2^b	91.2±0.0^a
a^*	3.8±0.1^a	0.9±0.0^b
b^*	26.8±0.4^a	10.0±0.0^b
ΔE	25.2±0.4^a	0.0±0.0^b
Water holding capacity (g water/g dw)	3.1±0.0^a	1.1±0.1^b
Oil holding capacity (g oil/g dw)	2.3±0.1^a	2.2±0.4^a

Data are shown as mean ± standard deviation (n=3). Values with different letters in the same row are significantly different ($p<0.05$). dw, dry weight; TDF, total dietary fiber; IDF, insoluble dietary fiber; SDF, soluble dietary fiber; GAE, gallic acid equivalent; DPPH radical, 2,2-diphenyl-1-picrylhydrazyl radical; TE, Trolox equivalent.

Effects of ratios of cashew apple pomace powder on proximate composition of pasta

The proximate composition of pasta fortified with CAPP is presented in Table 2. When the CAPP level in the pasta formulation increased from 0 to 20%, the lipid and ash content of the product increased by 2.1 times and 1.9 times, respectively, while its protein and starch content decreased by 48% and 15%, respectively. This is due to the increased level of CAPP in the pasta recipe and the high lipid and ash content as well as the low starch and protein content of CAPP (Table 1). At 5% CAPP level, the TDF, IDF and SDF content of the obtained pasta enhanced by 2.1, 2.7 and 1.3 times, respectively, compared to that of the control pasta (Table 2). The greater the CAPP level in the pasta recipe was, the higher was the dietary fiber content of the product. Similar results were reported when cucumber pomace powder [Saad *et al.*, 2021] and grape pomace powder [Balli *et al.*, 2021] were added to the pasta formulation. It should be noted that pasta with 5% CAPP or higher level can be claimed as high-dietary fiber pasta following the labeling guidelines of the European Union, in which food with TDF content higher than 6 g/100 g dw is considered a product high in fiber [Tolve *et al.*, 2020]. According to Oba-Yamamoto *et al.* [2022], low-starch and high-fiber pasta is proven to help control blood glucose levels and to prevent and/or take part in the treatment of type 2 diabetes.

Increase in CAPP level in the pasta formulation from 0% to 20% enhanced the IDF:SDF ratio from 1.3:1 to 4.0:1 (*w/w*). The pasta samples with 5% and 10% CAPP had IDF:SDF ratio close to the dietetic recommendations, *i.e.*, 3:1, *w/w* [Bader Ul Ain *et al.*, 2018]. The previous studies revealed that the IDF:SDF ratio of pasta with 10% wheat bran, tomato peel or coconut residue was 4.0:1 [Nguyen *et al.*, 2020], 2.2:1 [Padalino *et al.*, 2017] or 1.5:1 (*w/w*) [Sykut-Domańska *et al.*, 2020], respectively. Therefore, the pasta

Table 2. Proximate composition of pasta with different cashew apple pomace powder (CAPP) levels.

Component	Ratio of CAPP (%)				
	0	5	10	15	20
Protein (g/100 g dw)	15.2±0.7^{a}	12.9±0.6^{b}	10.3±0.4^{c}	9.1±0.2^{d}	7.9±0.3^{e}
Lipid (g/100 g dw)	1.8±0.2^{c}	2.2±0.8^{bc}	2.7±0.6^{ab}	3.0±0.8^{ab}	3.7±0.2^{a}
Ash (g/100 g dw)	0.8±0.1^{c}	1.2±0.0^{b}	1.3±0.1^{b}	1.4±0.1^{a}	1.5±0.1^{a}
Starch (g/100 g dw)	80.9±0.8^{a}	77.8±0.6^{b}	74.8±0.6^{c}	71.6±0.5^{d}	68.6±0.4^{e}
TDF (g/100 g dw)	3.5±0.1^{e}	7.3±0.2^{d}	9.7±0.1^{c}	12.0±0.4^{b}	14.2±0.2^{a}
IDF (g/100 g dw)	2.0±0.1^{e}	5.3±0.2^{d}	7.5±0.1^{c}	9.4±0.4^{b}	11.4±0.2^{a}
SDF (g/100 g dw)	1.5±0.2^{e}	2.0±0.1^{d}	2.3±0.1^{c}	2.6±0.1^{b}	2.8±0.1^{a}
IDF:SDF	1.3:1±0.1^{e}	2.6:1±0.1^{d}	3.3:1±0.2^{c}	3.6:1±0.3^{b}	4.0:1±0.1^{a}

Data are shown as mean ± standard deviation (n=3). Values with different letters in the same row are significantly different (p<0.05). dw, dry weight; TDF, total dietary fiber; IDF, insoluble dietary fiber; SDF, soluble dietary fiber.

supplemented with 10% CAPP had a fairly balanced IDF:SDF ratio as compared to that fortified with other dietary fiber sources.

Effects of ratios of cashew apple pomace powder on the total phenolic content and antioxidant capacity of pasta

Figure 1 presents the TPC and antioxidant capacity of pasta with different CAPP levels. Increase in CAPP ratio in the pasta recipe from 0 to 20% greatly improved TPC of the product. The TPC of pasta fortified with 10% CAPP was 7.6 times higher than that of the control pasta. It should be noted that at 10% fiber material level, the CAPP-incorporated pasta had much more total phenolics (794 mg GAE/100 g dw) than earlier analyzed grape pomace-supplemented pasta (257 mg GAE/100 g dw) [Tolve *et al.*, 2020], and olive pomace added pasta (228 mg GAE/100 g dw) [Simonato *et al.*, 2019].

The pasta with high CAPP level had improved antioxidant capacity. The DPPH radical scavenging activity and FRAP of pasta with 20% CAPP level increased by 18.2 times and 28.7 times, respectively, compared to those of the control pasta (Figure 1B and Figure 1C).

Close significant (p<0.05) correlations were observed for TPC and antioxidant capacity of the CAPP pasta samples. The correlation coefficients between TPC and DPPH radical scavenging activity as well as between TPC and FRAP were 0.955 and 0.980, respectively.

Effects of ratios of cashew apple pomace powder on cooking quality of pasta

The cooking quality of pasta with different CAPP levels is shown in Table 3. Increase in CAPP ratio in the pasta formulation from 0 to 20% decreased optimal cooking time of the product from 13.5 to 6.4 min. Reduction in optimal cooking time was also reported by Nguyen *et al.* [2020] when wheat bran was added to pasta recipe. According to these authors, the decrease in gluten content and the presence of fiber in pasta result in more channels for water diffusion from cooking water into pasta; the optimal cooking time of high fiber pasta is therefore reduced.

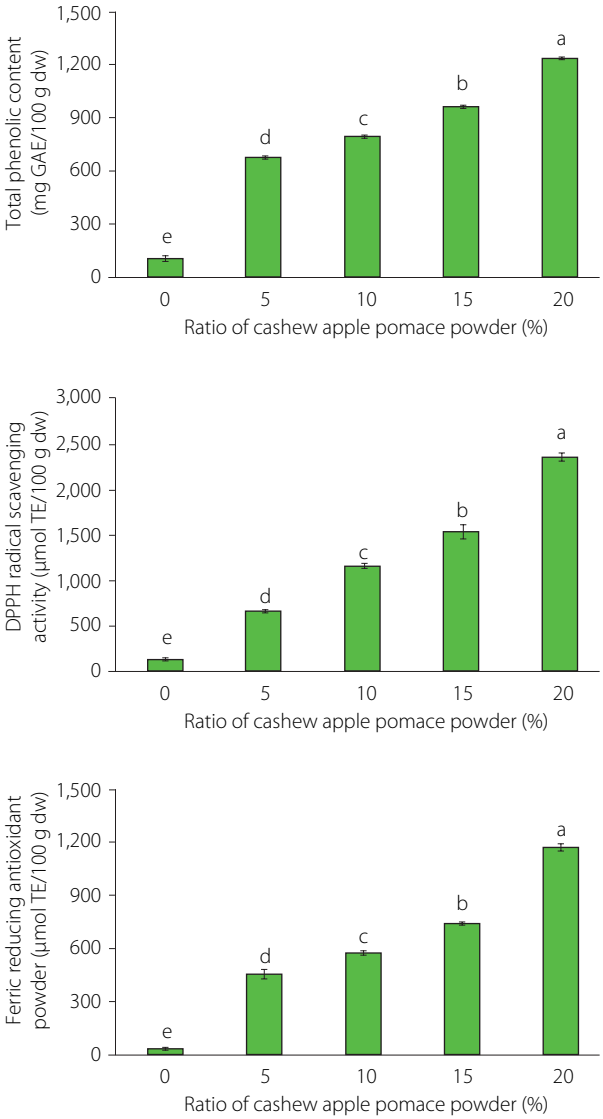

Figure 1. Total phenolic content (A), DPPH radical scavenging activity (B) and ferric reducing antioxidant power (C) of the pasta supplemented with different ratios of cashew apple pomace powder. GAE, gallic acid equivalent; dw, dry weight; TE, Trolox equivalent. Data are shown as mean ± standard deviation (n=3). Bars with different letters show significantly different values (p<0.05).

The cooking loss of pasta samples with 5–20% CAPP was 11–65% greater than that of the control (Table 3) mainly due to their decreased gluten content. As a consequence, the gluten system was weakened and the diffusion of starch and other components from the pasta into the cooking water was enhanced [Chusak *et al.*, 2020, Nguyen *et al.*, 2020]. High cooking loss was also recorded for pasta samples fortified with gac fruit [Chusak *et al.*, 2020] or berry powder [Bustos *et al.*, 2019].

Water absorption index presents the amount of water absorbed into the product during the cooking process while swelling index shows the change in the volume of cooked pasta compared to uncooked one [Chusak *et al.*, 2020]. Results provided in Table 3 reveal that the increase in CAPP ratio in the pasta formulation gradually reduced both WAI and SI. The water absorption index and swelling index of pasta with 20% CAPP dropped by 45% and 40%, respectively, compared to those of the durum semolina pasta. Similar trend has recently been observed by Chusak *et al.* [2020] when durum semolina was partially replaced by ripe gac fruit powder in the pasta recipe. The increased fiber content disrupted the starch-gluten network, allowing starch molecules to leak more into cooking water [Aravind *et al.*, 2012]. At the same time, dietary fiber has greater hydration dynamic than starch; the water is held more loosely by fiber than by starch [Wang *et al.*, 2020], leading to the decreased swelling index of the high-fiber pasta samples.

Effects of ratios of cashew apple pomace powder on physical properties of pasta

Textural properties of pasta samples with different CAPP ratios are presented in Table 4. When the CAPP ratio increased from 0 to 20%, the hardness of pasta rose by 46%. That can be explained by high water holding capacity of fiber in the pasta sample, leading to the prevention of water absorption and swelling of starch granules; this phenomenon caused the decrease in swelling index and made the cooked pasta become harder [Rakhesh *et al.*, 2015]. The increase in hardness of pasta was also recorded when tomato pomace powder [Padalino *et al.*, 2017] or soy okara powder were added to the product recipe [Kamble *et al.*, 2019].

Adhesiveness is the force required to remove the probe from the pasta sample. All pasta samples supplemented with CAPP had greater adhesiveness than the control pasta (Table 4). Increase in adhesiveness was previously reported when the ratio

Table 3. Cooking quality of pasta with different cashew apple pomace powder (CAPP) levels.

Cooking property	Ratio of CAPP (%)				
	0	5	10	15	20
Optimal cooking time (min)	13.5±0.0^{a}	11.5±0.3^{b}	9.2±0.2^{c}	8.5±0.1^{d}	6.4±0.1^{e}
Cooking loss (%)	4.6±0.2^{e}	5.1±0.2^{d}	6.1±0.2^{c}	7.2±0.2^{b}	7.6±0.2^{a}
Water absorption index	2.2±0.3^{a}	1.8±0.2^{b}	1.6±0.1^{bc}	1.4±0.1^{cd}	1.2±0.0^{d}
Swelling index	2.5±0.1^{a}	2.1±0^{b}	1.9±0.1^{c}	1.7±0.1^{cd}	1.5±0.1^{d}

Data are shown as mean ± standard deviation (n=3). Values with different letters in the same row are significantly different (p<0.05).

Table 4. Textural properties and instrumental color parameters of pasta with different cashew apple pomace powder (CAPP) levels.

Physical property	Ratio of CAPP (%)				
	0	5	10	15	20
Hardness (N)	1769±128^{c}	2068±23^{b}	2221±24^{b}	2433±167^{a}	2584±79^{a}
Adhesiveness	33±5^{c}	56±5^{b}	65±7^{b}	80±6^{a}	92±12^{a}
Springiness	0.94±0.03^{a}	0.85±0.03^{b}	0.85±0.03^{b}	0.80±0.02^{c}	0.79±0.02^{c}
Cohesiveness	0.53±0.04^{a}	0.45±0.02^{b}	0.43±0.03^{b}	0.40±0.03^{b}	0.40±0.00^{b}
Gumminess (g)	1042±23^{a}	985±29^{b}	980±25^{b}	909±32^{c}	901±27^{c}
Chewiness (g)	1001±60^{a}	800±51^{b}	797±26^{b}	641±31^{c}	647±30^{c}
Elongation rate (%)	192±18^{a}	138±7^{b}	119±10^{bc}	99±9^{c}	67±12^{d}
Tensile strength (kPa)	3.0±0.3^{b}	3.1±0.3^{b}	4.0±0.3^{a}	4.2±0.2^{a}	4.3±0.2^{a}
L*	87.1±0.1^{a}	82.7±0.6^{b}	81.1±0.2^{c}	80.0±0.3^{d}	78.4±0.1^{e}
a*	1.2±0.1^{d}	1.6±0.2^{c}	1.7±0.0^{c}	2.0±0.1^{b}	2.2±0.0^{a}
b*	7.8±0.2^{d}	9.7±0.5^{c}	11.1±0.1^{b}	12.6±0.3^{a}	12.5±0.2^{a}
ΔE	0.0±0.0^{e}	4.9±0.7^{d}	6.9±0.2^{c}	8.6±0.5^{b}	9.9±0.1^{a}

Data are shown as mean ± standard deviation (n=3). Values with different letters in the same row are significantly different (p<0.05). L^*, lightness; a^*, redness; b^*, yellowness; ΔE, total color difference.

of tomato pomace powder added to the pasta recipe was 15% [Padalino *et al.*, 2017]. The presence of fibers in pasta disrupted the continuity of its structure [Chusak *et al.*, 2020]. According to Bouasla *et al.* [2017], the change in adhesiveness is related to the fiber content and the dissolution of components such as starch, protein, soluble fiber in the cooking water. These components may form sticky layers on the surface of pasta strands [Rakhesh *et al.*, 2015].

Springiness represents the ability of pasta to recover its original shape after being subjected to an external force. At 20% CAPP ratio, the springiness of pasta decreased by 16% in comparison with that of the control (Table 4). Reduction in springiness was previously observed when apple pomace was added to pasta formulation [Xu *et al.*, 2020]. Bustos *et al.* [2011] explained that the decrease in springiness was related to the weak development of the protein-starch matrix due to the distribution of fiber in the pasta dough.

Cohesiveness measures the ability of pasta to withstand external forces before breaking, while gumminess is the force required to crush the pasta, and chewiness is the total force required to chew and swallow the product. The cohesiveness, gumminess, and chewiness of pasta with 20% CAPP decreased by 25%, 14%, and 35%, respectively in comparison with those of the control (Table 4). Decrease in cohesiveness and chewiness were also recorded for pasta samples supplemented with cucumber pomace [Saad *et al.*, 2021]. The presence of insoluble fiber in the product reduces the swelling of starch granules because of water competition, leading to negative change in textural properties [Saad *et al.*, 2021]. On the other hand, the disruption of the gluten network can also be a reason for the pasta to be broken more easily under external forces.

Among the textural properties of CAPP pasta, a close correlation was observed between the hardness as well as adhesiveness with the CAPP ratio in the pasta recipe. The CAPP level significantly ($p<0.05$), positively correlated with the hardness and adhesiveness and their correlation coefficients were 0.992 and 0.990, respectively. Similar correlation was reported when tomato pomace powder was supplemented to the pasta formulation [Padalino *et al.*, 2017].

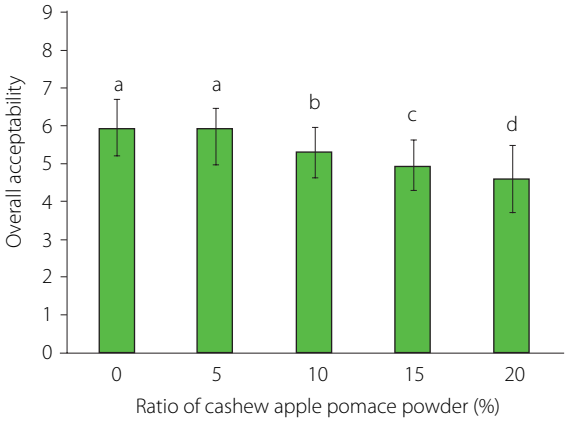

Figure 2. Overall acceptability of the pasta supplemented with different ratios of cashew apple pomace powder. Data are shown as mean ± standard deviation ($n=60$). Bars with different letters show significantly different values ($p<0.05$).

A tensile strength test is performed to clarify how much force is required to break pasta strands when they are pulled apart. Increase in CAPP ratio in the pasta recipe enhanced the tensile strength but decreased the elongation rate of pasta (Table 4). Shiau *et al.* [2020] also reported an increased tension strength as well as a reduced elongation rate of wheat noodles fortified with pitaya peel powder. According to the authors, the rigidity of fiber and the decrease in free water in the cooked pasta samples could cause the rise of tensile strength, while the decrease in elongation rate might be due to the weak gluten network of the high-fiber pasta.

Our study showed that the increased CAPP ratio in the pasta formulation negatively affected both textural and cooking properties of the product. Future studies on the interaction of CAPP fiber and protein-starch matrix of the blend dough are needed to clarify the effects of fiber on textural and cooking properties of high-fiber pasta.

The addition of CAPP to pasta recipe slightly enhanced darkness of the product since the L^* value of CAPP was lower than that of durum semolina (Table 4). Similar results were reported when fruit pomace such as apple pomace [Xu *et al.*, 2020] or grape pomace [Tolve *et al.*, 2020] was added to the pasta formulation. The redness (positive a^* value) and yellowness (positive b^* value) were observed for all pasta samples and their values varied in narrow ranges. Higher levels of CAPP caused higher ΔE value, which proved a greater difference in color between the CAPP added pasta and the control pasta.

Effects of ratios of cashew apple pomace powder on overall acceptability of pasta

The overall acceptability of all cooked pasta samples is shown in Figure 2. Pasta with 5% CAPP had a similar score to the control while higher level of CAPP led to the decreased overall acceptability. The decrease in sensory score was also recorded when adding legume flour [Wójtowicz & Mościcki, 2014] or partially-deoiled chia flour to the pasta recipe [Aranibar *et al.*, 2018]. It can be explained by the negative change in textural profile of cooked pasta. Texture is the key property for the evaluation of pasta quality [Poonsri *et al.*, 2019]. The increase in hardness may have strong effects on sensory properties of CAPP pasta since the customers did not favor pasta with high hardness [Prerana & Anupama, 2020]. Furthermore, the color of pasta is also a crucial property and is the first to affect the consumer acceptability [Sykut-Domańska *et al.*, 2020]. The pasta samples with high CAPP levels had a distinctly darker color compared to the control with light yellow color. Pasta sample with 10% CAPP had an average liking score of 5.3, which could be considered acceptable.

CONCLUSIONS

Use of CAPP in the pasta recipe significantly increased the dietary fiber and TPC content as well as the antioxidant capacity of the final product. Nevertheless, a high ratio of CAPP in the pasta formulation reduced its cooking quality, textural properties, and overall acceptability. The pasta with CAPP addition

level of 10% was considered high-fiber food with acceptable sensory quality. The interaction of CAPP fiber and protein-starch matrix of the blend dough needs to be investigated in the future to clarify the effects of fiber on textural properties and cooking quality of high-fiber pasta samples. Based on the present study results, CAPP may be found a potential ingredient for the development of different food products with high fiber and antioxidant content.

ACKNOWLEDGEMENTS

We acknowledge the support of time and facilities from Ho Chi Minh City University of Technology (HCMUT), VNU-HCM for this study.

RESEARCH FUNDING

This research WAS funded by Vietnam National University – Ho Chi Minh City (VNU-HCM) under grant number NCM2020-20-01.

CONFLICT OF INTERESTS

All authors of this manuscript declare no conflict of interest.

ORCID IDs

V.V.M. Le https://orcid.org/0000-0003-3284-207X
N.M.N. Ton https://orcid.org/0000-0002-3514-9193
T.T.T. Tran https://orcid.org/0000-0001-9942-7458

REFERENCES

1. AOAC International (2000). *Official Methods of Analysis of AOAC International*. 12th ed., Gaithersburg, MD, USA.
2. Aranibar, C., Pigni, N.B., Martinez, M., Aguirre, A., Ribotta, P., Wunderlin, D., Borneo, R. (2018). Utilization of a partially-deoiled chia flour to improve the nutritional and antioxidant properties of wheat pasta. *LWT – Food Science and Technology*, *89*, 381–387. https://doi.org/10.1016/j.lwt.2017.11.003
3. Aravind, N., Sissons, M., Egan, N., Fellows, C. (2012). Effect of insoluble dietary fibre addition on technological, sensory, and structural properties of durum wheat spaghetti. *Food Chemistry*, *130*(2), 299–309. https://doi.org/10.1016/j.foodchem.2011.07.042
4. Bader Ul Ain, H., Saeed, F., Arshad, M.U., Ahmad, N., Nasir, M.A., Amir, R.M., Kausar, R., Niaz, B. (2018). Modification of barley dietary fiber through chemical treatments in combination with thermal treatment to improve its bioactive properties. *International Journal of Food Properties*, *21*(1), 2491–2499. https://doi.org/10.1080/10942912.2018.1528454
5. Balli, D., Cecchi, L., Innocenti, M., Bellumori, M., Mulinacci, N. (2021). Food by-products valorisation: Grape pomace and olive pomace (pâté) as sources of phenolic compounds and fiber for enrichment of tagliatelle pasta. *Food Chemistry*, *355*, art. no. 129642. https://doi.org/10.1016/j.foodchem.2021.129642
6. Bianchi, F., Tolve, R., Rainero, G., Bordiga, M., Brennan, C.S., Simonato, B. (2021). Technological, nutritional and sensory properties of pasta fortified with agro-industrial by-products: a review. *International Journal of Food Science and Technology*, *56*(9), 4356–4366. https://doi.org/10.1111/ijfs.15168
7. Biney, K., Beta, T. (2014). Phenolic profile and carbohydrate digestibility of durum spaghetti enriched with buckwheat flour and bran. *LWT – Food Science and Technology*, *57*(2), 569–579. https://doi.org/10.1016/j.lwt.2014.02.033
8. Bouasla, A., Wójtowicz, A., Zidoune, M.N. (2017). Gluten-free precooked rice pasta enriched with legumes flours: Physical properties, texture, sensory attributes and microstructure. *LWT – Food Science and Technology*, *75*, 569–577. https://doi.org/10.1016/j.lwt.2016.10.005
9. Bustos, M.C., Paesani, C., Quiroga, F., León, A.E. (2019). Technological and sensorial quality of berry-enriched pasta. *Cereal Chemistry*, *96*(5), 967–976. https://doi.org/10.1002/cche.10201
10. Bustos, M.C., Pérez, G.T., León, A.E. (2011). Effect of four types of dietary fiber on the technological quality of pasta. *Food Science and Technology International*, *17*(3), 213–221. https://doi.org/10.1177/1082013210382303
11. Chami Khazraji, A., Robert, S. (2013). Interaction effects between cellulose and water in nanocrystalline and amorphous regions: A novel approach using molecular modeling. *Journal of Nanomaterials*, *2013*, art. no. 409676. https://doi.org/10.1155/2013/409676
12. Chusak, C., Chanbunyawat, P., Chumnumduang, P., Chantarasinlapin, P., Suantawee, T., Adisakwattana, S. (2020). Effect of gac fruit (*Momordica cochinchinensis*) powder on *in vitro* starch digestibility, nutritional quality, textural and sensory characteristics of pasta. *LWT – Food Science and Technology*, *118*, art. no. 108856. https://doi.org/10.1016/j.lwt.2019.108856
13. Duarte, F.N.D., Rodrigues, J.B., da Costa Lima, M., Lima, M.D.S., Pacheco, M.T.B., Pintado, M.M.E., de Souza Aquino, J., de Souza, E.L. (2017). Potential prebiotic properties of cashew apple (*Anacardium occidentale* L.) agro-industrial byproduct on *Lactobacillus* species. *Journal of the Science of Food and Agriculture*, *97*(11), 3712–3719. https://doi.org/10.1002/jsfa.8232
14. Foschia, M., Peressini, D., Sensidoni, A., Brennan, M.A., Brennan, C.S. (2015). How combinations of dietary fibres can affect physicochemical characteristics of pasta. *LWT – Food Science and Technology*, *61*(1), 41–46. https://doi.org/10.1016/j.lwt.2014.11.010
15. Gouw, V.P., Jung, J., Zhao, Y. (2017). Functional properties, bioactive compounds, and *in vitro* gastrointestinal digestion study of dried fruit pomace powders as functional food ingredients. *LWT – Food Science and Technology*, *80*, 136–144. https://doi.org/10.1016/j.lwt.2017.02.015
16. Jeyavishnu, K., Thulasidharan, D., Shereen, M.F., Arumugam, A. (2021). Increased revenue with high value-added products from cashew apple (*Anacardium occidentale* L.)—addressing global challenges. *Food and Bioprocess Technology*, *14*(6), 985–1012. https://doi.org/10.1007/s11947-021-02623-0
17. Kamble, D.B., Singh, R., Rani, S., Pratap, D. (2019). Physicochemical properties, *in vitro* digestibility and structural attributes of okara-enriched functional pasta. *Journal of Food Processing and Preservation*, *43*(12), art. no. e14232. https://doi.org/10.1111/jfpp.14232
18. Kaur, M., Dhaliwal, M., Kaur, H., Singh, M., Bangar, S.P., Kumar, M., Pandiselvam, R. (2022). Preparation of antioxidant-rich tricolor pasta using microwave processed orange pomace and cucumber peel powder: A study on nutraceutical, textural, color, and sensory attributes. *Journal of Texture Studies*, *53*(6), 834–843. https://doi.org/10.1111/jtxs.12654
19. Maphosa, Y., Jideani, V.A. (2016). Dietary fiber extraction for human nutrition—A review. *Food Reviews International*, *32*(1), 98–115. https://doi.org/10.1080/87559129.2015.1057840
20. Nielsen, S.S. (2017). *Food Analysis*. 5th edition. Springer, Cham, Switzerland. pp. 257–360. https://doi.org/10.1007/978-3-319-45776-5
21. Nguyen, S.N., Ngo, T.C.T., Tran, T.T.T., Ton, N.M.N., Le, V.V.M. (2020). Pasta from cellulase-treated wheat bran and durum semolina: Effects of vital gluten addition and/or transglutaminase treatment. *Food Bioscience*, *38*, art. no. 100782. https://doi.org/10.1016/j.fbio.2020.100782
22. Oba-Yamamoto, C., Takeuchi, J., Nakamura, A., Nomoto, H., Kameda, H., Cho, K.Y., Atsumi, T., Miyoshi, H. (2022). Impact of low-starch high-fiber pasta on postprandial blood glucose. *Nutrition, Metabolism and Cardiovascular Diseases*, *32*(2), 487–493. https://doi.org/10.1016/j.numecd.2021.10.019
23. Padalino, L., Conte, A., Lecce, L., Likyova, D., Sicari, V., Pellicanò, T.M., Poiana, M., Del Nobile, M.A. (2017). Functional pasta with tomato by-product as a source of antioxidant compounds and dietary fibre. *Czech Journal of Food Sciences*, *35*(1), 48–56. https://doi.org/10.17221/171/2016-CJFS
24. Poonsri, T., Jafarzadeh, S., Ariffin, F., Abidin, S.Z., Barati, Z., Latif, S., Müller, J. (2019). Improving nutrition, physicochemical and antioxidant properties of rice noodles with fiber and protein-rich fractions derived from cassava leaves. *Journal of Food and Nutrition Research*, *7*(4), 325–332. https://doi.org/10.12691/jfnr-7-4-10
25. Preethi, P., Mangalassery, S., Shradha, K., Pandiselvam, R., Manikantan, M.R., Reddy, S.V.R., Devi, S.R., Nayak, M.G. (2021). Cashew apple pomace powder enriched the proximate, mineral, functional and structural properties of cereal based extrudates. *LWT – Food Science and Technology*, *139*, art. no. 110539. https://doi.org/10.1016/j.lwt.2020.110539
26. Prerana, S., Anupama, D. (2020). Influence of carrot puree incorporation on quality characteristics of instant noodles. *Journal of Food Process Engineering*, *43*(3), art. no. e13270. https://doi.org/10.1111/jfpe.13270
27. Rakhesh, N., Fellows, C.M., Sissons, M. (2015). Evaluation of the technological and sensory properties of durum wheat spaghetti enriched with different dietary fibres. *Journal of the Science of Food and Agriculture*, *95*(1), 2–11. https://doi.org/10.1002/jsfa.6723

28. Saad, A.M., El-Saadony, M.T., Mohamed, A.S., Ahmed, A.I., Sitohy, M.Z. (2021). Impact of cucumber pomace fortification on the nutritional, sensorial and technological quality of soft wheat flour-based noodles. *International Journal of Food Science and Technology*, *56*(7), 3255–3268. https://doi.org/10.1111/ijfs.14970
29. Sangokunle, O.O., Sathe, S.K., Singh, P. (2020). Purified starches from 18 pulses have markedly different morphology, oil absorption and water absorption capacities, swelling power, and turbidity. *Starch-Stärke*, *72*(11–12), art. no. 2000022. https://doi.org/10.1002/star.202000022
30. Schweiggert, R.M., Vargas, E., Conrad, J., Hempel, J., Gras, C.C., Ziegler, J.U., Mayer, A., Jiménez, V., Esquivel, P., Carle, R. (2016). Carotenoids, carotenoid esters, and anthocyanins of yellow-, orange-, and red-peeled cashew apples (*Anacardium occidentale* L.). *Food Chemistry*, *200*, 274–282. https://doi.org/10.1016/j.foodchem.2016.01.038
31. Shiau, S.-Y., Li, G.-H., Pan, W.-C., Xiong, C. (2020). Effect of pitaya peel powder addition on the phytochemical and textural properties and sensory acceptability of dried and cooked noodles. *Journal of Food Processing and Preservation*, *44*(7), art. no. e14491. https://doi.org/10.1111/jfpp.14491
32. Silveira, A.G., Lopes, M.M.A., Pereira, E.C., de Castro, G.M.C., Germano, T.A., Oliveira, L.S., Ribeiro, P.R.V., Canuto, K.M., de Miranda, M.R.A., de Carvalho, J.M. (2021). Profile of phenolic compounds and antimicrobial potential of hydro-alcoholic extracts from cashew-apple coproducts. *Emirates Journal of Food and Agriculture*, *33*(2), 139–148. https://doi.org/10.9755/ejfa.2021.v33.i2.2566
33. Simonato, B., Trevisan, S., Tolve, R., Favati, F., Pasini, G. (2019). Pasta fortification with olive pomace: Effects on the technological characteristics and nutritional properties. *LWT – Food Science and Technology*, *114*, art. no. 108368. https://doi.org/10.1016/j.lwt.2019.108368
34. Stipanuk, M.H. (2019). Nutrients: History and Definitions. In M.H. Stipanuk, M.A. Caudill (Eds.), *Biochemical, Physiological, and Molecular Aspects of Human Nutrition - E-book*, Elsevier Health Sciences, St. Louis, Missouri, USA, pp. 6–7.
35. Sykut-Domańska, E., Zarzycki, P., Sobota, A., Teterycz, D., Wirkijowska, A., Blicharz-Kania, A., Andrejko, D., Mazurkiewicz, J. (2020). The potential use of by-products from coconut industry for production of pasta. *Journal of Food Processing and Preservation*, *44*(7), art. no. e14490. https://doi.org/10.1111/jfpp.14490
36. Tan, B.L., Norhaizan, M.E., Liew, W.-P.-P., Sulaiman Rahman, H. (2018). Antioxidant and oxidative stress: A mutual interplay in age-related diseases. *Frontiers in Pharmacology*, *9*, art. no. 1162. https://doi.org/10.3389/fphar.2018.01162
37. Tolve, R., Pasini, G., Vignale, F., Favati, F., Simonato, B. (2020). Effect of grape pomace addition on the technological, sensory, and nutritional properties of durum wheat pasta. *Foods*, *9*(3), art. no. 354. https://doi.org/10.3390/foods9030354
38. Wang, L., Zhao, H., Brennan, M., Guan, W., Liu, J., Wang, M., Wen, X., He, J., Brennan, C. (2020). *In vitro* gastric digestion antioxidant and cellular radical scavenging activities of wheat-shiitake noodles. *Food Chemistry*, *330*, art. no. 127214. https://doi.org/10.1016/j.foodchem.2020.127214
39. Wang, S., Gu, B.-J., Ganjyal, G.M. (2019). Impacts of the inclusion of various fruit pomace types on the expansion of corn starch extrudates. *LWT – Food Science and Technology*, *110*, 223–230. https://doi.org/10.1016/j.lwt.2019.03.094
40. Wójtowicz, A., Mościcki, L. (2014). Influence of legume type and addition level on quality characteristics, texture and microstructure of enriched precooked pasta. *LWT – Food Science and Technology*, *59*(2), 1175–1185. https://doi.org/10.1016/j.lwt.2014.06.010
41. Xu, J., Bock, J.E., Stone, D. (2020). Quality and textural analysis of noodles enriched with apple pomace. *Journal of Food Processing and Preservation*, *44*(8), art. no. e14579. https://doi.org/10.1111/jfpp.14579

ORIGINAL ARTICLE
http://journal.pan.olsztyn.pl

Polish Journal of Food and Nutrition Sciences
2023, Vol. 73, No. 1, 59–69
DOI: 10.31883/pjfns/159651
ISSN 1230-0322, e-ISSN 2083-6007

Effect of Different Cooking Methods on Lipid Content and Fatty Acid Profile of Red Mullet (*Mullus barbatus*)

Francesca Biandolino[1], Ermelinda Prato[1]*, Asia Grattagliano[2], Isabella Parlapiano[1]

[1]National Research Council, Water Research Institute (CNR-IRSA), Via Roma, 3, 74123 Taranto, Italy
[2]Department of Chemical Sciences and Technologies, University of Rome Tor Vergata, Via della Ricerca Scientifica, 1, 00133 Roma, Italy

This study investigated the effect of five in-house cooking methods (grilling, oven-cooking, frying, microwaving, and boiling) on lipid content and fatty acid composition in red mullet (*Mullus barbatus*). Moreover, the nutritional quality of the lipid fraction was evaluated by determining a number of lipid nutritional quality indices (LNQI). Moisture content of red mullet decreased after cooking, with the exception of boiled fish, while the lipid content significantly increased after microwave treatment and frying. After the latter, a ten-fold increase in lipid content was noted compared to fresh fish (from 2.1 to 21.1 g/100 g wet matter). All cooking methods caused significant changes in the fatty acid (FA) profile of *M. barbatus*. The content of saturated fatty acids (SFAs) varied significantly between raw and cooked fish with the lowest values determined for fried sample. Monounsaturated fatty acid (MUFA) content increased after oven cooking and frying, while polyunsaturated fatty acid (PUFA) content showed an opposite trend. The eicosapentaenoic acid (EPA) and docosahexaenoic (DHA) were the dominant fatty acids among *n*3 acids in all samples. EPA+DHA contribution in total FAs was significantly lower in the samples after oven cooking (19.6% total FAs) and frying (4.99% total FAs) than in the raw (25.5% of total FAs) fish. The *n*3/*n*6 ratio (range 1.25–3.65) decreased significantly after cooking; however, it remained above the recommended values for a healthy human nutrition (1:5). The PUFA/SFA ratio was between 0.69 in fried and 1.02 in boiled fish, both being greater than those recommended by the WHO/FAO [2003]. Atherogenicity index value decreased significantly after the cooking particularly in fried fish. The polyene index (PI), as a measure of PUFA damage, was in the range of 0.42–1.18. Although all cooking methods affected the FA profile, based on LNQI, it can be concluded that barbecue-grilling and boiling were the best cooking methods for healthy eating, due to their lowest effect on essential FAs.

Key words: lipid quality, nutritional indices, barbecue-grilling, oven-cooking, frying, microwaving, boiling, Mediterranean fish

INTRODUCTION

Consumed fish represent a precious ally for human health, since fish play a keystone role as a source of animal protein, long-chain *n*3 polyunsaturated fatty acids (PUFAs), and micronutrients, including vitamins and minerals [Wang *et al.*, 2020]. Moreover, fish have a relatively low energy value thus are recommended in a healthy and balanced diet [Rubio-Rodríguez *et al.*, 2010]. It is well known that long-chain *n*3 PUFAs present in fish lipids are associated with beneficial health outcomes. A high consumption of *n*3 PUFAs, more specifically eicosapentaenoic acid (EPA, 20:5*n*3) and docosahexaenoic acid (DHA, 22:6*n*3), leads to an increase in high-density lipoprotein (HDL) cholesterol content and a decrease in total cholesterol content, and in reduced levels of inflammatory markers [Asher *et al.*, 2021]. Indeed, they play a key beneficial role in anti-inflammatory metabolism, being the substrates in the synthesis of biologically active

***Corresponding Author:**
e-mail: linda.prato@irsa.cnr.it (E. Prato)

Submitted: 9 November 2022
Accepted: 23 January 2023
Published on-line: 16 February 2023

anti-inflammatory mediators involved in several pathologies such as neurodegenerative disorders, cardiovascular diseases, cancer, rheumatoid arthritis, and psoriasis [Calder & Yagoob, 2009; Chitre *et al.*, 2019; Simopoulos, 2008]. The World Health Organization (WHO) and Food and Agriculture Organization of the United Nations (FAO) recommend a regular fish consumption of at least one-two servings per week with each serving providing the equivalent of 250–500 mg of EPA+DHA [WHO/FAO, 2003].

Red mullet, *Mullus barbatus* (L. 1758), has a widespread geographical distribution that extends from the eastern Atlantic along the European and African coasts to the Mediterranean Sea and the Black Sea [Fisher, 1987]. It is one of the most valuable components of coastal Mediterranean demersal fisheries [Tserpes *et al.*, 2002]. Although there is considerable knowledge of red mullet biology, distribution and fishery [Fiorentino *et al.*, 2008; Tserpes *et al.*, 2002], information on their nutritional value is very scarce. They are usually eaten cooked with different methods including boiling, frying, roasting *etc*. Cooking processes inevitably affect the nutritive value of fish and especially profile of flavor compounds as well as contents and quality of proteins, lipids and vitamins [Wang *et al.*, 2020; Wei *et al.*, 2023]. Usually high temperatures used in these processes degrade nutrients through hydrolysis and oxidation. Fatty acids, mainly PUFAs, are considered to be especially susceptible to oxidation during high-temperature culinary treatments [Bastías *et al.*, 2017; Koubaa *et al.*, 2012]. On the other hand, fish protein digestibility was reported to increase upon cooking, due to their denaturation. In addition, cooking was shown to improve certain features of fillets, for example by developing good odor, appealing look, and removal of harmful microorganisms [Abou-Taleb *et al.*, 2021; Bognár, 1998; Koubaa *et al.*, 2012].

Several studies have previously investigated the effects of different cooking methods on the nutritional quality of fish [Alexi *et al.*, 2019; Biandolino *et al.*, 2021; Costa *et al.*, 2015; Gladyshev *et al.*, 2014; Hosseini *et al.*, 2014; Schneedorferová *et al.*, 2015]. Koubaa *et al.* [2012] investigated the effect of four cooking methods on the fatty acid profile of red mullet from the sea gulf of Gabes (Mediterranean Sea). They reported the best proportion of PUFA and *n*6/*n*3 ratio in steamed, oven-cooked, and microwaved fish as compared with fried red mullet. García-Arias *et al.* [2003] have also reported that frying affect the fatty acid composition of sardine with decreasing EPA and DHA, while oven-baking and grilling minimally affected the fatty acid content. Therefore, it is fundamental to inform consumers about the best cooking methods that have the least adverse effect on the nutritional value of fish. This should be done on the basis of scientific studies which examine the effects of different culinary treatments on contents of essential compounds and indicators of the nutritional values of fish, such as lipid nutritional quality indices (LNQI).

The objective of the present study was to determine the effect of five in-house cooking processes (barbecue-grilling, oven cooking, frying, microwaving, and boiling) on lipid content and fatty acid profile of red mullet *Mullus barbatus* (L. 1758). Moreover, in order to assess the nutritional quality of the lipid fraction after cooking, a number of fatty acid-related nutritional quality indices, for the first time for red mullet, was determined. These would help select the optimal cooking method to be recommended to consumers and nutritionists for fish culinary preparation.

MATERIALS AND METHODS

Fish origin and preparation

Fresh specimens of *Mullus barbatus* (L. 1758) were purchased from a local market in the city of Taranto (Southern Italy), just immediately after being caught from the Ionian Sea (Mediterranean Sea), during spring 2021. Similarly sized fish were selected to ensure that any biochemical and chemical differences were not size-dependent (length 10.4±0.7 cm, weight 23.6±1.7 g). They were immediately stored in icebox at 4°C and transported to the laboratory for processing and analysis. Fish were washed several times in tap water, and cooked with the whole body after being gutted and scaled, without removing the head and skin. They were randomly divided into six groups: each group consisted of about 45 individuals, with 15 samples for each replicate (n=3). One group was kept fresh-raw and used as control (raw). The others were cooked with following methods: barbecuing--grilling (embers, cooking time of about 6–8 min), oven-cooking (oven, 200°C for 10–15 min), frying (pan frying with 1 L of olive oil at a temperature of about 180°C for 10 min), microwaving (Samsung M17-13 microwave oven (Suwon, South Korea), 800 W, 2,450 MHz, cooked medium-high for 5 min), boiling (on 3 L of tap water for 10 min at 90–100°C). Once cooked, fish were gently drained for about 5 min on absorbent paper towels. The fresh and cooked fish were cut into small pieces, weighed in glass containers and frozen at –20°C, to be subsequently freeze-dried and homogenized.

Moisture, total lipid content, and fatty acid profile determination

The moisture content of cooked and fresh fish was determined by drying the sample in an oven at 105°C until a constant weight was obtained according to the AOAC method [AOAC, 2005].

Lipid extraction was performed according to the modified Folch method [Folch *et al.*, 1957]. Briefly, the fish samples were homogenized using an Ultra-Turrax homogenizer (IKA-Werke GmbH & Co., Staufen, Germany). After that, 0.5 g of homogenate of each sample was homogenized with 5 mL of a chloroform/ /methanol mixture (2:1, *v/v*), which contained 0.01% butylated hydroxytoluene (BHT) as the antioxidant. Next, 2 mL of a 0.88% potassium chloride solution was added and mixed thoroughly. After phase separation, the chloroform was evaporated until dryness. The total lipid content was determined gravimetrically and the results were expressed as g per 100 g wet matter (wm).

The content of fatty acids (FAs) in the total lipids of *M. barbatus* were determined as described by Biandolino *et al.* [2021]. FA methyl esters (FAMEs) were analyzed on a gas chromatograph (GC) (Hewlett Packard (HP)/Agilent 6890 N, Agilent Technologies, Inc., Santa Clara, CA, USA) equipped with a flame ionization detector (FID) and fitted with an Agilent HP-88 column (60 m × 0.25 mm id, 0.2 µm). Helium was used as the carrier

gas (1 mL/min). The column temperature program was as follows: 150 to 250°C at 4°C/min and held at 250°C. The fatty acids were identified by comparing retention times of corresponding peaks with those of a mixture of fatty acid methyl ester standards (Supelco 37 component FAME mix, Supelco Inc. Bellefonte, PA, USA). Relative quantities were expressed as % of total fatty acids. Quantification was made also using the technique of internal standardization with methyl nonadecanoate (98% purity Sigma-Aldrich Chemicals, Saint Louis, MO, USA). The results were expressed as mg/100 g wm.

Lipid nutritional quality indices

The LNQI of both raw and cooked fish were evaluated based on the fatty acid compositions of fish lipids. Indices of PUFAs/saturated fatty acids (SFAs), (MUFAs+PUFAs)/(SFAs–C18:0), *n6/n3* and *n3/n6* ratios, EPA+DHA, arachidonic acid (ARA)/DHA and ARA/EPA ratios were evaluated. The atherogenic (AI) and thrombogenic (TI) indices were estimated according to Equations (1) and (2), respectively [Ulbricht & Southgate, 1991], whereas the ratio of hypocholesterolemic/hypercholesterolemic fatty acids (HH) was calculated according to Equation (3) [Santos-Silva *et al.*, 2002].

$$AI = \frac{C12:0+4\times C14:0+C16:0}{\Sigma MUFAs + \Sigma PUFAs} \quad (1)$$

$$TI = \frac{C14:0+C16:0+C18:0}{0.5\ \Sigma MUFAs + 0.5\ \Sigma n6PUFAs + 3\ \Sigma n3PUFAs + \frac{\Sigma n3PUFAs}{\Sigma n6PUFAs}} \quad (2)$$

$$HH = \frac{C18:1+\Sigma selected\ PUFAs}{C14:0+C16:0} \quad (3)$$

where: selected PUFAs include C18:2*n6*, C20:4*n6*, C18:3*n3*, C20:5*n3*, C22:5*n*-3, and C22:6*n3*.

The Equations (4) and (5) were used to calculate the health-promoting index (HPI) and the unsaturation index (UI), respectively [Chen & Liu, 2020].

$$HPI = \frac{\Sigma UFAs}{C12:0+4\times C14:0+C16:0} \quad (4)$$

where: UFAs – unsaturated fatty acids.

$$UI = 1\times(\%\ monoenoics)+2\times(\%\ dienoics)+3\times(\%\ trienoics) +4\times(\%\ tetraenoics)+5\times(\%\ pentaenoics)+ 6\times(\%\ hexaenoics) \quad (5)$$

The polyene index (PI) was estimated based on the Equation (6) proposed by Pirestani *et al.* [2010].

$$PI = \frac{C20:5n3+22:6n3}{C16:0} \quad (6)$$

Statistical analysis

All analyses were performed in triplicate and the results were reported as mean values ± standard deviation (SD). Statistical analysis was performed by using Past software, version 4.03. Data were tested for normality of distributions and homogeneity of variances by means of the Kolmogorov-Smirnov test and the Levene test, respectively. Mean values were compared by one-way ANOVA to test the difference in nutrients between raw and cooked samples. When significant differences were found, a post hoc Tukey test ($p<0.05$) was applied. When requirements for normality were not met, the non-parametric Kruskal-Wallis test on ranks was applied ($p<0.05$). Hierarchical clustering analysis was used to graphically represent differences in the nutritional quality of the raw and cooked fish studied.

RESULTS AND DISCUSSION

Moisture and total lipids

In raw fish, the moisture content was 78.3 g/100 g of the total tissue weight and lipid content was 2.1 g/100 g wm (Figure 1). Previous studies reported slightly different data for the same species, in a range of 72–78 g/100 g for moisture content and 1.82–10.9 g/100 g wm for lipid content [Di Lena *et al.*, 2016; Kocatepe & Turan, 2012; Prato & Biandolino, 2012; Roncarati *et al.*, 2012]. Indeed, the chemical composition of fish varies greatly among species but also within the same species, depending on many variables, such as season and time of fishing, geographical area of fish life, feeding availability, age, sex, and physiological condition [Prato & Biandolino 2012].

The moisture content of red mullet showed a significant ($p<0.05$) decrease as a result of cooking treatments (except with boiling), reaching the minimum value after frying (61.2 g/100 g) (Figure 1). The lipid content significantly ($p<0.05$) increased after frying, which resulted in its about ten times higher value (21.1 g/100 g wm) compared to that determined for the raw fish (2.1 g/100 g wm). A significant ($p<0.05$) increase was also observed for microwaved fish (3.4 g/100 g wm). These results are

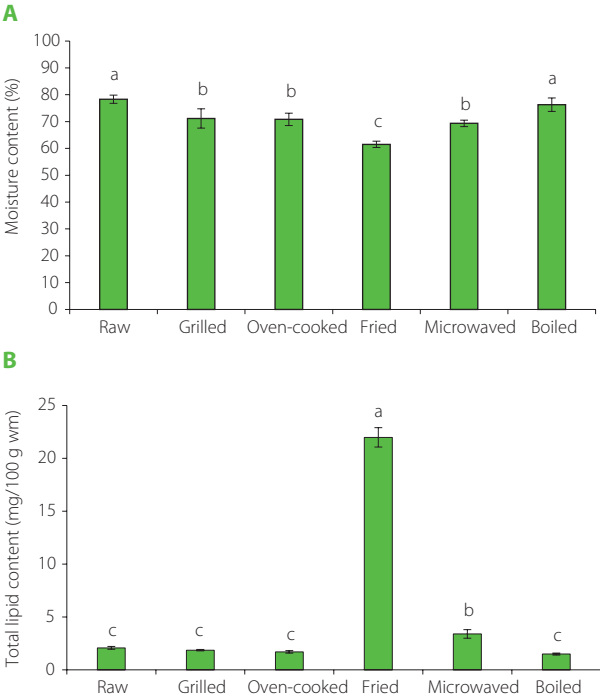

Figure 1. (**A**) Moisture content and (**B**) total lipid content based on wet matter (wm) of raw and cooked *Mullus barbatus*. Identical letters over bars show not significant differences ($p\geq0.05$).

in accordance with the findings reported by Weber *et al.* [2008], Naseri *et al.* [2013], Gokoglu *et al.* [2004], and Biandolino *et al.* [2021], in studies on fish and molluscs bivalves, which showed a significant lipid increase after cooking, which might be mainly due to moisture loss *via* evaporation inducing the concentration of fat in the final product and to the absorption of frying oil by the fish [Sampels, 2015]. Moreover, Quaglia & Bucarelli [2001] stated that, during frying, the exchange between lipids and water occurred through the pores opened during the water evaporation. It has also been found that lean fish tend to absorb higher quantities of frying oils than the fatty ones [Alexi *et al.*, 2019; Kalogeropoulos *et al.*, 2004]. The fish samples analyzed in this study were relatively lean, which suggests high oil absorption and explains the high oil content of the fried red mullet.

Fatty acid composition

The compositions of the most important fatty acids of lipids of raw and cooked red mullet and quantities of these fatty acids expressed as % of total FAs and as mg per 100 g of wm are shown in Table 1 and Table 2, respectively. The fatty acids exceeding a minimum of 0.1% total FAs in a minimum of one sample were considered and compared among the different cooking treatments. Quantitatively, the raw fish showed a profile of fatty acids favorable to consumer health with PUFAs (552 mg/100 g wm, 38.0% total FAs) as dominant FA group followed by SFAs (530 mg/100 g wm, 36.4% total FAs), and MUFAs. The latter showing the lowest value (372 mg/100 g wm, 25.6% total FAs). Lower PUFAs content compared to SFAs and MUFAs has been reported by Kocatepe & Turan [2012] and Koubaa *et al.* [2012] for *Mullus barbatus*. In our study, the raw fish contained palmitic acid (C16:0) as the main FA, followed by oleic (C18:1*n*9), DHA (C22:6*n*3), EPA (C20:5*n*3), palmitoleic (C16:1*n*7), and stearic (C18:0) acids. It is important to highlight the high content of oleic acid (C18:1*n*9) (14.0% total FAs) contributing approximately to 55.6% of total MUFAs. These results were similar to those reported by Merdzhanova *et al.* [2012] and Koubaa *et al.* [2012] for the same fish species.

Significant differences ($p<0.05$) were found between cooking methods, in terms of contents of total and individual saturated and unsaturated FAs (Table 1 and Table 2). It is noteworthy to consider that the variations in the fatty acid contents reflect the lipid content (Figure 1). For this reason, the fried and microwaved products showed significantly ($p<0.05$) higher contents

Table 1. Fatty acid (FA) profile (% of total FAs) of lipids extracted from raw and cooked *Mullus barbatus*.

FA	Raw	Grilled	Oven-cooked	Fried	Microwaved	Boiled
C14:0	3.98±0.20^{a}	3.62±0.24^{ab}	2.75±0.18^{c}	0.54± 0.06^{d}	3.22±0.44^{bc}	3.00±0.53^{c}
C15:0	1.62±0.25^{c}	3.12±0.15^{a}	2.22±0.25^{b}	0.45±0.02^{d}	3.03±0.13^{a}	2.25±0.29^{b}
C16:0	20.7±0.7^{b}	22.3±1.5^{a}	21.9±0.8^{ab}	11.9±0.1^{c}	20.7±0.4^{b}	21.9±1.0^{ab}
C17:0	1.56±0.06^{c}	1.75±0.23^{c}	2.57±0.09^{b}	0.60±0.09^{d}	3.19±0.42^{a}	3.32±0.26^{a}
C18:0	8.60±0.09^{a}	8.74±0.40^{a}	7.13±1.15^{b}	5.39±0.08^{c}	9.35±0.43^{a}	9.31±0.58^{a}
∑SFAs	36.4±1.1^{b}	39.5±1.5^{a}	36.6±0.5^{b}	18.9±0.3^{c}	39.5±1.0^{a}	39.8±0.7^{a}
C16:1	9.08±0.06^{a}	7.40±0.24^{b}	5.95±0.27^{d}	1.61±0.02^{f}	6.62±0.76^{c}	5.14±0.30^{e}
C17:1	1.21±0.15^{d}	2.00±0.09^{c}	2.23±0.09^{bc}	nd	2.82±0.11^{a}	2.50±0.49^{ab}
C18:1*n*9*c*	14.0±0.5^{c}	10.2±0.9^{d}	21.5±0.7^{b}	66.6±1.4^{a}	13.2±0.2^{c}	9.92±1.63^{d}
C20:1*n*9	1.29±0.10^{b}	1.24±0.13^{b}	1.13±0.32^{b}	nd	1.01±0.10^{b}	1.90±0.16^{a}
∑MUFAs	25.6±0.4^{c}	20.8±0.7^{e}	30.9±0.6^{b}	68.2±1.4^{a}	23.7±0.9^{d}	19.5±0.7^{e}
C18:2*n*6*c*	2.05±0.23^{b}	2.13±0.25^{b}	2.04±0.18^{b}	4.31±0.09^{a}	1.69±0.14^{c}	1.65±0.24^{c}
C18:3*n*3	2.62±0.08^{a}	2.11±0.26^{b}	1.83±0.35^{b}	1.02±0.45^{c}	1.00±0.08^{c}	2.09±0.15^{b}
C22:0+C20:3*n*6	0.22±0.02^{b}	0.27±0.03^{b}	0.87±0.22^{a}	nd	0.24±0.03^{b}	0.27±0.02^{b}
C20:3*n*3+C22:1	0.39±0.07^{c}	0.45±0.08^{c}	1.03±0.02^{a}	nd	0.70±0.09^{b}	0.34±0.05^{c}
C20:4*n*6	4.68±0.13^{c}	6.14±0.20^{b}	5.07±0.04^{c}	1.45±0.03^{d}	6.09±0.74^{b}	8.02±0.14^{a}
C20:5*n*3 (EPA)	12.2±0.7^{a}	10.6±1.7^{bc}	9.25±0.32^{c}	2.04±0.21^{d}	10.8±0.8^{ab}	9.91±0.23^{bc}
C22:5*n*3	2.47±0.27^{ab}	2.78±0.97^{ab}	2.10±0.23^{bc}	1.18±0.33^{c}	2.76±0.31^{ab}	3.28±0.69^{a}
C22:6*n*3 (DHA)	13.4±0.5^{b}	15.2±0.9^{a}	10.4±0.9^{c}	2.95±0.36^{d}	13.6±1.1^{b}	15.1±0.8^{a}
∑PUFAs	38.0±1.5^{bc}	39.7±1.3^{ab}	32.6±1.1^{d}	13.0±1.1^{e}	36.9±1.9^{c}	40.7±0.6^{a}
*n*3	31.0±1.4^{ab}	31.1±1.6^{a}	24.6±1.0^{c}	7.20±1.2^{d}	28.9±1.3^{b}	30.8±0.7^{ab}
*n*6	6.94±0.23^{c}	8.55±0.44^{b}	7.98±0.05^{b}	5.76±0.07^{d}	8.02±0.78^{b}	9.95±0.24^{a}

Values are means ± standard deviations of three separate replicates. Means with different letters (a–f) within each raw indicate significant differences ($p<0.05$). SFAs, saturated fatty acids; MUFAs, monounsaturated fatty acids; PUFAs, polyunsaturated fatty acids; nd, not detected; EPA, eicosapentaenoic acid; DHA, docosahexaenoic acid.

Table 2. Content of fatty acids (FAs) (mg/100 g wm) of lipids extracted from raw and cooked *Mullus barbatus*.

FA	Raw	Grilled	Oven-cooked	Fried	Microwaved	Boiled
C14:0	57.9±2.9^{b}	47.1±3.1^{bc}	32.7±2.1^{c}	83.3±8.8^{a}	76.4±10.4^{a}	31.2±5.5^{c}
C15:0	23.5 ±3.6^{c}	40.7 ±1.9^{b}	26.4 ±2.9^{c}	70.1±3.9^{a}	71.9±3.1^{a}	23.4±3.1^{c}
C16:0	301±11^{c}	290±19^{c}	260±10^{d}	1825±11^{a}	492±10^{b}	228±11^{e}
C17:0	21.7±0.8^{c}	22.8±3.0^{c}	30.6±1.1^{c}	92.3±11.3^{a}	75.7±10.2^{b}	34.5±2.7^{c}
C18:0	125±1^{c}	114±5^{cd}	84.7±8.6^{e}	830±12^{a}	222±10^{b}	96.8±6.1^{de}
∑SFAs	530±16^{c}	515 ±20^{c}	435±6^{d}	2902±47^{a}	938±24^{b}	414±7^{d}
C16:1	132±1^{c}	96.3±3.2^{d}	70.7±3.2^{ed}	249±3^{a}	157±18^{b}	53.5±3.1^{e}
C17:1	17.6±2.3^{c}	26.0±1.2^{b}	26.5±1.1^{b}	nd	67.1±2.6^{a}	26.0±5.1^{b}
C18:1*n9c*	204±7^{b}	133±11^{c}	256±8^{b}	10247±214^{a}	313±5^{b}	103±14^{c}
C20:1*n9*	18.7±2^{bc}	16.2±1.3^{bc}	13.4±3.7^{c}	nd	24.0±2.3^{a}	19.7±1.7^{b}
∑MUFAs	372± 6^{c}	271±10^{cd}	366±8^{b}	10496±212^{a}	562±21^{b}	202±7^{d}
C18:2*n6c*	29.8±3.3^{c}	27.7±3.3^{cd}	24.2±2.1^{cd}	664±14^{a}	40.1±3.2^{b}	17.2±2.5^{d}
C18:3*n3*	38.1±1.2^{b}	27.4±3.4^{b}	21.7±3.2^{a}	158±39^{a}	23.9±2.0^{b}	21. 8±1.6^{b}
C22:0+C20:3*n6*	3.18±0.28^{c}	3.6 ±0.27^{c}	10.4±2.0^{a}	nd	5.76±0.72^{b}	2.85±0.23^{c}
C20:3*n3*+C22:1	5.63±0.84^{c}	5.89±1.0^{c}	12.28±0.19^{b}	nd	16.6±2.1^{a}	3.57±0.49^{c}
C20:4*n6*	68.0±1.9^{c}	80.0±2.5^{c}	60.3±0.5^{c}	223±5^{a}	145±18^{b}	83.4±1.5^{c}
C20:5*n3* (EPA)	177±10^{c}	138±23^{cd}	110±4^{d}	315±32^{a}	257± 12^{b}	103±2^{d}
C22:5*n3*	36±3.9^{c}	36.3±8.7^{c}	24.9±2.8^{c}	182±41^{a}	65.6±7.3^{b}	34.2±7.1^{c}
C22:6*n3* (DHA)	195±8^{c}	198±11^{c}	123±11^{d}	454±56^{a}	323±27^{b}	157±8.5^{cd}
∑PUFAs	552±21^{c}	516±16^{cd}	387±13^{d}	1995±175^{a}	876±44^{b}	423±6^{cd}
n3	451±20^{c}	405±21^{cd}	292±12^{d}	1108±187^{a}	686±30^{b}	320±8^{cd}
n6	101±3^{c}	111±6^{c}	94.8±0.6^{c}	887±12^{a}	191±19^{b}	103±3^{c}

Values are means ± standard deviations of three separate replicates. Means with different letters (a–e) within each row indicate significant differences (p<0.05). SFAs, saturated fatty acids; MUFAs, monounsaturated fatty acids; PUFAs, polyunsaturated fatty acids; nd, not detected; EPA, eicosapentaenoic acid; DHA, docosahexaenoic acid; wm, wet matter.

of most of individual fatty acids (Table 2). When referring to the values based on the total FAs, the comparison of the raw sample with cooked ones revealed a significant (p<0.05) increase in the proportion of SFAs after most treatments, with the exception of frying (decrease from 36.4 to 18.8% total FAs, p<0.05), and oven-cooking (insignificant difference, p≥0.05). Palmitic and stearic acids were the dominant SFAs in the total FAs of cooked fish lipids, although with considerably lower values in the fried product (11.9% and 5.39% total FAs, respectively). Similar results were found by other authors for the same and other fish species [Kalogeropoulos *et al.*, 2004; Koubaa *et al.*, 2012; Weber *et al.*, 2008]. SFAs are traditionally considered as unhealthy components because the favor the increase in plasma concentration of cholesterol and low-density lipoprotein (LDL) cholesterol linked to cardiovascular disease (CVD), although conclusions from recent meta-analyses have not supported this association [Zhuang *et al.*, 2019]. Certainly, among SFAs, stearic acid has a neutral effect on cholesterol concentrations and thus on CVD risk, and this may be due to desaturation that rapidly converts it to oleic acid in the liver [Micha & Mozaffarian, 2010].

Cooking methods induced variations in the proportion of MUFAs (% total FAs), with the following order boiling=grilling<microwaving<raw<oven-cooking<frying (Table 1). Fried fish lipids showed the highest MUFA contribution in total FAs (68.2% total FAs), more than 2.5 fold higher than the raw sample (25.6% total FAs). The exchange between the frying oil and the fish lipids with the MUFA absorption from frying oil resulted in modification of the fish lipid FA profile [Hosseini *et al.*, 2014]. In our study, this resulted in a significant (p<0.05) increase of contribution of the fatty acid characteristic of olive oil (oleic acid, C18:1*n9*) in frying fish lipids, by about 4.7 times (66.6% total FAs), when compared to the raw sample (14.0% total FAs). A similar increase was reported by Al-Saghir *et al.* [2004] for fried salmon as compared to the raw one, by Kalogeropoulos *et al.* [2004] in a study on the effect of pan-frying in virgin olive oil on fatty acids of seafood, and by Zotos *et al.* [2013] for anchovies fried in olive oil. Oleic acid was the most represented MUFA in fish FAs after all cooking treatments, and in addition to frying, its contribution in the total FAs showed a significant increase after oven cooking (21.5% total FAs) (Table 1). However, a significant

decrease of oleic acid contribution in the total FAs was observed in lipids of grilled and boiled fish ($p<0.05$). Palmitoleic acid was the second most abundant MUFA for all cooking treatments, with values ranging from 1.61 to 7.40% of the total FAs and significantly lower compared to raw sample (9.08% total FAs) ($p<0.05$). Literature data reported that MUFAs and especially oleic acid had positive impact on various tissues in general and a beneficial effect on the cardiovascular system, with decreasing LDL cholesterol concentration in serum, the myocardial infarction rate, and platelet aggregation [Karacor & Cam, 2015]. Moreover, high oleic acid consumption has contributed to the prevention of the risk of developing inflammatory diseases by increasing leukotriene A3 levels, which is an inhibitor of pro-inflammatory LTB4 [Piccinin *et al.*, 2019].

Fish are a major source of marine-derived *n*3 PUFAs for the human diet. In recent years, the interest in *n*3 PUFAs increased because of their health beneficial effects and disease risk reduction, representing an incentive for the consumption of fish. However, fish is mainly consumed cooked; therefore, there is concern about the use of high-temperature processing, which may lead to the reduction of labile *n*3 PUFAs, resulting in a decrease of the nutritional value of the fish. Concerning the changes in the PUFAs before and after cooking, some important remarks can be made. In our study, a significant ($p<0.05$) decrease in PUFA proportion in the total FAs occurred after oven-cooking and frying treatments and a significant increase after boiling, while no significant ($p\geq0.05$) differences were found between the other cooking methods and the control (Table 1). In particular, contribution of PUFAs in the total FAs drastically decreased in olive oil fried samples when compared to raw sample, *i.e.* from 38.0% to 13.0% of the total FAs. Decrease of more than half was reported in literature [Kalogeropoulos *et al.*, 2004; Yazdan *et al.*, 2009; Zotos *et al.*, 2013]. However, previous studies have shown contradictory results regarding changes in the content of PUFAs of aquatic species during storage and cooking; according to some authors the PUFA contents tended to decrease [Saldanha & Bragagnolo, 2008], while other authors [Gladyshev *et al.*, 2007] have reported that cooking methods (boiling, frying, *etc.*) would not have the same effect on the PUFA content in many fish species.

Among PUFAs, the contribution of beneficial *n*3 fatty acids, including EPA and DHA, in the total FAs remained at satisfactory levels in cooked fish, although significantly ($p<0.05$) different than in the raw sample, except for microwaved fish, for which EPA and DHA remained unchanged ($p\geq0.05$) compared to the control (Table 1). Both acids reached the lowest ($p<0.05$) proportion in the fried product, with 2.04 and 2.95% for EPA and DHA, respectively. These values were consistent with literature data [Asghari *et al.*, 2013; Gladyshev *et al.*, 2007; Kalogeropoulos *et al.*, 2004; Weber *et al.*, 2008; Zhang *et al.*, 2011; Zotos *et al.*, 2013]. The content of EPA and DHA of fried red mullet expressed as g/100 g wm was higher than of the raw fish (Table 2). This increase can be explained by moisture loss and lipid increase during frying, but can also be due to the absorption of the fatty acids from the culinary fat used for this cooking method. Gladyshev *et al.* [2007] reported that among the different cooking methods (boiling, frying and roasting) used for humpback salmon processing, only frying significantly reduced EPA and DHA levels, attributing the PUFA decrease to the long duration of frying (15–20 min). In this study, the frying time was 10 min. Probably, this shorter frying time limited the oxidation and subsequent loss of PUFAs. ARA was the most abundant *n*6 PUFA in raw and grilled, oven-cooked, microwaved, and boiled fish followed by linoleic acid (C18:2*n*6) (Table 2). On the contrary, fried fish showed linoleic acid as the major *n*6 PUFA. The content of ARA increased significantly ($p<0.05$) after grilling, microwaving, and boiling compared with the raw fish.

Contribution of *n*3 and *n*6 PUFAs in the total FAs of raw red mullet lipids were 31.0% (absolute content of 451 g/100 g wm) and 6.94% (absolute content of 101 g/100 g ww) of total FAs, respectively (Table 1 and Table 2). Kocatepe & Turan [2012] found lower values than those with 11.6% for *n*3 and 1.49% for *n*6 FAs. In turn, Koubaa *et al.* [2012] reported 2.29 and 1.75% of the total FAs for *n*3 and *n*6, respectively. Both *n*3 and *n*6 PUFAs are fundamental for the formation of important structural lipids and elements of cell membranes. In addition, these PUFAs are precursors of eicosanoids, which influence the inflammation process and immune reactions [Simopoulos, 2008].

Cooking influenced *n*3 FAs proportion in the total FAs of red mullet lipids, showing a significant ($p<0.05$) decrease after oven-cooking (24.6% total FAs corresponding to 292 mg/100 g wm), but especially after frying with a decrease from 31.0% in the raw to 7.2% in the fried fish (Table 1 and Table 2). In the case of the absolute amounts (mg/100 g mw), as already explained above, the very high content reflects the high lipid content of the fried samples. The other cooking methods did not significantly ($p\geq0.05$) affect *n*3 PUFAs (Table 1). As regards the *n*6 PUFAs, a relative significant increase was observed with all cooking methods ($p<0.05$), except for frying. Despite all, the level of *n*3 FAs determined in raw and cooked samples was high and advantageous for human health because it prevents cardiovascular disease risk factors, while the low level of *n*6 FAs is required by the human body [Simopoulos, 2008].

Lipid nutritional quality indices (LNQI)

The dietary fish oil intake is associated with the prevention and treatment of different diseases, and this aspect has stimulated the need to define lipid nutritional quality indices to understand the lipids quality in fish. Among them, *n*3/*n*6 and PUFA/SFA ratios, AI, TI, and HH are useful to assess the impact of dietary lipid intake on cardiovascular health [Chen & Liu, 2020; Ulbricht & Southgate, 1991], while the HPI, UI, and EPA+DHA are useful to evaluate the content of high-quality PUFAs [Chen & Liu, 2020]. PUFAs of *n*3 and *n*6 families differ in their antithrombogenic and anti-inflammatory activity, which is most pronounced in the *n*3 family, particularly EPA and DHA. Therefore, these PUFAs are useful in the prevention and treatment of several diseases, such as CVD, hypertension, type 2 diabetes, rheumatoid arthritis, psychiatric disorders, obesity, and several cancers [Calder, 2006; Ulbricht & Southgate, 1991]. These findings are important

and should be taken into account when making dietary recommendations.

From a health point of view, it is important to consider a balanced *n*3/*n*6 ratio (1:1), although, in recent decades, developed countries have radically modified their dietary habits, by making their diets rich in SFAs and n*6* PUFAs, which has resulted in an unhealthy *n*3/*n*6 ratio. The recommended ratio differs between authors but it is always superior to 1 [Chow, 2008]. A ratio in favor of *n*6 PUFAs promotes the pathogenesis of many diseases, including CVD, atherosclerosis, obesity, cancer, and inflammatory and autoimmune diseases [Djuricic & Calder, 2021]. WHO/FAO [2003] recommend an *n*3/*n*6 ratio in the range of 1:8 and 1:5, as an ideal ratio, because five times higher levels of *n*6 FAs do not affect the conversion of *n*3 PUFA α-linolenic acid (18:3*n*3, ALA) to *n*3 highly unsaturated fatty acids (HUFA). The *n*3/*n*6 ratio of raw red mullet lipids was very favorable to human health, with a value of 4.47 (Table 3), and even though the *n*3/*n*6 ratio decreased for all cooking fishes ($p<0.05$), and in particular after frying (1.25), it was better than the above recommended standards. The significant decrease of this ratio after frying indicates that this cooking method has a high impact in the lipid quality of red mullet, suggesting a reduction of its nutritional value. Similar findings were reported by Kalogeropoulos *et al.* [2004] who observed an increase in the *n*6/*n*3 ratio in *M. barbatus* from 0.43 in raw to 1.23 in the fried sample.

The PUFA/SFA ratio assumes a great importance in the evaluation of the lipid quality because dietary recommendations and policies have shown that reducing SFA intake can prevent chronic diseases [Te Morenga & Montez, 2017]. In fact, it is known that the dietary PUFAs are involved in the reduction of LDH cholesterol, and in keeping serum cholesterol at lower levels, unlike SFAs. However, just as not all PUFAs exert a positive influence on cardiovascular prevention, not all SFAs negatively affect serum cholesterol. In general, a ratio of PUFA/SFA greater than 0.45 and at no less than 0.1 is recommended in human diets [Department of Health, 1994]. All values obtained in this study, both for raw (1.04) and cooked fish samples, were always well above the recommended value, although, a clear decrease was recorded for the fried (0.69) and oven-cooked (0.89) red mullet compared to the fresh fish (Table 3). Our results were in line with previous studies on Mediterranean species [Durmuş *et al.*, 2019; Özogul *et al.*, 2009]. However, the PUFA/SFA index does not take into account the important metabolic function of MUFAs in lowering LDL cholesterol levels in the blood and lowering the risk of heart disease and stroke. Similarly, it does not consider stearic acid as a SFA which does not cause the increase of plasma cholesterol [Djuricic & Calder, 2021]. For these reasons, another index was applied in which MUFAs were added and stearic acid was removed from the SFAs. The (MUFAs+PUFAs)/(SFAs–C18:0) value significantly ($p<0.05$) increased after frying and decreased after grilling compared to the raw samples (Table 3). For remaining cooking methods, this index did not differ significantly ($p\geq0.05$) from the raw sample. Biandolino *et al.* [2021] reported a significant increase of this index with all cooking methods used in their study for mussel (*Mytilus galloprovincialis*).

As regards the *n*6 PUFAs, ARA can be converted into eicosanoids, a group of lipid mediators, such as prostaglandins, thromboxanes, leukotrienes, hydroxy fatty acids, which exert essentially pro-inflammatory effects [Djuricic & Calder, 2021]. When the ARA/EPA ratio is between 1:1 and 5–10:1, both FAs are incorporated into membrane phospholipids, while when the ratio is higher, the incorporation of ARA is preferred [Whelan, 1996], determining the increases of pro-inflammatory and pro-aggregatory eicosanoids. Therefore, ARA/EPA and ARA/DHA

Table 3. Lipid nutritional quality indices of raw and cooked *Mullus barbatus*.

FA	Raw	Grilled	Oven-cooked	Fried	Microwaved	Boiled
EPA+DHA (% total FAs)	25.5±1.1^{a}	25.8±2.5^{a}	19.6±1.2^{b}	4.99±0.63^{c}	24.4±1.6^{a}	25.0±1.0^{a}
*n*3/*n*6 ratio	4.47±0.18^{a}	3.65±0.43^{b}	3.08±0.14^{c}	1.25±0.21^{d}	3.61±0.29^{b}	3.09±0.12^{c}
PUFAs/SFAs	1.04±0.08^{a}	1.00±0.09^{ab}	0.89±0.03^{c}	0.69±0.04^{d}	0.93±0.13^{bc}	1.02±0.02^{ab}
(MUFAs+PUFAs)/(SFAs–C18:0)	2.29±0.08^{b}	1.97±0.11^{c}	2.19±0.04^{bc}	6.03±0.12^{a}	2.01±0.10^{c}	1.97±0.03^{c}
ARA/DHA	0.35±0.02^{d}	0.41±0.02^{cd}	0.49±0.04^{ab}	0.50±0.04^{ab}	0.45±0.05^{cd}	0.53±0.02^{a}
ARA/EPA	0.38±0.02^{d}	0.59±0.10^{c}	0.55±0.04^{c}	0.71±0.10^{b}	0.56±0.02^{c}	0.81±0.01^{a}
AI	0.58±0.02^{ab}	0.61±0.02^{a}	0.52±0.02^{c}	0.17±0.04^{d}	0.55±0.02^{bc}	0.56±0.04^{abc}
TI	0.29±0.01^{b}	0.31±0.01^{ab}	0.33±0.02^{a}	0.30±0.03^{b}	0.31±0.01^{ab}	0.31±0.02^{ab}
HH	2.09±0.12^{bc}	1.90±0.16^{c}	2.12±0.04^{b}	6.41±0.12^{a}	2.06±0.10^{bc}	2.00±0.12^{bc}
HPI	1.74±0.12^{bc}	1.64±0.12^{c}	1.93±0.02^{b}	5.79±0.10^{a}	1.81±0.22^{bc}	1.75±0.13^{bc}
UI	212±8^{ab}	216±8^{ab}	185±6^{c}	119±4^{d}	207±9^{b}	220±4^{a}
PI	1.24±0.10^{a}	1.16±0.16^{a}	0.89±0.02^{b}	0.42±0.10^{c}	1.18±0.10^{a}	1.14±0.10^{a}

Values are means ± standard deviations of three separate replicates. Means with different letters (a–e) within each row indicate significant differences ($p<0.05$). SFAs, saturated fatty acids; MUFAs, monounsaturated fatty acids; PUFAs, polyunsaturated fatty acids; EPAs, eicosapentaenoic acid; DHA, docosahexaenoic acids; ARA, arachidonic acid; AI, atherogenic index; TI, thrombogenicity index; HH, hypocholesterolaemic/hypercholesterolaemic fatty acid ratio; HPI, health-promoting index; UI, unsaturation index; PI, polyene index.

ratios are both important, simple, rapid, and reliable indices for determining *n*3 FA status. In this study, all cooking methods significantly ($p<0.05$) increased the values of both indices of red mullet lipids, with the exception of the ARA/DHA ratio ($p\geq0.05$) as a result of grilling (Table 3).

In order to characterize the atherogenic and thrombogenic potential of food and to overcome the weaknesses of the PUFA/SFA ratio, considered too general, Ulbricht & Southgate [1991] developed AI and TI indices. Contrary to most indices, their lower value indicate a better food lipid nutritional quality. AI and TI less than 1.0 and 0.5, respectively, are recommended in the diet. Also for these indices, the raw and cooked red mullet showed very advantageous values. AI ranged from 0.17 (fried fish) to 0.61 (grilled fish), while TI ranged from 0.29 (raw fish) to 0.33 (oven-cooked fish) (Table 3). AI and TI of raw and cooked red mullet showed values within the ranges reported in literature for other fish, with 0.21 (*Sparus aurata*) to 1.41 (*Kutum roach*) for AI and 0.14 (*Sparus aurata*) to 0.87 (*Oreochromis niloticus*) for TI [Chen & Liu, 2020].

The ratio between hypocholesterolemic and hypercholesterolemic fatty acids (HH index) indicates the effects of specific fatty acids on cholesterol metabolism [Santos-Silva *et al.*, 2002]. The positive effects of HH have been ascribed to HH values around 2.40 and higher values are more beneficial [Ivanova & Hadzhinikolova, 2015]. The HH indices obtained in the present study ranged from 1.90 (grilled fish) to 6.41 (fried fish) (Table 3). The HH of raw fish was 2.09. In a previous study, Prato *et al.* [2020] indicated a lower value (1.25) for the raw red mullet probably due to the different sampling time, physiological state, and size of fish. However, the results fall within the range found by Rincón-Cervera *et al.* [2020] who reported HH for fish and shellfish species from South Pacific at 2.14 for yellowtail amberjack, 2.10 for palm ruff, 1.86 for croaker, 2.00 for mackerel, 2.23 for Chilean hake, 1.73 for jack mackerel, and 1.54 for Chilean sandperch.

The major change of AI (significantly higher decrease) and HH (significantly higher increase) in our study, occurred only after frying, that was due to the absorption of oleic acid from the frying media.

The health-promoting index (HPI) is the inverse of the AI and estimates the nutritional value of dietary lipids, providing information on the effect of FA composition on CVD [Chen & Liu, 2020]. Higher the HPI is, the more the lipids are beneficial to human health [Chen & Liu, 2020]. The results obtained for raw and cooked *M. barbatus* showed HPI between 1.64 (grilled fish) and 5.79 (fried fish) (Table 3). The level of the latter was determined by the high content of MUFAs of lipids, not the high content of PUFAs. HPI values of red mullet were much higher than the values of 0.16–0.68 reported by Chen & Liu [2020] for dairy products; thereby confirming that eating fish is more beneficial for human health compared to dairy products.

UI is used to evaluate the content of high-quality PUFAs in lipids. In this index, a different weight is attributed to the different unsaturated fatty acids, so a high value means a high degree of total unsaturation of lipids, favorable to maintain the lipid membrane fluidity [Pekkoh *et al.*, 2022]. In this study, UI of fried sample was the lowest (120), while these determined for boiled, grilled, and raw ones were the highest (220, 216, and 211, respectively) ($p<0.05$, Table 3). The UI values determined in this study for raw and cooked red mullet were generally higher than those found in other food products. Chen & Liu [2020] reported UI in ranges from 45 to 369 for macroalgae, from 125 to 155 for crops, from 73 to 124 for meat, and from 86 to 126 for dairy products.

The polyene index (PI) provides a measure of PUFA damage [Lubis & Buckle, 1990]. For red mullet, PI showed the lowest value for the fried red mullet (0.42) (Table 3), due to the lower EPA+DHA level compared to fish cooked with the other methods. All PI values, except that for the fried fish, were higher than those reported in the literature for other fish, *i.e.*, golden grey mullet (0.32–0.55) and gold band goatfish (0.50–0.56) [Küçükgülmez *et al.*, 2018]. In a study on the effect of cooking methods on fatty acid profile in rainbow trout, Asghari *et al.* [2013] reported values of PI lower than those presented in this study, but with similar trend, with fried fish showing the lowest value (0.27).

Hierarchical clustering analysis highlights graphically differences in the nutritional quality of *M. barbatus*, based on the fatty acid profiles (SFAs, MUFAs, PUFAs, *n*3 PUFAs, *n*6 PUFAs, EPA+DHA) and nutritional quality indices (*n*3/*n*6 ratio, PUFAs/SFAs ratio, HPI, UI, PI) (Figure 2). The fried and oven-cooked fish were clustered together because they were characterized by the lowest nutritional value, while fish cooked with the other methods formed second cluster – they were more desirable for human consumption for their beneficial lipids.

The EPA+DHA content is commonly used to assess the nutritional quality of marine animal products. The cooking of red mullet did not cause a significant ($p<0.05$) decrease in the relative EPA+DHA content when compared to the raw sample, except for oven-cooking and frying (Table 3). Indeed, after frying in olive oil, EPA+DHA decreased by about 5 times from 25.5% (raw fish) to 4.99% (fried fish) of the total FAs. This strong reduction was due to the olive oil uptake by fish during frying, which completely changed the fatty acid proportions. Similar results were reported by Asghari *et al.* [2013], Gladyshev *et al.* [2007], Hosseini *et al.* [2014], and Alexi *et al.* [2019]. Since the main benefits of fish consumption are mainly due to the intake of EPA

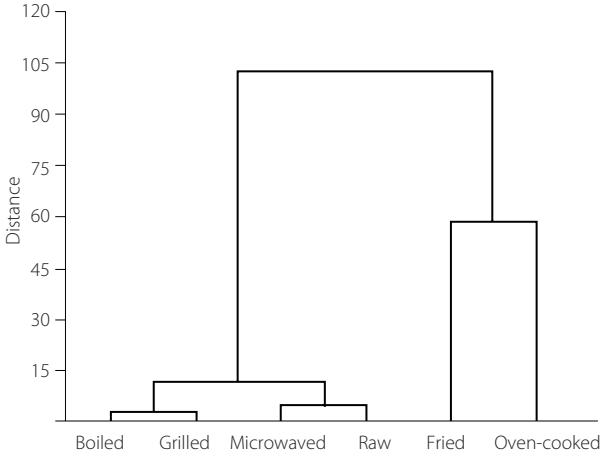

Figure 2. Hierarchical clustering analysis of *Mullus barbatus*, raw and cooked with five methods.

Table 4. Sum of eicosapentaenoic acid and docosahexaenoic acid (EPA+DHA) contents in raw and cooked red mullet (*Mullus barbatus*).

Cooking method	EPA+DHA (mg/100g wm)	Fish portion (g) containing recommended levels of EPA+DHA	
		250 mg	500 mg
Raw	371±17^{c}	67.3	135
Grilled	335±32^{cd}	74.5	149
Oven-cooked	233±14^{e}	107	215
Fried	768±88^{a}	32.5	65.1
Microwaved	580±38^{b}	43.1	86.3
Boiled	260±11de	96.0	192

Values are means ± standard deviations. Means in a column with different letters are significantly different ($p<0.05$); wm, wet matter.

and DHA, the sum of EPA+DHA represents a globally accepted index to evaluate the quality of fish. Dieticians and nutritionists are very interested in knowing the EPA and DHA content in fish to advice consumers on the optimal range of fish portion ensuring their adequate dietary intake. In this study, EPA+DHA content significantly decreased in the oven-cooked and boiled fish ($p<0.05$) when compared with the raw ones (371 mg/100 g mw) (Table 4). On the contrary, a significant increase of EPA+DHA was observed with frying and microwave cooking, due to highest lipid content. This fact was due to the higher total lipid triggered by these two cooking methods. Several health scientific agencies and national and international organizations have developed a series of guidelines to provide recommendations for the optimal dietary intake of EPA+DHA. The WHO/FAO [2003] and the European Food Safety Authority [EFSA Scientific Committee, 2015] recommend an intake of EPA+DHA of 250 mg for adults, with the addition of another 100–200 mg/day for women during pregnancy or lactation. According to the present study results, in order to obtain the daily intake of EPA+DHA (250–500 mg per day), it is necessary to consume a portion of only 32.5–65.1 g of fried red mullet. For the other cooking methods, a greater portion is needed to meet the daily requirement (Table 4). In a study on the effect of cooking methods on fatty acids in rainbow trout, Asghari *et al.* [2013] reported a portion of 154.8 g of microwaved, 234.3 g of fried, and 357.4 g of boiled trout, to ensure 1 g of EPA+DHA per day.

CONCLUSIONS

The lipid content and quality and fatty acid profile of the red mullet (*Mullus barbatus*) were affected by five different cooking methods examined in this study. Frying was the one that most of all affected lipid quality. Frying in olive oil markedly increased the content of oleic acid and, even if less, also of linoleic acids, while it decreased the contents of most of the other fatty acids. Based on the LNQI values, we can state that frying and oven-cooking worsened the lipid quality of red mullet, although this latter less drastically. The remaining cooking treatments, in general, caused slight changes in the fatty acid profile remaining valuable and healthier, in particular grilling and boiling appeared to be the most beneficial. Finally, for the most of cooking methods, it is sufficient to consume small portions to cover the daily intake recommended by the WHO/FAO for *n*3 fatty acids.

RESEARCH FUNDING

This study received no external funding.

CONFLICT OF INTERESTS

Authors declare no conflict of interest.

ORCID IDs

F. Biandolino https://orcid.org/0000-0002-3654-3926
I. Parlapiano https://orcid.org/0000-0001-5411-7712
E. Prato https://orcid.org/0000-0002-7917-6361

REFERENCES

1. Abou-Taleb, M., Ibrahim, S.M., El-Sherif, S., Talab, A.S. (2021). Effect of different cooking techniques on quality characteristics of some fish species. *Egyptian Journal of Aquatic Biology and Fisheries*, *25*(4), 899–907. https://doi.org/10.21608/ejabf.2021.195947
2. Alexi, N., Kogiannou, D., Oikonomopoulou, I., Kalogeropoulos, N., Byrne, D.V., Grigorakis, K. (2019). Culinary preparation effects on lipid and sensory quality of farmed gilthead seabream (*Sparus aurata*) and meagre (*Argyrosomus regius*): An inter-species comparison. *Food Chemistry*, *301*, art. no. 125263. https://doi.org/10.1016/j.foodchem.2019.125263
3. Al-Saghir, S., Thurner, K., Wagner, K.-H., Frisch, G., Luf, W., Razzazi-Fazeli, E., Elmadfa, I. (2004). Effects of different cooking procedures on lipid quality and cholesterol oxidation of farmed salmon fish (*Salmo salar*). *Journal of Agricultural and Food Chemistry*, *52*(16), 5290–5296. https://doi.org/10.1021/jf0495946
4. AOAC International (2005). *Official Methods of Analysis of AOAC International*. 18th ed., Washington, DC, USA.
5. Asghari, L., Zeynali, F., Sahari, M.A. (2013). Effects of boiling, deep-frying, and microwave treatment on the proximate composition of rainbow trout fillets: changes in fatty acids, total protein, and minerals. *Journal of Applied Ichthyology*, *29*(4), 847–853. https://doi.org/10.1111/jai.12212
6. Asher, A., Tintle, N.L., Myers, M., Lockshon, L., Bacareza, H., Harris, W.S. (2021). Blood omega-3 fatty acids and death from COVID-19: A pilot study. *Prostaglandins, Leukotrienes and Essential Fatty Acids*, *166*, art. no. 102250. https://doi.org/10.1016/j.plefa.2021.102250
7. Bastías, J.M., Balladares, P., Acuña, S., Quevedo, R., Muñoz, O. (2017). Determining the effect of different cooking methods on the nutritional composition of salmon (*Salmo salar*) and chilean jack mackerel (*Trachurus murphyi)* fillets. *PLoS ONE*, *12*(7), art. no. e0180993. https://doi.org/10.1371/journal.pone.0180993
8. Biandolino, F., Parlapiano, I., Denti, G., Di Nardo, V., Prato, E. (2021). Effect of different cooking methods on lipid content and fatty acid profiles *of Mytilus galloprovincialis*. *Foods*, *10*(2), art. no. 416. https://doi.org/10.3390/foods10020416
9. Bognár, A. (1998). Comparative study of frying to other cooking techniques influence on the nutritive value. *Grasas y Aceites*, *49*(3–4), 250–260. https://doi.org/10.3989/gya.1998.v49.i3-4.746
10. Calder, P.C. (2006). n-3 Polyunsaturated fatty acids, inflammation, and inflammatory diseases. *The American Journal of Clinical Nutrition*, *83*(6), 1505S–1519S. https://doi.org/10.1093/ajcn/83.6.1505S
11. Calder, P.C., Yaqoob, P. (2009). Omega-3 polyunsaturated fatty acids and human health outcome. *BioFactors*, *35*(3), 266–272. https://doi.org/10.1002/biof.42
12. Chen, J., Liu, H. (2020). Nutritional indices for assessing fatty acids: A mini-review. *International Journal of Molecular Sciences*, *21*(16), art. no. 5695. https://doi.org/10.3390/ijms21165695
13. Chitre, N.M., Moniri, N.H., Murnane, K.S. (2019). Omega-3 fatty acids as druggable therapeutics for neurodegenerative disorders. *CNS and Neurological Disorders – Drug Targets*, *18*(10), 735–749. https://doi.org/10.2174/1871527318666191114093749
14. Chow, C.K. (2008). *Fatty Acids in Foods and their Health Implications*. 3rd edition. CRC Press, Boca Raton, Florida, USA. https://doi.org/10.1201/9781420006902
15. Costa, S., Afonso, C., Cardoso, C., Batista, I., Chaveiro, N., Nunes, M.L., Bandarra, N.M. (2015). Fatty acids, mercury, and methylmercury bioaccessibility in salmon (*Salmo salar*) using an *in vitro* model: Effect of culinary treatment. *Food Chemistry*, *185*, 268–276. https://doi.org/10.1016/j.foodchem.2015.03.141

16. Department of Health (1994). *Reports on Health and Social Subjects No. 46: Nutritional aspects of cardiovascular disease. Report of the Cardiovascular Review Group Committee on Medical Aspects of Food Policy*. HMSO, London, UK. pp. 1–186.
17. Di Lena, G., Nevigato, T., Rampacci, M., Casini, I., Caproni, R., Orban, E. (2016). Proximate composition and lipid profile of red mullet (*Mullus barbatus*) from two sites of the Tyrrhenian and Adriatic seas (Italy): A seasonal differentiation. *Journal of Food Composition and Analysis*, *45*, 121–129. https://doi.org/10.1016/j.jfca.2015.10.003
18. Djuricic, I., Calder, P. (2021). Beneficial outcomes of omega-6 and omega-3 polyunsaturated fatty acids on human health: An update for 2021. *Nutrients*, *13*(7), art. no. 2421. https://doi.org/10.3390/nu13072421
19. Durmuş, M. (2019). Fish oil for human health: omega-3 fatty acid profiles of marine seafood species. *Food Science and Technology*, *39*(Suppl. 2), 454–461. https://doi.org/10.1590/fst.21318
20. EFSA Scientific Committee (2015). Statement on the benefits of fish/seafood consumption compared to the risks of methylmercury in fish/seafood. *European Food Safety Authority Journal*, *13*(1), art. no. 3982. https://doi.org/10.2903/j.efsa.2015.3982
21. Fiorentino, F., Badalamenti, F., D'Anna, G., Garofalo, G., Gianguzza, P., Gristina, M., Pipitone, C., Rizzo, P., Fortibuoni, T. (2008). Changes in spawning-stock structure and recruitment pattern of red mullet, *Mullus barbatus*, after a trawl ban in the Gulf of Castellammare (central Mediterranean Sea). *ICES Journal of Marine Science*, *65*(7), 1175–1183. https://doi.org/10.1093/icesjms/fsn104
22. Fisher, W., Schneider, M., Bauchot, M.L. (1987). *Fishes FAO d'identification des espèces pour les besoins de la pêche. Mediterranée et mer Noire. Zone de pêche 37. Volume I-II*. Commission des Communautés Européennes and FAO, Rome, Italy (in French).
23. Folch, J., Lees, M., Sloane Stanley, G.H. (1957). A simple method for the isolation and purification of total lipides from animal tissues. *Journal of Biological Chemistry*, *226*(1), 497–509. https://doi.org/10.1016/S0021-9258(18)64849-5
24. García-Arias, M.T., Álvarez Pontes, E., García-Linares, M.C, García-Fernández, M.C., Sánchez-Muniz, F.J. (2003). Cooking–freezing–reheating (CFR) of sardine (*Sardina pilchardus*) fillets. Effect of different cooking and reheating procedures on the proximate and fatty acid compositions. *Food Chemistry*, *83*(3), 349–356. https://doi.org/10.1016/S0308-8146(03)00095-5
25. Gladyshev, M.I., Sushchik, N.N., Gubanenko, G.A., Demirchieva, S.M., Kalachova, G.S. (2007). Effect of boiling and frying on the content of essential polyunsaturated fatty acids in muscle tissue of four fish species. *Food Chemistry*, *101*(4), 1694–1700. https://doi.org/10.1016/j.foodchem.2006.04.029
26. Gladyshev, M.I., Sushchik, N.N., Gubanenko, G.A., Makhutova, O.N., Kalachova, G.S., Rechkina, E.A., Malyshevskaya, K.K. (2014). Effect of the way of cooking on contents of essential polyunsaturated fatty acids in filets of zander. *Czech Journal of Food Sciences*, *32*(3), 226–231. https://doi.org/10.17221/365/2013-CJFS
27. Gokoglu, N., Yerlikaya, P., Cengiz, E. (2004). Effects of cooking methods on the proximate composition and mineral contents of rainbow trout (*Oncorhynchus mykiss*). *Food Chemistry*, *84*(1), 19–22. https://doi.org/10.1016/S0308-8146(03)00161-4
28. Hosseini, H., Mahmoudzadeh, M., Rezaei, M., Mahmoudzadeh, L., Khaksar, R., Khosroshahi, N.K., Babakhani, A. (2014). Effect of different cooking methods on minerals, vitamins and nutritional quality indices of *kutum roach* (*Rutilus frisii kutum*). *Food Chemistry*, *148*, 86–91. https://doi.org/10.1016/j.foodchem.2013.10.012
29. Ivanova, A., Hadzhinikolova, L. (2015). Evaluation of nutritional quality of common carp (*Cyprinus carpio* L.) lipids through fatty acid ratios and lipid indices. *Bulgarian Journal of Agricultural Science*, *21*(Suppl. 1), 180–185.
30. Kalogeropoulos, N., Andrikopoulos, N.K., Hassapidou, M. (2004). Dietary evaluation of Mediterranean fish and molluscs pan-fried in virgin olive oil. *Journal of the Science of Food and Agriculture*, *84*(13), 1750–1758. https://doi.org/10.1002/jsfa.1878
31. Karacor, K., Cam, M. (2015). Effects of oleic acid. *Medical Science and Discovery*, *2*(1), 125–132. https://doi.org/10.17546/msd.25609
32. Kocatepe, D., Turan, H. (2012). Proximate and fatty acid composition of some commercially important fish species from the Sinop region of the Black Sea. *Lipids*, *47*(6), 635–641. https://doi.org/10.1007/s11745-012-3658-1
33. Koubaa, A., Mihoubi, N.B., Abdelmouleh, A., Bouain, A. (2012). Comparison of the effects of four cooking methods on fatty acid profiles and nutritional composition of red mullet (*Mullus barbatus*) muscle. *Food Science and Biotechnology*, *21*(5), 1243–1250. https://doi.org/10.1007/s10068-012-0163-5
34. Küçükgülmez, A., Yanar, Y., Çelik, M., Ersor, B. (2018). Fatty acids profile, atherogenic, thrombogenic, and polyene lipid indices in golden grey mullet (*Liza aurata*) and gold band goatfish (*Upeneus moluccensis*) from Mediterranean Sea. *Journal of Aquatic Food Product Technology*, *27*(8), 912–918. https://doi.org/10.1080/10498850.2018.1508105
35. Lubis, Z., Buckle, K.A. (1990). Rancidity and lipid oxidation of dried-salted sardines. *International Journal of Food Science and Technology*, *25*(3), 295–303. https://doi.org/10.1111/j.1365-2621.1990.tb01085.x
36. Merdzhanova, A., Stancheva, M., Makedonski, L. (2012). Fatty acid composition of Bulgarian Black Sea fish species. *Ovidius University Annals of Chemistry*, *23*(1), 41–46. https://doi.org/10.2478/v10310-012-0006-5
37. Micha, R., Mozaffarian, D. (2010). Saturated fat and cardiometabolic risk factors, coronary heart disease, stroke, and diabetes: a fresh look at the evidence. *Lipids*, *45*(10), 893–905. https://doi.org/10.1007/s11745-010-3393-4
38. Naseri, M., Abedi, E., Mohammadzadeh, B., Afsharnaderi, A. (2013). Effect of frying in different culinary fats on the fatty acid composition of silver carp. *Food Science and Nutrition*, *1*(4), 292–297. https://doi.org/10.1002/fsn3.40
39. Özogul, Y., Özogul, F., Çiçek, E., Polat, A., Kuley, E. (2009). Fat content and fatty acid compositions of 34 marine water fish species from the Mediterranean Sea. *International Journal of Food Sciences and Nutrition*, *60*(6), 464–475. https://doi.org/10.1080/09637480701838175
40. Pekkoh, J., Phinyo, K., Thurakit, T., Lomakool, S., Duangjan, K., Ruangrit, K., Pumas, C., Jiranusornkul, S., Yooin, W., Cheirsilp, B., Pathom-aree, W., Srinuanpan, S. (2022). Lipid profile, antioxidant and antihypertensive activity, and computational molecular docking of diatom fatty acids as ACE inhibitors. *Antioxidants*, *11*(2), art. no. 186. https://doi.org/10.3390/antiox11020186
41. Piccinin, E., Cariello, M., De Santis, S., Ducheix, S., Sabbà C., Ntambi J.M., Moschetta A. (2019). Role of oleic acid in the gut-liver axis: From diet to the regulation of its synthesis via stearoyl-CoA desaturase 1 (SCD1). *Nutrients*, *11*(10), art. no. 2283. https://doi.org/10.3390/nu11102283
42. Pirestani, S., Sahari, M.A., Barzegar, M. (2010). Fatty acids changes during frozen storage in several fish species from South Caspian Sea. *Journal of Agricultural Science and Technology*, *12*(3), 321–329.
43. Prato, E., Biandolino, F. (2012). Total lipid content and fatty acid composition of commercially important fish species from the Mediterranean, Mar Grande Sea. *Food Chemistry*, *131*(4), 1233–1239. https://doi.org/10.1016/j.foodchem.2011.09.110
44. Prato, E., Fanelli, G., Parlapiano, I., Biandolino, F. (2020). Bioactive fatty acids in seafood from Ionian Sea and relation to dietary recommendations. *International Journal of Food Sciences and Nutrition*, *71*(6), 693–705. https://doi.org/10.1080/09637486.2020.1719388
45. Quaglia, G.B., Bucarelli, F.M. (2001). Effective process control in frying. In J.B. Rossell (Ed.), *Frying – Improving Quality*, Woodhead Publishing, Cambridge, England, pp. 236-265. https://doi.org/10.1533/9781855736429.3.236
46. Rincón-Cervera, M.Á., González-Barriga, V., Romero, J., Rojas, R., López-Arana, S. (2020). Quantification and distribution of omega-3 fatty acids in South Pacific fish and shellfish species. *Foods*, *9*(2), art. no. 233. https://doi.org/10.3390/foods9020233
47. Roncarati, A., Brambilla, G., Meluzzi, A., Iamiceli, A.L., Fanelli, R., Moret, I., Ubaldi, A., Miniero, R., Sirri, F., Melotti, P., di Domenico, A. (2012). Fatty acid profile and proximate composition of fillets from *Engraulis encrasicholus*, *Mullus barbatus*, *Merluccius merluccius* and *Sarda sarda* caught in Tyrrhenian, Adriatic and Ionian seas. *Journal of Applied Ichthyology*, *28*(4), 545–552. https://doi.org/10.1111/j.1439-0426.2012.01948.x
48. Rubio-Rodríguez, N., Beltrán, S., Jaime, I., de Diego, S.M., Sanz, M.T., Carballido, J.R. (2010). Production of omega-3 polyunsaturated fatty acid concentrates: A review. *Innovative Food Science and Emerging Technologies*, *11*(1), 1–12. https://doi.org/10.1016/j.ifset.2009.10.006
49. Saldanha, T., Bragagnolo, N. (2008). Relation between types of packaging, frozen storage and grilling on cholesterol and fatty acids oxidation in Atlantic hake fillets (*Merluccius hubbsi*). *Food Chemistry*, *106*(2), 619–627. https://doi.org/10.1016/j.foodchem.2007.06.021
50. Sampels, S. (2015). The effects of processing technologies and preparation on the final quality of fish products. *Trends in Food Science and Technology*, *44*(2), 131–146. https://doi.org/10.1016/j.tifs.2015.04.003
51. Santos-Silva, J., Bessa, R.J.B., Santos-Silva, F. (2002). Effects of genotype, feeding system and slaughter weight on the quality of light lambs: II. Fatty acid composition of meat. *Livestock Production Science*, *77*(2–3), 187–194. https://doi.org/10.1016/S0301-6226(01)00334-7
52. Schneedorferová, I., Tomčala, A., Valterová, I. (2015). Effect of heat treatment on the n-3/n-6 ratio and content of polyunsaturated fatty acids in fish tissues. *Food Chemistry*, *176*, 205–211. https://doi.org/10.1016/j.foodchem.2014.12.058

53. Simopoulos, A.P. (2008). The importance of the omega-6/omega-3 fatty acid ratio in cardiovascular disease and other chronic diseases. *Experimental Biology and Medicine*, *233*(6), 674–688. https://doi.org/10.3181/0711-MR-311
54. Te Morenga, L., Montez, J.M. (2017). Health effects of saturated and trans-fatty acid intake in children and adolescents: Systematic review and meta-analysis. *PLoS ONE, 12*(11), art. no. e0186672. https://doi.org/10.1371/journal.pone.0186672
55. Tserpes, G., Fiorentino, F., Levi, D., Cau, A., Murenu, M., Zamboni, A., Papacostantinou, C. (2002). Distribution of *Mullus barbatus* and *M. surmuletus* (Osteichthyes: Perciformes) in the Mediterranean continental shelf: implications for management. *Scientia Marina*, *66*(S2), 39–54. https://doi.org/10.3989/scimar.2002.66s239
56. Ulbricht, T.L.V., Southgate, D.A.T. (1991). Coronary heart disease: seven dietary factors. *The Lancet*, 338(8773), 985–992. https://doi.org/10.1016/0140-6736(91)91846-M
57. Wang, K., Bao, Y., Yang, H., Wang, Y., Dongpo, C., Regenstein, J.M., Zhou, P. (2020). Effect of core temperature on the oxidation of lipids and proteins during steam cooking of large-mouth bass (*Micropterus salmoides*). *Polish Journal of Food and Nutrition Sciences*, *70*(3), 301–312. https://doi.org/10.31883/pjfns/125836
58. Weber, J., Bochi, V.C., Ribeiro, C.P., Victório, A.M., Emanuelli, T. (2008). Effect of different cooking methods on the oxidation, proximate and fatty acid composition of silver catfish (*Rhamdia quelen*) fillets. *Food Chemistry*, *106*(1), 140–146. https://doi.org/10.1016/j.foodchem.2007.05.052
59. Wei, H., Wei, Y., Qiu , X., Yang, S., Chen, F., Ni, H., Li, Q. (2023). Comparison of potent odorants in raw and cooked mildly salted large yellow croaker using odor-active value calculation and omission test: Understanding the role of cooking method. *Food Chemistry*, *402*, art. no. 134015. https://doi.org/10.1016/j.foodchem.2022.134015
60. WHO/FAO (2003). *Diet, Nutrition, and the Prevention of Chronic Diseases. WHO Technical Report Series 916*. World Health Organization, Geneva, Switzerland.
61. Whelan, J. (1996). Antagonistic effects of dietary arachidonic acid and n-3 polyunsaturated fatty acids. *The Journal of Nutrition*, *126*(Suppl. 4), 1086S–1091S. https://doi.org/10.1093/jn/126.suppl_4.1086S
62. Yazdan, M., Jamilah, B., Yaakob, C.M., Sharifah, K. (2009). Moisture, fat content and fatty acid composition in breaded and non-breaded deep-fried black pomfret (*Parastromateus niger*) fillets. *International Food Research Journal*, *16*(2), 225–231.
63. Zhang, W., Li, P., Hu, X., Zhang, F., Chen, J., Gao, Y. (2011). Omega-3 polyunsaturated fatty acids in the brain: metabolism and neuroprotection. *Frontiers in Bioscience (Landmark edition)*, *16*(7), 2653–2670. https://doi.org/10.2741/3878
64. Zhuang, P., Cheng, L., Wang, J., Zhang, Y., Jiao, J. (2019). Saturated fatty acid intake is associated with total mortality in a nationwide cohort study. *The Journal of Nutrition*, *149*(1), 68–77. https://doi.org/10.1093/jn/nxy237
65. Zotos, A., Kotaras, A., Mikras, E. (2013). Effect of baking of sardine (*Sardina pilchardus*) and frying of anchovy (*Engraulis encrasicholus*) in olive and sunflower oil on their quality. *Food Science and Technology International*, *19*(1), 11–23. https://doi.org/10.1177/1082013212442179

ORIGINAL ARTICLE
http://journal.pan.olsztyn.pl

Polish Journal of Food and Nutrition Sciences
2023, Vol. 73, No. 1, 70–79
DOI: 10.31883/pjfns/160179
ISSN 1230-0322, e-ISSN 2083-6007

Purification and Characterization of a Low Molecular Weight Neutral Non-Starch Polysaccharide from *Panax ginseng* by Enzymatic Hydrolysis

Ying Ying[1,2], Chao Ma[2], Yajie Zhang[2], Xiaoping Li[2], Hongxin Wu[1]*

[1]Institute of Grassland Research, Chinese Academy of Agricultural Science, Huhhot, Inner Mongolia, 010010, P.R. China
[2]Beijing Key Laboratory of Forest Food Processing and Safety, College of Biological Sciences and Biotechnology, Beijing Forestry University, Beijing, 100083, P.R. China

In this study, a novel neutral non-starch polysaccharide (GP1A) was extracted using hot water from ginseng roots. Chemical characteristics, monosaccharide compositions and structure of GP1A were investigated using scanning electron microscopy, gel permeation chromatography, X-ray diffraction, Fourier transform infrared spectroscopy, gas chromatography with mass spectrometer, one-dimensional and two-dimensional nuclear magnetic resonance. The results indicated that the lyophilized GP1A was a homogeneous polysaccharide with a low molecular weight of 1.03 kDa. The dominating monosaccharides of GP1A were D-glucose, D-galactose, D-mannose, D-xylose and D-arabinose. The structure analysis indicated the main chain residues sequence of GP1A was α-D-Glc*p*-(6→3)-α-D-Gal*p*-(1→1)-α-D-Glc*p*-(3→4)-β-D-Man*p*-(2→2)-β-D-Ara*p* with branch chains of α-D-Glc*p* substituted at α-D-Gal*p* and β-D-Xyl*p* substituted at β-D-Man*p*.

Key words: ginseng polysaccharide, chromatographic separation, monosaccharide composition, structure analysis

INTRODUCTION

Ginseng (*Panax ginseng* C.A. Mey) root is a renowned medicine and component of functional food with numerous bioactivities, which are attributed to compounds contained in it, including ginsenosides, ginseng polysaccharides, polyacetylenic alcohols, peptides and fatty acids [Attele *et al.*, 1999]. Among these compounds, ginseng polysaccharides have aroused widespread concerns and showed numerous biological activities, such as anti-inflammatory, anti-tumor, immunoregulatory, anti-diabetic, and anti-fatigue effects [Huang *et al.*, 2021; Li *et al.*, 2018; Wang J. *et al.*, 2010; Wang K. *et al.*, 2020; Zhou *et al.*, 2020].

Various approaches are used to purify and characterize ginseng polysaccharides. Zhang *et al.* [2009] fractionated water-soluble ginseng polysaccharides into two neutral fractions and six acidic fractions by a combination of ethanol precipitation, ion-exchange and gel permeation chromatography. The neutral polysaccharides were starch-like glucan or a mixture of starch-like glucan and arabinogalactan. The acidic fractions were composed of neutral sugar, acidic sugar and/or galacturonic acid. Using α-amylase-assisted extraction method and anion exchange and gel permeation chromatography, Sun *et al.* [2015] fractionated the *Panax ginseng* root polysaccharides into several neutral and pectic fractions. The neutral fraction contained both amylopectin and amylose, and pectic polysaccharide fraction contained arabinogalactan, type-I rhamnogalacturonan and homogalacturonan-type pectin. These results revealed that water-soluble and insoluble polysaccharides were mainly composed of starch-like neutral polysaccharides.

***Corresponding Author:**
e-mail: **wuhongxin168@163.com** (Hongxin Wu)

Submitted: 19 October 2022
Accepted: 1 February 2023
Published on-line: 20 February 2023

The molecular weight (MW) of water-soluble ginseng polysaccharides ranged from 3.5 to 110 kDa and those of insoluble ginseng polysaccharides extracted with α-amylase-assisted methods ranged from 5.5 to 430 kDa [Sun *et al.*, 2015; Zhang *et al.*, 2009]. To date, most studies on neutral ginseng polysaccharides focused on starch-like high MW polysaccharides. However, further studies revealed that partial hydrolysis of type-I rhamnogalacturonan pectin fraction from ginseng polysaccharides, which decreased the MW from 110 kDa to 22 kDa, did not appreciably affected the ability of hydrolysate to enhance macrophage phagocytosis in comparison with parent pectin [Zhang *et al.*, 2012]. Also, it was reported that polysaccharides from the leaves of *Magnolia kwangsiensis* Figlar & Noot with low MW showed much higher antitumor activities than those with high MW [Zheng *et al.*, 2016]. In turn, polysaccharides extracted from *Ulva pertusa* Kjellman with low MW had stronger antioxidant activity compared with those of high MW [Shi, 2016]. A neutral polysaccharide isolated from American ginseng roots with the MW of 3.1 kDa showed significant anti-inflammatory effect [Wang *et al.*, 2015]. These findings indicated that low MW polysaccharides might exhibit high bioactivities. Although there have been a large number of studies on ginseng polysaccharides, understanding the character of low MW polysaccharide is inadequate.

The aim of our study was to establish a novel extraction, fractionation, and purification approach for the exploration of non-starch water-soluble ginseng polysaccharides. The novel neutral polysaccharide was obtained and further characterized using scanning electron microscopy (SEM), gel permeation chromatography (GPC), X-ray diffraction (XRD), Fourier transform infrared spectroscopy (FT-IR), gas chromatography-mass spectrometry (GC-MS), gas chromatography with flame ionization detection (GC-FID), and one-dimensional and two-dimensional nuclear magnetic resonance (NMR). The results could lay the foundation for the improvement of ginseng polysaccharide extraction and structure analysis.

MATERIALS AND METHODS

Chemicals, reagents and materials

Dried ginseng roots were obtained from Beijing Tong Ren Tang Co. (Beijing, China), and identified by Prof. Jianzhong Wang (Beijing Forestry University, Beijing, China). DEAE-52 was purchased from Shanghai Yuanye Bio-Technology Co., Ltd (Shanghai, China). Sephadex G-100 was purchased from Pharmacia Co. (Stockholm, Sweden). Papain, Coomassie brilliant blue G-250, α-amylase and bovine serum albumin were purchased from Sigma Chemical Co. (Saint Louis, MO, USA). Ethanol (95%, *v/v*), phenol and sulfuric acid were purchased from Beijing Chemical Co., Ltd (Beijing, China). Reference monosaccharide standards (D-glucose (D-Glc), D-galactose (D-Gal), D-xylose (D-Xyl), D-mannose (D-Man), and D-arabinose (D-Ara), trifluoroacetic acid and hexamethyl disilazane (HMDS) were purchased from Sinopharm Chemical Reagent Beijing Co., Ltd (Beijing, China). Trimethylchlorosilane (TMCS) and pyridine were purchased from J&K Scientific Co., Ltd (Beijing, China). All reagents used in experiments were of analytical grade.

Extraction of ginseng polysaccharides

Ginseng roots were extracted with hot water according to the method reported by Yu *et al.* [2017] with slight modifications. In detail, 50 g of ginseng root powders were defatted with 500 mL of 80% (*v/v*) ethanol two times at room temperature for 24 h each time. Residues were then extracted with 1000 mL of distilled water three times at 80°C for 3 h each time. The hot water extracts were collected and concentrated with a rotary evaporator (EYELA, Shanghai, China) to a final volume of about 100 mL. The concentrated extracts were precipitated with a five-fold volume of 95% (*v/v*) ethanol and left to stand overnight at 4°C. Finally, the precipitate was separated by filtration and dissolved in 100 mL of distilled water for further use.

Enzymatic hydrolysis of ginseng polysaccharides

To hydrolyse proteins of the crude extract, 20 U of papain were added to 100 mL of the extract solution, and the mixture was incubated at room temperature for 2 h [Yu *et al.*, 2017]. Then, it was heated at 100°C for 5 min to denature enzyme and stop the reaction, after which the precipitate was removed *via* centrifugation (2,100×*g*, 5 min). To further eliminate the starch from crude polysaccharide extract, α-amylase hydrolysis was performed as described by Sun *et al.* [2015]. Briefly, 80 U of α-amylase were added to 100 mL of the extract and incubated in a water bath at 50°C for 30 min. Following hydrolysis, the mixture was heated to 100°C and kept for 5 min to stop the reaction. The mixture was centrifuged at 2,100×*g* for 5 min after being cooled down to room temperature. Finally, supernatants were collected, lyophilized, and 4.66 g of crude polysaccharides (GP) were obtained for further fractionation.

Ion-exchange and gel permeation chromatography analysis

The GP was subsequently fractionated by anion exchange column chromatography according to a previous study with slight modifications [Zhang *et al.*, 2009]. Specifically, 600 mg of GP were dissolved in 20 mL distilled water and centrifuged at 4,200×*g* for 5 min. The supernatant was passed through a 0.45 μm filter and subsequently loaded onto a pre-treated chromatography column packed with DEAE-52 cellulose (1.6×40 cm). The GP was sequentially eluted from DEAE-52 column with distilled water (160 mL), followed by 80 mL of 0.1 M and 0.2 M NaCl solutions, respectively, at a flow rate of 1 mL/min. The eluate was collected at 8.0 mL per tube using an automatic collector (BSZ-100, Shanghai Jiapeng Technology Co., Ltd, Shanghai, China) and assayed for the distribution of the total sugars with phenol-sulfuric acid method [DuBois *et al.*, 1956]. The appropriate fractions were combined, concentrated, dialyzed against distilled water, and lyophilized to obtain one neutral fraction (132 mg, GP1) and two acidic fractions (GP2 and GP3). A 100-mg portion of GP1 was then dissolved in distilled water, loaded onto a Sephadex G-100 column (1.6×40 cm), and eluted with distilled water with a flow rate of 1.0 mL/min. The eluate (4.0 mL per tube) was collected and assayed for total sugar contents. The appropriate fractions were combined as GP1A, concentrated, and lyophilized

for further analysis. The original picture of the GP1A sample was shown in Figure 1.

Chemical composition analysis

The total sugar content was determined by phenol-sulfuric acid assay according to the literature, and the calculation was based on a calibration curve of glucose standard solution in the range of 10–50 μg/mL [DuBois *et al.*, 1956]. The total protein content was determined by Bradford assay, and calculated based on a calibration curve of a bovine serum albumin solution [Compton & Jones, 1985]. The total starch content was determined by measuring the absorbance at 620 nm using I_2-KI assay with amylose as a standard [McGrance *et al.*, 1998].

Characterizations of ginseng polysaccharides

The micro-structure and surface morphology of polysaccharides were observed using a scanning electron microscope (Quanta FEG 250, FEI Company, Hillsboro, OR, USA). Briefly, lyophilized polysaccharides were fixed on a silicon wafer, coated with gold, and then examined at 10 kV accelerating voltage under high vacuum. The micrographs were taken at ×1,000; ×2,000; ×10,000; and ×50,000 magnifications.

The homogeneity and MW distribution of ginseng polysaccharides were determined by the GPC system (Dawn Helios-II, Wyatt Technology, Santa Barbara, CA, USA). Appropriate amounts of GP1A were dissolved in distilled water and passed through a 0.45 μm filter membrane. An aliquot of 20 μL of the sample was loaded onto the column and then eluted with distilled water at a flow rate of 0.5 mL/min. The chromatogram was recorded with a differential refractive index detector (Shodex SB-806M, Showa Denko K. K, Tokyo, Japan) at 40°C. The MW of the fraction was calculated by comparing it with a calibration curve plotted for different MWs of dextran standards (MW of 1.0, 5.0, 12, 25, 50, 80, 150, 200, 500 kDa).

The crystallinity of ginseng polysaccharides was determined using the D8 Advance X-ray diffractometer (Bruker, Billerica, MA, USA). Under the high voltage of 40 kV, the sample was placed in a dish and scanned in the 2θ angle range of 5° to 60° at room temperature.

Figure 1. The original picture of GP1A sample.

The FT-IR spectra were acquired on a Spectrum GX FT-IR spectrometer (PerkinElmer, Inc, Waltham, MA, USA). In detail, 10 mg of the sample powder were dried for 48 h at 50°C in a blast oven (GZX-9070MBE, Boxun Co., Ltd, Shanghai, China) and then mixed with spectroscopic-grade potassium bromide powders. The mixture was pressed into a 1 mm dish and measured using the deuterated triglycine sulfate (DTGS) detector in the range of 4000–400 cm^{-1}.

Monosaccharide composition analysis

GC-MS and GC-FID techniques were used to identify and quantify monosaccharides of GP1A, respectively, after polysaccharide hydrolysis and derivatization of the product of hydrolysis. The hydrolysis of GP1A was performed according to a method reported by Yu *et al.* [2017] with slight modifications. In detail, 5 mg of the lyophilized sample were dissolved in 4.0 mL of 3 M trifluoroacetic acid (TFA) at 110°C for 4 h. After cooling down to room temperature, the excess reactants were removed by evaporation. The derivatization of degraded ginseng polysaccharides was performed using trimethylsilylation reagents according to a modified method described by Ruiz-Matute *et al.* [2011]. Briefly, 2 mg of degraded sample were dissolved in 1.0 mL of anhydrous pyridine. Then, 0.6 mL of HMDS and 0.3 mL of TMCS were added, and the mixture was heated at 50°C and kept for 30 min. After cooling down to room temperature, the derivatized sample was centrifuged at 4,200×*g* for 5 min. Then, 2 mg of each monosaccharide standards (D-Glc, D-Gal, D-Xyl, D-Man, and D-Ara) were derivatized with the same steps, respectively. For both, sample and standards, supernatants were collected and further analyzed by GC-MS and GC-FID under the same protocol.

Agilent 7890A and Agilent 5975C systems (Agilent Technologies, Inc., Santa Clara, CA, USA) were employed for GC-MS and GC-FID analyses, respectively. The injection and detection temperatures were 250°C and 280°C, respectively. The column (DB 5ms Ultra Inert, 30 m × 0.25 mm, film thickness 0.25 μm, Agilent Technologies, Inc.) temperature was programmed to increase from 180°C (maintained for 20 min) to 280°C (maintained for 10 min) at a rate of 20°C/min. Helium was used as the carrier gas and maintained at 1.0 mL/min. The volume of sample injection was 2.0 μL. The identification of monosaccharides was founded by comparing their mass spectra with the National Institute of Standards and Technology (NIST) library databases. Quantification was based on monosaccharide standards by comparing their peak areas with those of the samples (GC-FID separations). The results were shown as the percentage monosaccharide content of GP1A.

Primary structure analysis

All NMR spectra, including ^{1}H NMR, ^{13}C NMR, H–H correlation spectrometry (COSY), heteronuclear single-quantum coherence (HSQC) and heteronuclear multiple bond correlation (HMBC) spectra were recorded on an Avance III HD NMR spectrometer (Bruker), operating at 500 MHz and 25°C. After deuterium exchange in D_2O and double

lyophilization, 20 mg of the sample were dissolved in 0.5 mL of 99.9% D_2O, and the spectra were recorded under 500 MHz. Data collation was implemented using standard MestReNova software (Mestrelab Research SL, Santiago de Compostela, Spain).

Statistical analysis

All experiments were carried out in triplicate. All figures were drawn with the Origin software 10.4 (Origin Lab Corporation, Northampton, United Kingdom).

RESULTS AND DISCUSSION

Extraction and enzymatic hydrolysis of ginseng polysaccharides

In the preliminary step of ginseng root polysaccharides purification, the ethanol-soluble impurities were removed from root powder by ethanol (80%, *v/v*) extraction. Then starch, non-starch polysaccharides, and proteins remained in the residues were extracted with hot water (80°C) and precipitated by 95% (*v/v*) ethanol. After dissolving the precipitation in distilled water, starch and proteins in the solution were hydrolyzed with α-amylase and papain, which led to obvious decrease of starch and protein content from 9.18±0.13% and 1.53±0.04% to less than 0.01% (*w/w*), respectively. The extraction yield of enzymatically hydrolyzed crude ginseng polysaccharides (GP) reached about 9.32% (*w/w*).

Fractionation and purification of ginseng polysaccharides

For further fractionation and purification of ginseng polysaccharides, anion exchange chromatography and gel column chromatography were applied. Anion exchange column chromatography is the most commonly applied method for bulky polysaccharides purification at first, because the separation mechanism is not only ion-exchange but also adsorption-desorption. Anion exchange column chromatography is suitable for the separation of neutral and acidic polysaccharides by eluting with different ionic strength buffers [Yu *et al.*, 2017]. Because of the open framework and weak adsorption to polysaccharide, DEAE-cellulose was usually the first choice as an anion exchanger [Wang *et al.*, 2022]. In the present study, GP was fractionated into three fractions, GP1, GP2 and GP3 on a DEAE-52 anion exchange column chromatograph, as shown in Figure 2A. GP1 was eluted out by water, whereas GP2 and GP3 were obtained by elution with 0.1 M and 0.2 M NaCl solutions. GP1, GP2 and GP3 accounted for about 21.95%, 3.91% and 3.22% (*w/w*) of the total samples loaded, respectively. GP1, the major fraction was then purified using Sepharose G-100 gel column chromatography, which was commonly used to separate polysaccharides according to their size and shape [Kang *et al.*, 2019; Wang *et al.*, 2018]. Finally, GP1A was obtained by water elution, corresponding to a single and narrow peak as shown in Figure 2B, with a yield of 7.3% (*w/w*).

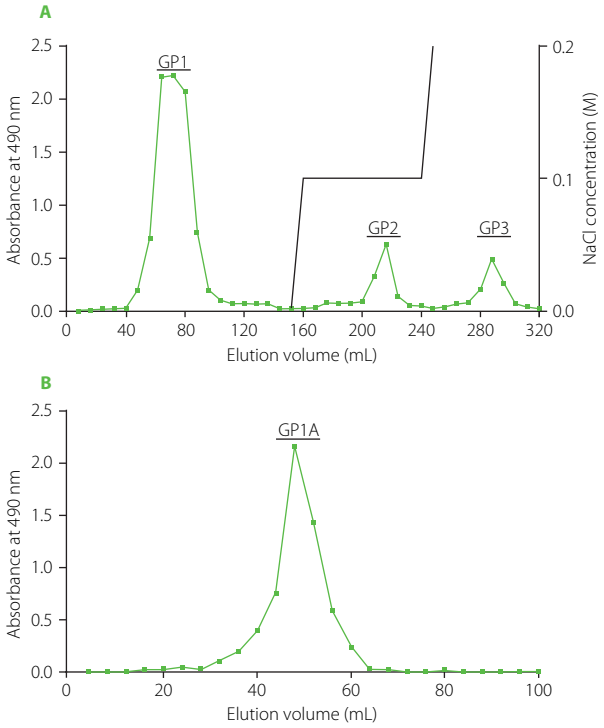

Figure 2. Chromatographic separation of crude polysaccharides of ginseng root on DEAE-52 anion exchange column by elution with different concentrations of NaCl (0.0 M, 0.1 M, and 0.2 M) (**A**) and GP1 on Sephadex G-100 column by elution with water (**B**).

Characterization of ginseng polysaccharide fraction

Surface morphology

The surface morphology and microstructure of GP1A revealed by SEM were shown in Figure 3. The SEM image magnified at ×1,000 (Figure 3A) revealed that GP1A was intensively concentrated and presented as irregular and lamellar shape. When magnified at ×2,000 (Figure 3B), GP1A showed representative honeycomb-like morphology with some small fragments on the surface, which was similar in the morphology of a neutral fraction of WPS-1 isolated from American ginseng [Yu *et al.*, 2017]. Further enlarged SEM images clearly presented smooth and compact structure, indicating that interactions among multiple molecules in GP1A were close and tight (Figures 3C and 3D). Obviously, the SEM observation demonstrated that the lyophilized GP1A powder was amorphous.

Homogeneity and MW distribution

The homogeneity and MW distribution of GP1A were assessed by GPC analysis. The GPC profile showed a single and sharp peak indicating that GP1A was homogeneous with high purity (Figure 4). The average MW of GP1A was 1.03 kDa, which was similar to a neutral polysaccharide PPQN (3.3 kDa) isolated from American ginseng, but far lower than those of other water-eluted polysaccharide fractions obtained from ginseng [Luo & Fang, 2008; Wang *et al.*, 2015]. In previous studies, low MW polysaccharides were usually discarded during the fractionation process, which is a huge waste of resources [Zheng *et al.*, 2016].

Crystallinity

The crystallinity of polysaccharides directly influences their physical properties such as solubility, flexibility and swelling ability

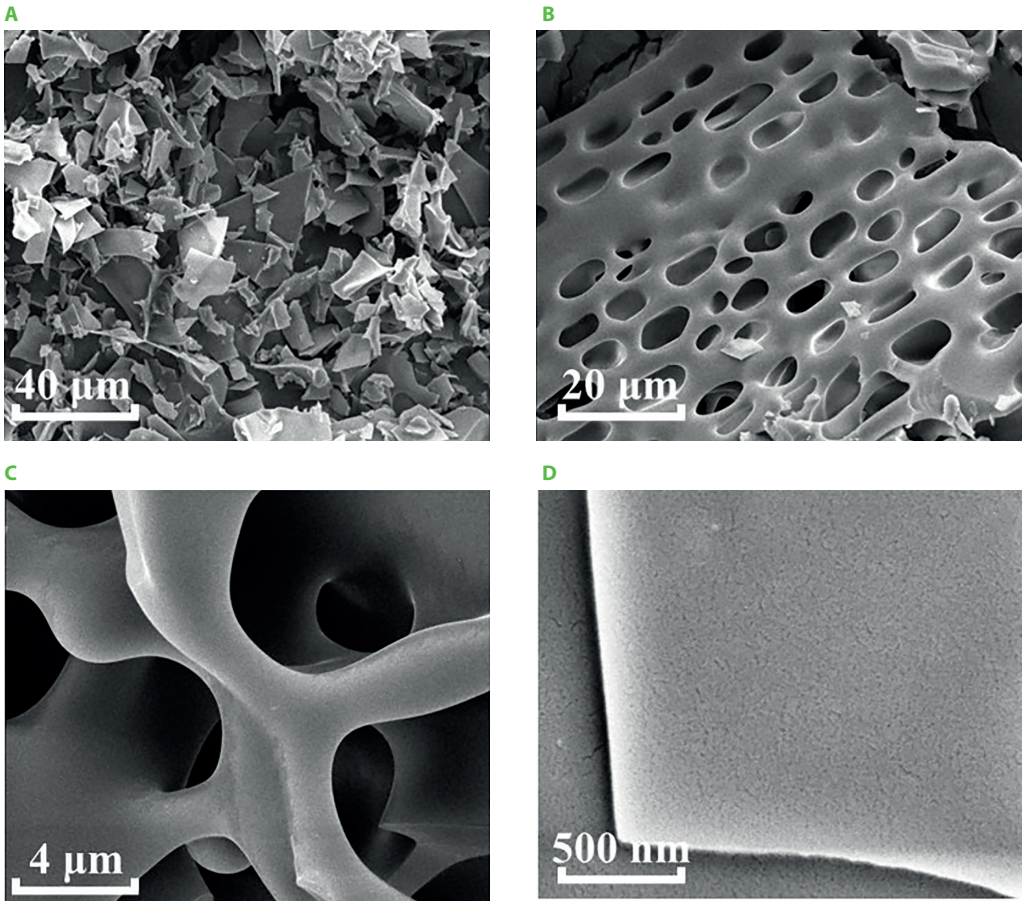

Figure 3. Scanning electron microscope images of ginseng polysaccharide GP1A at ×1,000 (**A**), ×2,000 (**B**), ×10,000 (**C**), and ×50,000 (**D**) magnification.

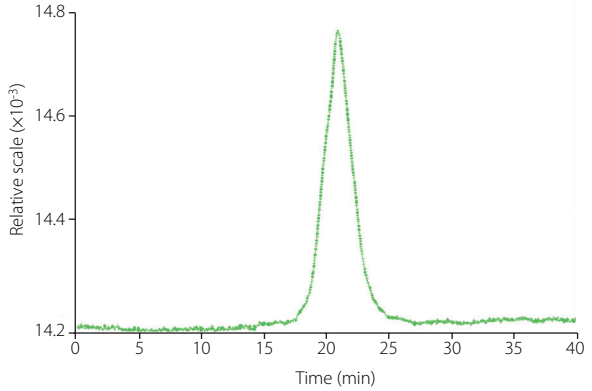

Figure 4. Gel permeation chromatography separation of ginseng polysaccharide GP1A for molecular weight determination.

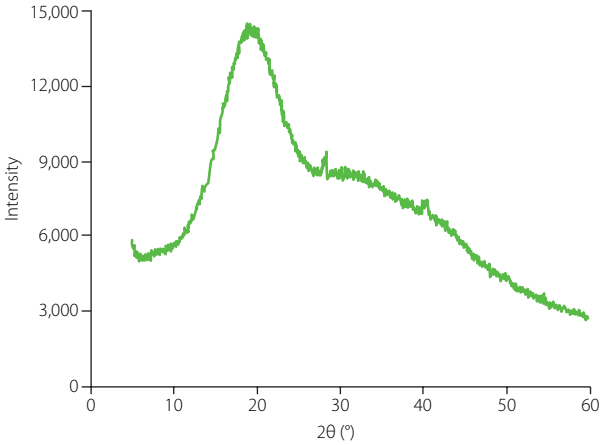

Figure 5. X-ray diffraction pattern of ginseng polysaccharide GP1A.

[Mazeau & Rinaudo, 2004]. XRD is a powerful technique for crystallinity analysis of polysaccharides [Park *et al.*, 2010]. The XRD pattern of GP1A was recorded between 5° and 60° (Figure 5), which suggested that GP1A was an amorphous polymer with low overall relative crystallinity (28.3%). The crystalline region of GP1A was realized at the angle (2θ) 19.05°, which was similar to that of water-soluble polysaccharides isolated from chickpea flour (19.6°) [Mokni Ghribi *et al.*, 2015]. Moreover, the XRD data was consistent with the SEM observation, both showed that GP1A occurred as amorphous powders.

Identification of molecular structures by FT-IR

The FT-IR spectrum of GP1A at range of 4,000–400 cm^{-1} (Figure 6) was recorded for qualitative analysis of functional groups. The spectrum showed no absorption at 1,650 cm^{-1} and 1,736 cm^{-1}, which corresponded to the stretching vibrations of C–O bonds in the acylamino group and the ester carbonyl group (C=O) in protonated carboxylic acid, indicating the absence of proteins and alduronic acids in GP1A [Jeddou *et al.*, 2016; Wang *et al.*, 2012]. The detected broad and strong absorption band at 3,379 cm^{-1} and the shoulder absorption

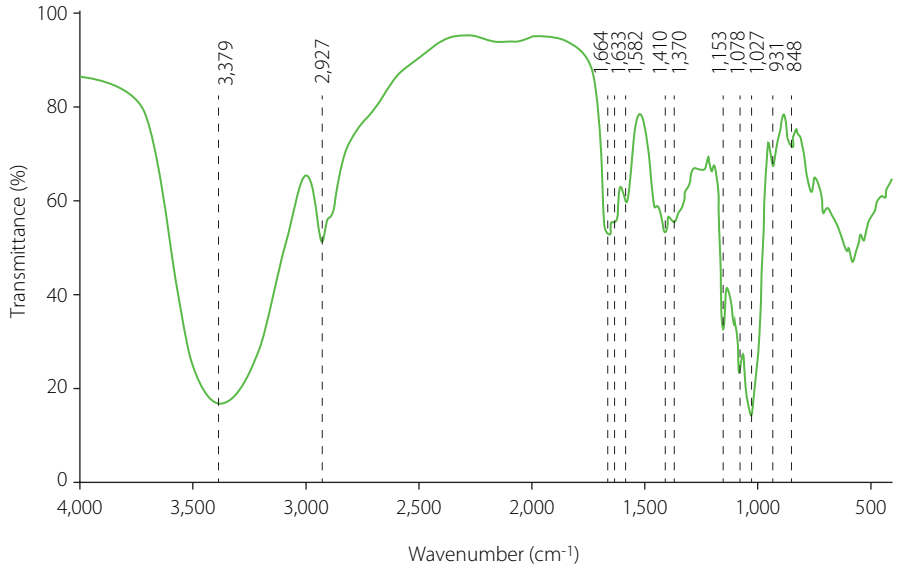

Figure 6. Fourier transform infrared spectrum of ginseng polysaccharide GP1A.

band at around 2,927 cm^{-1} were characteristic as absorption bands of polysaccharides and attributed to stretching vibrations of O–H and C–H, respectively [DuBois *et al.*, 1951]. The spectrum bands at around 1,664 cm^{-1} were assigned to the bound water [Zhao *et al.*, 2005]. The recorded band at 1410 cm^{-1} was reported to be the bending vibration of C–H [Romdhane *et al.*, 2017]. The specific bands in the 1,200–1,000 cm^{-1} region were ascribed to ring vibrations overlapped with the stretching vibrations of C–O–H side groups and the C–O–C glycosidic vibrations [Fan *et al.*, 2009]. The absorption peaks at 1,027 cm^{-1}; 1,078 cm^{-1};

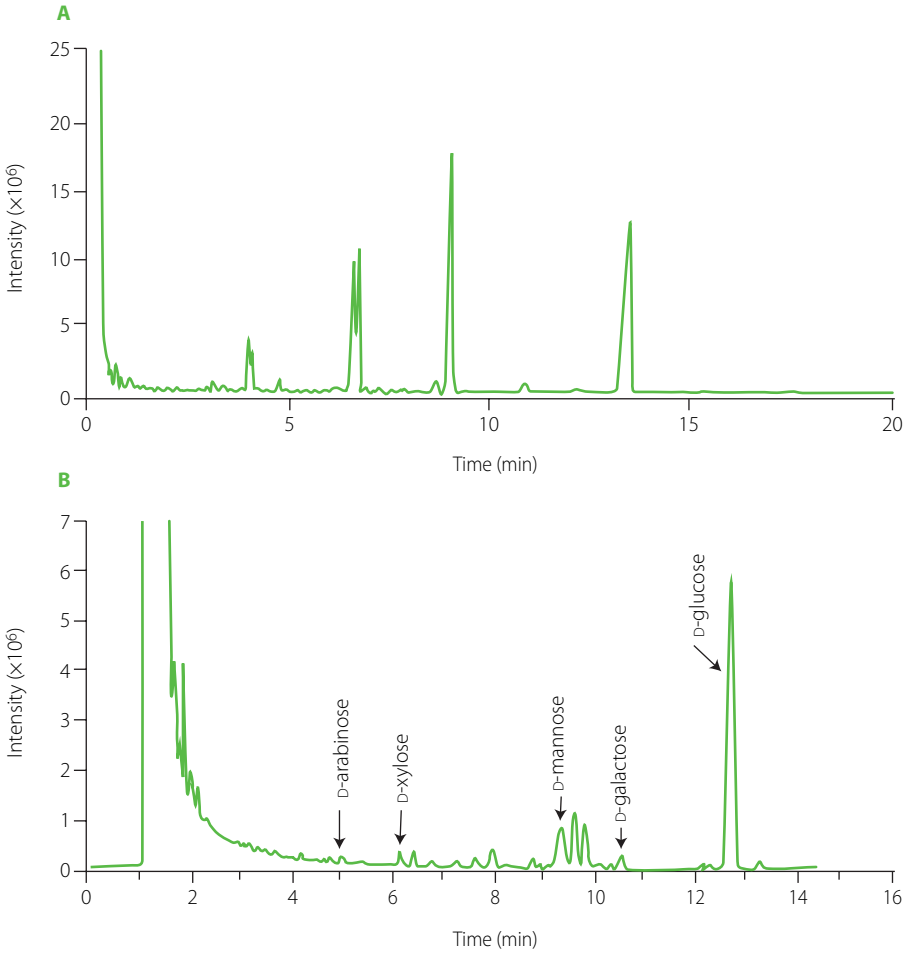

Figure 7. Total ion chromatogram of monosaccharides of ginseng polysaccharide GP1A obtained by gas chromatography–mass spectrophotometry (**A**) and National Institute of Standards and Technology database matching total ion chromatogram of monosaccharides of GP1A (**B**).

Table 1. Main silyl derivatives of monosaccharides identified in hydrolyzed ginseng root polysaccharide GP1A by gas chromatography–mass spectrometry analysis.

Monosaccharide derivative	Retention time (min)	Chemical formula	Sugar residue
1,2,3,4-Tetrakis-*O*-(trimethylsilyl)-β-D-xylopyranose	5.233	$C_{17}H_{42}O_5Si_4$	Xylose
1,2,3,5,6-Pentakis-*O*-(trimethylsilyl)-α-D-galactofuranose	7.694	$C_{21}H_{52}O_6Si_5$	Galactose
1,2,3,5-Tetrakis-*O*-(trimethylsilyl)-β-D-arabinofuranose	7.804	$C_{17}H_{42}O_5S_{i4}$	Arabinose
2,3,4,5,6-Pentakis-*O*-(trimethylsilyl)-β-D-mannose	10.03	$C_{21}H_{52}O_6Si_5$	Mannose
1,2,3,4,6-Pentakis-*O*-(trimethylsilyl)-α-D-glucose	14.27	$C_{21}H_{52}O_6Si_5$	Glucose

and 1,153 cm^{-1} indicated a pyranose form of polysaccharides [Luo *et al.*, 2010]. In general, the spectrum over the frequency range 960–730 cm^{-1} was assigned to either α- or β-D-glucopyranose, disregarding being reducing sugar, methyl glucosides, or polysaccharides. Specifically, α-anomers absorbed at 844±8 cm^{-1}, and β-anomers at 891±7 cm^{-1}. In the FT-IR spectrum of GP1A, no absorption band was observed at around 891 cm^{-1}, while an obvious band at 848 cm^{-1}s occurred, indicating the existence of α-D-glucopyranose. In summary, the FT-IR indicated that GP1A was a neutral polysaccharide without protein contaminants and suggested the existence of α-D-glucopyranose.

Monosaccharide composition

Total ion GC-MS chromatogram of main silyl monosaccharide derivatives identified in the hydrolyzed GP1A is shown in Figure 7. Comparing with NIST library database, the derivatives of D-xylose, D-galactose, D-arabinose, D-mannose, and D-glucose, containing α- and β-anomer were found (Table 1).

According to the GC-FID separations of standards and GP1A after hydrolysis and silylation (data not shown), GP1A was composed of D-glucose, D-galactose, D-mannose, D-xylose and D-arabinose in a molar ratio of 90.62:2.01:7.14:1.05:0.20. The neural polysaccharide fraction WGPN, isolated from ginseng by Zhang *et al.* [2009] was composed of glucose, galactose, arabinose with a molar ratio of 73.31:2.54:1.8 Another neutral ginseng polysaccharide WGPE-N isolated from hot water-extracted ginseng residues with the assistance of α-amylase was revealed to be composed of glucose, arabinose and galactose with a molar ratio of 94.8:2.9:2.3 [Sun *et al.*, 2015]. The homogeneous neutral polysaccharides PGPW with high MW of 350 kDa, isolated from ginseng roots, was reported to be composed of glucose, galactose, mannose, and arabinose with a molar ratio of 3.3:1.2:0.5:3.3 [Li *et al.*, 2012]. By comparing our results with those of ginseng polysaccharides reported previously, the present non-starch neutral polysaccharide was distinguished in monosaccharide composition.

The primary structure analysis

The ^{1}H NMR spectrum of GP1A is shown in Figure 8A. The ^{1}H signals at δ 5.0–5.4 ppm were assigned as anomeric protons of the *α*-glycosidic configuration and δ 4.4–5.0 ppm were

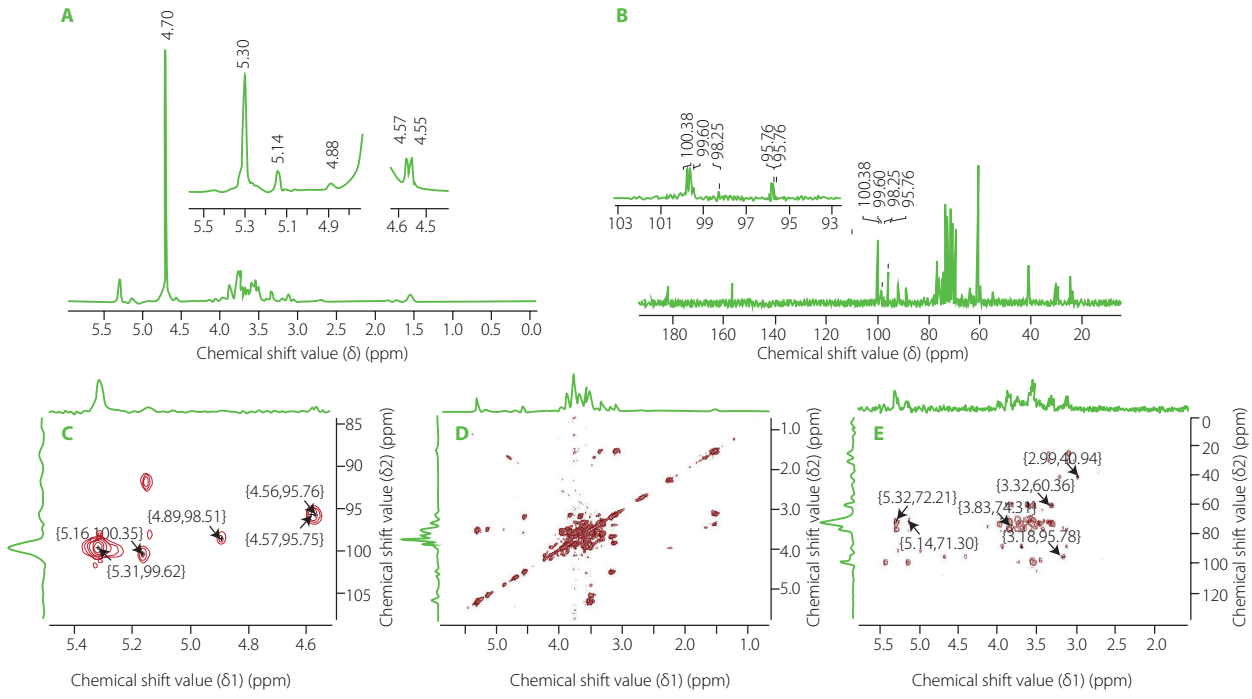

Figure 8. Proton nuclear magnetic resonance (^{1}H NMR) (**A**), carbon-13 nuclear magnetic resonance (^{13}C NMR) (**B**), heteronuclear single-quantum coherence (HSQC) (**C**), H–H correlation spectrometry (COSY) (**D**), heteronuclear multiple bond correlation (HMBC), (**E**) spectra (D_2O) of ginseng polysaccharide GP1A.

the β-glycosidic configuration [Wang *et al.*, 2017]. The ^{1}H signal at around δ 4.70 ppm was the solvent peak of D_2O. Five anomeric proton signals at δ 5.31, 5.14, 4.88, 4.58 and 4.56 ppm were present in the ^{1}H-NMR spectrum, indicating that GP1A was generally composed of five types of sugar residues. These results are consistent with that obtained from GC-MS analysis. The ^{13}C-NMR spectrum contained signals for five anomeric signals at δ 100.38, 99.60, 98.25, 95.76 and 95.75 ppm (Figure 8B). Combined with the HSQC (Figure 8C) and H-H COSY (Figure 8D) spectrum data and data in references, the anomeric proton and carbon signals at δ 5.31/99.60 ppm, 5.14/100.38 ppm, 4.88/98.25 ppm, 4.58/95.76 ppm and 4.56/95.76 ppm were assigned to α-D-Glc, α-D-Gal, β-D-Xyl, β-D-Man and β-D-Ara, respectively [Li *et al.*, 2012; Guo *et al.*, 2015; Meng *et al.*, 2017]. The signals of other sugar ring protons existed in the region of δ 3.40–4.40 ppm, whose corresponding carbons existed in the region of δ 60–80 ppm. The lack of carbon signals in the region δ 82–84 ppm was evident of the absence of furanosidic residues [Guo *et al.*, 2015]. The proton and carbon chemical shifts of sugar resides derived from the 1D and 2D NMR spectra were assigned in detail and summarized in Table 2.

The glycosyl sequence and linkage sites among residues were confirmed by the long-range ^{1}H-^{13}C correlations obtained from the HMBC spectrum (Figure 8E). Cross-peaks were found between α-D-Glc H1 (δ 5.31 ppm) and β-D-Man C6 (δ 72.29 ppm), α-D-Gal H3(δ 3.32 ppm) and α-D-Glc C6(δ 60.5 ppm), α-D-Gal H1(δ 5.14 ppm) and α-D-Glc C3(δ 71.90 ppm), β-D-Xyl H2 (δ 3.18 ppm) and β-D-Man C1 (δ 95.78 ppm), β-D-Man H2 (δ 3.83 ppm) and β-D-Ara C2 (δ 74.31 ppm) [He *et al.*, 2017; Yao *et al.*, 2021]. Above all, the GP1A ginseng polysaccharides were composed of five types of monosaccharides, and the main sequence was: α-D-Glcp-(6→3)-α-D-Galp-(1→1)-α-D-Glcp-(3→4)--β-D-Manp-(2→2)-β-D-Arap, with the branch chains of α-D-Glc*p* substituted at α-D-Gal*p* and β-D-Xyl*p* substituted at β-D-Man*p*. The deduced primary structure and the chemical structure of GP1A are shown in Figure 9.

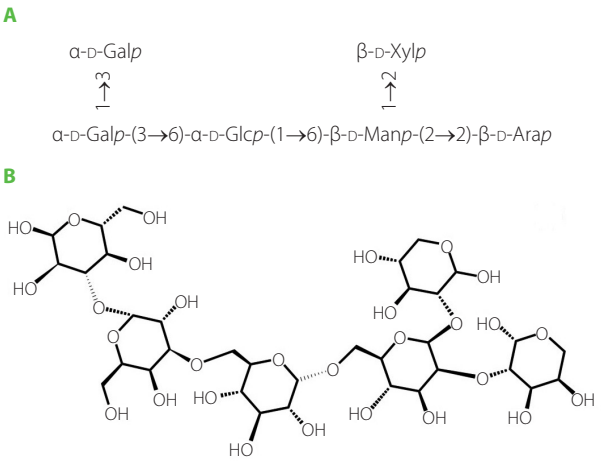

Figure 9. The deduced primary structure (**A**) and chemical structure (**B**) of ginseng polysaccharide GP1A. D-Glc, D-glucose; D-Gal, D-galactose; D-Xyl, D-xylose; D-Man, D-mannose; D-Ara, D-arabinose.

CONCLUSION

By a combination of removal of ethanol-soluble compounds, hot water extraction, ethanol precipitation, α-amylase and papain enzymatic hydrolysis, ion-exchange and gel permeation chromatography fractionation, a polysaccharide fraction GP1A was obtained from ginseng roots. GPC analysis revealed that GP1A was a homogenous polymer, with an average MW of 1.03 kDa, which was significantly lower than those of various polysaccharides reported previously. SEM and XRD analyses indicated that lyophilized GP1A was an amorphous powder with very low crystallinity. FT-IR analysis demonstrated that GP1A was a protein-free neutral polysaccharide, containing α-D-glucopyranose. GC-MS and GC-FID of the hydrolyzed GP1A revealed that major released monosaccharides were glucose, galactose, mannose, xylose and arabinose in a molar ratio of 90.62:2.01:7.14:1.05:0.20. The chemical structure was deduced by the one-dimensional and two-dimensional NMR. Therefore, the obtained GP1A polysaccharide was a novel neutral non-starch polysaccharide, which

Table 2. ^{1}H and ^{13}C nuclear magnetic resonance chemical shifts (ppm) for signals of ginseng root polysaccharide GP1A.

Structure		C-1(H-1)	C-2(H-2)	C-3(H-3)	C-4(H-4)	C-5(H-5)	C-6(H-6)
α-D-Glucose	^{1}H shifts	5.31	3.59	3.5	3.67	3.18	3.69
	^{13}C shifts	99.6	76.8	72.8	77	74	60.5
α-D-Galactose	^{1}H shifts	5.14	3.47	3.31	3.40	3.11	1.62
	^{13}C shifts	100.38	63.7	70.2	70.36	72.86	62.67
β-D-Xylose	^{1}H shifts	4.88	3.5	3.41	3.16	3.83	–
	^{13}C shifts	98.25	72.8	75.5	72.9	70.04	–
β-D-Mannose	^{1}H shifts	4.58	3.58	3.39	3.28	3.77	3.31
	^{13}C shifts	95.76	72.29	77	72.8	69.72	60.56
β-D-Arabinose	^{1}H shifts	4.56	3.19	3	3.89	3.12	–
	^{13}C shifts	95.76	74.01	63.74	70.80	66.87	–

The solvent of sample was D_2O (0.5 mL, 99.9%).

was distinguished from previously reported ones in both MW and monosaccharide composition.

RESEARCH FUNDING

This work was financially supported by the Central Public-interest Scientific Institution Basal Research Fund (NO. 1610332022004).

CONFLICT OF INTERESTS

The authors have no competing interests.

ORCID IDs

X. Li https://orcid.org/0000-0001-5451-9404
Ch. Ma https://orcid.org/0000-0001-6728-4114
H. Wu https://orcid.org/0000-0003-4809-5419
Y. Ying https://orcid.org/0000-0002-2926-6051
Y. Zhang https://orcid.org/0000-0003-2278-5905

REFERENCES

1. Attele, A.S., Wu, J.A., Yuan, C.-S. (1999). Ginseng pharmacology: Multiple constituents and multiple actions. *Biochemical Pharmacology*, *58*(11), 1658–1693. https://doi.org/10.1016/S0006-2952(99)00212-9
2. Compton, S.J., Jones, C.G. (1985). Mechanism of dye response and interference in the Bradford protein assay. *Analytical Biochemistry*, *151*(2), 369–374. https://doi.org/10.1016/0003-2697(85)90190-3
3. DuBois, M., Gilles, K., Hamilton, J.K., Smith, F. (1951). A colorimetric method for the determination of sugars. *Nature*, *168*, art. no. 167. https://doi.org/10.1038/168167a0
4. DuBois, M., Gilles, K.A., Hamilton, J.K., Rebers, P.A., Smith, F. (1956). Colorimetric method for determination of sugars and related substances. *Analytical Chemistry*, *28*(3), 350–356. https://doi.org/10.1021/ac60111a017
5. Fan, Y., He, X., Zhou, S., Luo, A., He, T., Chun, Z. (2009). Composition analysis and antioxidant activity of polysaccharide from *Dendrobium denneanum*. *International Journal of Biological Macromolecules*, *45*(2), 169–173. https://doi.org/10.1016/j.ijbiomac.2009.04.019
6. Guo, Q., Cui, S.W., Kang, J., Ding, H., Wang, Q., Wang, C. (2015). Non-starch polysaccharides from American ginseng: physicochemical investigation and structural characterization. *Food Hydrocolloids*, *44*, 320–327. https://doi.org/10.1016/j.foodhyd.2014.09.031
7. He, P.-F., He, L., Zhang, A.-Q., Wang, X.-L., Qu, L., Sun, P.-L. (2017). Structure and chain conformation of a neutral polysaccharide from sclerotia of *Polyporus umbellatus*. *Carbohydrate Polymers*, *155*, 61–67. https://doi.org/10.1016/j.carbpol.2016.08.041
8. Huang, J., Liu, D., Wang, Y., Liu, L., Li, J., Yuan, J., Jiang, Z., Jiang, Z., Hsiao, W.L.W., Liu, H., Khan, I., Xie, Y., Wu, J., Xie, Y., Zhang, Y., Fu, Y., Liao, J., Wang, W., Lai, H., Shi, A., Cai, J., Luo, L., Li, R., Yao, X., Fan, X., Wu, Q., Liu, Z., Yan, P., Lu, J., Yang, M., Wang, L., Cao, Y., Wei, H., Leung, E.L.-H. (2021). Ginseng polysaccharides alter the gut microbiota and kynurenine/tryptophan ratio, potentiating the antitumour effect of antiprogrammed cell death 1/programmed cell death ligand 1 (anti-PD-1/PD-L1) immunotherapy. *Gut*, *71*, 734–745. https://doi.org/10.1136/gutjnl-2020-321031
9. Jeddou, K.B., Chaari, F., Maktouf, S., Nouri-Ellouz, O., Helbert, C.B., Ghorbel, R.E. (2016). Structural, functional, and antioxidant properties of water-soluble polysaccharides from potatoes peels. *Food Chemistry*, *205*, 97–105. https://doi.org/10.1016/j.foodchem.2016.02.108
10. Kang, Q., Chen, S., Li, S., Wang, B., Liu, X., Hao, L., Lu, J. (2019). Comparison on characterization and antioxidant activity of polysaccharides from *Ganoderma lucidum* by ultrasound and conventional extraction. *International Journal of Biological Macromolecules*, *124*, 1137–1144. https://doi.org/10.1016/j.ijbiomac.2018.11.215
11. Li, C., Cai, J., Geng, J., Li, Y., Wang, Z., Li, R. (2012). Purification, characterization and anticancer activity of a polysaccharide from *Panax ginseng*. *International Journal of Biological Macromolecules*, *51*(5), 968–973. https://doi.org/10.1016/j.ijbiomac.2012.06.031
12. Li, J., Li, R., Li, N., Zheng, F., Dai, Y., Ge, Y., Yue, H., Yu, S. (2018). Mechanism of antidiabetic and synergistic effects of ginseng polysaccharide and ginsenoside Rb1 on diabetic rat model. *Journal of Pharmaceutical and Biomedical Analysis*, *158*, 451–460. https://doi.org/10.1016/j.jpba.2018.06.024
13. Li, Q., Xie, Y., Su, J., Ye, Q., Jia, Z. (2012). Isolation and structural characterization of a neutral polysaccharide from the stems of *Dendrobium densiflorum*. *International Journal of Biological Macromolecules*, *50*(5), 1207–1211. https://doi.org/10.1016/j.ijbiomac.2012.03.005
14. Luo, A., He, X., Zhou, S., Fan, Y., Luo, A., Chun, Z. (2010). Purification, composition analysis and antioxidant activity of the polysaccharides from *Dendrobium nobile* Lindl. *Carbohydrate Polymers*, *79*(4), 1014–1019. https://doi.org/10.1016/j.carbpol.2009.10.033
15. Luo, D., Fang, B. (2008). Structural identification of ginseng polysaccharides and testing of their antioxidant activities. *Carbohydrate Polymers*, *72*(3), 376–381. https://doi.org/10.1016/j.carbpol.2007.09.006
16. Mazeau, K., Rinaudo, M. (2004). The prediction of the characteristics of some polysaccharides from molecular modeling. Comparison with effective behavior. *Food Hydrocolloids*, *18*(6), 885–898. https://doi.org/10.1016/j.foodhyd.2004.04.004
17. McGrance, S.J., Cornell, H.J., Rix, C.J. (1998). A simple and rapid colorimetric method for the determination of amylose in starch products. *Starch/Stärke*, *50*(4), 158–163. https://doi.org/10.1002/(SICI)1521-379X(199804)50:4<158::AID-STAR158>3.0.CO;2-7
18. Meng, M., Cheng, D., Han, L., Chen, Y., Wang, C. (2017). Isolation, purification, structural analysis and immunostimulatory activity of water-soluble polysaccharides from *Grifola Frondosa* fruiting body. *Carbohydrate Polymers*, *157*, 1134–1143. https://doi.org/10.1016/j.carbpol.2016.10.082
19. Mokni Ghribi, A., Sila, A., Maklouf Gafsi, I., Blecker, C., Danthine, S., Attia, H., Bougatef, A., Besbes, S. (2015). Structural, functional, and ACE inhibitory properties of water-soluble polysaccharides from chickpea flours. *International Journal of Biological Macromolecules*, *75*, 276–282. https://doi.org/10.1016/j.ijbiomac.2015.01.037
20. Park, S., Baker, J.O., Himmel, M.E., Parilla, P.A., Johnson, D.K. (2010). Cellulose crystallinity index: measurement techniques and their impact on interpreting cellulase performance. *Biotechnology for Biofuels*, *3*(1), art. no. 10. https://doi.org/10.1186/1754-6834-3-10
21. Romdhane, M.B., Haddar, A., Ghazala, I., Jeddou, K.B., Helbert, C.B., Ellouz-Chaabouni, S. (2017). Optimization of polysaccharides extraction from watermelon rinds: Structure, functional and biological activities. *Food Chemistry*, *216*, 355–364. https://doi.org/10.1016/j.foodchem.2016.08.056
22. Ruiz-Matute, A.I., Hernández-Hernández, O., Rodríguez-Sánchez, S., Sanz, M.L., Martínez-Castro, I. (2011). Derivatization of carbohydrates for GC and GC-MS analyses. *Journal of Chromatography B*, *879*(17–18), 1226–1240. https://doi.org/10.1016/j.jchromb.2010.11.013
23. Shi, L. (2016). Bioactivities, isolation and purification methods of polysaccharides from natural products: A review. *International Journal of Biological Macromolecules*, *92*, 37–48. https://doi.org/10.1016/j.ijbiomac.2016.06.100
24. Sun, L., Wu, D., Ning, X., Yang, G., Lin, Z., Tian, M., Zhou, Y. (2015). α-Amylase-assisted extraction of polysaccharides from *Panax ginseng*. *International Journal of Biological Macromolecules*, *75*, 152–157. https://doi.org/10.1016/j.ijbiomac.2015.01.025
25. Wang, J., Li, S., Fan, Y., Chen, Y., Liu, D., Cheng, H., Gao, X., Zhou, Y. (2010). Anti-fatigue activity of the water-soluble polysaccharides isolated from *Panax ginseng C. A. Meyer*. *Journal of Ethnopharmacology*, *130*(2), 421–423. https://doi.org/10.1016/j.jep.2010.05.027
26. Wang, K., Zhang, H., Han, Q., Lan, J., Chen, G., Cao, G., Yang, C. (2020). Effects of astragalus and ginseng polysaccharides on growth performance, immune function and intestinal barrier in weaned piglets challenged with lipopolysaccharide. *Journal of Animal Physiology and Animal Nutrition*, *104*(4), 1096–1105. https://doi.org/10.1111/jpn.13244
27. Wang, L., Liu, H.-M., Qin, G.-Y. (2017). Structure characterization and antioxidant activity of polysaccharides from Chinese quince seed meal. *Food Chemistry*, *234*, 314–322. https://doi.org/10.1016/j.foodchem.2017.05.002
28. Wang, L., Yu, X., Yang, X., Li, Y., Yao, Y., Lui, E.M.K., Ren, G. (2015). Structural and anti-inflammatory characterization of a novel neutral polysaccharide from North American ginseng (*Panax quinquefolius*). *International Journal of Biological Macromolecules*, *74*, 12–17. https://doi.org/10.1016/j.ijbiomac.2014.10.062
29. Wang, R., Chen, P., Jia, F., Tang, J., Ma, F. (2012). Optimization of polysaccharides from *Panax japonicus C.A. Meyer* by RSM and its anti-oxidant activity. *International Journal of Biological Macromolecules*, *50*(2), 331–336. https://doi.org/10.1016/j.ijbiomac.2011.12.023
30. Wang, W., Li, X., Bao, X., Gao, L., Tao, Y. (2018). Extraction of polysaccharides from black mulberry fruit and their effect on enhancing antioxidant activity. *International Journal of Biological Macromolecules*, *120*(Part B), 1420–1429. https://doi.org/10.1016/j.ijbiomac.2018.09.132
31. Wang, W., Tan, J., Nima, L., Sang, Y., Cai, X., Xue, H. (2022). Polysaccharides from fungi: A review on their extraction, purification, structural features, and biological activities. *Food Chemistry: X*, *15*, art. no. 100414. https://doi.org/10.1016/j.fochx.2022.100414

32. Yao, H.-Y.-Y., Wang, J.-Q., Yin, J.-Y., Nie, S.-P., Xie, M.-Y. (2021). A review of NMR analysis in polysaccharide structure and conformation: Progress, challenge and perspective. *Food Research International*, 143, art. no. 110290. https://doi.org/10.1016/j.foodres.2021.110290
33. Yu, X.-H., Liu, Y., Wu, X.-L., Liu, L.-Z., Fu, W., Song, D.-D. (2017). Isolation, purification, characterization and immunostimulatory activity of polysaccharides derived from American ginseng. *Carbohydrate Polymers*, *156*, 9–18. https://doi.org/10.1016/j.carbpol.2016.08.092
34. Zhang, X., Li, S., Sun, L., Ji, L., Zhu, J., Fan, Y., Tai, G., Zhou, Y. (2012). Further analysis of the structure and immunological activity of an RG-I type pectin from *Panax ginseng*. *Carbohydrate Polymers*, *89*(2), 519–525. https://doi.org/10.1016/j.carbpol.2012.03.039
35. Zhang, X., Yu, L., Bi, H., Li, X., Ni, W., Han, H., Li, N., Wang, B., Zhou, Y., Tai, G. (2009). Total fractionation and characterization of the water-soluble polysaccharides isolated from *Panax ginseng C. A. Meyer*. *Carbohydrate Polymers*, *77*(3), 544–552. https://doi.org/10.1016/j.carbpol.2009.01.034
36. Zhao, G., Kan, J., Li, Z., Chen, Z. (2005). Structural features and immunological activity of a polysaccharide from *Dioscorea opposita* Thunb roots. *Carbohydrate Polymers*, *61*(2), 125–131. https://doi.org/10.1016/j.carbpol.2005.04.020
37. Zheng, Y.-F., Zhang, Q., Liu, X.-M., Ma, L., Lai, F. (2016). Extraction of polysaccharides and its antitumor activity on *Magnolia kwangsiensis* Figlar & Noot. *Carbohydrate Polymers*, *142*, 98–104. https://doi.org/10.1016/j.carbpol.2016.01.039
38. Zhou, H., Yan, Y., Zhang, X., Zhao, T., Xu, J., Han, R. (2020). Ginseng polysaccharide inhibits MDA-MB-231 cell proliferation by activating the inflammatory response. *Experimental and Therapeutic Medicine*, *20*(6), art. no. 229. https://doi.org/10.3892/etm.2020.9359

ORIGINAL ARTICLE
http://journal.pan.olsztyn.pl

Polish Journal of Food and Nutrition Sciences
2023, Vol. 73, No. 1, 80–94
DOI: 10.31883/pjfns/160186
ISSN 1230-0322, e-ISSN 2083-6007

Oral Supplementation with Three Vegetable Oils Differing in Fatty Acid Composition Alleviates High-Fat Diet-Induced Obesity in Mice by Regulating Inflammation and Lipid Metabolism

Waleed A.S. Aldamarany[1,2], Huang Taocui[3], Deng Liling[4], Yang Wanfu[1], Geng Zhong[1,5]*

[1]College of Food Science, Southwest University, Beibei District, Chongqing 400715, P.R. China
[2]Food Science and Technology Department, Faculty of Agriculture, Al-Azhar University (Assiut Branch), Assiut, Egypt
[3]Chongqing Academy of Agricultural Science, Chongqing 400060, P.R. China
[4]Science and Technology Department, Chongqing Medical and Pharmaceutical College, Chongqing 401334, P.R. China
[5]Chongqing Key Laboratory of Specialty Food Co-Built by Sichuan and Chongqing, Chongqing 400715, P.R. China

Obesity has become one of the most prevalent chronic diseases worldwide, which affects people's health and daily lives. Therefore, this study aimed to investigate the anti-obesity effects of perilla seed oil (PSO), sunflower oil (SFO), and tea seed oil (TSO) and their potential mechanisms in mice fed a high-fat diet (HFD). Mice were divided into five groups: ND, mice fed a normal diet; HFD, mice fed a high-fat diet; PSO, SFO, and TSO, mice fed a high-fat diet supplemented with PSO, SFO, and TSO at 2 g/kg body weight per day, respectively. Our findings showed that oral supplementation with all three oils for 8 weeks significantly reduced body weight, tissue weight, insulin resistance index, serum levels of alanine aminotransferase (ALT), aspartate aminotransferase (AST), and free fatty acids (FFA), and markedly alleviated hyperglycemia, hyperlipidemia, and hepatic steatosis in obese mice. It also decreased leptin, pro-inflammatory cytokines, such as tumor necrosis factor-alpha (TNF-α), interleukin (IL)-6, and (IL)-1beta (IL-1β), and increased anti-inflammatory adipokine adiponectin at both secretion and mRNA expression levels in the epididymal adipose tissue (EAT). Moreover, PSO, SFO, and TSO administration increased the expression levels of fatty acid β-oxidation-related genes, including peroxisome proliferator-activated receptor-alpha (PPAR-α), carnitine palmitoyltransferase 1a (CPT1a) and CPT1b, and thermogenesis-related genes such as uncoupling protein 1 (UCP1), and decreased the expression levels of lipid synthesis-related genes, including fatty acid synthase (FAS) and PPAR-γ in EAT. In conclusion, PSO, SFO, and TSO supplementation could have potential anti-obesity effects in HFD-fed mice by reducing inflammation and improving lipid metabolism.

Key words: perilla oil, sunflower oil, tea seed oil, anti-obesity effect, inflammation, lipid metabolism

ABBREVIATIONS

ALT, alanine aminotransferase; AST, aspartate aminotransferase; CPT1a, carnitine palmitoyltransferase 1a; CPT1b, carnitine palmitoyltransferase 1b; CVD, cardiovascular disease; FAS, fatty acid synthase; HDL-C, high-density lipoprotein cholesterol; HFD, high-fat diet; IL-1β, interleukin-1beta; IL-6, interleukin-6; LDL-C, low-density lipoprotein cholesterol; ND, normal diet; PPAR-α, peroxisome proliferator-activated receptor-alpha; PPAR-γ, peroxisome proliferator-activated receptor-gamma; PSO, perilla seed oil; PUFA, polyunsaturated fatty acids; qRT-PCR: quantitative real-time reverse-transcription PCR; SFA, saturated fatty acids; SFO, sunflower oil; TC, total cholesterol; TNF-α, tumor necrosis

***Corresponding Author:**
Tel: 0086-18696747591, e-mail: gzhong@swu.edu.cn (G. Zhong)

Submitted: 3 December 2022
Accepted: 2 February 2023
Published on-line: 28 February 2023

factor-alpha; TG, triglycerides; TSO, tea seed oil; UCP1, uncoupling protein 1; USFA, unsaturated fatty acids.

INTRODUCTION

Obesity is considered one of the most prevalent health problems worldwide, with an alarming increase in the number of obese people every year [Gregg & Shaw, 2017]. In recent years, obesity prevalence has more than doubled, with more than 1.9 billion overweight individuals globally, at least 600 million of whom were clinically obese [Zhang *et al.*, 2019]. Previous studies have demonstrated that obesity can be caused by a variety of factors, including a high-fat diet (HFD), and that it is linked to a range of metabolic disorders, such as type 2 diabetes, dyslipidemia, non-alcoholic fatty liver disease, and cardiovascular disease (CVD) [Li & Ji, 2018; Parto & Lavie, 2017]. Indeed, the onset and development of metabolic disorders have been associated with increased production of pro-inflammatory hormones and cytokines, such as leptin, resistin, tumor necrosis factor-alpha (TNF-α), interleukin-6 (IL-6), and interleukin-1beta (IL-1β), together with a decrease in the production of anti-inflammatory adipokines such as adiponectin [Ouchi *et al.*, 2011].

Inflammation-mediated pathways are likely to play an important role in metabolism regulation [Stienstra *et al.*, 2012]. It has been shown that the peroxisome proliferator-activated receptor-alpha (PPAR-α) plays a crucial role in metabolism regulation, primarily through enhancing β-oxidation by increasing the expression of its associated genes [Takahashi *et al.*, 2016]. Carnitine palmitoyltransferase 1 (CPT1), a PPAR target gene, is necessary for fatty acid transfer into the mitochondria for β-oxidation [Chen *et al.*, 2017]. Additionally, several genes related to lipid metabolism are linked to adipose tissue inflammation. For example, PPAR-α activation can reduce inflammatory cytokine production by suppressing nuclear factor kappa B (NF-κB) signaling, whereas peroxisome proliferator-activated receptor gamma (PPAR-γ) activation can inhibit macrophage activation and the production of inflammatory cytokines, such as TNF-α, IL-1β, and IL-6 [Decara *et al.*, 2020]. Furthermore, the uncoupling protein 1 gene (UCP1), found in the inner mitochondrial membrane, plays a crucial role in adipose tissue's browning and affects lipid metabolism [Mishra *et al.*, 2021]. Although UCP1 protein is abundant in brown adipose tissue, its presence in a white fat cell indicates that it has transformed into a light brown (beige) fat cell. Activation of brown and beige adipocytes can affect systemic energy metabolism, promoting substrate oxidation and energy expenditure, regardless of its use as a therapeutic target for many metabolic conditions, such as diabetes and obesity [Whitehead *et al.*, 2021]. Therefore, regulating lipid metabolism and the expression of genes related to inflammation is a beneficial approach to alleviating obesity.

In recent years, vegetable oils have received much attention due to their health advantages and possible use as alternative drugs to treat various diseases. Epidemiological evidence indicates that *n*3 and *n*6 polyunsaturated fatty acids (PUFAs) and *n*9 monounsaturated fatty acids (MUFAs) can be used as an alternative to saturated fatty acids (SFAs) with additional health benefits [Bjermo *et al.*, 2012]. Tea seed oil (TSO) is an edible vegetable oil produced from pressed ripe tea (*Camellia oleifera*) seeds and has a fatty acid composition similar to olive oil [Tung *et al.*, 2019]. It is principally composed of oleic acid (78 to 86%), and the percentage of unsaturated fatty acids (USFAs) in TSO may be as high as 90%, which is the highest proportion of USFAs found in any edible oil to date [He *et al.*, 2011]. Sunflower oil (SFO) is a popular edible vegetable oil produced from crushed sunflower seeds (*Helianthus annuus*) that is mainly used for frying and has a high content of oleic and linoleic acids. Adeleke & Babalola [2020] demonstrated that SFO provides several health benefits, including blood pressure control, cholesterol reduction, diabetes management, and many other health benefits. Perilla (*Perilla frutescens*) is a Lamiaceae family annual plant commonly grown in most Asian nations, including South Korea, China, and Japan, and is recognized to confer many health benefits [Thomas *et al.*, 2020b]. Perilla seed oil (PSO) is a good source of *n*3 PUFAs, particularly α-linolenic acid, and has numerous health benefits such as anti-inflammatory, anti-oxidant, and anti-obesity effects [Asif, 2011]. Though many different oils are used in our daily lives, only a few studies have compared the health effects of oils with different fatty acid (FA) compositions.

Therefore, the aim of this study was to assess the effects of PSO, SFO, and TSO on mice with HFD-induced obesity. The biochemical and physiological indicators of obesity-associated disorders were examined to evaluate the impact of the three studied oils. Furthermore, quantitative real-time reverse-transcription PCR (qRT-PCR) was used to explore the molecular mechanisms of tested oils against obesity. The findings of this study could contribute to the exploration and development of safe and effective dietary supplements for obesity treatment.

MATERIALS AND METHODS

Materials and reagents

Tea (*Camellia oleifera*) seeds were obtained from Chongqing Amber Tea Oil Co., Ltd. (Youyang, Chongqing, China). Perilla (*Perilla frutescens*) seeds were purchased from Chongqing Qingzhong Road Perilla Planting Professional Cooperative (Pengshui, Chongqing, China). Sunflower (*Helianthus annuus*) seeds were obtained from the biggest local supermarkets (Beibei, Chongqing, China). The following PCR primers were purchased from Sangon Biotech (Shanghai) Co., Ltd. (Shanghai, China): glyceraldehyde 3-phosphate dehydrogenase (GAPDH), leptin, adiponectin, TNF-α, IL-1β, IL-6, PPAR-α, PPAR-γ, fatty acid synthase (FAS), carnitine palmitoyltransferase 1a (CPT1a), carnitine palmitoyltransferase 1b (CPT1b), and UCP1. All chemicals and reagents used were analytical grade and bought from commercial sources.

Seed oil extraction

The cold pressing method was used in the lab for crushing the seeds and extracting the oil using a screw press machine. The seeds were pressed at room temperature with a temperature of 50±10°C inside the press, and the resulting oil temperature was 39±1°C. Next, the oil was clarified by centrifugation at 5,000 rpm for 15 min (desktop refrigerated centrifuge 5810R, Eppendorf

Ltd., Hamburg, Germany) and filtered through fine cheesecloth. The oil samples were stored at 4°C in dark-colored glass vials until further use.

Fatty acid composition analysis

The FA profile was determined using gas chromatography after conversion to fatty acid methyl esters (FAMEs) [Huang *et al.*, 2015]. The FAMEs were obtained by mixing 100 mg of oil and 0.2 mL of 2 M methanolic potassium hydroxide solution with 2 mL of *n*-hexane at 50°C for 15 min. The gas chromatograph was a Shimadzu GC-2010 plus (Shimadzu, Tokyo, Japan) with a flame ionization detector and a DB-FFAP silica capillary column (30 m × 0.53 mm; film thickness 0.50 m) attached. As a carrier gas, nitrogen (flowing rate, 10 mL/min) was used, and the analysis was designed as follows: for 1 min, maintain a temperature of 50°C, the temperature was then raised at a rate of 15°C/min to 170°C and then at a rate of 2°C/min from 170 to 250°C; the temperature was maintained at 250°C for the next 10 min. The detector and injector temperatures were set at 270°C and 230°C, respectively.

TABLE 1. Compositions of normal and high-fat diets.

Ingredient	Normal diet		High-fat diet	
	g	kcal	g	kcal
Sucrose	350	1,400	70	280
Corn starch	315	1,260	0	0
Casein	200	800	200	800
L-Cystine	3	12	3	12
Cellulose	55	0	55	0
Maltodextrin	35	140	125	500
Soybean oil	30	270	30	270
Lard	15	135	240	2,160
Whole milk powder	1.5	13.5	5	45
NaCl	5	0	5	0
Calcium carbonate	5.5	0	5.5	0
Dicalcium phosphate	15	0	15	0
Potassium citrate	16.5	0	16.5	0
Mineral/ vitamin mix	10	40	10	40
Total	**1,056.5**	**4,070.5**	**780**	**4,107**
	g%	kcal%	g%	kcal%
Protein	19.81	20	27.16	20
Fat	4.54	10	36.79	60
Carbohydrate	69.34	70	27.42	20
Total		**100**		**100**
(kcal/g)	3.85		5.26	

The concentration of each FAME was calculated by the area under the peak using ChemStation software (Agilent Technologies Inc., Wilmington, DE, USA). The results were expressed as a percentage of the total FAs.

Animal experimental design

Fifty healthy male Kunming (KM) mice (7-weeks old, weight 30±2 g) were obtained from Jiangsu Xietong Pharmaceutical Bio-engineering Co., Ltd., Nanjing, China (quality certificate number: SCXK (XIANG) 2019-0004). All mice were housed in a specific pathogen-free (SPF) barrier laboratory of the College of Pharmaceutical Sciences, Southwest University (facility license number: SYXK (YU) 2020-0006) in a controlled laboratory environment (12 h light/dark cycle, 25±2°C temperature, and 55±5% relative humidity) with free access to food and water throughout the experiment.

After a week of acclimation, the mice were randomly divided into five groups (n=10 per group): a control group (ND) fed a standard diet (contains 10% fat, 3.85 kcal/g, Jiangsu Xietong Pharmaceutical Bio-engineering Co., Ltd., Nanjing, China); HFD (model group) fed a HFD (contains 60% fat, 5.26 kcal/g, Jiangsu Xietong Pharmaceutical Bio-engineering Co., Ltd., Nanjing, China); PSO group; SFO group; TSO group (PSO, SFO, and TSO groups were fed with the same HFD but supplemented with 2 g/kg body weight per day with PSO, SFO, and TSO, respectively) by oral gavage for 8 consecutive weeks. The composition of ND and HFD is shown in Table 1. Mice in the ND and HFD groups were administered the same dose of saline solution to create the same treatment stress (gavage procedure). All experimental animal procedures were approved and supervised by the Institutional Animal Care and Use Committee (IACUC) of Southwest University, Chongqing, China (IACUC No. approved: IACUC-20210225-06) following the legislation and regulations governing the care and use of laboratory animals. The experimental design is shown in Figure 1A.

Dosage information

The dietary oil doses were chosen based on previous studies from our group and others using different oils [Cheng *et al.*, 2014; Hirabara *et al.*, 2013; Huang *et al.*, 2021; Wang *et al.*, 2020]. They were calculated based on body surface area, as reported by Reagan-Shaw *et al.* [2008]. According to this suggestion, a daily oil intake of 2 g/kg body weight per day in mice is precisely equivalent to 162 mg/kg body weight per day in humans *(i.e.*, 9.72 g per day for a 60 kg individual), which is markedly less than the daily intake recommended by the Chinese Nutrition Society (25–30 g per day) [Wang *et al.*, 2016].

Measurement of body weight and food consumption

At the initiation of the experiment and at the end of each other week, body weight was measured. A sensitive electronic scale was used to weigh an empty scoop container. Then, the mice were placed inside the container and weighed individually. The weight of each mouse was calculated as the difference in weight between the empty container and the container with the mouse inside. Furthermore, throughout the experiment,

food weight was measured daily in a container of known weight and weighed using an electronic weighing balance. The food weight was obtained from the weight difference between the empty container and the container with the food inside. The food consumption was calculated by subtracting the remaining food weight from the served food weight.

Sample collection

After the end of the experiment, all mice were fasted overnight, and blood samples were taken by uprooting eyeballs after light narcotizing with ether (1.90%) for serum preparation. The serum was obtained after blood clotting by centrifugation at 3,500 rpm for 15 min at 4°C and then stored at −80°C until use. The mice were then executed by cervical dislocation, and the organs and adipose tissue, including the liver, kidney, lung, spleen, perirenal adipose tissue (PAT), and epididymal adipose tissue (EAT), were excised, weighed separately, and stored at −80°C until analysis.

Serum biochemical analysis

The biochemical analysis kits for insulin (cat. no. H203-1-2), glucose (cat. no. A154-1-1), total cholesterol (TC; cat. no. A111-1-1), triglycerides (TG; cat. no. A110-1-1), high-density lipoprotein cholesterol (HDL-C; cat. no. A112-1-1), low-density lipoprotein cholesterol (LDL-C; cat. no. A113-1-1), alanine aminotransferase (ALT; cat. no. C009-2-1), and aspartate aminotransferase (AST; cat. no. C010-2-1) were used to measure the serum concentrations of insulin, glucose, TC, TG, HDL-C, LDL-C, ALT, and AST, according to the manufacturer's instructions (Nanjing Jiancheng Biology Engineering Institute, Nanjing, China). The free fatty acid (FFA) levels were measured using the colorimetric method with a serum FFA kit (cat. no. E1001; Applygen Technologies Inc., Beijing, China). Moreover, very low-density lipoprotein cholesterol (vLDL-C) was calculated as TG/5 according to the Friedewald formula [Friedewald *et al.*, 1972], while the atherogenic index was calculated by the Equation (1):

$$\text{Atherogenic index} = (TC - HDL\text{-}C)/HDL\text{-}C \quad (1)$$

The homeostatic model assessment for insulin resistance (HOMA-IR) index and the homeostatic model assessment for insulin sensitivity (HOMA-IS) index were calculated as previously reported [Qu *et al.*, 2019a].

ELISA analysis

The enzyme-linked immunosorbent assay (ELISA) kits for leptin (cat. no. ml-1015883), adiponectin (cat. no. ml-42683), and pro-inflammatory cytokines, including TNF-α (cat. no. ml-1015901), IL-1β (cat. no. ml-67771), and IL-6 (cat. no. ml-67768), were used to determine the levels of leptin, adiponectin, TNF-α, IL-1β, and IL-6 in EAT, following the manufacturer's instructions (Shanghai ML-BIO Biotechnology Co., Ltd., Shanghai, China).

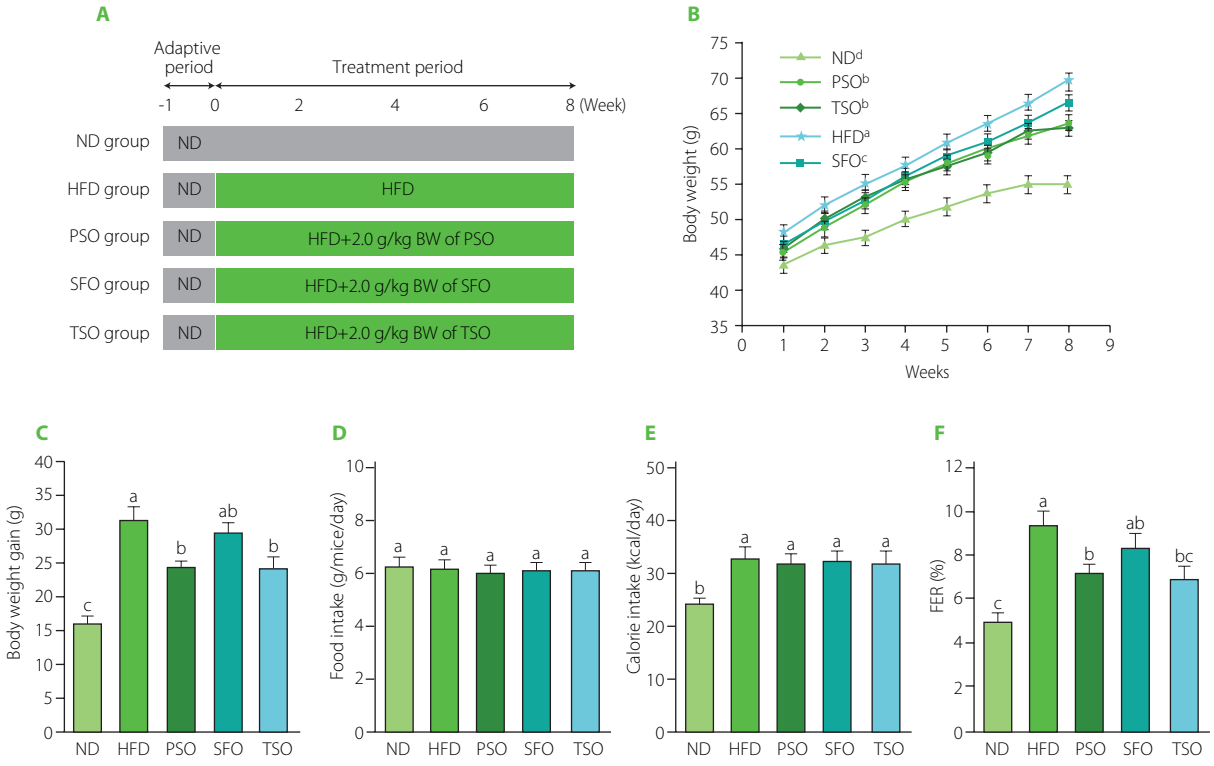

FIGURE 1. Perilla seed oil (PSO), sunflower oil (SFO), and tea seed oil (TSO) supplementation reduced body weight gain but not food intake in HFD-induced obese mice. (**A**) Scheme of the study design; (**B**) Body weight growth of mice consuming the specified diets for the 8 weeks; (**C**) Body weight gain of mice at the end of the study period; (**D**) Food intake of mice during the study period; (**E**) Calorie intake of mice during the study period; (**F**) Food efficiency ratio (FER) calculated as body weight gain (g/day)/food intake (g/day)×100 of mice after 8 weeks of food intervention. ND, mice fed a normal diet; HFD, mice fed a high-fat diet; PSO, SFO, and TSO, mice fed a high-fat diet supplemented with PSO, SFO, and TSO at 2 g/kg body weight per day, respectively. Data are presented as mean ± standard deviation (n=8). Means with different letters (a–c) were considered significantly different at $p<0.05$, according to Tukey's test.

RNA extraction from tissues and quantification by real-time qRT-PCR

To measure the differences in relative mRNA expression, we used qRT-PCR. The total RNA was extracted from the frozen EAT using TRIzol reagent (CoWin Biosciences (CWBIO), MA, USA) according to the manufacturer's protocols, and the quality of total RNA was evaluated using a Nano-Drop One spectrophotometer (Thermo Scientific, Wilmington, DE, USA). Then, the cDNA was reverse transcribed from the total RNA using the HiFiScript gDNA Removal cDNA Synthesis Kit (Jiangsu Cowin Biotech Co., Ltd., Changping, Beijing, China). qRT-PCR was performed using SYBR PRIME qPCR Kits (Fast HS) on a CFX thermocycler system (Bio-Rad, Hercules, CA, USA). PCR amplification was performed as follows: 95°C for 5 min and 40 cycles of amplification at 94°C for 20s, 94°C for 10s, 50–60°C for 10s, and 72°C for 10s. Relative quantification was calculated using the $2^{-\Delta\Delta CT}$ method, and GAPDH, a housekeeping gene, was utilized to normalize the level of the target gene expression. The primer sequences used in this study are shown in Table 2.

Histological analysis

The liver and EAT, freshly isolated from each of the five mice groups, were quickly fixed in 4% paraformaldehyde for 24 h at room temperature. The tissues were subsequently coated in paraffin and sliced into 5 µm thick sections. After staining slices with hematoxylin and eosin (H&E), histopathological alterations were examined using a light microscope (Olympus, Tokyo, Japan). The EAT number and size were measured by the software Image J (NIH Image, Bethesda, Rockville, MD, USA).

Statistical analysis

All data were obtained from at least three replications and presented as a means ± standard deviation (SD). Statistical analysis was performed using Statistix Analytical Software version 9.0 (Analytical Software, Tallahassee, FL, USA). The variances among the collected data were assessed by one-way ANOVA using the Tukey's test, and differences at $p<0.05$ were considered statistically significant. The figures were designed by OriginPro 2021 software (OriginLab, Co., Northampton, MA, USA).

RESULTS AND DISCUSSION

Fatty acid composition

The fatty acid (FA) composition of the seed oils tested is shown in Table 3. Eleven FAs were detected in cold-pressed PSO, SFO, and TSO, of which six were SFAs, three were MUFAs, and the last two were PUFAs. Among six SFAs (myristic, palmitic, stearic, arachidic, behenic, and lignoceric acids), two were dominant: palmitic acid, which ranged from 5.02% in SFO to 8.64% in TSO, and stearic acid, which varied from 2.04% in TSO to 5.52% in SFO. Although there were minor variances in SFA content among the oils studied, SFO had the highest total SFA content (12.01%). Three MUFAs (palmitoleic, oleic, and gadoleic acids) were identified in all samples, but only one was dominant: oleic acid, which ranged from 15.62% in PSO to 78.33% in TSO. TSO had the highest MUFA content, which was substantially different from the other oils ($p<0.05$).

Among PUFAs, C18:2*n*6 and C18:3*n*3 contents varied from 8.50% and 0.11% to 50.66% and 61.58%, respectively. Linoleic acid was the most abundant FA in SFO, followed by PSO and TSO, while only PSO had a high content of α-linolenic acid. There were significant differences ($p<0.05$) in PUFA content among all tested oil samples, with PSO (74.24%) having the greatest content, followed by SFO (51.10%) and TSO (9.05%). The SFA:USFA ratio was 1:7, 1:8, and 1:8 in SFO, PSO, and TSO, respectively, suggesting all three examined oils have a low ratio of SFA:USFA. Interestingly, several previous studies have established that the SFA:USFA ratio is a significant health predictor, and diets high in MUFAs with a low SFA to USFA ratio may alleviate obesity [Liao *et al.*, 2010; Yang *et al.*, 2017].

TABLE 2. The primer sequences used for qPCR.

Gene name	Forward primer (5'– 3')	Reverse primer (5'–3')
GAPDH	GCTGAGTATGTCGTGGAGT	GTTCACACCCATCACAAAC
TNF-α	GTCTACTGAACTTCGGGGTGAT	GGCTACAGGCTTGTCACTCG
IL-1β	CCAACAAGTGATATTCTCCATGAG	ACTCTGCAGACTCAAACTCCA
IL-6	CTCTGCAAGAGACTTCCATCC	GAATTGCCATTGCACAACTC
Leptin	GAGACCCCTGTGTCGGTTC	CTGCGTGTGTGAAATGTCATTG
Adiponectin	TGTTCCTCTTAATCCTGCCCA	CCA ACCTGCACAAGTTCCCTT
PPAR-α	GGATGTCACACAATGCAATTCGCT	CAGCGAGTAGCGCATAGTCA
PPAR-γ	AGGCCGAGAAGGAGAAGCTGTTG	TGGCCACCTCTTTGCTCTGCTC
FAS	GCTTGCTGGCTCACAGTTAAG	AGGTTGGTGTACCCCCATTC
CPT1a	GGACTCCGCTCGCTCATT	GAGATCGATGCCATCAGGGG
CPT1b	CATGTATCGCCGCAAACTGG	CCTGGGATGCGTGTAGTGTT
UCP1	GTGAACCCGACAACTTCCGAA	TGCCAGGCAAGCTGAAACTC

TABLE 3. Fatty acid composition of sunflower, perilla, and tea seed oils (% total fatty acids).

FAs	SFO	PSO	TSO
Myristic acid (C14:0)	0.074±0.002^{a}	0.024±0.004^{b}	0.034±0.002^{b}
Palmitic acid (C16:0)	5.02±0.14^{c}	6.68±0.28^{b}	8.64±0.19^{a}
Palmitoleic acid (C16:1*n*7)	0.056±0.006^{c}	0.201±0.006^{a}	0.097±0.003^{b}
Stearic acid (C18:0)	5.52±0.16^{a}	2.45±0.25^{b}	2.04±0.05^{b}
Oleic acid (C18:1*n*9)	36.48±1.31^{b}	15.62±0.93^{c}	78.33±1.28^{a}
Linoleic acid (C18:2*n*6)	50.66±1.08^{a}	12.66±0.28^{b}	8.50±0.22^{c}
α-Linolenic acid (C18:3*n*3)	0.11±0.02^{b}	61.58±0.33^{a}	0.55±0.15^{b}
Arachidic acid (C20:0)	0.33±0.01^{a}	0.16±0.01^{b}	0.04±0.01^{c}
Gadoleic acid (C20:1*n*11)	0.13±0.01^{b}	0.09±0.01^{b}	0.49±0.06^{a}
Behenic acid (C22:0)	0.82±0.09^{a}	0.03±0.01^{b}	0.02±0.01^{b}
Lignoceric acid (C24:0)	0.24±0.02^{a}	0.03±0.02^{b}	0.03±0.01^{b}
SFAs	12.01±0.12^{a}	9.37±0.37^{c}	10.81±0.24^{bc}
MUFAs	36.66±1.31^{b}	15.91±0.93^{c}	78.91±1.34^{a}
PUFAs	51.10±1.10^{b}	74.24±0.36^{a}	9.05±0.36^{c}
USFAs	87.76±0.66^{b}	90.15±0.68^{a}	87.96±0.98^{b}
SFAs:USFAs	1:7	1:8	1:8

Data are presented as mean ± standard deviation (n=3). Different letters in the same row indicate significant differences at p<0.05, according to Tukey's test. FA, fatty acids; SFO, sunflower oil; PSO, perilla seed oil; TSO, tea seed oil; SFAs, saturated fatty acids; MUFAs, monounsaturated fatty acids; PUFAs, polyunsaturated fatty acids; USFAs, unsaturated fatty acids.

Effects of PSO, SFO, and TSO supplementation on body weight and food intake in obese mice

Body weight is considered one of the most axiomatic indicators to judge obesity cases in mice. Here, during the experiment, the body weight growth of the HFD group increased faster than in the ND, PSO, SFO, and TSO groups (Figure 1B). The PSO and TSO groups had lower body weights than those in the HFD group after 8 weeks of oil supplementation, but there were no significant differences (p≥0.05) in body weight gain among the SFO and HFD groups, indicating that PSO and TSO supplementation could effectively prevent the body weight gain induced by the HFD (Figure 1C). In contrast, there were no significant differences (p≥0.05) between all the dietary oil and HFD groups in terms of food consumption (Figure 1D) and calorie intake (Figure 1E). Additionally, the HFD group's food efficiency ratio (FER) was higher than that of the ND group (p<0.05), while the FER was significantly decreased after 8 weeks of supplementation with dietary oils, particularly in the PSO and TSO groups (Figure 1F).

Moreover, HFD feeding increased the relative weight of the liver, while dietary oil supplementation reversed this trend (Table 4). However, there were no significant differences (p≥0.05) in the relative weight of the kidney, lung, and spleen among the five mice groups. In contrast, compared to the HFD group, PSO, SFO, and TSO administration significantly reduced the proportion of EAT and PAT relative to the body weight (p<0.05).

To sum up, dietary oil supplementation reduced body and organ weight gain but had no impact on food and calorie intake compared to the HFD group. In agreement with our results, α-linolenic acid-rich kiwifruit seed oil administered over 12 weeks decreased body weight gain without affecting food intake [Qu *et al.*, 2019b]. Also, black raspberry seed oil, which is high in α-linolenic acid, reduced body weight but had no impact on food intake when administered for 10 weeks in db/db mice [Lee *et al.*, 2016]. Cui *et al.* [2017] revealed that fish oil ingestion for 12 weeks caused body weight reduction in HFD-induced obese mice. In our study, there were no significant differences in food consumption among the five groups; therefore, the effect of dietary oil supplementation on body weight was not associated with the decrease in food intake.

Effects of PSO, SFO, and TSO supplementation on serum lipid profile levels

Obesity is strongly linked to changes in serum biochemistry. As a result, we used commercial kits to examine the effect of oil supplementation on serum lipid profile levels. As shown in Figure 2A, TG concentrations in the serum of mice of ND, HFD, PSO, SFO, and TSO groups were 1.60, 2.59, 2.13, 2.21, and 2.06 mmol/L, respectively, with the HFD group having a substantially higher TG concentration than the other groups (p<0.05). After 8 weeks of oils supplementation, the levels of TC were significantly lower (p<0.05) in the PSO, SFO, and TSO groups, by 25.70%, 15.36%, and 22.30%, respectively, compared with the HFD group (Figure 2B). However, the results of HDL-C showed no significant differences (p≥0.05) in the HDL-C levels among the HFD and all other treatment groups, with

TABLE 4. The relative tissue weights in mice of ND, HFD, PSO, SFO, and TSO groups (g/100 g body weight).

Item	ND	HFD	PSO	SFO	TSO
Liver	3.32±0.19^{c}	4.43±0.27^{a}	3.69±0.21^{b}	3.75±0.29^{b}	3.78±0.23^{b}
Kidney	1.17±0.20^{a}	1.15±0.09^{a}	1.17±0.16^{a}	1.08±0.18^{a}	1.11±0.14^{a}
Lung	0.48±0.06^{a}	0.43±0.08^{a}	0.44±0.05^{a}	0.43±0.05^{a}	0.48±0.09^{a}
Spleen	0.22±0.06^{a}	0.23±0.11^{a}	0.24±0.06^{a}	0.24±0.04^{a}	0.26±0.09^{a}
Epididymal adipose tissue	2.47±0.32^{c}	5.21±0.79^{a}	4.12±0.69^{b}	4.32±0.56^{b}	4.21±0.48^{b}
Perirenal adipose tissue	0.47±0.09^{c}	1.01±0.14^{a}	0.60±0.07^{bc}	0.79±0.07^{b}	0.61±0.10^{bc}

Data are presented as mean ± standard deviation (n=8 for each group). Different letters in the same row indicate significant differences at p<0.05, according to Tukey's test. ND, mice fed a normal diet; HFD, mice fed a high-fat diet; PSO, SFO, and TSO, mice fed a high-fat diet supplemented with PSO, SFO, and TSO at 2 g/kg body weight per day, respectively.

the highest levels being observed in the ND group (Figure 2C). Notably, the high HDL-C level in the HFD group may represent an adaptive response to the increased demand for lipid transport [Wolf & Phil, 1996]. Furthermore, compared with the HFD group, the serum LDL-C levels were significantly reduced by 44.62%, 32.31%, and 51.79% in the PSO, SFO, and TSO groups, respectively (Figure 2D). As shown in Figure 2E, the dietary oil intervention reduced serum vLDL-C levels in TSO group; however, there were no significant differences between the HFD, PSO, and SFO groups. Moreover, compared to the HFD group, the PSO, SFO, and TSO groups exhibited a reduction in atherogenic index values of 42.5%, 15%, and 35.4%, respectively (Figure 2F).

Our study revealed that long-term intake of PSO, SFO, and TSO reduced serum lipid profile levels and atherogenic index values, which are risk factors for CVD. These findings are consistent with the report by Lian *et al.* [2020] who showed that replacing SFAs with USFAs in the Western diet improved the blood lipid profile, increased USFA levels in plasma, and reduced the risk of atherosclerosis in mice. Consumption of fish oil caused significantly lower body weight and blood lipid concentrations in HFD-induced obese mice [Pradhan

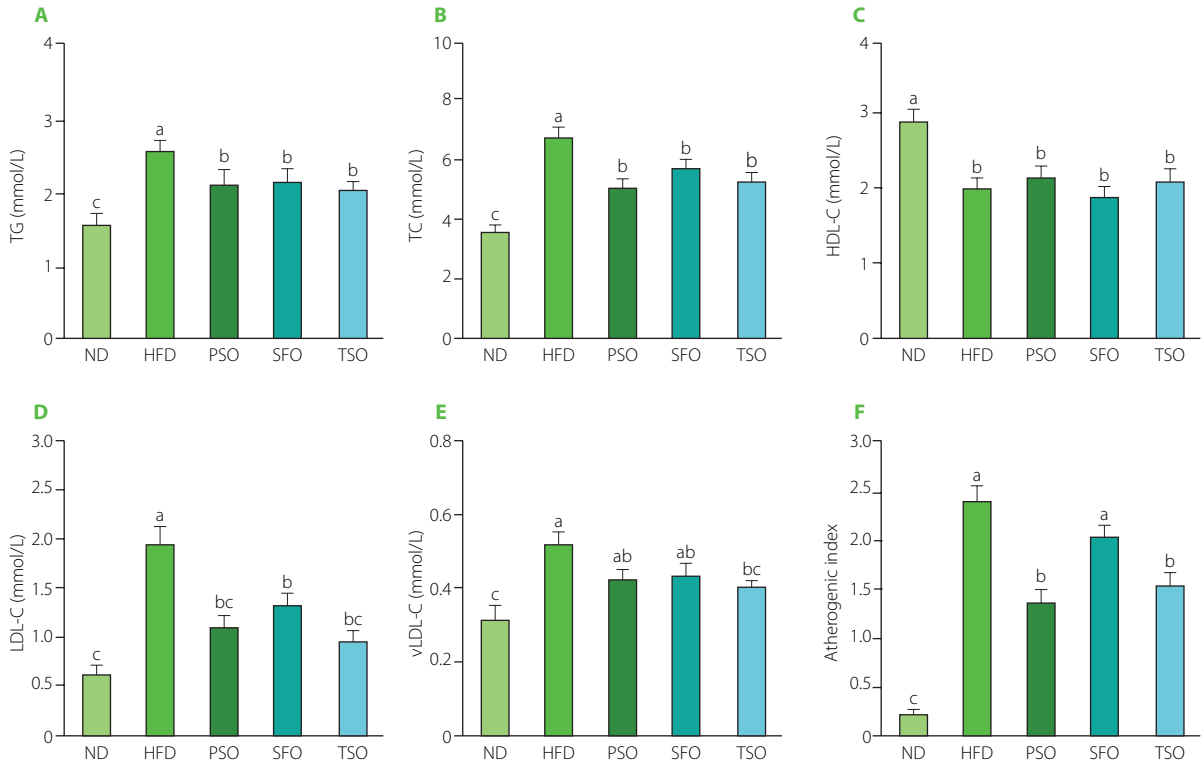

FIGURE 2. Perilla seed oil (PSO), sunflower oil (SFO), and tea seed oil (TSO) supplementation reduced the serum lipid levels and atherogenic index in HFD--induced obese mice. (**A**) Triglycerides, TG; (**B**) Total cholesterol, TC; (**C**) High-density lipoprotein cholesterol, HDL-C; (**D**) Low-density lipoprotein cholesterol, LDL-C; (**E**) Very low-density lipoprotein cholesterol, vLDL-C; (**F**) Atherogenic index. ND, mice fed a normal diet; HFD, mice fed a high-fat diet; PSO, SFO, and TSO, mice fed a high-fat diet supplemented with PSO, SFO, and TSO at 2 g/kg body weight per day, respectively. Data are presented as mean ± standard deviation (n=8). Means with different letters (a–c) were considered significantly different at p<0.05, according to Tukey's test.

et al., 2020]. In a similar study, oral treatment of camellia oil considerably reduced fat deposits, serum TC, TG, LDL-C, and the atherogenic index, as well as significantly elevated HDL-C concentration in HFD-induced obese mice [Huang *et al.*, 2021]. Our findings showed that PSO, SFO, and TSO consumption could remarkably improve lipid metabolism, alleviate dyslipidemia, and reduce the risk of atherosclerosis development in HFD-fed mice.

Effects of PSO, SFO, and TSO supplementation on fat tissue histopathology

The EAT, a metabolically active and anatomically distinct abdominal fat depot, is commonly employed to investigate adipose tissue in rodent studies [Wang *et al.*, 2018]. As shown in Figure 3A, histopathology examination (H&E staining) of EAT revealed that HFD feeding encouraged adipocyte hypertrophy and that the HFD group had lower adipocyte numbers and larger adipose cell sizes than the ND group (Figures 3B and C). On the contrary, oral supplementation with dietary oils alleviated these effects, where the adipocytes of EAT in all treatment groups were small and closely organized with morphological integrity, particularly in PSO and TSO, suggesting that the studied oils have the potential to attenuate fat accumulation in mice caused by a HFD. Our results agreed with the previous studies, which showed that perilla oil supplementation reduced the adipocyte size and ameliorated the percentage of fat tissue in diabetic KK-Ay mice fed with HFD [Wang *et al.*, 2018]. Another study indicated that consuming kiwifruit seed oil for 12 weeks reduced fat tissue weight compared with the HFD group, and this finding was corroborated by fat tissue histological examination in obese mice [Qu *et al.*, 2019b]. These results indicate that supplementation with PSO, SFO, and TSO could reduce fat accumulation in adipose tissue.

Effects of PSO, SFO, and TSO supplementation on liver function indicators and hepatic steatosis in obese mice

The liver is widely known for its role in detoxification and metabolic regulation. Therefore, it is critical to preserve the normal structure of the liver. To investigate the influence of oil supplementation on liver function, we measured the activity of serum AST and ALT, which are liver function representative markers that reflect the degree of liver injury [Chang *et al.*, 2019]. As shown in Figures 4A and B, the ALT and AST levels were the lowest in the ND group mice. On the contrary, the HFD group mice had the highest levels, indicating liver injury. Also, ALT and AST levels were significantly reduced ($p<0.05$) in all dietary oil groups except the SFO group, where there were no significant differences in ALT levels compared to the HFD group. Furthermore, the effects of dietary oil supplementation on HFD-induced hepatic steatosis in mice by histological examination were investigated. H&E staining showed that the HFD-fed mice had more serious microvesicular steatosis and lipid droplet accumulation in hepatocytes than the ND-fed mice. At the same time, supplementation with dietary oils alleviated these adverse effects (Figure 4C), suggesting that the examined oils have a robust protective effect against HFD-induced liver injury. Our findings are consistent with prior observations in other rodent models that USFA oils have a defensive impact in HFD-induced obese mice [Su *et al.*, 2016]. Our results allow us to conclude that PSO, SFO, and TSO supplementation could suppress HFD-induced obesity and regulate lipid metabolism by enhancing liver function and its structural integrity.

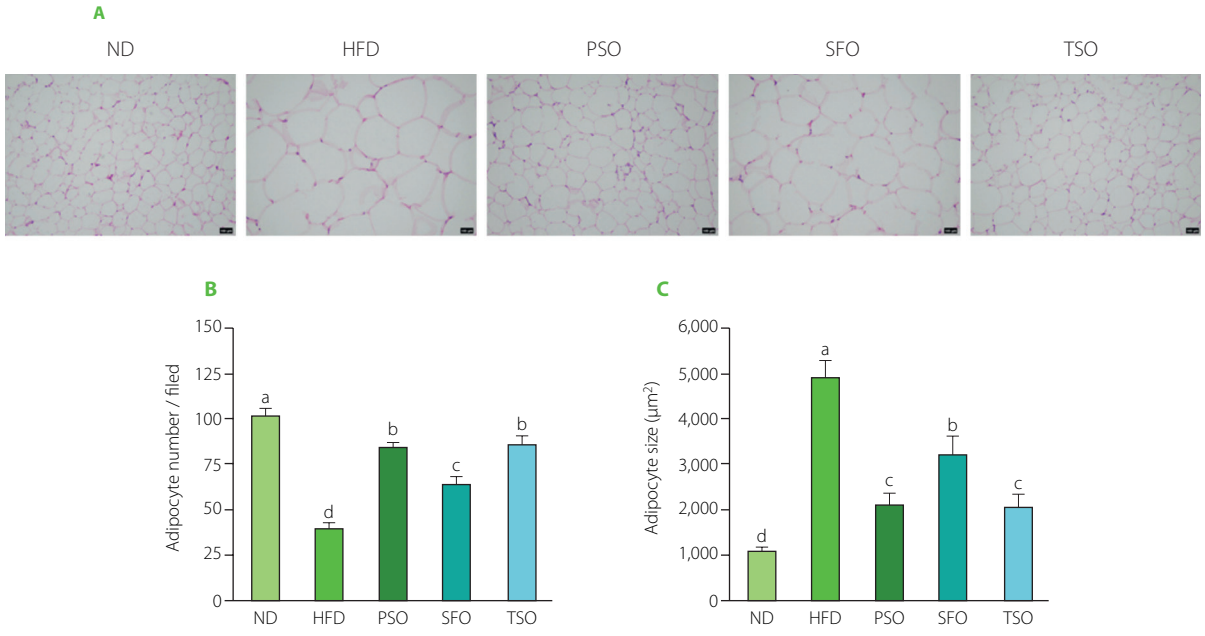

FIGURE 3. Perilla seed oil (PSO), sunflower oil (SFO), and tea seed oil (TSO) supplementation reduced adipocyte hypertrophy and increased adipocyte numbers in the histopathological examination of epididymal adipose tissue. (**A**) Histological analysis of epididymal adipose tissue (hematoxylin and eosin staining, ×100 magnification); (**B**) Adipocyte numbers; (**C**) Adipocyte size. ND, mice fed a normal diet; HFD, mice fed a high-fat diet; PSO, SFO, and TSO, mice fed a high-fat diet supplemented with PSO, SFO, and TSO at 2 g/kg body weight per day, respectively. Data are presented as mean ± standard deviation (n=6–8). Means with different letters (a–d) were considered significantly different at $p<0.05$, according to Tukey's test.

Effects of PSO, SFO, and TSO supplementation on serum glucose, insulin, and FFA levels

Next, commercial kits were used to investigate the effects of dietary oil supplementation on serum concentrations of insulin, glucose, and FFA in HFD-induced obese mice. Consumption of HFD generated a substantial rise in blood glucose concentration (10.57 mmol/L), which was much higher than in the ND group (5.82 mmol/L, $p<0.05$). In contrast, compared to the HFD group, supplementation with dietary oils markedly reduced the fasting serum glucose concentrations by 22.99%, 14.66%, and 17.88% in the PSO, SFO, and TSO, respectively (Figure 5A). In addition, the serum insulin level was remarkably higher in the HFD group compared to the ND group. After 8 weeks of dietary oil intervention, there were significant differences in insulin concentrations across all treatment groups except the SFO group ($p<0.05$, Figure 5B). Insulin resistance is characterized as an organ's inability to respond to insulin. The HOMA-IR and HOMA-IS indices are common indicators used to estimate insulin resistance and sensitivity in diabetic patients. In our study, dietary oil supplementation for 8 weeks notably improved the HOMA-IR index; however, there were no significant differences in the HOMA-IS index among the SFO, TSO, and HFD groups (Figures 5C and D). Previous studies have found that supplementation with kiwifruit seed oil, which is also high in USFAs, reduced insulin and glucose levels in the blood and improved the indicator of insulin resistance in mice with HFD-induced obesity [Qu *et al.*, 2019a, b].

The liver is an important organ in lipid metabolic pathways because it takes up FFAs from the blood as well as produces, transports, and stores lipid metabolites. It is established that obesity, insulin resistance, type 2 diabetes, dyslipidemia, CVD, and atherosclerosis have all been associated with high levels of FFAs [Henderson, 2021]. Furthermore, a potential association between inflammation and serum FFAs has been suggested in both animal and human studies. A high level of FFAs in the bloodstream is closely associated with the onset of inflammation, noted by the increase in the secretion of IL-6 and TNF-α in adipose tissues [Neeland *et al.*, 2018]. Additionally, inflammatory cytokines promote lipolysis and raise FFA levels, contributing to endothelial dysfunction and increasing the risk of atherosclerosis [Ormseth *et al.*, 2013]. As shown in Figure 5E, the serum FFA level in the HFD group (0.71 mmol/L) increased by 255% compared to the level in the ND group (0.20 mmol/L). After 8 weeks of dietary oil supplementation, the FFA levels in the serum were significantly reduced by 42%, 46%, and 28% in the PSO, SFO, and TSO groups, respectively, but still higher than those in the ND group. Our findings indicate that consumption of PSO, SFO, and TS could alleviate hyperglycemia, insulin resistance, atherosclerosis, and inflammation by preventing lipolysis and reducing serum FFA levels in HFD-fed mice in a FA composition-dependent way.

Effects of PSO, SFO, and TSO supplementation on secretion and mRNA expression of inflammatory cytokines in EAT

Generally, adipose tissue produces a variety of factors with biological activity, including inflammatory hormones (leptin and adiponectin), pro-inflammatory cytokines (TNF-α, IL-1β, and IL-6), and anti-inflammatory cytokines (IL-10) [Hummasti & Hotamisligil, 2010]. Furthermore, in obese individuals, adipocyte hypertrophy promotes an increase in the release of inflammatory cytokines, which induces adipose tissue metabolic inflammation and progressively leads to chronic low-grade inflammation

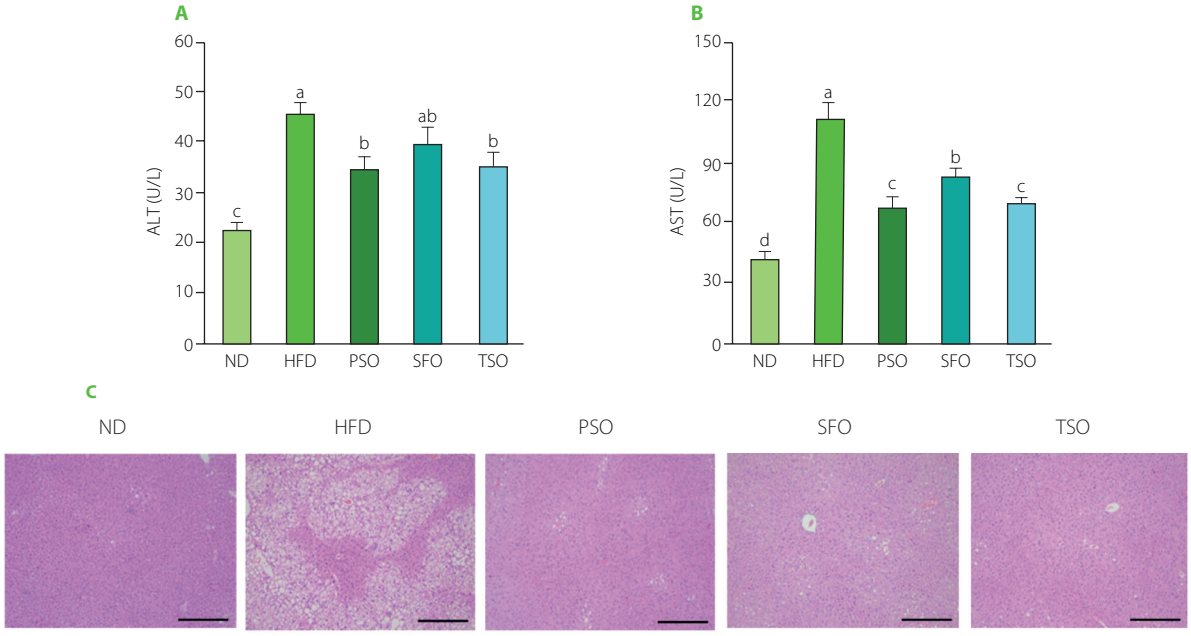

FIGURE 4. Perilla seed oil (PSO), sunflower oil (SFO), and tea seed oil (TSO) supplementation improved liver function indicators and alleviated liver steatosis. (**A**) Alanine aminotransferase (ALT) activity; (**B**) Aspartate aminotransferase (AST) activity; (**C**) Histological analysis of liver tissue (hematoxylin and eosin staining, ×100 magnification). ND, mice fed a normal diet; HFD, mice fed a high-fat diet; PSO, SFO, and TSO, mice fed a high-fat diet supplemented with PSO, SFO, and TSO at 2 g/kg body weight per day, respectively. Data are presented as mean ± standard deviation (n=6–8). Means with different letters (a–d) were considered significantly different at p<0.05, according to Tukey's test.

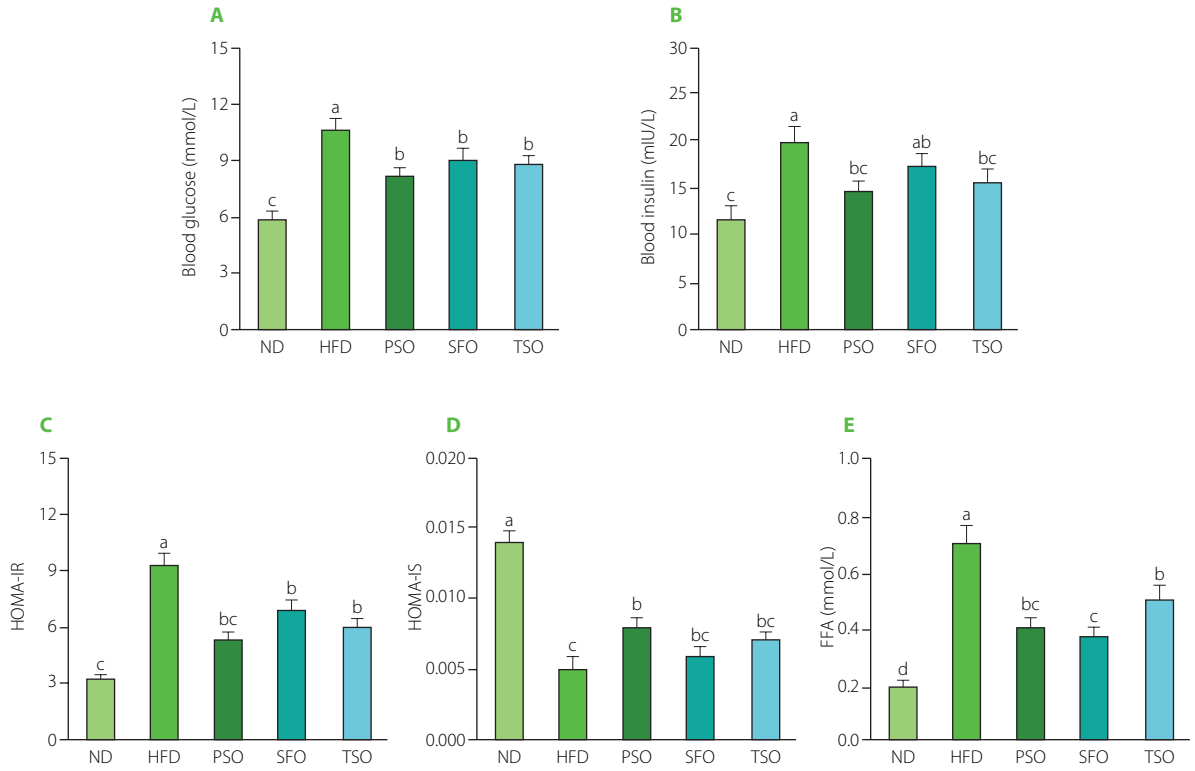

FIGURE 5. Perilla seed oil (PSO), sunflower oil (SFO), and tea seed oil (TSO) supplementation alleviated diet-induced hyperglycemia, improved insulin resistance, and reduced serum free fatty acid (FFA) levels. (**A**) Fasting glucose level; (**B**) Insulin level; (**C**) Insulin resistance (HOMA-IR) index; (**D**) Insulin sensitivity (HOMA-IS) index; (**E**) FFA level. ND, mice fed a normal diet; HFD, mice fed a high-fat diet; PSO, SFO, and TSO, mice fed a high-fat diet supplemented with PSO, SFO, and TSO at 2 g/kg body weight per day, respectively. Data are presented as mean ± standard deviation (n=8). Means with different letters (a–d) were considered significantly different at p<0.05, according to Tukey's test.

[Hummasti & Hotamisligil, 2010; Oh & Olefsky, 2012]. Therefore, obesity is commonly related to chronic low-grade inflammation. Thus, secretion and mRNA expression levels of inflammation-related genes in the EAT were measured to clarify whether consuming vegetable oils can alleviate the inflammation caused by a HFD.

It is well known that leptin, an adipose-derived hormone, regulates body weight by affecting food consumption and energy expenditure [Williams *et al.*, 2009], and its levels increase in patients with obesity and decrease in individuals with weight loss. Obesity stimulates the secretion and production of pro-inflammatory cytokines such as TNF-α, IL-6, and IL-1β in adipose tissue [Trayhurn & Wood, 2004]. TNF-α has been linked to the development of obesity, insulin resistance, and type 2 diabetes [Golshani *et al.*, 2015]. Furthermore, IL-6 has a potent pro-inflammatory effect, which can increase TNF-α levels [Park *et al.*, 2005]. On the other hand, adiponectin also modulates lipid and glucose metabolism, protects against chronic inflammation, and improves insulin sensitivity [Pajvani *et al.*, 2004]. Its lower levels are associated with obesity and related diseases such as type 2 diabetes, non-alcoholic fatty liver disease, and insulin resistance [Ebrahimi *et al.*, 2022]. As shown in Figure 6A, HFD feeding led to a 3.45-fold rise in EAT levels of leptin in the HFD group compared with the ND group (p<0.05). At the same time, dietary oil supplementation lowered leptin levels by 40.31%, 37.19%, and 35.54% in the PSO, SFO, and TSO groups, respectively, compared to the HFD group. Moreover, EAT levels of pro-inflammatory cytokines (TNF-α, IL-6, and IL-1β) were considerably higher in the HFD group when compared to the ND group; however, following 8 weeks of dietary oil supplementation, the concentrations decreased in the PSO, SFO, and TSO groups (Figures 6B, C, and D). On the contrary, supplementation with dietary oils significantly elevated the EAT levels of anti-inflammatory adipokine adiponectin by 20.20%, 11.74%, and 10.64% in the PSO, SFO, and TSO groups, respectively, when compared with the HFD group (p<0.05, Figure 6E). Furthermore, the same trends were approximately found in mRNA expression levels (Figure 6F). Our results were consistent with the previous studies, which showed that the HFD supplemented with fish oil lowered leptin levels while increasing adiponectin levels in adipose tissue [Sundaram *et al.*, 2016]. Thomas *et al.* [2020a] found that perilla oil administration reduced pro-inflammatory cytokines in serum and colon, and the effects were comparable to those obtained from fish oil in HFD-induced inflammation in mice. Wu *et al.* [2020] observed that camellia oil intake significantly reduced pro-inflammatory cytokine levels (TNF-α, IL-1β, and IL-6) in rats with acetic acid-induced colitis. Another study also demonstrated that kiwifruit seed oil supplementation decreased the mRNA expression of pro-inflammatory cytokines (TNF-α, IL-6, and IL-1β) in a dose-dependent way, compared to the HFD group [Qu *et al.*, 2019b]. Furthermore, fish oil addition to a HFD significantly raised adiponectin levels and lowered

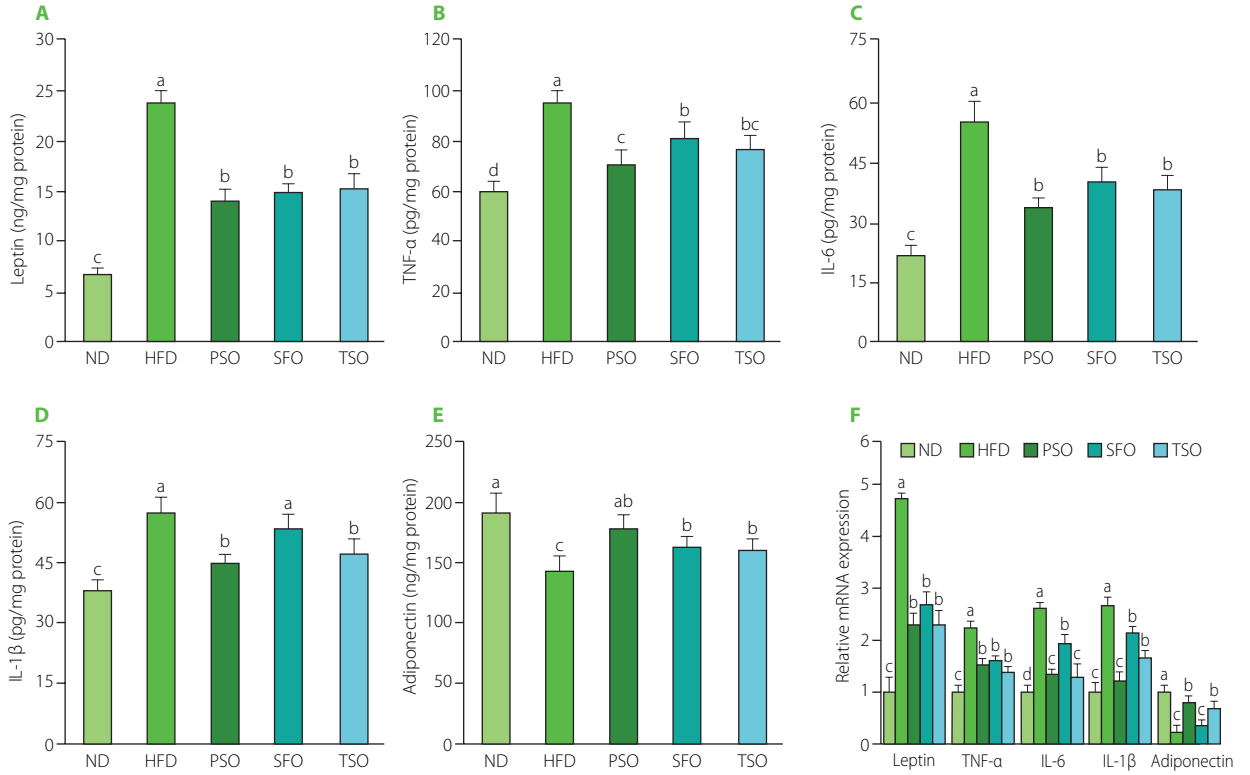

FIGURE 6. Effects of perilla seed oil (PSO), sunflower oil (SFO), and tea seed oil (TSO) supplementation on the secretion and mRNA expression levels of inflammatory cytokines of epididymal adipose tissue in HFD-induced obese mice. (**A**) Leptin; (**B**) tumor necrosis factor-alpha, (IL-6), and TNF-α; (**C**) interleukin-6, IL-6; (**D**) interleukin-1beta, IL-1β; (**E**) Adiponectin; (**F**) Relative mRNA expression. ND, mice fed a normal diet; HFD, mice fed a high-fat diet; PSO, SFO, and TSO, mice fed a high-fat diet supplemented with PSO, SFO, and TSO at 2 g/kg body weight per day, respectively. Data are presented as mean ± standard deviation (n=8). Means with different letters (a–d) were considered significantly different at p<0.05, according to Tukey's test.

leptin levels in serum and EAT mRNA expression, according to a study published by Monk *et al.* [2019]. Our findings show that USFA in the examined oils could relieve low-grade adipose tissue inflammation in obese mice.

Effects of PSO, SFO, and TSO supplementation on mRNA expressions of lipid metabolism-related genes of EAT in mice

Next, the effects of oils supplementation on specific essential lipid metabolism-related genes were also examined to clarify further the mechanism and possible effect of vegetable oils on lipid metabolism dysfunction. Several regulatory factors, including the nuclear receptor family of peroxisome proliferator-activated receptors (PPARs), have been found to play a vital regulatory role in energy homeostasis and metabolic functions [Wagner & Wagner, 2020]. Numerous PPAR subtypes have been identified, among which are PPAR-α and PPAR-γ. PPAR-α controls the expression of several lipid metabolism-related genes and is a critical target for treating lipid metabolism disorders [Kersten & Stienstra, 2017]. PPAR-γ regulates the primary genes involved in the production and lipid metabolism, as well as the transport and accumulation of FAs [Janani & Ranjitha Kumari, 2015]. In addition, FAS, the major adipogenesis enzyme involved in lipid synthesis, is a sign of the obesity therapeutic impact [Noratto *et al.*, 2016]. As shown in Figure 7A, the mRNA expression level of PPAR-α was up-regulated in the three oil-supplemented groups compared to the HFD group (p<0.05), and there were no significant differences (p≥0.05) among the PSO and TSO groups. Compared to the ND group, the expression levels of PPAR-γ (Figure 7B) and FAS (Figure 7C) were significantly increased, but after 8 weeks of dietary oils intervention, the expression levels of those genes were substantially lower than those in the HFD group (p<0.05). Supplementation with dietary oils significantly reduced FAS expression, which indicated the downregulation of FA synthesis. Importantly, dietary oils also suppressed lipid accumulation by inactivating the expression of PPAR-γ [Jiang *et al.*, 2014; Zhang *et al.*, 2020]. Altogether, these findings indicate that PSO, SFO, and TSO could exert anti-obesity effects by downregulating lipid synthesis and accumulation.

Moreover, we also measured mRNA expression levels of both CPT1a and CPT1b, which are enzymes controlling the rate in the pathway of FA β-oxidation [Kliewer *et al.*, 2001]. Consumption of HFD resulted in downregulated mRNA expression levels of both CPT1a and CPT1b compared to the ND group, while the levels were significantly increased in all dietary oil groups (p<0.05, Figures 7D and E). Next, we measured the mRNA expression levels of thermogenesis-linked genes, such as UCP1, which is considered a morphological and functional sign of thermogenic adipocyte production [Zhang *et al.*, 2016]. As shown in Figure 6F, the expression levels of the UCP1 gene were significantly up-regulated after 8 weeks of dietary oil intake in both the PSO and TSO groups compared to the levels in the HFD group, but there were no significant differences between the SFO

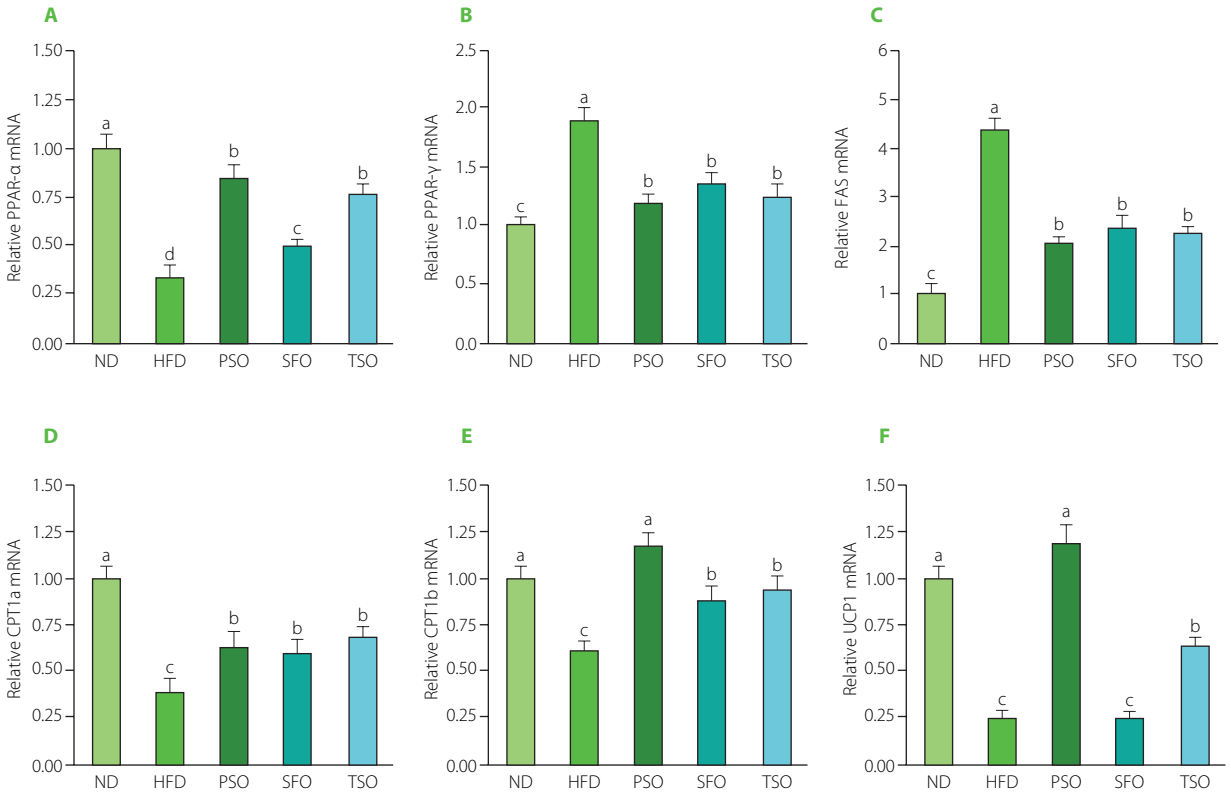

FIGURE 7. Effects of perilla seed oil (PSO), sunflower oil (SFO), and tea seed oil (TSO) supplementation on the mRNA expression levels of lipid metabolism-related genes in epididymal adipose tissue. (**A**) peroxisome proliferator-activated receptor-alpha, PPAR-α; (**B**) peroxisome proliferator-activated receptor-gamma, PPAR-γ; (**C**) fatty acid synthase, FAS; (**D**) carnitine palmitoyl transferase 1a, CPT1a; (**E**) carnitine palmitoyltransferase 1b, CPT1b; (**F**) uncoupling protein 1, UCP1. ND, mice fed a normal diet; HFD, mice fed a high-fat diet; PSO, SFO, and TSO, mice fed a high-fat diet supplemented with PSO, SFO, and TSO at 2 g/kg body weight per day, respectively. Data are presented as mean ± standard deviation (n=8). Means with different letters (a–d) were considered significantly different at $p<0.05$, according to Tukey's test.

and HFD groups. Notably, it has been reported that activating UCP1-expressing adipocytes has effective potential as an anti-diabetic and anti-obesity agent by increasing energy consumption and lowering adiposity in mice [Bond & Ntambi, 2018]. Our findings were consistent with the previous studies, which found that up-regulation of FA oxidation by PPAR-α was associated with a decrease in fat accumulation in HFD-induced obesity [Bremer, 2001; Hirako *et al.*, 2010]. Another study revealed that HFD supplemented with perilla, olive, and safflower oils exerted anti-obesity effects by reducing expression levels of genes associated with lipid synthesis (PPAR-γ and FAS) and increased expression levels of genes related to FA β-oxidation (PPAR-α) in both liver and adipose tissue in mice with obesity and colon inflammation triggered by HFD [Thomas *et al.*, 2020a]. A similar study also showed that consumption of kiwifruit seed oil had anti-obesity effects by increasing mRNA expression levels of FA β-oxidation-related genes (PPAR-α, CPT1a, and CPT1b) and energy metabolism and thermogenesis (UCP2) while decreasing mRNA expression levels of lipid synthesis-related genes (PPAR-γ and FAS) in obese mice induced by HFD [Qu *et al.*, 2019a, b]. Our study found that PSO, SFO, and TSO supplementation suppressed PPAR-γ and FAS expressions and enhanced PPAR-α, CPT1a, CPT1b, and UCP1 expressions to different degrees, revealing that dietary oil supplementation had a strong inhibitory effect on lipid metabolism disorders in HFD-fed mice.

The FA composition analysis showed that PSO, SFO, and TSO had an incredibly high content of USFAs and a low SFA:USFA ratio (Table 3), indicating that the anti-obesity properties of these oils are probably due to the high content of USFA and the low SFA:USFA ratio, especially in PSO and TSO. Previous studies have shown that a low SFA:USFA ratio is beneficial for health [Li *et al.*, 2015; Thomas *et al.*, 2020a]. Interestingly, although the three oils studied showed similar anti-obesity effects in HFD-fed mice, there were some subtle differences in the metabolic effects. Notably, dietary oils vary in FA composition and the presence of other active minor compounds, such as tocopherols, carotenoids, *etc*. These variations are believed to lead to various biochemical pathways and, thus, different metabolic impacts [Altberg *et al.*, 2020]. For instance, the molecular technicalities that underlie the effects of PSO in preventing lipid accumulation, inhibiting hyperglycemia, and improving lipid metabolism and chronic inflammation are likely related to the bioconversion of α-linolenic acid to eicosapentaenoic acid (C20:5*n*3) and docosahexaenoic acid (C22:6*n*3) [González-Mañán *et al.*, 2012]. These findings highlight the necessity of replacing SFAs with USFAs and the potential applications for by-products of these dietary oils in the context of a balanced and healthy dietary pattern. However, the mechanisms through which PSO, SFO, and TSO ameliorate inflammation and lipid metabolism in HFD-induced obese mice must be further investigated. It has been shown that the gut microbiota is a critical factor in body

health regulation and might be a target for treating inflammation, obesity and other chronic diseases [Scheithauer *et al.*, 2020]. Therefore, an exciting study will be conducted to explore whether PSO, SFO, and TSO supplementation can ameliorate obesity by modulating the gut microbiota composition compared with one of the most commonly used anti-obesity drugs.

CONCLUSIONS

In this study, we investigated the effect of oral supplementation with PSO, SFO, and TSO, oils with different fatty acid compositions, on HFD-induced obesity in KM mice. The results of the animal study demonstrated that oils supplementation could reduce body weight and tissue weight but not food intake in HFD-induced obese mice. Furthermore, PSO, SFO, and TSO supplementation alleviated hyperlipidemia, hyperglycemia, and hepatic steatosis induced by HFD, reduced serum FFA levels, and improved insulin resistance, liver function, and the atherogenic index. Additionally, the results showed that dietary oil supplementation suppressed HFD-induced adipose tissue inflammation in mice by reducing both secretion and mRNA expression levels of pro-inflammatory cytokines and increasing secretion and mRNA expression levels of anti-inflammatory adipokines. Likewise, the qPCR assay of lipid metabolism-related genes showed that dietary oil supplementation improved lipid metabolism by increasing FA β-oxidation and thermogenesis and suppressing lipid synthesis in EAT. Taken together, PSO, SFO, and TSO supplements could have potential anti-obesity implications by suppressing inflammation and improving lipid metabolism in HFD-induced obese mice.

RESEARCH FUNDING

This work was financially supported by the Chongqing Modern Mountainous Characteristic Efficient Agricultural Industrial Technology System (Innovation Team No. 2021 [4]); Key R&D projects of Sichuan Science and Technology Plan (2020YFN0148).

CONFLICT OF INTERESTS

The authors declare no conflict of interest.

ORCID IDs

W.A.S. Aldamarany https://orcid.org/0000-0001-6975-4271
G. Zhong https://orcid.org/0000-0001-5572-8355

REFERENCES

1. Adeleke, B.S., Babalola, O.O. (2020). Oilseed crop sunflower (*Helianthus annuus*) as a source of food: Nutritional and health benefits. *Food Science and Nutrition*, *8*(9), 4666–4684. https://doi.org/10.1002/fsn3.1783
2. Altberg, A., Hovav, R., Chapnik, N., Madar, Z. (2020). Effect of dietary oils from various sources on carbohydrate and fat metabolism in mice. *Food and Nutrition Research*, *64*, art. no. 4287. https://doi.org/10.29219/fnr.v64.4287
3. Asif, M. (2011). Health effects of omega-3,6,9 fatty acids: *Perilla frutescens* is a good example of plant oils. *Oriental Pharmacy and Experimental Medicine*, *11*(1), 51–59. https://doi.org/10.1007/s13596-011-0002-x
4. Bjermo, H., Iggman, D., Kullberg, J., Dahlman, I., Johansson, L., Persson, L., Berglund, J., Pulkki, K., Basu, S., Uusitupa, M., Rudling, M., Arner, P., Cederholm, T., Ahlström, H., Risérus, U. (2012). Effects of *n*-6 PUFAs compared with SFAs on liver fat, lipoproteins, and inflammation in abdominal obesity: a randomized controlled trial. *The American Journal of Clinical Nutrition*, *95*(5), 1003–1012. https://doi.org/10.3945/ajcn.111.030114
5. Bond, L.M., Ntambi, J.M. (2018). UCP1 deficiency increases adipose tissue monounsaturated fatty acid synthesis and trafficking to the liver. *Journal of Lipid Research*, *59*(2), 224–236. https://doi.org/10.1194/jlr.M078469
6. Bremer, J. (2001). The biochemistry of hypo- and hyperlipidemic fatty acid derivatives: metabolism and metabolic effects. *Progress in Lipid Research*, *40*(4), 231–268. https://doi.org/10.1016/S0163-7827(01)00004-2
7. Chang, Y., Li, H., Ren, H., Xu, H., Hu, P. (2019). Misclassification of chronic hepatitis B natural history phase: Insight from new ALT, AST, AKP, and GGT reference intervals in Chinese children. *Clinica Chimica Acta*, *489*, 61–67. https://doi.org/10.1016/j.cca.2018.11.034
8. Chen, G., Li, H., Zhao, Y., Zhu, H., Cai, E., Gao, Y., Liu, S., Yang, H., Zhang, L. (2017). Saponins from stems and leaves of *Panax ginseng* prevent obesity *via* regulating thermogenesis, lipogenesis and lipolysis in high-fat diet-induced obese C57BL/6 mice. *Food and Chemical Toxicology*, *106*(Part A), 393–403. https://doi.org/10.1016/j.fct.2017.06.012
9. Cheng, Y.-T., Wu, S.-L., Ho, C.-Y., Huang, S.-M., Cheng, C.-L., Yen, G.-C. (2014). Beneficial effects of Camellia Oil (*Camellia oleifera* Abel.) on ketoprofen-induced gastrointestinal mucosal damage through upregulation of HO-1 and VEGF. *Journal of Agricultural and Food Chemistry*, *62*(3), 642–650. https://doi.org/10.1021/jf404614k
10. Cui, C., Li, Y., Gao, H., Zhang, H., Han, J., Zhang, D., Li, Y., Zhou, J., Lu, C., Su, X. (2017). Modulation of the gut microbiota by the mixture of fish oil and krill oil in high-fat diet-induced obesity mice. *PLoS ONE*, *12*(10), art. no. e0186216. https://doi.org/10.1371/journal.pone.0186216
11. Decara, J., Rivera, P., López-Gambero, A.J., Serrano, A., Pavón, F.J., Baixeras, E., Rodríguez de Fonseca, F., Suárez, J. (2020). Peroxisome proliferator-activated receptors: Experimental targeting for the treatment of inflammatory bowel diseases. *Frontiers in Pharmacology, 11*, art. no. 730. https://doi.org/10.3389/fphar.2020.00730
12. Ebrahimi, R., Shanaki, M., Mohassel Azadi, S., Bahiraee, A., Radmard, A.R., Poustchi, H., Emamgholipour, S. (2022). Low level of adiponectin predicts the development of nonalcoholic fatty liver disease: Is it irrespective to visceral adiposity index, visceral adipose tissue thickness and other obesity indices? *Archives of Physiology and Biochemistry*, *128*(1), 24–31. https://doi.org/10.1080/13813455.2019.1661496
13. Friedewald, W.T., Levy, R.I., Fredrickson, D.S. (1972). Estimation of the concentration of low-density lipoprotein cholesterol in plasma, without use of the preparative ultracentrifuge. *Clinical Chemistry*, *18*(6), 499–502. https://doi.org/10.1093/clinchem/18.6.499
14. Golshani, H., Haghani, K., Dousti, M., Bakhtiyari, S. (2015). Association of TNF-α 308 G/A polymorphism with type 2 diabetes: A case-control study in the Iranian Kurdish ethnic group. *Osong Public Health and Research Perspectives*, *6*(2), 94–99. https://doi.org/10.1016/j.phrp.2015.01.003
15. González-Mañán, D., Tapia, G., Gormaz, J.G., D'Espessailles, A., Espinosa, A., Masson, L., Varela, P., Valenzuela, A., Valenzuela, R. (2012). Bioconversion of α-linolenic acid to n-3 LCPUFA and expression of PPAR-alpha, acyl Coenzyme A oxidase 1 and carnitine acyl transferase I are incremented after feeding rats with α-linolenic acid-rich oils. *Food and Function*, *3*(7), 765–772. https://doi.org/10.1039/c2fo30012e
16. Gregg, E.W., Shaw, J.E. (2017). Global health effects of overweight and obesity. *The New England Journal of Medicine*, *377*(1), 80–81. https://doi.org/10.1056/NEJMe1706095
17. He, L., Zhou, G.-Y., Zhang, G.-Y., Liu, J.-A. (2011). Research progress on the health function of tea oil. *Journal of Medicinal Plants Research*, *5*(4), 485–489.
18. Henderson, G.C. (2021). Plasma free fatty acid concentration as a modifiable risk factor for metabolic disease. *Nutrients*, *13*(8), art. no. 2590. https://doi.org/10.3390/nu13082590
19. Hirabara, S.M., Folador, A., Fiamoncini, J., Lambertucci, R.H., Rodrigues, C.F., Rocha, M.S., Aikawa, J., Yamazaki, R.K., Martins, A.R., Rodrigues, A.C., Carpinelli, A.R., Pithon-Curi, T.C., Fernandes, L.C., Gorjão, R., Curi, R. (2013). Fish oil supplementation for two generations increases insulin sensitivity in rats. *The Journal of Nutritional Biochemistry*, *24*(6), 1136–1145. https://doi.org/10.1016/j.jnutbio.2012.08.014
20. Hirako, S., Kim, H., Arai, T., Chiba, H., Matsumoto, A. (2010). Effect of concomitantly used fish oil and cholesterol on lipid metabolism. *The Journal of Nutritional Biochemistry*, *21*(7), 573–579. https://doi.org/10.1016/j.jnutbio.2009.02.013
21. Huang, B., Wang, X., Liang, X. (2015). Effects of tea cultivars and oil extraction process on fatty acid component in tea seed. *Journal of the Chinese Cereals and Oils Association*, *30*(1), 65–70 and 75.
22. Huang, T., Zhou, W., Ma, X., Jiang, J., Zhang, F., Zhou, W., He, H., Cui, G. (2021). Oral administration of camellia oil ameliorates obesity and modifies the gut microbiota composition in mice fed a high-fat diet. *FEMS Microbiology Letters*, *368*(10), art. no. fnab063. https://doi.org/10.1093/femsle/fnab063

23. Hummasti, S., Hotamisligil, G.S. (2010). Endoplasmic reticulum stress and inflammation in obesity and diabetes. *Circulation Research*, *107*(5), 579–591. https://doi.org/10.1161/CIRCRESAHA.110.225698
24. Janani, C., Ranjitha Kumari, B.D. (2015). PPAR gamma gene – A review. *Diabetes and Metabolic Syndrome: Clinical Research and Reviews*, *9*(1), 46–50. https://doi.org/10.1016/j.dsx.2014.09.015
25. Jiang, Y., Liu, D., Kong, X., Xu, Y., Chen, W., Lin, N. (2014). Huogu I formula prevents steroid-induced osteonecrosis in rats by down-regulating PPARγ expression and activating Wnt/LRP5/β-catenin signaling. *Journal of Traditional Chinese Medicine*, *34*(3), 342–350. https://doi.org/10.1016/S0254-6272(14)60100-X
26. Kersten, S., Stienstra, R. (2017). The role and regulation of the peroxisome proliferator activated receptor alpha in human liver. *Biochimie*, *136*, 75–84. https://doi.org/10.1016/j.biochi.2016.12.019
27. Kliewer, S.A., Xu, H.E., Lambert, M.H., Willson, T.M. (2001). Peroxisome proliferator-activated receptors: from genes to physiology. *Recent Progress in Hormone Research*, *56*, 239–263. https://doi.org/10.1210/rp.56.1.239
28. Lee, H.J., Jung, H., Cho, H., Lee, K., Kwak, H.-K., Hwang, K.T. (2016). Dietary black raspberry seed oil ameliorates inflammatory activities in *db/db* mice. *Lipids*, *51*(6), 715–727. https://doi.org/10.1007/s11745-016-4159-4
29. Li, Y., Hruby, A., Bernstein, A.M., Ley, S.H., Wang, D.D., Chiuve, S.E., Sampson, L., Rexrode, K.M., Rimm, E.B., Willett, W.C., Hu, F.B. (2015). Saturated fats compared with unsaturated fats and sources of carbohydrates in relation to risk of coronary heart disease: A prospective cohort study. *Journal of the American College of Cardiology*, *66*(14), 1538–1548. https://doi.org/10.1016/j.jacc.2015.07.055
30. Li, Z., Ji, G.E. (2018). Ginseng and obesity. *Journal of Ginseng Research*, *42*(1), 1–8. https://doi.org/10.1016/j.jgr.2016.12.005
31. Lian, Z., Perrard, X.D., Peng, X., Raya, J.L., Hernandez, A.A., Johnson, C.G., Lagor, W.R., Pownall, H.J., Hoogeveen, R.C., Simon, S.I., Sacks, F.M., Ballantyne, C.M., Wu, H. (2020). Replacing saturated fat with unsaturated fat in Western diet reduces foamy monocytes and atherosclerosis in male *Ldlr*$^{-/-}$ mice. *Arteriosclerosis, Thrombosis, and Vascular Biology*, *40*(1), 72–85. https://doi.org/10.1161/ATVBAHA.119.313078
32. Liao, F.-H., Liou, T.-H., Shieh, M.-J., Chien, Y.-W. (2010). Effects of different ratios of monounsaturated and polyunsaturated fatty acids to saturated fatty acids on regulating body fat deposition in hamsters. *Nutrition*, *26*(7–8), 811–817. https://doi.org/10.1016/j.nut.2009.09.009
33. Mishra, B.K., Madhu, S.V., Aslam, M., Agarwal, V., Banerjee, B.D. (2021). Adipose tissue expression of UCP1 and PRDM16 genes and their association with postprandial triglyceride metabolism and glucose intolerance. *Diabetes Research and Clinical Practice*, *182*, art. no. 109115. https://doi.org/10.1016/j.diabres.2021.109115
34. Monk, J.M., Liddle, D.M., Hutchinson, A.L., Wu, W., Lepp, D., Ma, D.W.L., Robinson, L.E., Power, K.A. (2019). Fish oil supplementation to a high-fat diet improves both intestinal health and the systemic obese phenotype. *The Journal of Nutritional Biochemistry*, *72*, art. no. 108216. https://doi.org/10.1016/j.jnutbio.2019.07.007
35. Neeland, I.J., Poirier, P., Després, J.P. (2018). Cardiovascular and metabolic heterogeneity of obesity: Clinical challenges and implications for management. *Circulation*, *137*(13), 1391–1406. https://doi.org/10.1161/CIRCULATIONAHA.117.029617
36. Noratto, G., Chew, B.P., Ivanov, I. (2016). Red raspberry decreases heart biomarkers of cardiac remodeling associated with oxidative and inflammatory stress in obese diabetic db/db mice. *Food and Function*, *7*(12), 4944–4955. https://doi.org/10.1039/C6FO01330A
37. Oh, D.Y., Olefsky, J.M. (2012). Omega 3 fatty acids and GPR120. *Cell Metabolism*, *15*(5), 564–565. https://doi.org/10.1016/j.cmet.2012.04.009
38. Ormseth, M.J., Swift, L.L., Fazio, S., Linton, M.F., Raggi, P., Solus, J.F., Oeser, A., Bian, A., Gebretsadik, T., Shintani, A., Stein, C.M. (2013). Free fatty acids are associated with metabolic syndrome and insulin resistance but not inflammation in systemic lupus erythematosus. *Lupus*, *22*(1), 26–33. https://doi.org/10.1177/0961203312462756
39. Ouchi, N., Parker, J.L., Lugus, J.J., Walsh, K. (2011). Adipokines in inflammation and metabolic disease. *Nature Reviews Immunology*, *11*(2), 85–97. https://doi.org/10.1038/nri2921
40. Pajvani, U.B., Hawkins, M., Combs, T.P., Rajala, M.W., Doebber, T., Berger, J.P., Wagner, J.A., Wu, M., Knopps, A., Xiang, A.H., Utzschneider, K.M., Kahn, S.E., Olefsky, J.M., Buchanan, T.A., Scherer, P.E. (2004). Complex distribution, not absolute amount of adiponectin, correlates with thiazolidinedione-mediated improvement in insulin sensitivity. *Journal of Biological Chemistry*, *279*(13), 12152–12162. https://doi.org/10.1074/jbc.M311113200
41. Park, H.S., Park, J.Y., Yu, R. (2005). Relationship of obesity and visceral adiposity with serum concentrations of CRP, TNF-α and IL-6. *Diabetes Research and Clinical Practice*, *69*(1), 29–35. https://doi.org/10.1016/j.diabres.2004.11.007
42. Parto, P., Lavie, C.J. (2017). Obesity and cardiovascular diseases. *Current Problems in Cardiology*, *42*(11), 376–394. https://doi.org/10.1016/j.cpcardiol.2017.04.004
43. Pradhan, S., Panchali, T., Paul, B., Khatun, A., Rao Jarapala, S., Mondal, K.C., Ghosh, K., Chakrabarti, S. (2020). Anti-obesity potentiality of Tapra fish (*Opisthopterus tardoore*) oil. *Journal of Food Biochemistry*, *44*(11), art. no. e13448. https://doi.org/10.1111/jfbc.13448
44. Qu, L., Liu, Q., Zhang, Q., Liu, D., Zhang, C., Fan, D., Deng, J., Yang, H. (2019a). Kiwifruit seed oil ameliorates inflammation and hepatic fat metabolism in high-fat diet-induced obese mice. *Journal of Functional Foods*, *52*, 715–723. https://doi.org/10.1016/j.jff.2018.12.003
45. Qu, L., Liu, Q., Zhang, Q., Tuo, X., Fan, D., Deng, J., Yang, H. (2019b). Kiwifruit seed oil prevents obesity by regulating inflammation, thermogenesis, and gut microbiota in high-fat diet-induced obese C57BL/6 mice. *Food and Chemical Toxicology*, *125*, 85–94. https://doi.org/10.1016/j.fct.2018.12.046
46. Reagan-Shaw, S., Nihal, M., Ahmad, N. (2008). Dose translation from animal to human studies revisited. *The FASEB Journal*, *22*(3), 659–661. https://doi.org/10.1096/fj.07-9574LSF
47. Scheithauer, T.P.M., Rampanelli, E., Nieuwdorp, M., Vallance, B.A., Verchere, C.B., van Raalte, D.H., Herrema, H. (2020). Gut microbiota as a trigger for metabolic inflammation in obesity and type 2 diabetes. *Frontiers in Immunology*, *11*, art. no. 571731. https://doi.org/10.3389/fimmu.2020.571731
48. Stienstra, R., Tack, C.J., Kanneganti, T.-D., Joosten, L.A.B., Netea, M.G. (2012). The inflammasome puts obesity in the danger zone. *Cell Metabolism*, *15*(1), 10–18. https://doi.org/10.1016/j.cmet.2011.10.011
49. Su, J., Ma, C., Liu, C., Gao, C., Nie, R., Wang, H. (2016). Hypolipidemic activity of peony seed oil rich in α-linolenic, is mediated through inhibition of lipogenesis and upregulation of fatty acid β-oxidation. *Journal of Food Science*, *81*(4), H1001–H1009. https://doi.org/10.1111/1750-3841.13252
50. Sundaram, S., Bukowski, M.R., Lie, W.-R., Picklo, M.J., Yan, L. (2016). High-fat diets containing different amounts of n3 and n6 polyunsaturated fatty acids modulate inflammatory cytokine production in mice. *Lipids*, *51*(5), 571–582. https://doi.org/10.1007/s11745-015-4093-x
51. Takahashi, H., Chi, H.-Y., Mohri, S., Kamakari, K., Nakata, K., Ichijo, N., Nakata, R., Inoue, H., Goto, T., Kawada, T. (2016). Rice koji extract enhances lipid metabolism through proliferator-activated receptor alpha (PPARα) activation in mouse liver. *Journal of Agricultural and Food Chemistry*, *64*(46), 8848–8856. https://doi.org/10.1021/acs.jafc.6b03516
52. Thomas, S.S., Cha, Y.-S., Kim, K.-A. (2020a). Effect of vegetable oils with different fatty acid composition on high-fat diet-induced obesity and colon inflammation. *Nutrition Research and Practice*, *14*(5), 425–437. https://doi.org/10.4162/nrp.2020.14.5.425
53. Thomas, S.S., Cha, Y.-S., Kim, K.-A. (2020b). Perilla oil alleviates high-fat diet--induced inflammation in the colon of mice by suppressing nuclear factor--kappa B activation. *Journal of Medicinal Food*, *23*(8), 818–826. https://doi.org/10.1089/jmf.2019.4675
54. Trayhurn, P., Wood, I.S. (2004). Adipokines: inflammation and the pleiotropic role of white adipose tissue. *British Journal of Nutrition*, *92*(3), 347–355. https://doi.org/10.1079/BJN20041213
55. Tung, Y.-T., Hsu, Y.-J., Chien, Y.-W., Huang, C.-C., Huang, W.-C., Chiu, W.-C. (2019). Tea seed oil prevents obesity, reduces physical fatigue, and improves exercise performance in high-fat-diet-induced obese ovariectomized mice. *Molecules*, *24*(5), art. no. 980. https://doi.org/10.3390/molecules24050980
56. Wagner, N., Wagner, K.-D. (2020). The role of PPARs in disease. *Cells*, *9*(11), art. no. 2367. https://doi.org/10.3390/cells9112367
57. Wang, F., Zhu, H., Hu, M., Wang, J., Xia, H., Yang, X., Yang, L., Sun, G. (2018). Perilla oil supplementation improves hypertriglyceridemia and gut dysbiosis in diabetic KKAy mice. *Molecular Nutrition and Food Research*, *62*(24), art. no. 1800299. https://doi.org/10.1002/mnfr.201800299
58. Wang, J., He, Y., Yu, D., Jin, L., Gong, X., Zhang, B. (2020). Perilla oil regulates intestinal microbiota and alleviates insulin resistance through the PI3K/AKT signaling pathway in type-2 diabetic KKAy mice. *Food and Chemical Toxicology*, *135*, art. no. 110965. https://doi.org/10.1016/j.fct.2019.110965
59. Wang, S.-S., Lay, S., Yu, H.-N., Shen, S.-R. (2016). Dietary Guidelines for Chinese Residents (2016): comments and comparisons. *Journal of Zhejiang University – Science B*, *17*(9), 649–656. https://doi.org/10.1631/jzus.B1600341
60. Whitehead, A., Krause, F.N., Moran, A., MacCannell, A.D.V., Scragg, J.L., McNally, B.D., Boateng, E., Murfitt, S.A., Virtue, S., Wright, J., Garnham, J., Davies, G.R., Dodgson, J., Schneider, J.E., Murray, A.J., Church, C., Vidal-Puig, A., Witte, K.K.,

Griffin, J.L., Roberts, L.D. (2021). Brown and beige adipose tissue regulate systemic metabolism through a metabolite interorgan signaling axis. *Nature Communications*, *12*(1), art. no. 1905. https://doi.org/10.1038/s41467-021-22272-3

61. Williams, K.W., Scott, M.M., Elmquist, J.K. (2009). From observation to experimentation: leptin action in the mediobasal hypothalamus. *The American Journal of Clinical Nutrition*, *89*(3), 985S–990S. https://doi.org/10.3945/ajcn.2008.26788D
62. Wolf, G., Phil, D. (1996). High-fat, high-cholesterol diet raises plasma HDL cholesterol: Studies on the mechanism of this effect. *Nutrition Reviews*, *54*(1), 34–35. https://doi.org/10.1111/j.1753-4887.1996.tb03772.x
63. Wu, C.-C., Tung, Y.-T., Chen, S.-Y., Lee, W.-T., Lin, H.-T., Yen, G.-C. (2020). Anti-inflammatory, antioxidant, and microbiota-modulating effects of camellia oil from *Camellia brevistyla* on acetic acid-induced colitis in rats. *Antioxidants*, *9*(1), art. no. 58. https://doi.org/10.3390/antiox9010058
64. Yang, S.-C., Lin, S.-H., Chang, J.-S., Chien, Y.-W. (2017). High fat diet with a high monounsaturated fatty acid and polyunsaturated/saturated fatty acid ratio suppresses body fat accumulation and weight gain in obese hamsters. *Nutrients*, *9*(10), art. no. 1148. https://doi.org/10.3390/nu9101148
65. Zhang, C., Wu, W., Li, X., Xin, X., Liu, D. (2019). Daily supplementation with fresh *Angelica keiskei* juice alleviates high-fat diet-induced obesity in mice by modulating gut microbiota composition. *Molecular Nutrition and Food Research*, *63*(14), art. no. 1900248. https://doi.org/10.1002/mnfr.201900248
66. Zhang, H., Zhang, W., Yun, D., Li, L., Zhao, W., Li, Y., Liu, X., Liu, Z. (2020). Alternate-day fasting alleviates diabetes-induced glycolipid metabolism disorders: roles of FGF21 and bile acids. *The Journal of Nutritional Biochemistry*, *83*, art. no. 108403. https://doi.org/10.1016/j.jnutbio.2020.108403
67. Zhang, X., Zhang, Q.-X., Wang, X., Zhang, L., Qu, W., Bao, B., Liu, C.-A., Liu, J. (2016). Dietary luteolin activates browning and thermogenesis in mice through an AMPK/PGC1α pathway-mediated mechanism. *International Journal of Obesity*, *40*(12), 1841–1849. https://doi.org/10.1038/ijo.2016.108

ORIGINAL ARTICLE
http://journal.pan.olsztyn.pl

Polish Journal of Food and Nutrition Sciences
2023, Vol. 73, No. 1, 95–107
DOI: 10.31883/pjfns/161366
ISSN 1230-0322, e-ISSN 2083-6007

Influence of Synthetic Antioxidants Used in Food Technology on the Bioavailability and Metabolism of Lipids – *In Vitro* Studies

Anna Antończyk, Magdalena Mika*, Agnieszka Wikiera

Department of Biotechnology and General Technology of Food, Faculty of Food Technology, University of Agriculture, ul. Balicka 122, 30-149 Krakow, Poland

Synthetic antioxidants, such as butylated hydroxytoluene (BHT), butylated hydroxyanisole (BHA), and tert-butylhydroquinone (TBHQ), have been widely used for many years to stabilise lipids in foods. Nonetheless, their effect on the bioavailability and metabolism of lipids stabilised with them still remains unknown. To investigate this issue, *in vitro* digestion of a model high-fat product (20 g fat/100 g) without antioxidants and supplemented with BHT, BHA and TBHQ (100 mg/kg) was conducted, followed by studies using the Caco-2 and Hep G2 cell lines. BHT, BHA and TBHQ increased intestinal absorption of triacylglycerols and modified the structure of chylomicrons (CM). The addition of BHT and TBHQ inhibited apolipoprotein-IV (apoA-IV) synthesis. At the same time, smaller chylomicrons were secreted, but their amount was greater than in the model product without antioxidants. In contrast, BHA activated apoA-IV synthesis, resulting in the formation of fewer but very large CMs. Of concern was the significant decrease in apoA-IV in cells upon the use of BHT and TBHQ, which can lead to obesity due to the lack of the sensation of feeling full after eating high-fat foods stabilised with these antioxidants. Furthermore, the efficiency of CM remnant (CMR) uptake by hepatocytes was inversely correlated with their size. The large CMRs generated for samples with BHA were not absorbed by hepatocytes, which can lead to atherosclerosis. The results of our *in vitro* study shed new light on the role of synthetic phenolic antioxidants used in food technology as potential obesity and atherosclerosis triggers and suggested the need for further research that will clearly separate antioxidants that promote the development of these diseases from those, which do not do that.

Key words: butylated hydroxytoluene, butylated hydroxyanisole, tert-butylhydroquinone, chylomicrons, lipid digestion, intestinal absorption

ABBREVIATIONS

ACC, acetyl-CoA carboxylase; AG, acylglycerols; AMPK, AMP-dependent kinase; BHA, butylated hydroxyanisole; BHT, butylated hydroxytoluene; CD36 receptor, fatty acid translocase; CE, cholesterol esters; Chol, cholesterol; CM, chylomicrons; CMR, chylomicron remnants; DG, diacylglycerols; DM, dry matter; DMEM, Dulbecco's modified eagle medium; FFA, free fatty acids; LPL, lipoprotein lipase; MDA, malondialdehyde; MG, monoacylglycerols; MTP, microsomal triglyceride transfer protein; pACC, phosphorylated ACC; pAMPK, phosphorylated AMPK; tACC, total ACC; tAMPK, total AMPK; TBA, 2-thiobarbituric acid; TBARS, thiobarbituric acid-reactive substances; TBHQ, tert-butylhydroquinone; TCA, trichloroacetic acid; TEER, transepithelial electrical resistance; TEP, 1,1,3,3-tetraethoxypropane; TG, triacylglycerols.

INTRODUCTION

Synthetic antioxidants, such as butylated hydroxytoluene (BHT), butylated hydroxyanisole (BHA), and tert-butylhydroquinone

***Corresponding Author:**
Tel.: +48 12 662 47 03; e-mail: magdalena.mika@urk.edu.pl (M. Mika)

Submitted: 28 September 2022
Accepted: 17 February 2023
Published on-line: 7 March 2023

(TBHQ), are commonly used as antioxidants in the food industry. The use of antioxidants ensures the prolonged freshness of food by stabilising its nutritional value, taste, and colour. Synthetic phenolic antioxidants are primarily used to stabilise frying fats and instant products that have gained popularity among consumers in recent years. Thanks to their ability to quench free radicals, they not only prolong the freshness of food, but also protect consumers from the adverse effects of lipid oxidation products that are important factors in the pathogenesis of atherosclerosis [Plat *et al.*, 2014; Björkhem *et al.*, 1991]. The permitted amount of BHT added to food is 100 mg/kg of fat, while TBHQ and BHA can be used in twice the amount [Commission Regulation (EU) No 1129/2011 of 11 November 2011]. Excessive or improper use of synthetic antioxidants may have carcinogenic effects [Xu *et al.*, 2021].

Although synthetic phenolic antioxidants have been widely used to stabilise dietary lipids for many years, their role in regulating the bioavailability and metabolism of lipids stabilised with them still remains unclear. Data available in the literature indicate that diet supplementation with synthetic antioxidants modifies the metabolism of lipids, affecting their blood profile [Nam *et al.*, 2013; Nishizono *et al.*, 2000; Sun *et al.*, 2020] and body weight of the animals fed [Hung *et al.*, 2019; Nam *et al.*, 2013 Nishizono *et al.*, 2000; Sun *et al.*, 2020; Safer & Al-Nughamish, 1999]. However, these data are scarce and do not show at which stages the changes in lipid metabolism do occur. Moreover, published results are sometimes inconclusive or even contradictory. For example, various effects can be observed not only between antioxidants [Nam *et al.*, 2013; Sun *et al.*, 2020], but also for the same antioxidant tested by different researchers [Hung *et al.*, 2019; Nam *et al.*, 2013; Nishizono *et al.*, 2000]. Studies with rodents, rabbits, and even primates (rhesus macaque) have shown that the addition of BHT or BHA to the diet caused a significant increase in levels of triacylglycerols (TG) and the cholesterol low-density lipoprotein (LDL) and very-low-density lipoprotein (VLDL) fractions in the blood with a concomitant decrease in hepatic TG level [Björkhem *et al.*, 1991; Sun *et al.*, 2020]. In contrast, the addition of TBHQ to animal diets resulted in a decreased blood TG content [Nam *et al.*, 2013; Nishizono *et al.*, 2000]. Using a low dose of TBHQ (0.001–0.0028%) reduced blood TG levels by 22% in diabetic rats [Nam *et al.*, 2013; Nishizono *et al.*, 2000] and in mice fed a high-fat diet [Nam *et al.*, 2013]. It has also been noted that the addition of BHT [Safer & Al-Nughamish, 1999] or BHA [Sun *et al.*, 2020] to the diet in amounts not exceeding 0.1% resulted in higher body weight gains in experimental animals. However, the effect of TBHQ on body weight is not clear and may depend on the species. Administering this antioxidant to mice at 0.001% along with a high-fat diet for 32 days reduced body weight gain by approximately 61% and reduced the amount of lipids stored in adipocytes [Nam *et al.*, 2013]. At the same time, in rats with diabetes mellitus (induced by streptozotocin) that were fed a standard diet with 0.0028% TBHQ for 15 days, an increase in body weight gain was observed even though the animals ate less food than those from the control group [Nishizono *et al.*, 2000]. On the other hand, enriching pig diets with 0.006% TBHQ for 34 days did not affect their body weight gains [Hung *et al.*, 2019].

The bioavailability of lipids from the diet entails digestion in the gastrointestinal (GI) tract followed by intestinal absorption. Digested in the GI tract, triacylglycerols are hydrolysed to free fatty acids (FFA) and monoacylglycerols (MG), which are absorbed by intestinal cells. In enterocytes, the products of lipid digestion are converted back into TG and released into the bloodstream in the form of chylomicrons (CMs). CMs secreted by enterocytes into the bloodstream enable the transport of exogenous TG and exogenous cholesterol [Acevedo-Fani & Singh, 2022]. In addition to TG and cholesterol esters (CE) forming a hydrophobic core, CMs have a hydrophilic envelope that includes apoB48 and apoA-IV. One of the crucial functions of these proteins is to facilitate lipid emulsification in blood plasma. The first of these proteins is considered a CM marker because there is only one apoB48 molecule per chylomicron [Phillips *et al.*, 1997], *i.e.,* more apoB48 determines more CMs. In contrast, the amount of apoA-IV secreted with CM varies, and the regulation of apoA-IV synthesis is unknown. In recent years, apoA-IV has been found to regulate satiety, and a deficiency of this protein has been linked to obesity, arteriosclerosis and diabetes development [Kohan *et al.*, 2013, 2015]. Postprandially, TGs included in CMs undergo lipolysis catalysed by lipoprotein lipase (LPL). LPL activity can be inhibited by apoC-III protein synthesised by liver cells and binding to the CM. The chylomicron remnants (CMRs), formed after TG hydrolysis, are then absorbed by hepatocytes and the apoE protein is involved in the process. The absorption of FFA and CMRs by hepatocytes may affect: (i) CD 36 receptor (fatty acid translocase), which is involved in the absorption of fatty acids by cells, (ii) microsomal triglyceride transfer protein (MTP) , which participates in the formation of lipoproteins secreted by enterocytes and hepatocytes into the bloodstream, and (iii) the activity AMP-dependent kinase (AMPK) affecting the intensity of the cell's uptake of FFA [Harmel *et al.*, 2014]. In addition, AMPK influences lipid metabolism in hepatocytes by controlling the lipogenesis mainly by modifying the activity of acetyl-CoA carboxylase (ACC), a key enzyme of the FA biosynthetic pathway.

Based on the presented analysis of literature data, it can be hypothesised that BHT, BHA and TBHQ, used as antioxidants in high-fat products, can significantly affect both the bioavailability and metabolism of lipids stabilised with them. To verify this hypothesis, we conducted *in vitro* study entailing: digestion, intestinal absorption (cell line Caco-2) and liver metabolism (cell line Hep G2).

MATERIALS AND METHODS

Materials and reagents

Raw pork fat (no stabilising agent added) was purchased in the company store Szubryt (Chelmiec, Poland), and wheat bread was purchased at the local bakery Pawlak (Cracow, Poland). Aicar, amphotericin B, BHA, BHT, bile salts, Compound C, Dulbecco's modified eagle medium (DMEM), ethylenedinitrilotetraacetic acid (EDTA), fetal bovine serum, glutamine, glycerol, LPL, pancreatin, phosphate buffered saline (PBS), penicillin,

pepsin, protease inhibitor, streptomycin, 2-thiobarbituric acid (TBA), TBHQ, trichloroacetic acid (TCA), 1,1,3,3-tetraethoxypropane (TEP), trypan blue, and β-mercaptoethanol were purchased from Sigma-Aldrich (Saint Louis, MO, USA). Antibodies: anti-apoE, anti-apoA-I, anti-apoA-IV, anti-apoB100, anti-apoB48, anti-CD36, anti-MTP, anti-tACCα, and anti-pACC were purchased from Santa Cruz Biotechnology (Dallas, TX, USA); Grb-2, β-actin and anti-β-actin were purchased from Sigma-Aldrich; anti-apoC-III was purchased from MyBioSource (San Diego, CA, USA); anti-pAMPK was purchased from Cell Signaling Technology (Danvers, MA, USA); and anti-Grb-2 from was purchased from BD Transduction Laboratories (San Francisco, CA, USA). Human colorectal adenocarcinoma ATCC HTB-37 (Caco-2) and hepatocellular carcinoma ATCC HB-8065 (Hep G2) cell lines were purchased from the American Type Culture Collection (Manassas, VA, USA).

Model product preparation

The model high-fat product contained 80 g/100 g wheat bread (dried for 24 h and ground to a grain size of 0.5 mm in diameter) and 20 g/100 g lard rendered from raw pork fat. The ingredients were mixed for 10 min, and the resulting product was divided into four parts. To three of them BHT, BHA and TBHQ were added at 100 mg/kg fat (0.002 g/100 g model product), respectively, and the fourth without antioxidants served as the control. All antioxidants were used in the same dose, but not exceeding the permitted dose in food set in the Commission Regulation (EU) No 1129/2011 of 11 November 2011 on permitted additives. The model product immediately after preparation was used for the *in vitro* digestion.

In vitro digestion

The procedure of the *in vitro* digestion described by Minekus *et al.* [2014] with minor modifications was followed in the study. The scheme of its course is shown in Figure 1. Briefly, the model products (2 g) were placed in screw cap flasks (n=16 for each product), and 1 mL of simulated salivary fluid (SSF: pH 7; 18.8 mM K^+; 13.6 mM Na^+; 19.5 mM Cl^-; 3.7 mM $H_2PO_4^-$; 13.7 mM HCO_3^-; 0.15 mM Mg^{2+}; 0.12 mM NH_4^+; 1.5 mM Ca^{2+}) was added to each. The flasks were shaken for 10 min in a water bath (37°C), and then 2.8 mL of simulated gastric fluid (SGF: 7.8 mM K^+; 72.2 mM Na^+; 70.2 mM Cl^-; 0.9 mM $H_2PO_4^-$; 25.5 mM HCO_3^-; 0.1 mM Mg^{2+}; 1 mM NH_4^+; 0.15 mM Ca^{2+}) was added to each mixture, and the pH of the samples was brought to 2 using 1 M HCl. Simultaneously, a solution of pepsin in SGF was prepared and added to the mixture at a volume of 0.2 mL (12 kU). Pepsin activity in the digestion mixture was 2 kU/mL. Gastric digestion was carried out in a water bath with shaking for 2 h (37°C). Of the 16 replicates intended for gastric digestion, 4 were assigned for the future characterisation of gastric emulsion and 12 for the subsequent digestion step.

The pepsin-catalysed reaction was stopped by adding 5.2 mL of simulated intestinal fluid (SIF: 7.6 mM K^+; 123.4 mM Na^+; 55.5 mM Cl^-; 0.8 mM $H_2PO_4^-$; 85 mM HCO_3^-; 0.33 mM Mg^{2+}; 0.6 mM Ca^{2+}) and 1 M NaOH to bring the pH to 7.2. Then, 0.4 mL of bile salts solution (60 mg/g of the model product) was added to the samples, and after thorough mixing, another 0.4 mL of pancreatin solution (4.8 mg/g of the model product) was added. Solutions of bile salts (30%, *w/v*) and pancreatin (2.4%, *w/v*) were prepared using the SIF solution. Intestinal digestion was conducted in a shaking water bath (150 swings/min) at 37°C for 2 h. Of the 12 replicates intended for intestinal digestion, 4 were used for duodenal emulsion examination, and 8 for intestinal absorption examination. The mixtures intended for the intestinal absorption examination were centrifuged (10°C, 750×*g*, 10 min), and the resulting supernatant was stored at –80°C.

Assays of emulsion characteristics

The samples after *in vitro* digestion under gastric and duodenal conditions were left for 10 min to separate the emulsified layer (the time was determined by the Stokes sedimentation equation) and measure its volume. The emulsification degree was defined as the percentage of the emulsified layer in the total sample volume.

Fat droplets in the emulsion were stained with Sudan III and analysed by microscopy (Zeiss Axio Observer Z1 inverted microscope equipped with digital camera and Zen 2012 software, Carl Zeiss, Jena, Germany). Droplet size was estimated using Lucia measurement software (Laboratory Imagining, Prague, Czechia).

Evaluation of lipid absorption and metabolism *in vitro*

The design of the procedure for the *in vitro* evaluation of the absorption and metabolism of model high-fat products after digestion, and the parameters determined at each stage are presented in Figure 1.

Cell lines and culture

Human colorectal adenocarcinoma ATCC HTB-37 (Caco-2) and hepatocellular carcinoma ATCC HB-8065 (Hep G2) cell lines were grown in DMEM, supplemented with 20% fetal bovine serum, 2% glutamine, 10 µg/mL of streptomycin, 100 U/mL of penicillin, and 25 µg/mL of amphotericin B at 37°C in a humidified atmosphere of 5% CO_2.

Cytotoxicity assays

Caco-2 cells at 5×10^4 were seeded onto 24-well plates and, after 24 h of culture, were incubated (2 h) with the BHA, BHT and TBHQ (2 µg/mL). Then, cells present in the fluid and detached from the medium with a 0.1% EDTA solution in PBS were centrifuged (250×*g*, 5 min, 20°C) and stained with 0.4% trypan blue in 0.81% sodium chloride and 0.06% potassium phosphate. The stained cells were counted in a Bürker chamber. The percentage of dead cells was determined.

Intestinal absorption assays

Caco-2 cells were grown in DMEM in inserts with a pore diameter of 3 µm and a growth area of 0.9 cm^2 (Thermo Fisher Scientific, Waltham, MA, USA) at 37°C with 5% CO_2 concentration. Transmembrane electrical resistance (TEER; EVOM device with STX2 electrode, WPI company, Sarasota, FL, USA) was measured every other day. The culture was terminated when the membrane was entirely covered with a monolayer of morphologically mature

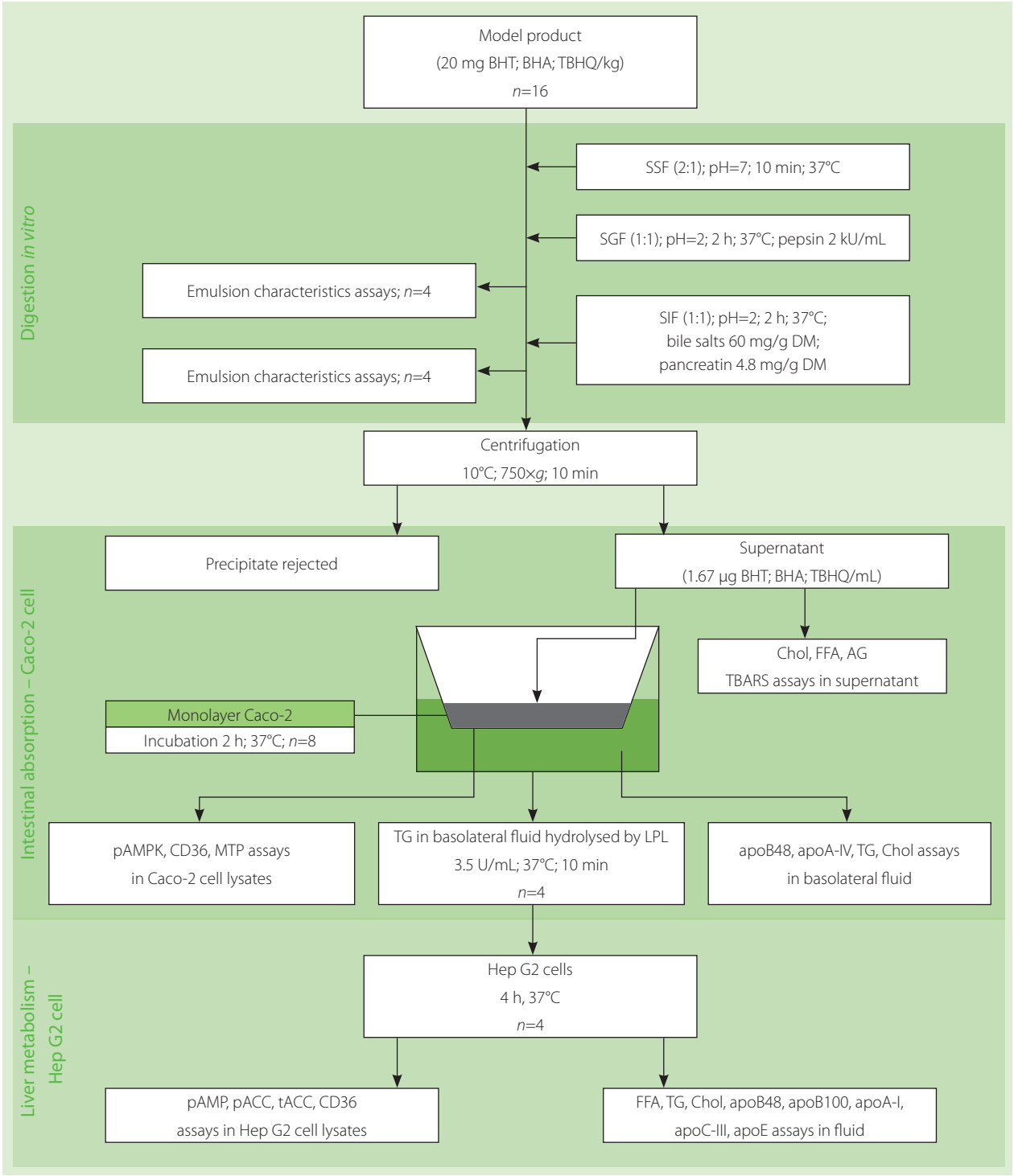

Figure 1. Scheme of study design, *in vitro* digestion, intestinal absorption and liver metabolism.

cells, and the TEER reached 200–300 Ω and persisted for two days. Then, the growth medium was removed from the apical and basal compartments, and PBS was added. Cells were incubated for 15 min at 37°C, after which TEER was measured. After the removal of PBS, 0.5 mL of the supernatant obtained after *in vitro* digestion was placed in the apical chamber. Next, 1 mL of colourless DMEM (1 g/L glucose, no glutamine) was placed in the basal chamber. The experiment duration and final membrane pore size were set at 2 h and 3 µm, respectively, based on preliminary experiments.

At the same time, a study was conducted to determine the effect of AMPK on the secretion of chylomicrons into the the basolateral fluid . To this end, 0.5 mL of the supernatant obtained after *in vitro* digestion of the model product without antioxidants was applied to the monolayer of Caco-2 cells. Aicar (final concentration of 500 µM) or Compound C (final concentration of 10 µM) was added to the supernatant. Then, 1 mL of colourless DMEM was placed in the basal chamber. Cells (*n*=8) were incubated for 2 h. In all experiments, the basolateral fluid was collected after the 2-h incubation and stored at –80°C for further analysis. Cells

were washed with PBS and incubated in this buffer for 15 min at 37°C; then, TEER was measured. Subsequently, PBS was removed, and the cells were lysed.

Preparation of the lysates of Caco-2 cells and Hep G2 cells

Lysis buffer (50 mM Tris-HCl, pH 7.5, 100 mM NaF, 2 mM EDTA, 10 mM β-mercaptoethanol, 10% glycerol, 5 µg/mL protease inhibitor mixture) was added to the cells in the culture dishes, which were subsequently incubated for 5 min at 4°C. The cells were then transferred to Eppendorf tubes and centrifuged (3,500×*g*, 5 min, 4°C). The lysates were stored at –80°C for further analysis.

Study of metabolism in hepatocytes – Hep G2 cell model

To this end, 3.5 U/mL lipoprotein lipase was added to 0.5 mL of basolateral fluid obtained after culturing Caco-2 cells and incubated at 37°C for 10 min. The mixture thus obtained was administered to Hep G2 cells growing on 12-well plates with a growth area of 2 cm^2 and incubated for 4 h at 37°C (n=4). After incubation, the fluid from wells was collected and stored at –80°C for further analysis. Cells were washed with PBS and then lysed (following the procedure described in subsection "Preparation of the lysates of Caco-2 cells and Hep G2 cells").

Analytical methods

Western-blot procedure

ApoB100, apoB48, tACC, pACC, apoE, apoA-I, apoA-IV, CD36, MTP, pAMPK, and apoC-III were determined by Western blotting [Mika *et al.*, 2021]. According to the scheme shown in Figure 1, apoB 48 and apoA-IV were determined in the basolateral fluid; pAMPK, CD36 and MTP were determined in Caco-2 cell lysates; apoB48, apoB100, apoA-I, apoC-III and apoE were determined in the fluid obtained after incubation with Hep G2 cells; whereas pAMPK, pACC, tACC and CD36 were determined in Hep G2 cells lysates. Briefly, the samples (50 µg of protein) were mixed with loading buffer (50 mM Tris-HCl, pH 6.8, 0.4% sodium dodecyl sulphate, 10 mM β-mercaptoethanol, 20% glycerol, 0.02 mg/mL bromophenol blue), denatured at 95°C for 5 min and separated either in 6% (for apoB100, apoB48, total-ACCα and phospho-ACC detection), 10% (for apoE, apoA-I, apoA-IV, CD36, MTP and pAMPK detection) or 15% (for apoC-III detection) polyacrylamide gels. , Grb-2 and β-actin were used as reference proteins. After electrophoresis and electroblotting, the nitrocellulose membranes were blocked by incubation in a TBS-Tween buffer (10 mM Tris-HCl, pH 7.6, 0.5 M NaCl, 0.5% Tween 20) with 5% non-fat milk for 1 h at room temperature. The primary antibodies (anti-apoE, anti-apoA-I, anti-apoA-IV, anti-apoB100, anti-apoB48, anti-CD36, anti-MTP, anti-tACCα, anti-pACC, anti-apoC-III, anti-pAMPK, anti-Grb-2, and anti-β-actin) were diluted in the same buffer and the blot was incubated for 12 h at 4°C. The dilution of primary antibodies was 1:1,000 and that of secondary antibodies was 1:4,000. After extensive washing in a TBS-Tween buffer, the membranes were incubated with goat anti-rabbit horseradish peroxidase conjugated antibodies for 1 h at room temperature, washed again, and subjected to chemiluminescent signal detection. The protein band intensities were quantified using Freeware image analysis software (ImageJ; https://imagej.nih.gov/ij).

The enzyme-linked immunosorbent assay (ELISA)

The concentration of apoB48 in the basolateral fluid obtained after incubation with Caco-2 cells was also determined by an immunoenzymatic method using an ELISA kit from BioSciences (Allentown, PA, USA). An apoB48 solution (0–188 nM) was used as a standard. The coefficient of variation of the ELISA was <10% (intra-assay) and <12% (inter-assay). ELISA was performed using a microplate reader Model 680 from BioRad (Hercules, CA, USA).

Acylglycerol (AC) assays

The sum of mono-, di- and triacylglycerols was determined using BioSystems lipoprotein lipase/glycerophosphate oxidase/peroxidase enzymatic assay (Sriperumbudur, Tamil Nadu, India). AC was determined in the supernatant obtained after *in vitro* digestion, in the basolateral fluid obtained after incubation with Caco-2 cells and in the fluid obtained after incubation with Hep G2. To this end, 10 µL of the test sample was added to 1 mL of the reagent, and the mixture was incubated for 15 min at room temperature. Absorbance was measured at 500 nm wavelength using a flow single beam spectrophotometer Specord 40 (AnalytikJena, Jena, Germany). The TG solution with a concentration of 0–18 µM was used to plot the standard curve.

Cholesterol (Chol) assays

Free and esterified cholesterol content was determined using a cholesterol esterase/cholesterol oxidase/peroxidase enzymatic assay kit from BioSysteme. Cholesterol fractions were determined in: the supernatant obtained after *in vitro* digestion, the basolateral fluid obtained after incubation with Caco-2 cells, and the fluid obtained after incubation with Hep G2. To this end, 10 µL of the test sample was added to 1 mL of the reagent, and the mixture was incubated for 10 min at room temperature. Absorbance was measured at 500 nm wavelength using a Specord 40 spectrophotometer (AnalytikJena). A Chol solution with a concentration of 0–0.8 µM was used to plot the standard curve.

Free fatty acids (FFA) assays

The concentration of free fatty acids was determined using the enzymatic assay NEFA-HR acyl-CoA synthase/acyl-CoA oxidase/peroxidase kit from Wako Chemicals GmbH (Neuss, Germany). FFA were determined in: the supernatant obtained after *in vitro* digestion, the basolateral fluid obtained after incubation with Caco-2 cells, the basolateral fluid after incubation with LPL, and the fluid obtained after incubation with Hep G2. To this end, 10 µL of the test sample was added to 0.5 mL of the reagent, and the mixture was incubated for 7 min at 37°C. Absorbance was measured at 546 nm wavelength using Specord 40 spectrophotometer (AnalytikJena). A Wako calibrator (FFA concentration up to 4 mM) was used as a standard.

Thiobarbituric acid reactive substances (TBARS) assays

The supernatant (0.5 mL) obtained after *in vitro* digestion of the model product was mixed with 0.5 mL of 0.01% (*w/v*) ethanolic BHT solution (to protect against the formation of peroxidation products during analysis). Next, 0.5 mL of a 10% (*w/v*) solution of trichloroacetic acid (TCA) in 0.25 M HCl and 0.5 mL of a 0.67% (*w/v*) solution of thiobarbituric acid (TBA) in 0.25 M HCl were added and the mixture was incubated at 100°C for 20 min. After cooling, the sample was centrifuged (850×*g*, 15 min, 4°C), and absorbance was measured at 535 nm wavelength (spectrophotometer Specord 40, AnalytikJena). An aqueous solution of TEP with a concentration up to 2 µM malondialdehyde (MDA) was used to prepare a standard curve.

Statistical analysis

Data were expressed as means values ± standard deviation (n=4). Statistical analysis was performed using Statistica 13.3 (StatSoft Polska, Cracow, Poland). One-way ANOVA with post hoc Bonferroni's test was used to compare groups. Whereas, in order to examine the relationship between the variables, the Pearson correlation coefficient (r) was calculated. In statistical analyses, a level of significance of <5% was considered significant.

RESULTS AND DISCUSSION

Effects of BHT, BHA and TBHQ on *in vitro* fat digestion

Fat digestion in the human gastrointestinal tract is a process involving emulsification and hydrolysis catalysed by salivary, gastric, and pancreatic lipases. These enzymes work at the interface; hence, lipolysis effectiveness depends, among other things, on the degree of fat emulsification. The effect of synthetic antioxidants on fat emulsification after digestion of a model product under gastric and under duodenal conditions was determined by evaluating the emulsification degree and fat droplet size in the emulsified layer at both stages (Table 1). Some representative images of fat droplets in the emulsion stained with Sudan III are shown in Figure 2. Emulsification degree after gastric digestion ranged from

Table 1. Emulsification degree and diameter of fat droplets of model products with antioxidants and without antioxidants (control) after their *in vitro* digestion under stomach and duodenal conditions, and concentrations of thiobarbituric acid reactive substances (TBARS), free fatty acids (FFA), acylglycerols (AG) and cholesterol (Chol) after digestion under duodenal conditions.

Parameter	Digestion stage	Control	BHT	BHA	TBHQ
Emulsification degree (%)	Stomach	54.0±3.8^{b}	54.3±5.9^{b}	68.8±4.2^{a}	61.2±5.9^{ab}
	Duodenum	100^{a}	100^{a}	100^{a}	100^{a}
Diameter of fat droplets (µm)	Stomach	13.0±2.7^{a}	10.4±2.5^{a}	10.6±1.3^{a}	11.8±1.8^{a}
	Duodenum	2.41±0.93^{b}	4.22±2.38^{a}	2.08±1.29^{b}	2.46±0.83^{b}
TBARS concentration (µmol/L)	Duodenum	0.24±0.13^{a}	0.22±0.12^{a}	0.22±0.13^{a}	0.23±0.11^{a}
FFA concentration (mmol/L)	Duodenum	2.05±0.32^{a}	2.31±0.46^{a}	2.34±0.23^{a}	2.56±0.23^{a}
AG (TG+DG+MG) concentration (mmol/L)	Duodenum	3.34±0.76^{a}	3.63±1.43^{a}	4.02±0.43^{a}	3.76±0.41^{a}
Chol concentration (mmol/L)	Duodenum	0.47±0.02^{a}	0.45±0.03^{a}	0.44±0.04^{a}	0.41±0.06^{a}

BHT, butylated hydroxytoluene; BHA, butylated hydroxyanisole; TBHQ, tert-butylhydroquinone; TG, triacylglycerols; DG, diacylglycerols; MG, monoacylglycerols; Data are mean ± standard deviation (n=4). Values with different letters within a row differ significantly (post hoc Bonferroni's test, p<0.05).

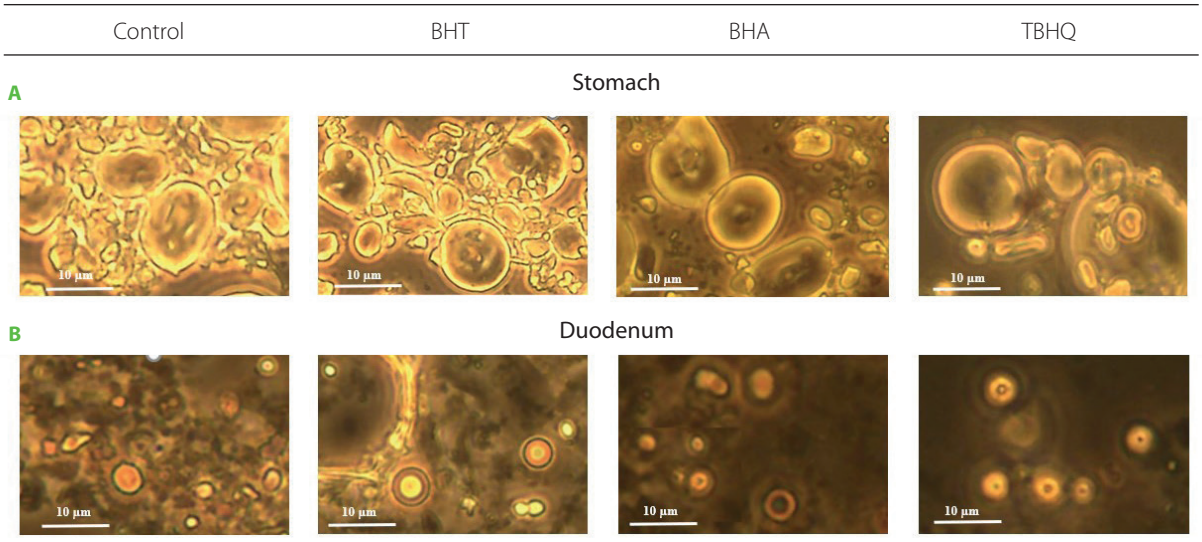

Figure 2. Fat droplets stained with Sudan III in the emulsion after *in vitro* digestion of a model product without (control) and with antioxidants in the stomach (**A**) and in the duodenum (**B**). Scale bars were placed on each image. BHT, butylated hydroxytoluene; BHA, butylated hydroxyanisole; TBHQ, tert-butylhydroquinone.

54.0% to 68.8% and differed significantly ($p<0.05$) from the control only for BHT (14.7% higher). No significant differences ($p\geq0.05$) were observed in the mean size of droplets forming emulsions (Table 1, Figure 2). However, the leading site of lipid digestion is the duodenum; thus, changes in emulsion characteristics at this stage have the key effect on its hydrolysis. After intestinal digestion, the emulsified layer was already 100% in all samples, including the control, although in the case of BHT, the droplets forming the emulsion had significantly larger diameters compared to the other samples (Table 1, Figure 2). At this stage of *in vitro* digestion, the favourable changes in emulsion characteristics after gastric digestion observed for BHA were not maintained. The emulsification progress observed between the stomach and duodenum was due to the action of bile salts and advanced TG hydrolysis, and the measured fat droplet diameters were consistent with the values noted in the human gastrointestinal tract [Armand *et al.*, 1999].

Further analyses showed that the synthetic antioxidants did not affect fat digestibility. Indeed, the contents of FFA and AG in the supernatants obtained after *in vitro* digestion of the model product with or without BHT, BHA and TBHQ did not differ significantly ($p\geq0.05$), (Table 1). Even the addition of BHT did not inhibit fat hydrolysis, although the emulsion formed in its presence had significantly larger droplets. Hence, it can be concluded that pancreatic lipase activity was only to some extent dependent on the degree of substrate emulsification, with fat droplets from 2.1 to 4.2 µm in diameter being hydrolysed with the same strength.

Furthermore, at this stage, the progression of FA peroxidation in the control sample was excluded. No differences were noted in the TBARS content between samples with and without the antioxidants (Table 1). Lipid peroxidation could significantly modify the intestinal absorption of FFA [Courtois *et al.*, 2002].

Effects of synthetic phenolic antioxidants on intestinal absorption

The effect of synthetic phenolic antioxidants on the bioavailability of lipids from an *in vitro* digested model product stabilised with these antioxidants was examined using the Caco-2 cell line. The selection of Caco-2 cells as the best model for the study of bioavailability was determined by their ability to differentiate into cells morphologically and physiologically similar to normal intestinal cells, *i.e.* the production of tight connections between each other and the formation of a brush border, the ability to produce enzymes (*e.g.*, alkaline phosphatase, sucrase and aminopeptidase) and systems that transport substances from the lumen of the digestive tract to the bloodstream. The antioxidants were found to be non-toxic to Caco-2 cells under the conditions used; the visibility of the cells was 95.8–97.9% and was not significantly different ($p\geq0.05$) from that of the control (Table 2).

In the intestinal absorption model, Caco-2 cells take FFA and monoacylglycerols (MG) from the mixture placed in the apical chamber and use them to synthesise TGs that are part of the CMs secreted into the basolateral fluid. In our study, apoB48, apoA-IV, TG, and Chol levels were assayed in the basolateral fluid after incubation of Caco-2 cells with supernatants obtained after *in vitro* digestion of model hight-fat products. The results are shown in Table 2 and Figure 3A. The addition of antioxidants increased the absorption rate of TG and decreased the absorption rate of Chol. The absorption rates of TG and Chol in the control were 7.0% and 13.8%, respectively, and in the presence of synthetic phenolic antioxidants ranged from 7.8% to 8.5% for TG and from 8.6% to 13.1% for Chol. The antioxidants caused a 22–38% increase in TG secretion by Caco-2 cells compared to the control. BHA also caused a significant ($p<0.05$) alteration in Chol absorption, reducing its uptake by about 40%. All of the antioxidants also significantly regulated the ability of Caco-2 cells to release apoB48 and thus affected the amount of CMs formed. Most of the apoB48 was released by cells incubated with BHT and TBHQ, 2.1 and 2.6 times more than the cells with the control sample, respectively. These values were also comparable to or greater than those observed when AMPK inhibitor was used. Furthermore, the presence of synthetic antioxidants significantly ($p<0.05$) affected the amount of apoA-IV released by Caco-2 cells (Figure 3A). In extreme cases, *i.e.*, when incubated with the antioxidants BHT and TBHQ, the concentration in the basolateral fluid was about 90% lower than for the control. Such a significant postprandial decrease in apoA-IV may translate into a lack of satiety after consuming high-fat foods stabilised with these antioxidants. There was a very strong inverse correlation ($r=-0.94$) between the amount of apoB48 and apoA-IV released by Caco-2 cells. To sum up, the presence of antioxidants significantly modified the structure of CMs secreted by

Table 2. Viability of Caco-2 cells, intestinal absorption rate of triacylglycerols (TG) and cholesterol (Chol) of *in vitro* digested products without (control) and with antioxidants, and the concentration of TG, Chol and apoB48 secreted by Caco-2 cells into basolateral fluid after their treatment with digested model products.

Parameter	Control	Antioxidant			Regulator of AMPK activity	
		BHT	BHA	TBHQ	Aicar	Compound C
Cell viability (%)	97.4±2.6^{a}	96.3±2.9^{a}	97.9±2.1^{a}	95.8±3.1^{a}	-	-
TG concentration (mmol/L)	0.232±0.031^{c}	0.283±0.012^{b}	0.314±0.021^{ab}	0.321±0.022^{ab}	0.152±0.031^{d}	0.342±0.032^{a}
Chol concentration (mmol/L)	0.065±0.010^{a}	0.059±0.015^{a}	0.038±0.008^{b}	0.046±0.009^{ab}	0.069±0.013^{a}	0.071±0.016^{a}
apoB48 concentration (nmol/L)	1.62±0.65^{c}	3.43±0.44^{ab}	0.54±0.26^{d}	4.28±0.51^{a}	0.84±0.43^{cd}	2.98±0.69^{bc}
TG absorption rate (%)	7.0	7.8	7.8	8.5	-	-
Chol absorption rate (%)	13.8	13.1	8.6	11.2	-	-

BHT, butylated hydroxytoluene; BHA, butylated hydroxyanisole; TBHQ, tert-butylhydroquinone; AMPK, AMP dependent kinase; Aicar, AMPK activator; Compound C, AMPK inhibitor. Data are mean ± standard deviation ($n=4$). Values with different letters within a row differ significantly (post hoc Bonferroni's test, $p<0.05$).

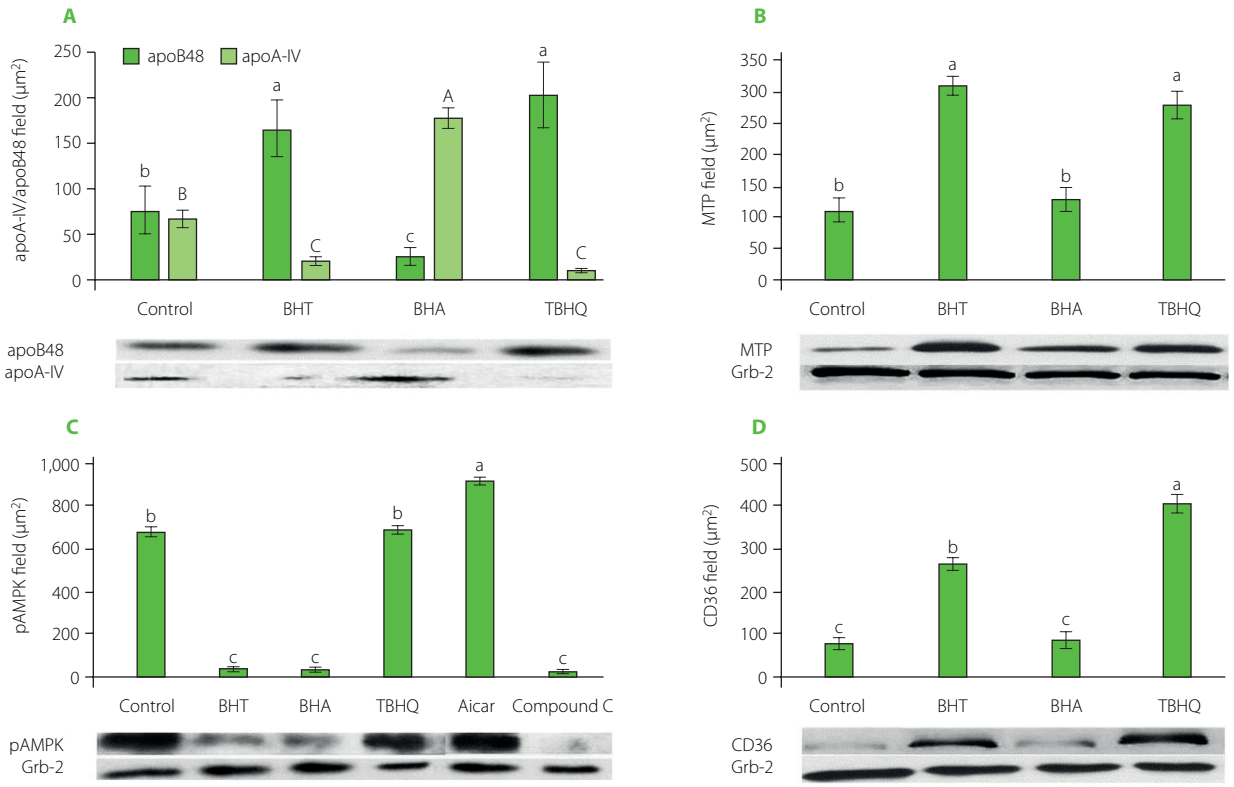

Figure 3. The amount of apoB48 and apoA-IV secreted by Caco-2 cells (**A**) and levels of microsomal triglyceride transfer protein, MTP (**B**), phospho-AMP dependent kinase, pAMPK (**C**) and fatty acid translocase, CD36 (**D**) in Caco-2 cells after their treatment with digested model products without antioxidants (control) and with butylated hydroxytoluene (BHT), butylated hydroxyanisole (BHA) and tert-butylhydroquinone (TBHQ). Aicar, AMPK activator; Compound C, AMPK inhibitor. Data are mean ± standard deviation (n=4). Significant differences among gropus were marked with different letters (post hoc Bonferroni's test, p<0.05).

Caco-2 cells. In the case of BHA, the increase in the amount of secreted TGs uncorrelated with the increase in the amount of apoB48 resulted in the formation of less numerous but large CMs additionally stabilised by apoA-IV. In contrast, in the presence of BHT and TBHQ, the CMs formed were more numerous but smaller than in the control sample. This observation, with all proportions maintained, is shown in Figure 4. The scheme shows that for every very large CM released by Caco-2 cells in the presence of BHA, there are as many as 7 and 8 small CMs released in the presence of BHT and TBHQ, respectively, and only 3 intermediate-sized CMs released in the control sample. The importance of apoA-IV in the transport of higher amounts of TG through CM was previously demonstrated in studies performed on porcine intestinal epithelial cells [Lu *et al.*, 2006].

Factors that may contribute to the changes in the composition of secreted CMs are the CD36 transporter located, among others, in the intestinal brush-border membrane and involved in CM formation. Mice with deletion of the CD36 gene secrete less apoB48 [Nassir *et al.*, 2007; Tran *et al.*, 2011]. Another important factor regulating CM synthesis may be the MTP. This protein is located in the endoplasmic reticulum of cells and is primarily responsible for transporting and attaching lipids to apoB48. The absence of MTP occurs in abetalipoproteinemia patients in whom hepatocytes and enterocytes are unable to synthesise lipoprotein B [Burnett *et al.*, 2022]. AMPK, whose metformin-mediated activation has been linked to the inhibition of intestinal absorption of FFA, may also play an essential role in CM synthesis and secretion [Harmel *et al.*, 2014]. The effects

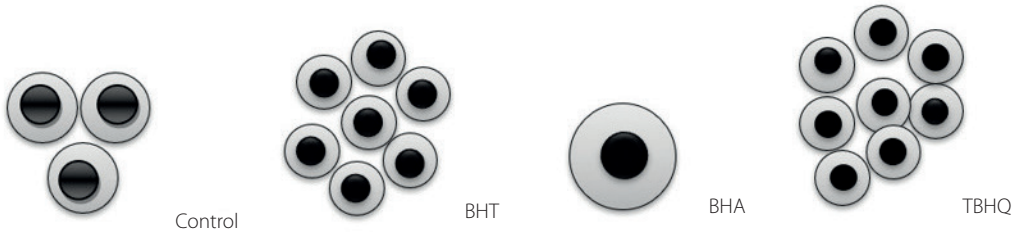

Figure 4. Scheme of the number and size of chylomicrons (CMs) secreted by Caco-2 cells treated with the digested model product without antioxidants (control) and with butylated hydroxytoluene (BHT), butylated hydroxyanisole (BHA) and tert-butylhydroquinone (TBHQ) at 100 mg/kg fat. The amount of CMs was estimated from the amount of apoB48, and their size from the amount of triacylglycerols (grey) and cholesterol (black) *per* apoB48 molecule.

of BHT, BHA, and TBHQ on the levels of these proteins in Caco-2 cells are shown in Figure 3 B–D. Similar to Compound C, BHT significantly decreased the amount of pAMPK in Caco-2 cells and simultaneously increased the expression of CD36 and MTP approximately threefold. The ability of Caco-2 cells to synthesise these proteins also increased in the presence of TBHQ, although this antioxidant did not affect the AMPK activity. The BHA worked differently, which decreased the level of pAMPK but did not affect the intensity of CD36 and MTP synthesis by Caco-2 cells.

The juxtaposition of these results with the previously described effects of BHT, BHA, and TBHQ on the ability of Caco-2 cells to release TG and apoB48 (Table 2) showed significant relationships. An inverse correlation (r=–0.72) was observed between the amount of TG secreted by cells and the degree of AMPK phosphorylation. Similar relationships were previously shown for metformin, which enhanced AMPK activity and suppressed intestinal absorption of FFA [Harmel *et al.*, 2014].

A very strong correlation was also found between the amount of apoB48 secreted by Caco-2 cells and the amount of CD36 (r=0.91) and MTP (r=0.99) in cells. The relationship between the amount of CD36 transporter and the amount of CM secreted by enterocytes was observed by Nassir *et al.* [2007]. However, in their study, decreased amounts of apoB48 were also accompanied by reduced amounts of secreted TG and apoA-IV. In contrast, in our study, BHA caused an increase in the TG uptake and a decrease in the level of CMs, necessitating an increase in apoA-IV synthesis to allow the transport of increased lipids by fewer CMs.

Effects of BHT, BHA and TBHQ on chylomicron catabolism: The Hep G2 cell model

CM catabolism begins with TG hydrolysis catalysed by lipoprotein lipase (LPL) bound to the luminal surface of endothelial cells in capillaries. The FFA released by its action are used by fat tissue and muscles, among others. Effective hydrolysis of TGs transported by CMs depends on the concentration of apoC-III. Due to the presence of hydrophobic residues, this apoprotein exhibits the ability to bind on the surface of lipoproteins and thus restrict LPL access to the substrate [Larsson *et al.*, 2013]. Consequently, the removal of TG-rich CMs from the bloodstream is impaired, and the time of postprandial hypertriglyceridemia is prolonged. In our study, all antioxidants induced enhanced apoC-III secretion by Hep G2 cells (Figure 5A). The greatest increase in the amount of apoC-III (of approximately 70%) was determined for the samples with BHT. For the other antioxidants, the increase in the amount of proteins was about 40%. Due to the study design, the involvement of apoC-III in lipoprotein lipase inhibition was observed. However, in feeding studies, a significant increase in TG concentration (2.5-fold) was observed in the blood of rabbits fed a high-cholesterol diet with 1% BHT [Björkhem *et al.*, 1991]. The authors could not explain the mechanism of the observed changes but suggested that they were related to the inhibition of lipoprotein lipase activity. The involvement of apoC-III in disorders of lipid metabolism has been the subject of many studies. A comparison of apoC-III levels in obese and normal-weight subjects showed that increased body weight is associated with elevated levels of this protein [Talayero *et al.*, 2014]. In addition, high plasma apoC-III levels correlate with the occurrence of coronary artery disease [Onat *et al.*, 2003].

After TG hydrolysis of CMs, CMRs are formed containing mainly CE and apoB48 (apoA-IV is an exchangeable protein and is transferred to HDL). Since there is only one apoB48 molecule *per* CMR molecule, their size is determined primarily by the amount of cholesterol transported. Caco-2 cells under the influence of BHA secreted the largest CMs containing the highest amount of both TG and CE (Figure 4). Consequently, the resulting CMRs had the largest diameters. In contrast, CMRs in TBHQ and BHT samples were significantly smaller. The efficiency of uptake of the remnants by Hep G2 cells in the control sample was about 63% (Table 3). The smaller CMRs formed in the BHT- and TBHQ-supplemented samples were more efficiently taken up by the cells, and after 4 h of incubation, their absorption rates were 85.0% and 99.5%, respectively. In contrast,

Table 3. Absorption rate of chylomicron remnants (CMR) and cholesterol (Chol) by Hep G2 cells and concentration of triacylglycerols (TG), free fatty acids (FFA), Chol, endogenous fatty acids (EFA) and endogenous cholesterol (EChol) in the fluid obtained after incubation of Hep G2 cells with digested and treated with Caco-2 cell model products.

Parameter	Control	BHT	BHA	TBHQ
CMR concentration (nmol/L)	0.603±0.051^{a}	0.514±0.032^{b}	0.512±0.043^{b}	0.021±0.011^{c}
TG concentration (mmol/L)	0.761±0.083^{b}	1.022±0.075^{a}	0.781±0.049^{b}	1.010±0.052^{a}
Chol concentration (mmol/L)	0.081±0.008^{a}	0.061±0.005^{b}	0.092±0.009^{a}	0.056±0.006^{b}
FFA concentration (mmol/L)	0.298±0.011^{a}	0.281±0.012^{ab}	0.266±0.014^{b}	0.239±0.015^{c}
CMR absorption rate (%)	62.8	85.0	4.4	99.5
FFA absorption rate (%)	57.3	66.9	71.7	75.2
EFA concentration (mmol/L)	1.59±0.119^{b}	2.22±0.222^{a}	1.40±0.128^{b}	2.07±0.156^{a}
EChol concentration (mmol/L)	0.018±0.009^{b}	0.002±0.003^{c}	0.053±0.011^{a}	0.009±0.008^{bc}

BHT, butylated hydroxytoluene; BHA, butylated hydroxyanisole; TBHQ, tert-butylhydroquinone. Data are mean ± standard deviation (n=4). Values with different letters within a row differ significantly (post hoc Bonferroni's test, p<0.05).

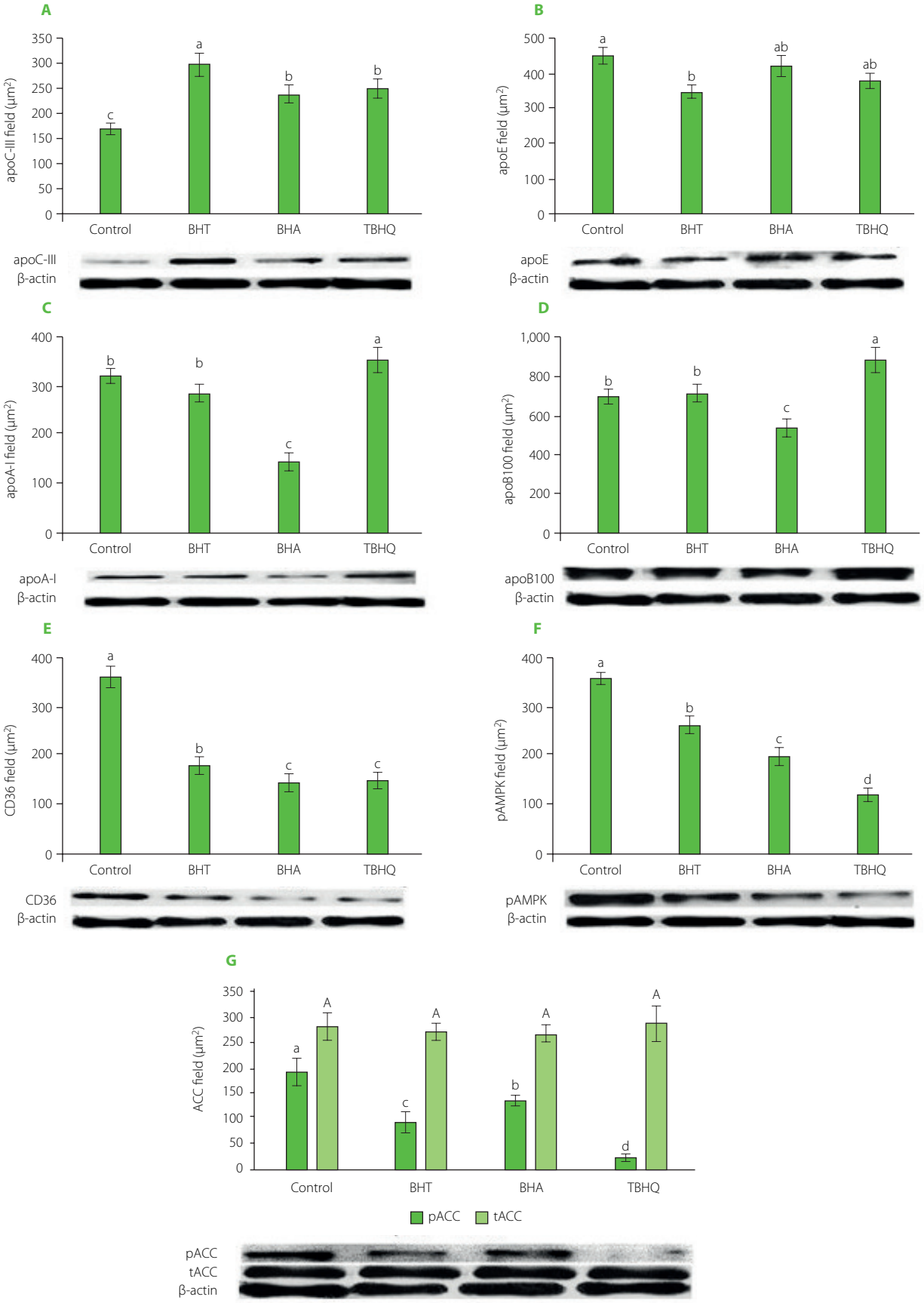

Figure 5. The amount of apoC-III (**A**), apoE (**B**), apoA-I (**C**) and apoB100 (**D**) secreted by Hep G2 cells and levels of CD36 (**E**), pAMPK (**F**) and ACC (**G**) in Hep G2 cells after their treatment with basolateral fluid obtained after incubation of Caco-2 cells with the supernatant received after *in vitro* digestion of a model product without (control) and with antioxidants. BHT, butylated hydroxytoluene; BHA, butylated hydroxyanisole; TBHQ, tert-butylhydroquinone; CD36, fatty acid translocase; pAMPK, phospho-AMP dependent kinase; ACC, acetyl-CoA carboxylase. Data are mean ± standard deviation (n=4). Significant differences among gropus were marked with different letters (post hoc Bonferroni's test, p<0.05).

the uptake of large CMRs formed in the BHA-containing sample was strongly inhibited, and the amount of particles taken up by the cells reached only 4.4% at the end of incubation. A very strong correlation was found between CMR size and absorption rate (r=0.995).

CMRs are taken up from the bloodstream by liver cells mainly *via* membrane-bound LDL receptors [Martins *et al.*, 2000]. It is known that this process requires the presence of apoE, as CMRs cannot bind to LDL receptors *via* apoB48 because this protein lacks the β2 domain responsible for this process [Hinsdale *et al.*, 2002]. In our study, cells secreted 25% less apoE in the BHT-supplemented sample, but this did not affect the efficiency of CMR removal (Figure 5B).

Efficient CMR uptake by hepatocytes allows cholesterol-rich particles to be removed from the bloodstream. The disruption of this mechanism observed in the samples with BHA may result in the uptake of remnants by macrophages and lead to atherosclerosis [Bentley *et al.*, 2011]. CMRs lack TG, which makes their diameter small enough to get inside macrophages [Proctor & Mamo, 2003]. This can lead to the formation of foam cells that contribute to the development of atherosclerosis [Yu & Mamo, 2000].

In the samples with the addition of the tested antioxidants, Hep G2 cells took up FFA formed after hydrolysis of TGs present in CM more efficiently (Table 3). To identify the mechanism by which synthetic phenolic antioxidants modify the FFA uptake, CD36 receptor and pAMPK levels were examined. Each of the antioxidants tested caused a decrease in CD36 protein content (Figure 5E), as well as in the amount of the active form of AMPK (Figure 5F) in Hep G2 cells. A strong correlation (r=0.833) was found between AMP-dependent kinase activity and the amount of CD36 transporter. Furthermore, strong inverse correlations were determined between FFA uptake and the amount of both pAMPK (r=–0.983) and CD36 transporter (r=–0.919).

Effects of BHT, BHA and TBHQ on lipid metabolism in Hep G2 cells

FFA, derived from dietary lipids, can be used as an energy source (β-oxidation process) or for TG synthesis. TGs and CEs formed in the liver enter into the VLDL or HDL. The marker apoprotein of VLDL is apoB100. For every molecule of VLDL, there is one molecule of apoB100. The primary function of VLDL is to distribute lipids and cholesterol (LDL formed from VLDL after hydrolysis of the TG portion by LPL) into the body's cells. ApoB100 is a large protein with a molecular weight of 550 kDa [Hegele, 2009]. Within this protein, there is a hydrophobic region that allows the binding of TG and a hydrophilic region that shows an affinity for the aqueous environment of blood. In addition, apoB100 has a binding domain for LDL receptors. This allows the uptake of LDL particles by peripheral tissue cells [Gruffat *et al.*, 1996].

The effect of BHT, BHA and TBHQ on hepatic lipid metabolism was studied using the Hep G2 cell line, which is currently the most frequently used model of human hepatocytes, distinguished from others by its phenotype most similar to the hepatic, *e.g.*, the synthesis of albumin and other proteins, including coagulation factors [Coward *et al.*, 2009]. In the presence of TBHQ, Hep G2 cells secreted significantly more VLDL (apoB100) than the cells of the control sample, whereas BHA contributed to their suppressed secretion (Figure 5D). VLDL-transported CEs are formed from Chol produced in the liver or taken up by hepatocytes as CMR. In our study, a very strong inverse correlation was determined between Chol synthesis in Hep G2 cells and the efficiency of CMR uptake by these cells (r=–0.945). In addition, hepatocytes of the BHA-supplemented sample synthesised almost three times more Chol than the cells of the control samples and nearly 26 times more than the BHT- or TBHQ-supplemented samples (Table 3). Although Caco-2 cells absorbed the least cholesterol in the presence of BHA, the fact that CMR uptake by hepatocytes was completely inhibited resulted in such an intense biosynthesis of Chol that we ultimately determined the highest cholesterol concentration in the culture fluid of Hep G2 cells in these samples. Also, FA synthesis was strongly correlated (r=0.874) with the efficiency of CMR uptake by hepatocytes. Cells in which the CMR uptake was inhibited synthesised less FA (Table 3). Thus, CMR uptake efficiency correlated strongly with the amount of VLDL lipoprotein secreted (r=0.887). Cells that removed most of the CMR under TBHQ treatment secreted the most VLDL.

Of the antioxidants tested, only BHA did not increase TG synthesis in hepatocytes (Table 3). To synthesise TG, hepatocytes use FFA derived from ingested fat and fatty acids produced from non-lipid components. The decrease in hepatic AMPK activation is responsible for inhibiting FA β-oxidation and activating FA and TG biosynthesis [Ford *et al.*, 2015]. Silencing the expression of the gene encoding AMPK in the liver results in increased lipogenesis and increased plasma TG levels [Andreelli *et al.*, 2006]. AMP-dependent kinase controls lipogenesis primarily by altering the degree of phosphorylation of ACC, a key enzyme of the FA biosynthesis pathway. In the case of ACC, the active form of the enzyme is unphosphorylated. All antioxidants tested decreased the amount of the active form of AMPK (Figure 5F) and increased the amount of the active form of ACC (Figure 5G). A strong correlation was determined between ACC activity and the intensity of FA biosynthesis in hepatocytes (r=0.711).

The antioxidants tested also affected the amount of apoA-I synthesised by Hep G2 cells (Figure 5C). ApoA-I is the major structural and functional protein of HDL particles. It accounts for up to 60% of all proteins that make up this lipoprotein and plays a vital role in a process called reverse cholesterol transport. The presence of ApoA-I enables the transfer of cholesterol and phospholipids from cells to HDL particles. This protein attaches to the ATP-A1-binding cassette transporter (ABCA1) located on the cell surface and regulates the function of lecithin-cholesterol acetyltransferase (LCAT), which catalyses cholesterol esterification [Asztalos & Schaefer, 2003]. Reverse cholesterol transport is particularly important in removing excess cholesterol from macrophages and transporting it to the liver. The level of this protein in the fluid after the culture of Hep G2 cells allowed us to evaluate the potential effect of the tested compounds on the production of HDL particles by hepatocytes. TBHQ and BHA significantly (p<0.05)

modified the secretion of apoA-I (Figure 5C). For the TBHQ-supplemented sample, higher amounts of apoA-I were determined than in the control sample, whereas for the BHA-supplemented sample, a decrease in the level of this protein was found. In contrast, BHT had no significant ($p \geq 0.05$) effect on apoA-I content in Hep G2 cell culture fluid. Therefore, it can be concluded that the use of TBHQ as a food additive can increase HDL fraction cholesterol levels, reducing the risk of atherosclerosis. However, the composition of the apoproteins that make up the HDL fraction plays an essential role in the efficient transport of cholesterol to the liver. Lipoproteins with apoC-III bound on the surface perform less efficiently [Luo *et al.*, 2017]. In human studies, it has been observed that the plasma of patients diagnosed with coronary artery disease has a high content of apoC-III-rich HDL particles [Luo *et al.*, 2017; Riwanto *et al.*, 2013; Xiong *et al.*, 2015]. In our study, synthetic phenolic antioxidants contributed to increased apoC-III secretion (Figure 5A). Hence, stimulating hepatocytes to produce higher apoC-III may result in higher HDL levels that do not protect against atherosclerosis.

CONCLUSIONS

Synthetic phenolic antioxidants (BHT, BHA, or TBHQ) used in the food industry significantly modify the bioavailability and metabolism of lipids. *In vitro* studies have shown that these antioxidants used at a dose of 100 mg/kg of fat do not affect the digestibility of fat, but induce an increase in the intestinal absorption of TG and modify CM structure. The addition of BHT and TBHQ inhibited apoA-IV synthesis. At the same time, smaller chylomicrons were secreted, but their amount was greater than in the sample without antioxidants. In contrast, BHA activated apoA-IV synthesis, resulting in the formation of fewer but very large CMs. The observed significant decrease in apoA-IV secretion in the BHT- and TBHQ-supplemented samples may result in a lack of satiety after consumption of high-fat foods stabilised with these antioxidants. Also of concern is the increased secretion of apoC-III by hepatocytes observed in the presence of the antioxidants tested, especially with the addition of BHT. Indeed, an increase in LPL inhibitory apoprotein may lead to hyperlipidemia associated with increased CM catabolism time. The efficiency of hepatocyte uptake of CMRs resulting from catabolism was inversely correlated with their size. The small CMRs formed in the samples with BHT and TBHQ were almost entirely taken up, while the uptake of large CMRs present in the samples with BHA by Hep G2 cells was minimal. The prolongation of CMR catabolism time with BHA can lead to hyperlipidemia, the consequences of which include atherosclerosis. Furthermore, the inhibition of CMR uptake in the presence of BHA resulted in a substantial enhancement of cholesterol biosynthesis in hepatocytes. The results of our *in vitro* study shed new light on synthetic phenolic antioxidants used in food technology in the possible generation of obesity and atherosclerosis. However, at this stage of research, it is impossible to clearly separate antioxidants that promote the development of these diseases from those, which do not do that. To this end, further studies on macrophage cell lines must be carried out to verify CMR uptake, and *in vivo* studies should be conducted on a properly selected animal model to assess the impact of apoA-IV on the feeling of satiety and food intake.

RESEARCH FUNDING

This research did not receive any specific grant from funding agencies in the public, commercial, or not-for-profit sectors.

CONFLICT OF INTERESTS

The authors declare that the research was conducted in the absence of any commercial or financial relationships that could be construed as a potential conflict of interest.

ORCID IDs

M. Mika https://orcid.org/0000-0002-6682-6505
A. Wikiera https://orcid.org/0000-0002-5736-8469

REFERENCES

1. Acevedo-Fani, A., Singh, H. (2022). Biophysical insights into modulating lipid digestion in food emulsions. *Progress in Lipid Research*, *85*, art. no. 101129. https://doi.org/10.1016/j.plipres.2021.101129
2. Andreelli, F., Foretz, M., Knauf, C., Cani, P.D., Perrin, C., Iglesias, M.A., Pillot, B., Bado, A., Tronche, F., Mithieux, G., Vaulont, S., Burcelin, R., Viollet, B. (2006). Liver adenosine monophosphate-activated kinase-α2 catalytic subunit is a key target for the control of hepatic glucose production by adiponectin and leptin but not insulin. *Endocrinology*, *147*(5), 2432–2441. https://doi.org/10.1210/en.2005-0898
3. Armand, M., Pasquier, B., André, M., Borel, P., Senft, M., Peyrot, J., Salducci, J., Portugal, H., Jaussan, V., Lairon, D. (1999). Digestion and absorption of 2 fat emulsions with different droplet sizes in the human digestive tract. *The American Journal of Clinical Nutrition*, *70*(6), 1096–1106. https://doi.org/10.1093/ajcn/70.6.1096
4. Asztalos, B.F., Schaefer, E.J. (2003). High-density lipoprotein subpopulations in pathologic conditions. *The American Journal of Cardiology*, *91*(7A), 12–17. https://doi.org/10.1016/S0002-9149(02)03383-0
5. Bentley, C., Hathaway, N., Widdows, J., Bejta, F., De Pascale, C., Avella, M., Wheeler-Jones, C.P.D., Botham, K.M., Lawson, C. (2011). Influence of chylomicron remnants on human monocyte activation *in vitro*. *Nutrition, Metabolism and Cardiovascular Diseases*, *21*(11), 871–878. https://doi.org/10.1016/j.numecd.2010.02.019
6. Björkhem, I., Henriksson-Freyschuss, A., Breuer, O., Diczfalusy, U., Berglund, L., Henriksson, P. (1991). The antioxidant butylated hydroxytoluene protects against atherosclerosis. *Arteriosclerosis and Thrombosis: A Journal of Vascular Biology*, *11*(1), 15–22. https://doi.org/10.1161/01.ATV.11.1.15
7. Burnett, J.R., Hooper, A.J., Hegele, R.A. (2022). Abetalipoproteinemia. In M.P. Adam, D.B. Everman, G.M. Mirzaa, R.A. Pagon, S.E. Wallace, L.J.H. Bean, K.W. Gripp, A. Amemiya (Eds.), *GeneReviews® [Internet]*, University of Washington, Seattle, Washington, USA, pp. 1993–2023.
8. Commission Regulation (EU) No 1129/2011 of 11 November 2011 amending Annex II to Regulation (EC) No 1333/2008 of the European Parliament and of the Council by establishing a Union list of food additive. https://eur-lex.europa.eu/LexUriServ/LexUriServ.do?uri=OJ:L:2011:295:0001:0177:EN:PDF
9. Courtois, F., Delvin, E., Ledoux, M., Seidman, E., Lavoie, J.-C., Levy, E. (2002). The antioxidant BHT normalizes some oxidative effects of iron + ascorbate on lipid metabolism in Caco-2 cells. *The Journal of Nutrition*, *132*(6), 1289–1292. https://doi.org/10.1093/jn/132.6.1289
10. Coward, S.M, Legallais, C., David, B., Thomas, M., Foo, Y., Mavri-Damelin, D., Hodgson, H.J., Selden, C. (2009). Alginate-encapsulated Hep G2 cells in a fluidized bed bioreactor maintain function in human liver failure plasma. *Artificial Organs*, *33*(12), 1117–1126. https://doi.org/10.1111/j.1525-1594.2009.00821.x
11. Ford, R.J., Fullerton, M.D., Pinkosky, S.L., Day, E.A., Scott, J.W., Oakhill, J.S., Bujak, A.L., Smith, B.K., Crane, J.D., Blümer, R.M., Marcinko, K., Kemp, B.E., Gerstein, H.C., Steinberg, G.R. (2015). Metformin and salicylate synergistically activate liver AMPK, inhibit lipogenesis and improve insulin sensitivity. *Biochemical Journal*, *468*(1), 125–132. https://doi.org/10.1042/BJ20150125
12. Gruffat, D., Durand, D., Graulet, B., Bauchart, D. (1996). Regulation of VLDL synthesis and secretion in the liver. *Reproduction Nutrition Development*, *36*(4), 375–389. https://doi.org/10.1051/rnd:19960404

13. Harmel, E., Grenier, E., Ouadda, A.B., Chebly, M.E., Ziv, E., Beaulieu, J.F., Sané, A., Spahis, S., Laville, M., Levy, E. (2014). AMPK in the small intestine in normal and pathophysiological conditions. *Endocrinology*, *155*(3), 873–888. https://doi.org/10.1210/en.2013-1750
14. Hegele, R.A. (2009). Plasma lipoproteins: genetic influences and clinical implications. *Nature Reviews Genetics*, *10*(2), 109–121. https://doi.org/10.1038/nrg2481
15. Hinsdale, M.E., Sullivan, P.M., Mezdour, H., Maeda, N. (2002). ApoB-48 and apoB-100 differentially influence the expression of type-III hyperlipoproteinemia in APOE*2 mice. *Journal of Lipid Research*, *43*(9), 1520–1528. https://doi.org/10.1194/jlr.M200103-JLR200
16. Hung, Y.T., Hanson, A.R., Urriola, P.E., Johnston, L.J., Kerr, B.J., Shurson, G.C. (2019). Addition of tert-butylhydroquinone (TBHQ) to maize oil reduces lipid oxidation but does not prevent reductions in serum vitamin E in nursery pigs. *Journal of Animal Science and Biotechnology*, *10*, art. no. 51. https://doi.org/10.1186/s40104-019-0362-5
17. Kohan, A.B., Wang, F., Li, X., Vandersall, A.E., Huesman, S., Xu, M., Yang, Q., Lou, D., Tso, P. (2013). Is apolipoprotein A-IV rate limiting in the intestinal transport and absorption of triglyceride? *American Journal of Physiology-Gastrointestinal and Liver Physiology*, *304*(12), G1128–G1135. https://doi.org/10.1152/ajpgi.00409.2012
18. Kohan, A.B., Wang, F., Lo, C-M., Liu, M., Tso, P. (2015). ApoA-IV: current and emerging roles in intestinal lipid metabolism, glucose homeostasis, and satiety. *American Journal of Physiology-Gastrointestinal and Liver Physiology*, *308*, G472–G481. https://doi.org/10.1152/ajpgi.00098.2014
19. Larsson, M., Vorrsjö, E., Talmud, P., Lookene, A., Olivecrona, G. (2013). Apolipoproteins C-I and C-III inhibit lipoprotein lipase activity by displacement of the enzyme from lipid droplets. *Journal of Biological Chemistry*, *288*(47), 33997–34008. https://doi.org/10.1074/jbc.M113.495366
20. Lu, S., Yao, Y., Cheng, X., Mitchell, S., Leng, S., Meng, S., Gallagher, J.W., Shelness, G.S., Morris, G.S., Mahan, J., Frase, S., Mansbach, C.M., Weinberg, R.B., Black, D.D. (2006). Overexpression of apolipoprotein A-IV enhances lipid secretion in IPEC-1 cells by increasing chylomicron size. *Journal of Biological Chemistry*, *281*(6), 3473–3483. https://doi.org/10.1074/jbc.M502501200
21. Luo, M., Liu, A., Wang, S., Wang, T., Hu, D., Wu, S., Peng, D. (2017). ApoCIII enrichment in HDL impairs HDL-mediated cholesterol efflux capacity. *Scientific Reports*, *7*(1), art. no. 2312. https://doi.org/10.1038/s41598-017-02601-7
22. Martins, I.J., Hone, E., Chi, C., Seydel, U., Martins, R.N., Redgrave, T.G. (2000). Relative roles of LDLr and LRP in the metabolism of chylomicron remnants in genetically manipulated mice. *Journal of Lipid Research*, *41*(2), 205–213. https://doi.org/10.1016/S0022-2275(20)32054-X
23. Mika, M., Wikiera, A., Antończyk, A., Grabacka, M. (2021). The impact of catechins included in high fat diet on AMP-dependent protein kinase in apoE knock-out mice. *International Journal of Food Sciences and Nutrition*, *72*(3), 348–356. https://doi.org/10.1080/09637486.2020.1817345
24. Minekus, M., Alminger, M., Alvito, P., Ballance, S., Bohn, T., Bourlieu, C., Carrière, F., Boutrou, R., Corredig, M., Dupont, D., Dufour, C., Egger, L., Golding, M., Karakaya, S., Kirkhus, B., Le Feunteun, S., Lesmes, U., Macierzanka, A., Mackie, A., Marze, S., McClements, D.J., Ménard, O., Recio, I., Santos, C.N., Singh, R.P., Vegarud, G.E., Wickham, M.S.J., Weitschies, W., Brodkorb, A. (2014). Standardised static *in vitro* digestion method suitable for food – an international consensus. *Food and Function*, *5*(6), 1113–1124. https://doi.org/10.1039/C3FO60702J
25. Nam, K.-W., Kim, Y.H., Kwon, H.J., Rhee, S.-K., Kim, W.-J., Han, M.-D. (2013). *tert*-Butylhydroquinone reduces lipid accumulation in C57BL/6 mice with lower body weight gain. *Archives of Pharmacal Research*, *36*(7), 897–904. https://doi.org/10.1007/s12272-013-0109-3
26. Nassir, F., Wilson, B., Han, X., Gross, R.W., Abumrad, N.A. (2007). CD36 Is important for fatty acid and cholesterol uptake by the proximal but not distal intestine. *Journal of Biological Chemistry*, *282*(27), 19493–19501. https://doi.org/10.1074/jbc.M703330200
27. Nishizono, S., Hayami, T., Ikeda, I., Imaizumi, K. (2000). Protection against the diabetogenic effect of feeding *tert*-butylhydroquinone to rat prior to the administration of streptozotocin. *Bioscience, Biotechnology, and Biochemistry*, *64*(6), 1153–1158. https://doi.org/10.1271/bbb.64.1153
28. Onat, A., Hergenç, G., Sansoy, V., Fobker, M., Ceyhan, K., Toprak, S., Assmann, G. (2003). Apolipoprotein C-III, a strong discriminant of coronary risk in men and a determinant of the metabolic syndrome in both genders. *Atherosclerosis*, *168*(1), 81–89. https://doi.org/10.1016/S0021-9150(03)00025-X
29. Phillips, M.L., Pullinger, C., Kroes, I., Kroes, J., Hardman, D.A., Chen, G., Curtiss, L.K., Gutierrez, M.M., Kane, J.P., Schumaker, V.N. (1997). A single copy of apolipoprotein B48 is present on the human chylomicron remnant. *Journal of Lipid Research*, *38*(6), 1170–1177. https://doi.org/10.1016/S0022-2275(20)37199-6
30. Plat, J., Theuwissen, E., Husche, C., Lütjohann, D., Gijbels, M.J.J., Jeurissen, M., Shiri-Sverdlov, R., van der Made, I., Mensink, R.P. (2014). Oxidised plant sterols as well as oxycholesterol increase the proportion of severe atherosclerotic lesions in female LDL receptor$^{+/-}$ mice. *British Journal of Nutrition*, *111*(1), 64–70. https://doi.org/10.1017/S0007114513002018
31. Proctor, S.D., Mamo, J.C.L. (2003). Intimal retention of cholesterol derived from apolipoprotein B100– and apolipoprotein B48–containing lipoproteins in carotid arteries of Watanabe heritable hyperlipidemic rabbits. *Arteriosclerosis, Thrombosis, and Vascular Biology*, *23*(9), 1595–1600. https://doi.org/10.1161/01.ATV.0000084638.14534.0A
32. Riwanto, M., Rohrer, L., Roschitzki, B., Besler, C., Mocharla, P., Mueller, M., Perisa, D., Heinrich, K., Altwegg, L., von Eckardstein, A., Lüscher, T.F., Landmesser, U. (2013). Altered activation of endothelial anti- and proapoptotic pathways by high-density lipoprotein from patients with coronary artery disease. Role of high-density lipoprotein-proteome remodeling. *Circulation*, *127*(8), 891–904. https://doi.org/10.1161/CIRCULATIONAHA.112.108753
33. Safer, A.M., Al-Nughamish, A.J. (1999). Hepatotoxicity induced by the anti-oxidant food additive, butylated hydroxytoluene (BHT), in rats: An electron microscopical study. *Histology and Histopathology*, *14*(2), 391–406. https://doi.org/10.14670/HH-14.391
34. Sun, Z., Tang, Z., Yang, X., Liu, Q.S., Liang, Y., Fiedler, H., Zhang, J., Zhou, Q., Jiang, G. (2020). Perturbation of 3-*tert*-butyl-4-hydroxyanisole in adipogenesis of male mice with normal and high fat diets. *Science of the Total Environment*, *703*, art. no. 135608. https://doi.org/10.1016/j.scitotenv.2019.135608
35. Talayero, B., Wang, L., Furtado, J., Carey, V.J., Bray, G.A., Sacks, F.M. (2014). Obesity favors apolipoprotein E- and C-III-containing high density lipoprotein subfractions associated with risk of heart disease. *Journal of Lipid Research*, *55*(10), 2167–2177. https://doi.org/10.1194/jlr.M042333
36. Tran, T.T.T., Poirier, H., Clément, L., Nassir, F., Pelsers, M.M.A.L., Petit, V., Degrace, P., Monnot, M.-C., Glatz, J.F.C., Abumrad, N.A., Besnard, P., Niot, I. (2011). Luminal lipid regulates CD36 levels and downstream signaling to stimulate chylomicron synthesis. *Journal of Biological Chemistry*, 286(28), 25201–25210. https://doi.org/10.1074/jbc.M111.233551
37. Xiong, X., Liu, H., Hua, L., Zhao, H., Wang, D., Li, Y. (2015). The association of HDL-apoCIII with coronary heart disease and the effect of statin treatment on it. *Lipids in Health and Disease*, *14*, art. no. 127. https://doi.org/10.1186/s12944-015-0129-8
38. Xu, X., Liu, A., Hu, S., Ares, I., Martínez-Larrañaga, M.-R., Wang, X., Martínez, M., Anadón, A., Martínez, M.-A. (2021). Synthetic phenolic antioxidants: Metabolism, hazards and mechanism of action. *Food Chemistry, 353*, art. no. 129488. https://doi.org/10.1016/j.foodchem.2021.129488
39. Yu, K.C.-W., Mamo, J.C.L. (2000). Chylomicron-remnant-induced foam cell formation and cytotoxicity: a possible mechanism of cell death in atherosclerosis. *Clinical Science*, *98*(2), 183–192. https://doi.org/10.1042/CS19990182

Polish Journal of Food and Nutrition Sciences

72 VOLUME'S REVIEWERS

The Editors gratefully thank the following reviewers for their valuable help in reviewing manuscripts published in this volume and other papers reviewed between 1st January 2022 and 31st December 2022.

Almoselhy R., Food Technology Research Institute, Agricultural Research Center, Giza, Egypt
Amarowicz R., Institute of Animal Reproduction and Food Research of the Polish Academy of Sciences, Olsztyn, Poland
Anwar A., National Research Centre, Dokki, Cairo, Egypt
Aoe S., Otsuma Women's University, Tokio, Japan

Balzan S., University of Padova, Padova, Italy
Barbin D.F., University of Campinas, Campinas, Brazil
Bauza-Kaszewska J., Bydgoszcz University of Science and Technology, Bydgoszcz, Poland
Berthold-Pluta A., Warsaw University of Life Sciences, Warsaw, Poland
Bordonaro M., *Geisinger* Commonwealth School of Medicine, Denville, PA, USA
Bryła M., Institute of Agricultural and Food Biotechnology – State Research Institute, Warsaw, Poland

Cabral A., Federal University of Rio Grande do Norte, Rio Grande do Norte, Brazil
Carocho M., Polytechnic Institute of Bragança, Bragança, Portugal
Çelik E., Hacettepe University, Ankara, Turkey
Chen K., Zhejiang Gongshang University, Zhejiang, China
Chiavaro E., University of Parma, Parma, Italy
Culetu A., National Institute of Research & Development for Food Bioresources – IBA Bucharest, Bucharest, Romania
Cvetković D., University of Niš, Niš, Serbia
Czubiński J., Poznań University of Life Sciences, Poznań, Poland

Denev P.N., Institute of Organic Chemistry with Centre of Phytochemistry, Bulgarian Academy of Sciences, Plovidiv, Bulgaria
Dib J.R., National Scientific and Technical Research Council, San Miguel de Tucumán, Argentina
Djuričić I.D., University of Belgrade, Belgrade, Serbia
Dmytrukha N., Institute for Occupational Health of the National Academy of Medical Science of Ukraine, Kiev, Ukraine
Drabińska N., Institute of Animal Reproduction and Food Research of the Polish Academy of Sciences, Olsztyn, Poland
du Plessis H., Agricultural Research Council, ARC Infruitec-Nietvoorbij, Stellenbosch, South Africa

Fecka I., Wrocław Medical University, Wrocław, Poland
Ferreira S.S., University of Aveiro, Aveiro, Portugal

Gai, F., Institute of Sciences of Food Production, Italian National Research Council, Grugliasco, Italy
Gerschenson L., Buenos Aires University, Buenos Aires, Argentina
Ghane S., Shivaji University, Kolhapur, India
Grembecka M., Medical University of Gdansk, Gdansk, Poland
Grzegorzewska M., Institute of Horticulture - National Research Institute, Skierniewice, Poland
Grzelak-Błaszczyk K., Lodz University of Technology, Lodz, Poland

Jahanban-Esfahlan A., Tabriz University of Medical Sciences, Tabriz, Iran
Jakobek L., Josip Juraj Strossmayer University of Osijek, Osijek, Croatia
Janiak M., Institute of Animal Reproduction and Food Research of the Polish Academy of Sciences, Olsztyn, Poland
Jeleń H., Poznan University of Life Sciences, Poznań, Poland
Jurgoński A., Institute of Animal Reproduction and Food Research of the Polish Academy of Sciences, Olsztyn, Poland

Kakurinov V., University of Macedonia, Skopje, North Macedonia
Karamać M., Institute of Animal Reproduction and Food Research of the Polish Academy of Sciences, Olsztyn, Poland
Khwaldia K., Institut National de Recherche et d'Analyse Physico-Chimique, Sidi Thabet, Tunisia
Kocot A., Institute of Animal Reproduction and Food Research of the Polish Academy of Sciences, Olsztyn, Poland
Kozłowska M., Warsaw University of Life Sciences – SGGW, Warsaw, Poland
Kumar M., ICAR – Central Institute for Research on Cotton Technology, Mumbai, India
Kutralam-Muniasamy G., Center for Research and Advanced Studies of the National Polytechnic Institute, Mexico City, Mexico

Lee S., University of São Paulo, São Paulo, Brazil
Lesiow T., Wrocław University of Economics, Wrocław, Poland
Li G., Jiangxi Agricultural University, Nanchang, China
Lo Scalzo R., CREA – Council for Agricultural Research and Economics, Roma, Italy
Lopez-Martinez L., Coordinación de Tecnologia de Alimentos de Origen Vegetal, CONACYT-CIAD, Mexico

Marudova M., Plovdiv University "Paisii Hilendarski", Plovdiv, Bulgaria
Matusevicius P., Lithuanian University of Health Sciences, Veterinary Academy, Kaunas, Lithuania
Michalska-Ciechanowska A., Wrocław University of Environmental and Life Sciences, Wrocław, Poland
Miladinovic B., University of Niš, Niš, Serbia
Minnaar P., Agricultural Research Council, Infruitec-Nietvoorbij, Stellenbosch, South Africa
Mlcek J., Tomas Bata University in Zlín, Zlín , Czech Republic
Mohanty G., North Orissa University, Odisha, India
Mohsen S., Cairo University, Giza, Egypt

Needham T., Czech University of Life Sciences Prague, Prague, Czech Republic

Ozkan K., Yildiz Technical University, İstanbul, Turkey

Pan J., Chinese Academy of Sciences, Beijing, China
Parada-Alfonso F., National University of Colombia, Bogota, Colombia
Pawlak R., East Carolina University, Greenville, United States
Pegg R., University of Georgia, Athens, United States
Pérez-Ramírez I.F., Universidad Autónoma de Querétaro, Querétaro, Mexico
Pindi W., Universiti Malaysia Sabah., Kota Kinabalu, Malaysia
Popardowski E., University of Agriculture in Krakow, Krakow, Poland
Pourfarzad A., University of Guilan, Rasht, Iran

Ramirez Ascheri J.L., Brazilian Agricultural Research Corporation (EMBRAPA), Brasília, Brazil
Ratcliffe N.M., University of the West of England, Bristol, UK
Russo P., University of Foggia, Foggia, Italy
Rutkowska J., Warsaw University of Life Sciences, Warsaw, Poland
Rybicka I., Poznań University of Economics and Business, Poznań, Poland

Salejda A., Wrocław University of Environmental and Life Sciences, Wrocław, Poland
Sawicki T., University of Warmia and Mazury in Olsztyn, Olsztyn, Poland
Serrano M., Miguel Hernández University of Elche, Elche, Spain
Shimoyamada M., University of Shizuoka, Shizuoka, Japan
Skowron K., Nicolaus Copernicus University in Toruń, Collegium Medicum of L. Rydygier in Bydgoszcz, Bydgoszcz, Poland
Slavisa S., University of Belgrade, Belgrade, Serbia
Sommer A., Gdańsk University of Technology, Gdańsk, Poland
Soriano García M., National Autonomous University of Mexico, Mexico City, Mexico
Špánik I., Slovak University of Technology in Bratislava, Bratislava, Slovakia
Srivastava A., University of Georgia, Athens, United States
Starowicz M., Institute of Animal Reproduction and Food Research of the Polish Academy of Sciences, Olsztyn, Poland
Strączkowski M., Medical University of Bialystok, Bialystok, Poland
Szumny A., Wrocław University of Environmental and Life Sciences, Wrocław, Poland
Szwajgier D., University of Life Sciences in Lublin, Lublin, Poland

Tacias-Pascacio V., Tuxtla Gutierrez Institute of Technology, Tuxtla Gutiérrez, Mexico
Tao Y., Nanjing Agricultural University, Nanjing, China
Tomaszewska-Gras J., Poznań University of Life Sciences, Poznań, Poland
Topalović A., University of Montenegro, Podgorica, Montenegro
Tsukamoto C., Iwate University, Morioka, Japan
Turabi Yolaçaner E., Hacettepe University, Ankara, Turkey

Uzel R.S., Yaşar University, Izmir, Turkey

Venditti A., La Sapienza, University of Rome, Rome, Italy

Wangtueai S., Chiang Mai University, Chiang Mai, Thailand
Wiczkowski W., Institute of Animal Reproduction and Food Research of the Polish Academy of Sciences, Olsztyn, Poland
Wiśniewska J., Institute of Animal Reproduction and Food Research of the Polish Academy of Sciences, Olsztyn, Poland
Wronkowska M., Institute of Animal Reproduction and Food Research of the Polish Academy of Sciences, Olsztyn, Poland

Yilmaz E., Çanakkale Onsekiz Mart University, Çanakkale, Turkey

INSTRUCTIONS FOR AUTHORS

SUBMISSION. Original contributions relevant to food and nutrition sciences are accepted on the understanding that the material has not been, nor is being, considered for publication elsewhere. All papers should be submitted and will be processed electronically via Editorial Manager system (available from PJFNS web site: http://journal.pan.olsztyn.pl). On submission, a corresponding author will be asked to provide: Cover letter; Files with Manuscripts, Tables, Figures/Photos; and Names of two potential reviewers (one from the author's homeland – but outside author's Institution, and the other from abroad). All papers which have been qualified as relevant with the scope of our Journal are reviewed. All contributions, except the invited reviews are charged. Proofs will be sent to the corresponding author and should be returned within one week since receipt. No new material may be inserted in the text at proof stage. It is the author's duty to proofread proofs for errors.

Authors should very carefully consider the preparation of papers to ensure that they communicate efficiently, because it permits the reader to gain the greatest return for the time invested in reading. Thus, we are more likely to accept those that are carefully designed and conform the instruction. Otherwise, papers will be rejected and removed from the online submission system.

SCOPE. The Polish Journal of Food and Nutrition Sciences publishes original, basic and applied papers, and reviews on fundamental and applied food research, preferably these based on a research hypothesis, in the following Sections:

Food Technology:
- Innovative technology of food development including biotechnological and microbiological aspects
- Effects of processing on food composition and nutritional value

Food Chemistry:
- Bioactive constituents of foods
- Chemistry relating to major and minor components of food
- Analytical methods

Food Quality and Functionality:
- Sensory methodologies
- Functional properties of food
- Food physics
- Quality, storage and safety of food

Nutritional Research:
- Nutritional studies relating to major and minor components of food (excluding works related to questionnaire surveys)

"News" section:
- Announcements of congresses
- Miscellanea

OUT OF THE SCOPE OF THE JOURNAL ARE:
- Works which do not have a substantial impact on food and nutrition sciences
- Works which are of only local significance i.e. concern indigenous foods, without wider applicability or exceptional nutritional or health related properties
- Works which comprise merely data collections, based on the use of routine analytical or bacteriological methods (i.e. standard methods, determination of mineral content or proximate analysis)
- Works concerning biological activities of foods but not providing the chemical characteristics of compounds responsible for these properties
- Nutritional questionnaire surveys
- Works related to the characteristics of foods purchased at local markets
- Works related to food law
- Works emphasizing effects of farming / agricultural conditions / weather conditions on the quality of food constituents
- Works which address plants for non-food uses (i.e. plants exhibiting therapeutic and/or medicinal effects)

TYPES OF CONTRIBUTIONS. *Reviews*: (at least: 30 pages and 70 references) these are critical and conclusive accounts on trends in food and nutrition sciences; *Original papers*: (maximally: 30 pages and 40 references) these are reports of substantial research; *Reports on post and forthcoming scientific events, and letters to the Editor* (all up to three pages) are also invited (free of charge).

REVIEW PROCESS. All scientific contributions will be peer-reviewed on the criteria of originality and quality. Submitted manuscripts will be preevaluated by Editor-in-Chief and Statistical Editor (except for review articles), and when meeting PJFNS' scope and formal requirements, they will be sent to a Section Editor who upon positive preevaluation will assign at least two reviewers from Advisory Board Members, reviewers suggested by the author or other experts in the field. Based on the reviews achieved, Section Editor and Editor-in--Chief will make a decision on whether a manuscript will be accepted for publication, sent back to the corresponding author for revision, or rejected. Once a manuscript is sent back to the corresponding author for revision, all points of the reviews should be answered or rebuttal should be provided in the Explanation letter. The revised manuscripts will be checked by Section Editor and by the original reviewers (if necessary), and a final decision will be made on acceptance or rejection by both Section Editor and Editor-in-Chief.

Polish Journal of Food and Nutrition Sciences uses CrossCheck's iThenticate software to detect instances of similarity in submitted manuscripts. In publishing only original research, PJFNS is committed to deterring plagiarism, including self-plagiarism.

COPYRIGHT LICENSE AGREEMENT referring to Authorship Responsibility and Acknowledgement, Conflict of Interest and Financial Disclosure, Copyright Transfer, are required for all authors, i.e. *Authorship Responsibility and Acknowledgement*: Everyone who has made substantial intellectual contributions to the study on which the article is based (for example, to the research question, design, analysis, interpretation, and written description) should be an author. It is dishonest to omit mention of someone who has participated in writing the manuscript ("ghost authorship") and unfair to omit investigator who have had important engagement with other aspects of the work. All contributors who do not meet the criteria for authorship should be listed in an Acknowledgments section. Examples of those who might be acknowledged include a person who provided purely technical help, writing assistance, or a department chairperson who provided only general support. Any financial and material support should also be acknowledged. *Conflict of Interest and Financial Disclosure*: Authors are responsible for disclosing financial support from the industry or other conflicts of interest that might bias the interpretation of results. *Copyright License Agreement*: Authors agree to follow the Creative Commons Attribution-Non--Commercial-NoDerivs 4.0 License.

A manuscript will not be published once the signed form has not been submitted to the Editor with the manuscript revised after positive reviews.

CHANGES TO AUTHORHIP. Authors are expected to consider carefully the list and order of authors before submitting their manuscript and provide the definitive list of authors at the time of the original submission. Any addition, deletion or rearrangement of author names in the authorship list should be made only before the manuscript has been accepted and only if approved by the journal Editor. To request such a change, the Editor must receive the following from the corresponding author: (a) the reason for the change in author list and (b) written confirmation (e-mail, letter) from all authors that they agree with the addition, removal or rearrangement. In the case of addition or removal of authors, this includes confirmation from the author being added or removed.

ETHICAL APPROVAL OF STUDIES AND INFORMED CONSENT. For all manuscripts reporting data from studies involving human participants or animals, formal approval by an appropriate institutional review board or ethics committee is required and should be described in the Methods section. For those investigators who do not have formal approval from ethics review committees, the principles outlined in the Declaration of Helsinki should be followed. For investigations of humans, state in the Methods section the manner in which informed consent was obtained from the study participants (i.e., oral or written). Editors may request that authors provide documentation of the formal review and recommendation from the institutional review board or ethics committee responsible for oversight of the study.

UNAUTHORIZED USE. Unauthorized use of the PJFNS name, logo, or any content for commercial purposes or to promote commercial goods and services (in any format, including print, video, audio, and digital) is not permitted by IAR&FR PAS.

MANUSCRIPTS. A manuscript in English must be singlesided, preferably in Times New Roman (12) with 1.5-point spacing, without numbers of lines. The Editor reserves the right to make literary corrections and to make suggestions to improve brevity. English is the official language. The English version of the paper will be checked by Language Editor. Unclear and unintelligible version will be returned for correction.

Every paper should be divided under the following headings in this order: a **Title** (possibly below 150 spaces); the **Name(s)** of the author(s) in full. In paper with more than one author, the asterisk indicates the name of the author to whom correspondence and inquiries should be addressed, otherwise the first author is considered for the corre-spondence. Current full postal address of the indicated corresponding author or the first author must be given in a footnote on the title page; the **Place(s)** where the work was done including the institution name, city, country if not Poland. In papers originated from several institu-tions the names of the authors should be marked with respective superscripts; the **Key words** (up to 6 words or phrases) for the main topics of the paper; an **Abstract** (up to 250 words for regular papers and reviews) summarizing briefly main results of the paper, no literature references; an **Introduction** giving essential background by saying why the research is important, how it relates to previous works and stating clearly the objectives at the end; **Materials and Methods** with sufficient experimental details permitting to repeat or extend the experiments. Literature references to the methods, sources of material, company names and location (city, country) for specific instruments must be given. Describe how the data were evaluated, including selection criteria used; **Results and Discussion** presented together (in one chapter). Results should be presented concisely and organized to supplement, but not repeat, data in tables and figures. Do not display the data in both tabular and graphic form. Use narrative form to present the data for which tables or figures are unnecessary. Discussion should cover the implications and consequences, not merely recapitulating the results, and it must be accomplished with concise **Conclusions**; **Acknowledgements** should be made to persons who do not fill the authorship criteria (see: Authorship forms); **Research funding** should include financial and material support; **Conflict of Interests**: Authors should reveal any conflicts of interest that might bias the interpretation of results; and **References** as shown below.

REFERENCES each must be listed alphabetically at the end of the paper (each should have an Arabic number in the list) in the form as follows: **Periodicals** – names and initials of all the authors, year of publication, title of the paper, journal title as in Chemical Abstracts, year of publication, volume, issue, inclusive page numbers, or article id.; **Books** – names and initials of all the authors, names of editors, chapter title, year of publication, publishing company, place of publication, inclusive page numbers; **Patents** – the name of the application, the title, the country, patent number or application number, the year of publication.

For papers published in language other than English, manuscript title should be provided in English, whereas a note on the original language and English abstract should be given in parentheses at the end.

The reference list should only include peer-reviewed full-text works that have been published or accepted for publication. Citations of MSc/PhD theses and works unavailable to international Editors, Reviewers, and Readers should be limited as much as possible.

References in the text must be cited by name and year in square parentheses (e.g.: one author – [Tokarz, 1994]; two authors – [Słonimski & Campbell, 1987]; more than two authors – [Amarowicz *et al*., 1994]). If more than one paper is published in the same year by the same author or group of authors use [Tokarz, 1994a, b]. Unpublished work must only be cited where necessary and only in the text by giving the person's name.

Examples:

Article in a journal:

Słonimski, B.A., Campbell, L.D., Batista, E., Howard B. (2008). Gas chromatographic determination of indole glucosinolates. Journal of Science and Food Agriculture, 40(5), 131–143.

Asher, A., Tintle, N.L., Myers, M., Lockshon, L., Bacareza, H., Harris, W.S. (2021). Blood omega-3 fatty acids and death from COVID-19: A pilot study. *Prostaglandins, Leukotrienes and Essential Fatty Acids, 166*, art. no. 102250.

Book:

Weber, W., Ashton, L., Milton, C. (2012). Antioxidants – Friends or Foes? 2nd edition. PBD Publishing, Birmingham, UK. pp. 218–223.

Chapter in a book:

Uden, C., Gambino, A., Lamar, K. (2016). Gas chromatography. In M. Queresi, W. Bolton (Eds.), CRC Handbook of Chromatography, CRC Press Inc., Boca Raton, Florida, USA, pp. 44–46.

ABBREVIATIONS AND UNITS. Abbreviations should only be used when long or unwieldy names occur frequently, and never in the title; they should be given at the first mention of the name. Metric SI units should be used. The capital letter L should be used for liters. Avoid the use of percentages (% g/g,% w/w; Mol%; vol%), ppm, ppb. Instead, the expression such as g/kg, g/L, mg/kg, mg/mL should be used. A space must be left between a number and a symbol (e.g. 50 mL not 50mL). A small x must be used as multiplication sign between numeric values (e.g. 5 × 102 g/mL). Statistics and measurements should be given in figures, except when the number begins a sentence. Chemical formulae and solutions must specify the form used. Chemical abbreviations, unless they are internationally known, Greek symbols and unusual symbols for the first time should be defined by name. Common species names should be followed by the Latin at the first mention, with contracting it to a single letter or word for subsequent use.

FIGURES should be submitted in separate files. Each must have an Arabic number and a caption. Captions of all Figures should be provided on a separate page "Figure Captions". Figures should be comprehensible without reference to the text. Self-explanatory legend to all figures should be provided under the heading "Legends to figures"; all abbreviations appearing on figures should be explained in figure footnotes. Three-dimensional graphs should only be used to illustrate real 3D relationships. Start the scale of axes and bars or columns at zero, do not interrupt them or omit missing data on them. Figures must be cited in Arabic numbers in the text.

TABLES should be submitted in separate files. They should be as few in number and as simple as possible (like figures, they are expensive and space consuming), and include only essential data with appropriate statistical values. Each must have an Arabic number and a caption. Captions of all Tables should be provided on a separate page "Table Captions". Tables should be self-explanatory; all abbreviations appearing in tables should be explained in table footnotes. Tables must be cited in Arabic numbers in the text.

PAGE CHARGES. A standard publication fee has been established at the rate of 450 EUR + tax (if applicable, e.g. for private persons) irrespective of the number of pages and tables/figures. For Polish Authors an equivalent fee was set at 1950 PLN + VAT. Payment instructions will be sent to Authors via e-mail with acceptance letter.

Information on publishing and subscription is available from:

Ms. Joanna Molga
Editorial Office of Pol. J. Food Nutr. Sci.
Institute of Animal Reproduction and Food Research Tuwima 10 Str., 10–748 Olsztyn 5, Poland
phone (48 89) 523–46–70, fax (48 89) 523–46–70;
e-mail: pjfns@pan.olsztyn.pl; http://journal.pan.olsztyn.pl

Nutrition